The effect of feed pH and *in-situ* pH adjustment on the behaviour of an anaerobic sequencing batch reactor treating synthetic winery wastewater

by

Jason Smit

Thesis presented in partial fulfilment
of the requirements for the Degree
of
MASTER OF ENGINEERING
(CHEMICAL ENGINEERING)

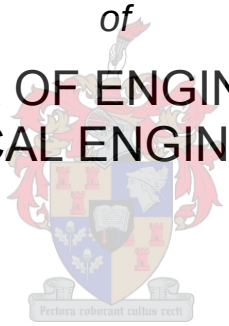

in the Faculty of Engineering
at Stellenbosch University

Supervisors
Professor A.J. Burger
Professor G. Sigge

March 2017

Stellenbosch University https://scholar.sun.ac.za

Declaration

By submitting this thesis electronically, I declare that the entirety of the work contained therein is my own, original work, that I am the sole author thereof (save to the extent explicitly otherwise stated), that reproduction and publication thereof by Stellenbosch University will not infringe any third party rights and that I have not previously in its entirety or in part submitted it for obtaining any qualification.

Date: ……March 2017……

Copyright © 2017 Stellenbosch University

All rights reserved

Stellenbosch University https://scholar.sun.ac.za

Abstract

Legal requirements and high production costs have resulted in wineries having to seek alternative methods of reducing operating costs with regards to the reduction of fresh water intake as well as treating the wastewater they produce. Winery wastewater typically contains varying concentrations of monosaccharides, volatile fatty acids and ethanol. To legally dispose of winery wastewater, its chemical oxygen demand (COD) needs to be reduced to below 400 mg/ℓ when disposing between 50 and 500 m^3 daily. An anaerobic sequencing batch reactor (ASBR) has been recommended as a possible method to treat winery wastewater due to several benefits over typical aerobic systems. Anaerobic digestion systems produce useful biogas and, compared to aerobic digestion systems, generate low volumes of sludge. These advantages, together with the simplicity and relatively low installation costs of sequencing batch reactor (SBR) systems, make ASBR technology an attractive option for treatment of winery wastewater.

Winery wastewaters have varying pH (3.5 – 8.0) due to the various sources from the plant. As such, the main objective of this study was to determine whether an ASBR can be operated with *in-situ* pH control and without adjusting the feed alkalinity.

Exploratory simulations were performed with the Anaerobic Digestion Model no. 1 (ADM1) to understand where the potential problems could occur with the experimental ASBR. Sludge retention in the ASBR was simulated through the incorporation of a clarification model in the ADM1. The simulation results indicated that winery wastewater with high monosaccharide concentrations would cause a sudden drop in pH early in the ASBR process due to rapid production of volatile fatty acids. It therefore followed that *in-situ* pH control would be required. The ADM1 was found to be unstable when poor initial guesses of the soluble and sludge component concentrations were used in the simulations. With the ADM1 simulation, the pH was identified as the variable which would easily indicate instability in the model.

Following the ADM1 simulations, a 14-litre laboratory scale ASBR was used to treat different synthetic winery wastewaters while operating with *in-situ* pH control. Two artificial feed solutions were prepared, the first with a high ammonium sulphate concentration and the second without ammonium sulphate. Both solutions contained high concentrations of glucose and fructose. The ASBR could handle the ammonium sulphate between organic loading rates (OLRs) 1.1 and 2.1 g-COD_{feed}.$ℓ^{-1}_{ASBR}$.day^{-1}. Under these conditions, the ASBR achieved a COD reduction of at least 60 %. In the absence of ammonium sulphate, the ASBR achieved a COD reduction of at least 80 %.

Stellenbosch University https://scholar.sun.ac.za

Biogas containing methane, carbon dioxide and nitrogen was produced. Theoretically excluding the nitrogen from the biogas resulted in a methane fraction in excess of 80 mol%, with the balance being carbon dioxide.

KOH was dosed as a nutrient. Correcting the feed pH to 7.4, allows for an approximate saving of 8 – 12% on the total amount of KOH required for feed substrate dosing and *in-situ* pH control. *In-situ* pH control was deemed to be the most important during the first five hours of a batch. After this, the methanogens generally consumed acetic acid fast enough to counter the effect that volatile fatty acid formation has on the pH of the system.

Stellenbosch University https://scholar.sun.ac.za

Opsomming

Weens wetsvereistes en hoë produksiekoste moet wynkelders met alternatiewe metodes vorendag kom om bedryfskoste te verlaag wat die vermindering van varswaterinname en die behandeling van afvalwater betref. Die afvalwater van wynkelders bevat gewoonlik wisselende konsentrasies monosakkariede, vlugtige vetsure en etanol. Om op ’n wettige manier van kelderafvalwater ontslae te raak, moet die chemiese suurstofbehoefte (CSB) tot onder 400 mg/ℓ verminder word om daagliks met tussen 50 en 500 m^3 weg te doen. ’n Anaërobiese opeenvolgende lotreaktor (AOLR) word aanbeveel as ’n moontlike metode om kelderafvalwater te behandel omdat dit verskeie voordele bo tipiese aërobiese stelsels inhou. Anaërobiese verteerstelsels produseer byvoorbeeld nuttige biogas en, vergeleke met aërobiese verteerstelsels, lae volumes slyk. Hierdie voordele, tesame met die eenvoud en betreklik lae installasiekoste van opeenvolgende lotreaktor- (OLR-)stelsels, maak AOLR-tegnologie dus ’n aanloklike moontlikheid vir die behandeling van afvalwater.

Kelderafvalwater het ’n wisselende pH (3.5 – 8.0) as gevolg van die verskillende bronne in die aanleg. Daarom was die hoofdoel van hierdie studie om te bepaal of ’n AOLR bedryf kan word met in situ-pH-beheer en sonder om die alkaliniteit van die toevoer aan te pas.

Ondersoekende simulasies is uitgevoer met die anaërobiese verteermodel nr 1 (“ADM1”) om te verstaan waar moontlike probleme met die eksperimentele AOLR kan voorkom. Slykbehoud in die AOLR is gesimuleer deur die insluiting van ’n verhelderingsmodel by die ADM1. Die simulasieresultate het getoon dat kelderafvalwater met hoë monosakkariedkonsentrasies ’n skielike pH-daling vroeg in die AOLR-proses sal veroorsaak as gevolg van die snelle produksie van vlugtige vetsure. In situ-pH-beheer sou dus nodig wees. Daar is bevind dat die ADM1 onstabiel is wanneer swak aanvanklike raaiskote van die oplosbare en slykkomponentkonsentrasies in die simulasies gebruik word. Die pH is uitgewys as die veranderlike in die ADM1-simulasie wat maklik op onstabiliteit in die model sal dui.

Na aanleiding van die ADM1-simulasies is ’n laboratoriumskaal-AOLR van 14 liter gebruik om verskillende sintetiese kelderafvalwaters te behandel terwyl in situ-pH-beheer toegepas word. Twee kunsmatige toevoeroplossings is voorberei: die eerste met ’n hoë ammoniumsulfaatkonsentrasie, en die tweede sonder ammoniumsulfaat. Albei oplossings het hoë konsentrasies glukose en fruktose bevat. Die AOLR kon die ammoniumsulfaat tussen organiese ladingstempo’s (OLT’s) van 1.1 en 2.1 $g\text{-}CSB_{toevoer}.ℓ^{-1}_{AOLR}.dag^{-1}$ hanteer. In hierdie omstandighede het die AOLR ’n CSB-vermindering van ten minste 60% behaal. Sonder ammoniumsulfaat is ’n CSB-vermindering van ten minste 80% verkry.

Stellenbosch University https://scholar.sun.ac.za

Biogas wat uit metaan, koolstofdioksied en stikstof bestaan, is geproduseer. Toe die stikstof teoreties van die biogas uitgesluit is, is ’n metaaninhoud van meer as 80 mol% verkry en het die res uit koolstofdioksied bestaan.

KOH is as ’n voedingstof toegedien. Die regstelling van die toevoer-pH tot 7.4 maak ’n besparing van ongeveer 8 – 12% moontlik op die totale hoeveelheid KOH wat vir toevoersubstraattoediening en in situ-pH-beheer vereis word. In situ-pH-beheer was die belangrikste gedurende die eerste vyf uur van ’n lot. Daarna het die metanogene die asynsuur oor die algemeen vinnig genoeg verteer om die uitwerking van vlugtigevetsuurvorming op die pH van die stelsel teen te werk.

Stellenbosch University https://scholar.sun.ac.za

Acknowledgements

I would like to thank the following people for making this study possible:

- My main supervisor, Prof Burger, for advice, guidance and continuous encouragement during the course of the project.
- My co-supervisor, Prof Sigge, for advice on anaerobic digestion.
- The Department of Process Engineering for financial support during the study.
- The analytical laboratory staff, Hanlie Botha, Levine Simmers and Jaco van Rooyen for input with analytical work.
- The workshop staff, oom Anton and oom Jos, for help with the improvement of the experimental setup as well as the morning coffees.
- Nardus Uys for assistance with PLC programming.
- The laboratory staff, Alvin, Linda and Ollie for general assistance in the large lab.
- Jeanne Louw for assistance in gas analysis and ASBR advice.
- Some close friends, Jacques, Willem, Jowandré, Bradley and Oliver for all sorts of help.
- My parents, Wimpie and Karin, for the continuous support and patience throughout the project.

Stellenbosch University https://scholar.sun.ac.za

Nomenclature

Abbreviation	Term
ADM1	Anaerobic Digestion Model No. 1
ASBR	Anaerobic Sequencing Batch Reactor
ASBBR	Anaerobic Sequencing Batch Biofilm Reactor
COD	Chemical Oxygen Demand
F:M	Food-to-Microorganism ratio
GC	Gas Chromatography
HPLC	High Pressure Liquid Chromatography
HHV	Higher Heating Value
IA	Intermediate Alkalinity
LCFA	Long Chain Fatty Acids
OLR	Organic Loading Rate
ORP	Oxidation Reduction Potential
PA	Partial Alkalinity
SAR	Sodium Absorption Ratio
SBR	Sequencing Batch Reactor
SRB	Sulphate Reducing Bacteria
TA	Total Alkalinity
VDF	Volumetric Discharge Fraction
VFA	Volatile Fatty Acid

Stellenbosch University https://scholar.sun.ac.za

Table of contents

Stellenbosch University https://scholar.sun.ac.za

Stellenbosch University https://scholar.sun.ac.za

Stellenbosch University https://scholar.sun.ac.za

Stellenbosch University https://scholar.sun.ac.za

List of tables

Stellenbosch University https://scholar.sun.ac.za

List of figures

Stellenbosch University https://scholar.sun.ac.za

Stellenbosch University https://scholar.sun.ac.za

Stellenbosch University https://scholar.sun.ac.za

Stellenbosch University https://scholar.sun.ac.za

Chapter 1 - Introduction

1.1. Motivation for the study

With the increase in industrial water usage and a limited fresh water supply, it is necessary for industries to reuse water where possible. The wine industry uses large amounts of water to produce wine during the post-harvest period. This has created two main problems for the wine industry. Firstly, they need to maintain a profitable wine making operation while reducing the fresh potable water intake. Secondly, wineries need to dispose of large volumes of effluent in an environmentally friendly manner.

An anaerobic digester system has been recommended to treat winery wastewater due to several advantages it has over aerobic systems. The two main benefits is a lower sludge production and the generation of methane, which can be used for heating purposes (Chernicharo, 2007). The anaerobic sequencing batch reactor (ASBR) is a semi-continuous batch process that can be used by wineries to reduce their wastewater treatment cost. The focus was on keeping the ASBR system as simple as possible by minimising the required process units for a large scale treatment plant.

The Anaerobic Digestion Model No. 1 (ADM1) (Batstone *et al*., 2002) is a detailed model that describes the anaerobic digestion process. In this study, ADM1 was used as a tool to understand the anaerobic digestion process that occurs in the ASBR. The programmed ADM1 was kept as simple as possible to determine whether *in-situ* pH control is required for an ASBR. It was determined that the pH of the system is greatly affected by the various group of anaerobic bacteria groups and possible pH control would be required in the ASBR.

A lab-scale ASBR with *in-situ* pH control was used to determine the effect that the varying pH of winery wastewater had on the overall performance of the system. The anaerobic digestion process produces various volatile fatty acids (VFAs) which needs to be neutralised with additional alkalinity or a basic solution. ASBRs are often operated by adding alkalinity to the feed substrate to remove the requirement for *in-situ* pH control. However, this study used KOH for *in-situ* pH control instead of adding alkalinity to the feed substrate. KOH was used as potassium is considered to be one of the least toxic cations to anaerobic bacteria (Gerardi, 2003).

1.1.1. Winery wastewater composition and volumes produced

The quality and quantity of winery wastewater produced in the wine making process is dependent on location, time of year and wine making methods (Conradie *et al*., 2014). South Africa generally produces winery wastewater with a lower chemical oxygen demand (COD) than European wineries.

Stellenbosch University https://scholar.sun.ac.za

However, this comes at the cost of producing more wastewater (Conradie *et al*., 2014; Mosse *et al*., 2011; Mulidzi *et al*., 2002).

Conradie *et al*. (2014) evaluated several global winery wastewater studies and found that the COD of the wastewater from wineries vary between 340 and 49000 mg/ℓ. Additionally, the pH varied between 3.5 and 7.9. The amount of wastewater produced per litre of wine varied between 1 and 8 litres.

Mulidzi *et al*. (2002) investigated 10 wineries in the Northern and Western Cape Provinces of South Africa during the wine making session. A summary of the study can be found below in Table 1-1. It is important to note that the quality of the wastewater is greatly dependent on where it is sampled.

Table 1-1: Winery wastewater characteristics as determined by Mulidzi et al. (2002)

Variable	Measured Range
COD [mg/ℓ]	300 – 59000
pH	3.5 – 8.0
Total Solids [mg/ℓ]	200 – 18000
Suspended Solids [mg/ℓ]	1000 – 5000
Electrical Conductivity [mS/m]	40 – 350
Sodium Absorption Ration [SAR]	0.1 - 35

Mosse *et al*. (2011) found that the majority of the COD in winery wastewater is made up of maltose, glucose and fructose, whereas Fillaudeau *et al*. (2008) found that 80% of the COD was made up from ethanol. However, the advantage of anaerobic digestion system is that they can be used to treat both wastewater types. Nonetheless, it is important for a system to be capable of handling these changes.

1.1.2. Legal requirements for winery wastewater disposal

Several methods of winery wastewater disposal exist. However, the most common method is through irrigation onto uncultivated land (van Schoor, 2005). Even for disposal via irrigation, the National Water Act (1998) requires the disposed water to be of a particular quality. Table 1-2 presents a summary of wastewater disposal requirements. Due to out-of-specification pH and COD, winery wastewater needs to be treated so that they adhere to the regulations.

Stellenbosch University https://scholar.sun.ac.za

Table 1-2: Legal limitations for the irrigation of wastewater (adapted from van Schoor (2005))

Variable	Maximum irrigated volume per day		
	50m³	**500m³**	**2000m³**
Electrical conductivity [mS/m]	< 200	<200	70 – 150
pH	6.0 – 9.0	6.0 – 9.0	5.5 – 9.5
COD [mg/ℓ]	< 5000	< 400	< 75
Faecal coli-forms	< 100 000	< 100 000	< 1000
Sodium adsorption ratio	< 5	<5	-

1.2. Research objectives

The main objective of this study was to determine whether an ASBR with *in-situ* pH control can be used to treat winery wastewater. This was achieved by:

1. Using the ADM1 to understand the anaerobic digestion process within an ASBR.
2. Evaluating the performance of an ASBR with regards to COD reduction, biogas production, and *in-situ* pH control requirements, during the treatment of synthetic winery wastewater.
3. Comparing the performance of an ASBR during the operation with the feed pH control and *in-situ* pH control.

1.3. Thesis outline

The focus of **Chapter 2** is on the literature of anaerobic digestion and the ASBR process. Initially, it provides a background on the anaerobic digestion process in terms of microbial activity and the effect controllable process parameters has on its performance. Furthermore, the ASBR process is discussed along with a short summary of similar studies on winery or organic wastewater.

Chapter 3 provides an overview of the experimental approach followed in this study where the exact details can be found in Appendix B. Before experiments were performed, the ADM1 was used to describe and understand the digestion process within an ASBR (**Chapter 4**). **Chapter 5** focuses on experimental results showing that an ASBR can be operated without additional alkalinity and solely with *in-situ* pH control. **Chapter 6** compares and discusses the results obtained when varying the feed substrate's pH to the ASBR. The conclusions and recommendations are offered in **Chapter 7**.

Stellenbosch University https://scholar.sun.ac.za

Chapter 2 - Literature review: Anaerobic wastewater treatment

2.1. Anaerobic digestion

Anaerobic digestion is a collection of reactions that break down organic matter to form biogas through the use of microorganisms in an oxygen free environment (Chernicharo, 2007). Winery wastewater is consists of several different types of organic components that can be broken down in the anaerobic digestion process. The main components include monosaccharides, VFAs and ethanol (Batstone *et al*., 2004; Malandra *et al.*, 2003).

2.1.1. Microbial and biochemical aspects of anaerobic digestion

The anaerobic digestion process consists of several interdependent, complex sequential and parallel biological reactions performed by various groups of bacteria (Batstone *et al*., 2002; Parawira, 2004). A schematic of anaerobic digestion process is shown in Figure 2-1. The digestion process can be categorised into four main phases, namely:

- Disintegration and hydrolysis
- Acidogenesis
- Acetogenesis
- Methanogenesis

Also indicated in Figure 2-1 are seven different pathways that are used to describe the various sub processes that occur during the acidogenesis, acetogenesis and methanogenesis steps (Batstone *et al*., 2002).

Stellenbosch University https://scholar.sun.ac.za

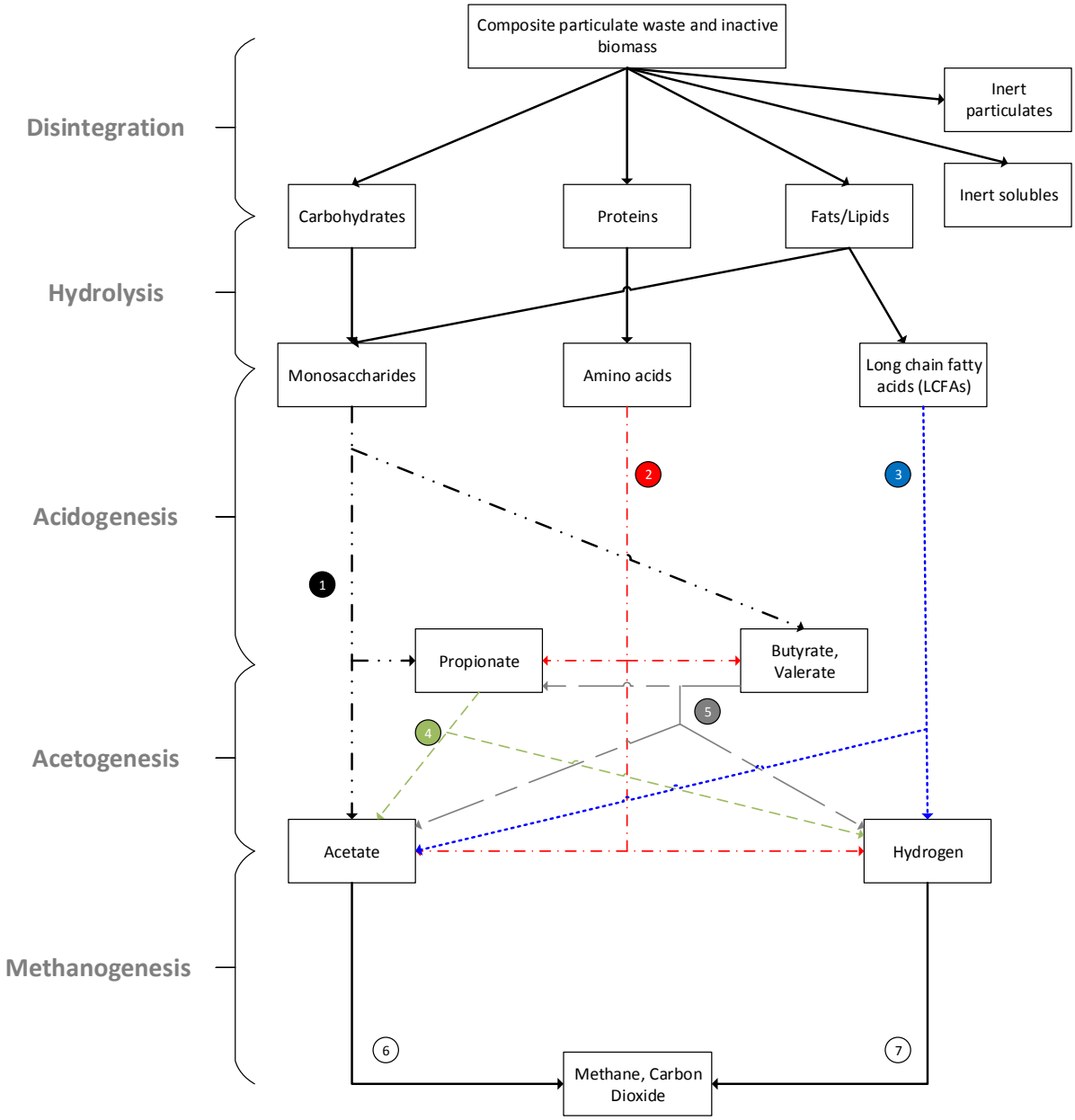

Figure 2-1: Main anaerobic digestion pathways. (1) Acidogenesis from monosaccharides; (2) Acidogenesis from amino acids; (3) Acetogenesis from LCFAs; (4) Acetogenesis from propionate; (5) Acetogenesis from butyrate and valerate; (6) aceticlastic methanogenesis; (7) Hydrogenotrophic methanogenesis. (Adapted from Batstone et al. (2002))

a. Disintegration and hydrolysis

Complex particulate waste and biomass need to be broken down into simpler dissolved materials which can be digested by other groups of microorganisms. This complex material is reduced through a process known as disintegration and hydrolysis.

Complex particulates are broken down into carbohydrates, protein, lipids, inert solubles and inert particulates in the disintegration phase of this step (Batstone *et al.*, 2002). After disintegration took

Stellenbosch University https://scholar.sun.ac.za

place, the hydrolysis phase of the process can take place. During the hydrolysis phase, hydrolytic bacteria convert carbohydrates, proteins and lipids into monosaccharides, amino acids and long chain fatty acids (LCFAs) (Parawira, 2004). The hydrolysis step is usually a slow process under anaerobic conditions, resulting in it being the overall rate limiting step (Chernicharo, 2007). Several factors have indicated that they influence the hydrolysis step and include:

- Operating temperature
- Substrate residence time
- Substrate composition
- Biomass particle size
- pH of the treated substrate
- Product concentration from the hydrolysis phase (e.g. volatile fatty acids)

b. Acidogenesis

Acidogenic bacteria converts monosaccharides, amino acids and LCFAs into alcohols, ketones and volatile fatty acids (VFAs) (Chernicharo, 2007). The acids that are produced during this phase are organic acids such as acetic, propionic, butyric and valeric acid. However, the type of acid and amount of acid produced is dependent on the operating conditions such as the operating temperature, pressure, acid concentrations and type of bacteria used in the process (Sigge, 2005).

The acidogenesis step is usually the fastest step in the anaerobic digestion (Mosey and Fernades, 1989). The glucose degradation reactions that take place during the acidogenesis step are provided in Table 2-1.

Table 2-1: Acidogenesis reactions of glucose degradation (adapted from Batstone et al.(2002))

Glucose degradation reaction	Main product	ΔG^0 [kJ]
$C_6H_{12}O_6 + 4H_2O \rightarrow 2CH_3COO^- + 2HCO_3^- + 4H^+ + 4H_2$	Acetate	-206
$C_6H_{12}O_6 + 2H_2 \rightarrow 2CH_3CH_2COO^- + 2H_2O + 2H^+$	Propionate	-358
$C_6H_{12}O_6 \rightarrow CH_3CH_2CH_2COOH + 2CO_2 + 2H_2$	Butyrate	N/A
$C_6H_{12}O_6 \rightarrow 2CH_3CHOHCOO^- + 2H^+$	Lactate	-198
$C_6H_{12}O_6 \rightarrow 2CH_3CH_2OH + 2CO_2$	Ethanol	-226

The acidogenesis reactions of amino acids proceed either through the Stickland oxidation-reduction paired fermentation process or via the oxidation of a single amino acid (Batstone *et al*., 2002). Further

Stellenbosch University https://scholar.sun.ac.za

information on this can be found in Batstone *et al*. (2002) and Parawira (2004). It is not discussed here as amino acids do not form a significant portion of the COD within winery wastewater.

The concentration of individual VFAs produced in the acidogenesis stage is an important step in the overall performance of the digestion process (Parawira *et al*., 2004). In this step, acetic and butyric acids are preferred precursors for the formation of methane in the later anaerobic digestion process.

c. Acetogenesis

During the acetogenesis phase, acetogenic bacteria degrade VFAs and alcohols into acetate, carbon dioxide and hydrogen (Chernicharo, 2007). This conversion forms an important intermediate for the production of biogas which is used later in the methanogenesis phase. The main reactions that take place in the acetogenesis phase are summarised in Table 2-2.

Table 2-2: Acetogenic reactions (adapted from Bitton (2005) and Parawira (2004))

Substrate	Acetogenesis reaction	Product	ΔG^0 [kJ]
Ethanol	$CH_3CH_2OH + H_2O \rightarrow CH_3COO^- + H^+ + 2H_2$	Acetate	+9.6
Propionate	$CH_3CH_2COO^- + 3H_2O \rightarrow CH_3COO^- + H^+ + HCO_3^- + 3H_2$	Acetate	+76.1
Butyrate	$CH_3CH_2CH_2COO^- + 2H_2O \rightarrow 2CH_3COO^- + H^+ + 2H_2$	Acetate	+48.1
Lactate	$CH(CHO)_2CO^- + 2H_2O \rightarrow CH_3COO^- + H^+ + HCO_3^- + 2H_2$	Acetate	-4.2

The acetogenic bacteria are slow growing, organic loading, temperature and pH sensitive bacteria (Parawira, 2004). For this bacteria to thrive, a hydrogen partial pressure is required for acetic acid conversion (Bitton, 2005). Therefore, hydrogen monitoring of the system can be used as an indicator for the performance of an anaerobic digester.

Hydrogen has been recognised as a controlling factor in the anaerobic digestion process (Archer *et al*., 1986). If the partial pressure of the hydrogen becomes too high, the acetate conversion is reduced and the substrate is converted back into propionic acid, butyric acid and ethanol rather than the desired product, methane (Bitton, 2005; Gerardi, 2003). Methanogens help to keep the hydrogen tension low as required by the acetogenic bacteria.

d. Methanogenesis

During the methanogenesis step, methanogens use H_2, CO_2 and acetic acid to form methane and carbon dioxide (Bitton, 2005). The methanogens are broken up into two sub-categories and their reactions are shown in Table 2-3 below:

Stellenbosch University https://scholar.sun.ac.za

- Hydrogenotrophic methanogens – these convert hydrogen and carbon dioxide into methane
- Acetotrophic methanogens – these convert acetate into methane and carbon dioxide

Table 2-3: Methanogenic reactions (adapted from Bitton (2005) and Parawira (2004))

Methanogenic reaction	Main product	ΔG^0 [kJ]
$CO_2 + 4H_2 \rightarrow CH_4 + 2H_2O$	Methane	-135.6
$CH_3COOH + H_2O \rightarrow CH_4 + CO_2 + H_2O$	Methane	-31.0

About 70% of methane is produced from acetic acid (Solera *et al*., 2002). However, the hydrogen pathway is more energy yielding in the process as it produces a biogas with a higher methane content. The hydrogen pathway is not rate limiting when the hydrogen partial pressure is kept low in the system.

The anaerobic digestion process can become unstable when the hydrogen partial pressure increases. This will lead to an accumulation of VFAs and a decrease in pH. Consequently this inhibits pH sensitive methanogens, thereby, resulting in a failure of the anaerobic digestion process (Parawira *et al*., 2007). When the pH of the system is reduced, the hydrogen partial pressure increases.

Acetotrophic methanogens growth rate is lower than that of hydrogenotrophic methanogens which could lead to an accumulation of hydrogen and the subsequent reverse reaction of acetic acid to propionic acid (Gerardi, 2003).

2.1.2. Process parameters that control anaerobic digestion

Several environmental factors affect the growth rate of anaerobic bacteria. Several of these factors can be controlled or measured to ensure growth of anaerobic bacteria (Chernicharo, 2007). These include:

- Temperature
- pH, alkalinity and VFAs
- Organic loading rate and hydraulic retention time
- Solid and hydraulic retention time
- Presence of inhibitory substances
- Oxidation reduction potential

Stellenbosch University https://scholar.sun.ac.za

a. Temperature

Microorganisms cannot control the internal temperature of the cell. Consequently their temperature is determined by the ambient temperature directly around the cell (Gerardi, 2003). Therefore, it is important to maintain the temperature of the digester to ensure stable operation.

Anaerobic bacteria is broken up into three temperature ranges within which they can operate (Gerardi, 2003):

- Psychrophilic bacteria: 5 – 25°C
- Mesophilic bacteria: 20 – 45°C
- Thermophilic bacteria: 50 – 122°C

Outside the above mentioned temperature ranges, the bacteria for that specific group cannot grow. Increasing the temperature for methanogens outside its operating range can lead to the bacteria being killed. However, the other groups of anaerobic bacteria often only become dormant and will return to the proper state if the environmental conditions are favoured for its growth (Chen *et al*., 2009; Liu *et al*., 2014). This is shown with anaerobic bacteria being heat treated to kill the methanogens so that it can be used to operate a digester for bio-hydrogen production.

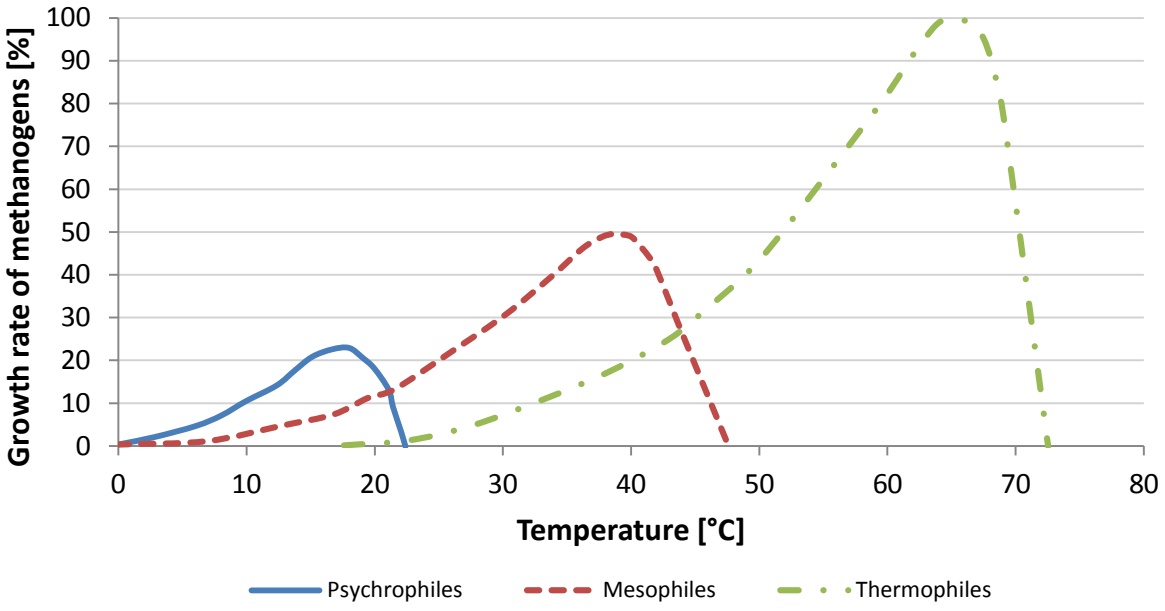

Figure 2-2: Temperature effect on the methanogenic biomass growth rate (redrawn from Chernicharo (2007))

The specific growth rate for each temperature range varies across the temperature band (Chernicharo, 2007). For each type of bacteria, the growth rate increases until it reaches a maximum. Thereafter, the

Stellenbosch University https://scholar.sun.ac.za

growth decreases sharply as the temperature increases. The effect of temperature on the three types of methanogenic bacteria can be seen below in Figure 2-2. Anaerobic digesters are often operated just below the maximum growth rate to allow for temperature variations within the reactors without greatly affecting the methanogenic bacteria growth rate. Acetotrophic methanogens is more sensitive to temperature change than hydrogenotrophic methanogens (Chernicharo, 2007).

Due to the methanogenic growth rate, full scale anaerobic digesters operate in three temperature ranges, namely (Chernicharo, 2007):

- Ambient temperature: 20 – 25°C
- Mesophilic temperature: 30 – 37°C
- Thermophilic temperature: 50 – 55°C

The conversion rates of bacteria increases with increased operating temperature, however, the stability of the process decreases (Fannin, 1987). In other words, a thermophilic digester is more temperature sensitive and less stable than a mesophilic digester. Thermophilic digesters were found to only tolerate a ±0.8°C change in operating temperature compared to a mesophilic digester operating with higher VFAs concentration (Fannin, 1987). This temperature sensitivity makes temperature control difficult in large systems due to the temperature gradients as a result of localised heating or cooling. The difficulty with sensitive temperature control of a thermophilic digester gives preference to rather operate a digester under mesophilic conditions.

In ambient and mesophilic operating ranges, the digestion process cannot kill pathogens and longer retention times are required of up to 32 days (Bitton, 2005) for low rate anaerobic digester systems.

Within the mesophilic temperature range there are two optimal temperatures for anaerobic digestion. The acidogenic bacteria have an optimal temperature of 30°C whereas the methanogens prefer 35°C (Gerardi, 2003). Methanogens can cause an anaerobic digester to fail due to not consuming acetic acid fast enough. Therefore, it would be preferred to operate the digester at a temperature that is favourable for methanogens.

b. pH, alkalinity and volatile acids

Alkalinity, volatile fatty acids (VFAs) and pH are closely related to each other and are important control parameters to ensure stable operation of an anaerobic digester. The optimum growth rate of anaerobic bacteria is greatly dependent on the system's pH.

Stellenbosch University https://scholar.sun.ac.za

Methanogens have a wide pH operating range of 6.0 - 8.0 within in which stability can be achieved. However, the optimum pH for methanogens growth is between 6.6 and 7.4 (Chernicharo, 2007). Outside the pH range of 6.0 - 8.0, methanogens become inhibited.

The optimum growth rate for acidogenic bacteria occurs in a pH range of 5.0 - 6.0 (Chernicharo, 2007). In this pH range, VFAs will be produced, however, methane formation is unlikely. The production of VFAs results in a natural pH reduction, provided there is not sufficient buffering capacity in the digester. To reduce the risk of the process failing, pH control is required or alkalinity needs to be added to the digester.

Anaerobic digesters can be operated in the acid-phase where they are operated at a pH below 5.5 to promote biohydrogen production and prevent methane production (Wu *et al*., 2010; Yu *et al*., 2002; Zhu *et al*., 2009). However, this results in an accumulation of VFAs in the effluent of the anaerobic digester.

Wang *et al.* (2009) investigated whether acetic acid, propionic acid, butyric acid and ethanol could have an inhibitory effect on methanogenic bacteria in an anaerobic digester. They found that acetic acid, butyric acid and ethanol at concentrations of 2400, 1800 and 2400 mg/ℓ, respectively, showed no significant inhibition. However, propionic acid showed significant methanogenic inhibition at concentrations above 900 mg/ℓ. This supports the fact that butyric acid formation instead of propionic acid formation from monosaccharides should be favoured.

The alkalinity of an anaerobic digester is the capacity of the system to buffer a change in the pH. Alkalinity is mainly related to carbonic acid and volatile acids (Metcalf & Eddy, 2003). The carbonic acid is formed when carbon dioxide is released in the anaerobic digestion process and then dissolved into the water. Calcium, magnesium and ammonium bicarbonate are buffering substances which are found in anaerobic digesters. In the digestion process, ammonium bicarbonate is used in the process when proteins in the feed sludge are broken down (Metcalf & Eddy, 2003). For small scale systems, alkalinity can be increased in the system by adding sodium carbonate or ammonia bicarbonate. Whereas, lime is used to adjust pH for most large scale systems due to its low cost (Metcalf & Eddy, 2003). Some studies have indicated that it is important to check the bicarbonate alkalinity as it is the only usable alkalinity to neutralise VFAs (Colmenarejo *et al*., 2004; Lee, 2008).

A two point titration of the effluent can be used to determine the partial (PA), intermediate (IA) and total alkalinity (TA). The Ripley ratio is equivalent to the IA divided by PA (Ripley *et al.*, 1986). Essentially this provides a ratio of VFAs to bicarbonate in the system. Generally if the Ripley ratio is below 0.3, the continuous anaerobic digester process is stable, however, some plants have had ratios below 0.8 and

Stellenbosch University https://scholar.sun.ac.za

were still stable (Drosg, 2013). In a batch system, the Ripley ratio will be time dependent. It is important to define the end points of the titration that is used to determine the IA and PA. Generally, the first titration point is pH 5.75 and the second point is pH 4.3 or pH 4.5 (Drosg, 2013; Du Preez, 2010).

c. Toxic material and inhibitory compounds

A review article by Chen *et al.* (2014) identified and explained the mechanisms through which compounds have an inhibitory or toxic effect on anaerobic digestion. These compounds include:

- Chlorophenols
- Halogenated aliphatics
- Long chain fatty acids
- Ammonia
- Sulphide
- Heavy metals

Chlorophenols is a group of chemicals produced when adding chlorine to phenol which is used in pesticides (Chen *et al.*, 2014). Therefore, they can find their way into winery wastewater.

Nitrogen, in the presence of free amino nitrogen, ammonia and ammonium, is an important nutrient to ensure successful fermentation for wine production (Conradie *et al.*, 2014). Free ammonia (NH_3) diffuses through cell membrane faster, causing a proton and/or K^+ deficiency when compared to ionised ammonium (NH_4^+), therefore, making it more toxic (Chen *et al.*, 2014). At 35°C and pH 7.0, nitrogen will be in the NH_4^+ form, however, increasing the pH above 7.4, this will start to rapidly convert to NH_3 (Gerardi, 2003). Therefore, operating the digester at pH 7.0, ammonia toxicity can be avoided. However, ammonia concentrations below 200 mg/ℓ can be used as a nitrogen source for the growth of anaerobic bacteria.

Sulphur dioxide (SO_2) is used in winemaking as an antimicrobial agent. Sulphate reducing bacteria (SRB) compete with acetotrophic methanogens for acetate as a substrate to form hydrogen sulphide gas (H_2S) with the use of sulphate (Gerardi, 2003). Kinetic studies have shown that SBRs generally have higher growth rates and higher affinity for substrate than acetotrophic methanogens in an environment where sulphate supply is not limiting (Bitton, 2005). A summary of these reactions is provided in Table 2-4. Sulphate has a low inhibitory effect on methane forming bacteria, however, the H_2S gas formed passes through the bacterial cell wall and attack the enzyme systems within the cell (Gerardi, 2003).

Stellenbosch University https://scholar.sun.ac.za

Table 2-4: Sulphate consumption reactions by sulphate reducing bacteria

SRB reaction
$SO_4^{-2} + 4H_2 \rightarrow H_2S + 2H_2O + 2OH^-$
$SO_4^{-2} + CH_3COOH \rightarrow H_2S + 2HCO_3^-$

d. Nutrient requirements

The two macronutrients required for anaerobic bacteria is nitrogen and phosphorous and the feed nutrient ratio is often presented as COD:N:P (Gerardi, 2003). The minimum recommended nitrogen and phosphorous required for an anaerobic digester is 4% and 1%, respectively of the COD fed.

Micronutrients such as cobalt, iron, nickel and sulphur are required at less than 0.2% of the COD fed (Gerardi, 2003). Although SRB uses sulphur to form H_2S, it is still required as a micronutrient to assist cell growth.

e. Oxidation reduction potential

Using oxidation-reduction potential (ORP) in an anaerobic digester provides a nett measurement of the relative amount of oxidised and reduced compounds (Gerardi, 2003). A summary of the favoured cellular activity based on ORP measurements can be found below in Table 2-5. This provides a simple way to check whether an anaerobic digester is operating correctly or whether there are problems with it and operational adjustments are required.

Table 2-5: Summary of cellular activity with oxidation reduction potential measurements (Modified from Gerardi (2003))

Approximate ORP measurement [mV]	Carrier molecule for organic compound degradation	Digester operating conditions	Respiration process
> +50	O_2	Oxic	Aerobic
+50 to -50	NO_3^- or NO_2^-	Anaerobic	Anoxic
< -50	SO_4^{-2}	Anaerobic	Fermentation; sulphate reduction
< -100	Organic compounds	Anaerobic	Fermentation; mixed acid production
< -300	CO_2	Anaerobic	Fermentation; methane production

Stellenbosch University https://scholar.sun.ac.za

It should be noted that the respiration process at a specific ORP is the favoured process, but does not mean that the others cannot occur at that measurement. Archilha *et al*. (2010) measured ORP values between -400 and -450 mV for the effluent from an ASBR while treating synthetic domestic wastewater containing sulphates.

Wang *et al*. (2006) found that an ORP value of less than -150mV should be avoided to prevent propionic acid-type fermentation. Khanal and Huang (2003) found that an increase in ORP from -280mV to -180mV results in an increased yield of methane for an anaerobic digester. Lee (2008) found that the operating range of ORP measurements should be between -390mV and -310mV for maximum VFA production (hydrogen as the main biogas) and minimum methane production within an anaerobic digester.

2.1.3. Biogas production and methane potential

Biogas production is an important indicator for the performance of an anaerobic digester. The biogas produced is mainly composed of about 60-70% CH_4 and 30-40% CO_2 (Metcalf & Eddy, 2003). Along with these two components, trace amounts of H_2, H_2O, N_2 and H_2S are also formed depending on the feed substrate, sludge composition and operating conditions.

The methane yield provides an indication of the nett energy recovery of the process. It is defined as the volume methane produced per COD removed per volume of wastewater fed to the reactor per day as presented in Eq. 2-1:

$$Y_{CH_4} = \frac{Q_{CH_4}}{Q_F(COD_{in} - COD_{out})} \qquad \textbf{Eq. 2-1}$$

The maximum theoretical methane yield at STP that can be produced from glucose is 0.35 ℓ.g-$COD^{-1}_{removed}$ (Chernicharo, 2007). This value is used to design large scale anaerobic digesters, however, a more conservative methane yield of 0.2 ℓ.g-$COD^{-1}_{removed}$ is expected for operational digesters (Metcalf & Eddy, 2003). Deviations from the maximum yield can be caused by gas leaks or change in composition of the feed substrate.

2.2. Anaerobic sequencing batch reactor process overview

The anaerobic sequencing batch reactor (ASBR) process is a four stage process that uses anaerobic biomass to reduce the organic concentration of the wastewater being treated within a single reactor vessel (Chernicharo, 2007). This is a discontinuous process as it treats a batch at a time as shown in Figure 2-3. The four stages that make up the ASBR process are:

Stellenbosch University https://scholar.sun.ac.za

1. Feed
2. React
3. Settling
4. Decant

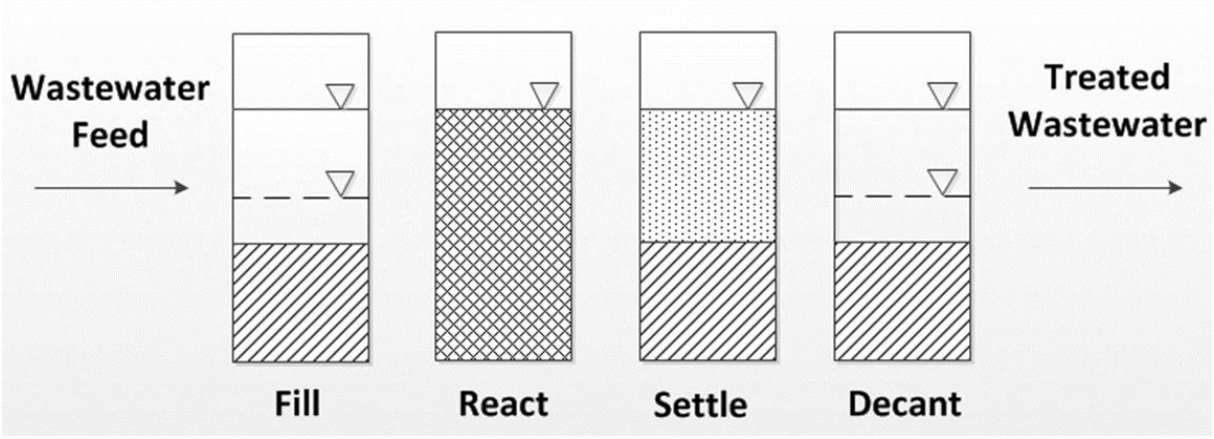

Figure 2-3: Four stages that make up the ASBR process

2.2.1. Feed stage

The feeding stage is considered to be the time the that ASBR is fed until it is full (Chernicharo, 2007). There is no specific required feed flow rate of the wastewater into the ASBR. However, a higher flow rate into the ASBR will result in improved initial mixing in the reactor. Consequently, there is an increase in liquid mass transfer between the wastewater and biomass. It is important to not allow oxygen into the ASBR during this stage of the process as it could have a negative effect on the anaerobic bacteria.

Various feed strategies are used for ASBRs. The feed strategies can be either batch or fed-batch. An increase in feed time, results in low initial substrate concentrations, thereby, avoiding initial organic overloading (Archilha *et al.*, 2010). Fed-batch feeding allows a higher organic loading rate (OLR) operation whilst reducing the effect possible substrate overload.

2.2.2. React stage

The react stage generally forms the longest stage of a batch-fed ASBR, therefore, it is considered to be the stage where anaerobic digestion process occurs (Chernicharo, 2007).

The contents of the reactor need to be mixed to increase the contact between the organic wastewater and the biomass (Pinho *et al.*, 2004; Zaiat *et al.*, 2001). During the react stage, the reactor contents can be mixed intermittently or continuously. Mixing can occur by three different methods, namely, gas or

Stellenbosch University https://scholar.sun.ac.za

liquid recycling or mechanically. The mixing must be such that the biomass remains in suspension to promote mass transfer (Pinho *et al*., 2005). Efficient mixing reduces temperature, pH and organic matter gradients throughout the reactor (Degrémont, 2007).

The duration of the react stage is determined by the characteristics of the wastewater, desired quality of effluent, concentration of biomass and temperature of the ASBR process (Metcalf & Eddy, 2003).

2.2.3. Settling stage

During this stage, the mixing of the reactor is stopped to allow the biomass in the reactor to settle. This stage of the process allows the reactor to perform as a clarifier, consequently, removing the need for an additional clarifier in the process (Metcalf & Eddy, 2003).

During this stage the anaerobic digestion reactions continue, which could cause a change in the pH of the process. However, the operation of the ASBR should be such that very little VFA formation should occur during this stage. Nonetheless, *in-situ* pH control should not occur to prevent pH gradients from forming in the reactor during this stage.

The time required for this step is dependent on the biomass settling characteristics (Zaiat *et al*., 2001). Therefore, granular biomass is preferred to enhance the settling of the biomass during this stage of the process.

2.2.4. Decant stage

This volume that is drained is dependent on the HRT (Hydraulic retention time) and operating volume of the ASBR (Metcalf & Eddy, 2003). This volume that is decanted is the same as the volume that is fed into the reactor during the feed stage of the process.

A gas bag or equaliser tank should be used to equalise the pressure in the ASBR when the liquid contents of the reactor is removed. This will aid in the prevention of oxygen from entering the system and prevent the ASBR vessel from imploding.

Stellenbosch University https://scholar.sun.ac.za

2.3. Factors influencing the performance of the ASBR process

The performance of an anaerobic digestion process is measured in several different ways depending on the treatment requirement is. The main measurable variables for assessing the performance of an anaerobic digester are:

- COD reduction
- Methane yield
- Biogas composition
- Biogas production volume
- Effluent alkalinity

More complex variables can also be measured such as individual VFA concentrations, nutrient concentration, sludge composition, etc.

The design variables affecting ASBR performance are:

- Mixing strategy
- Feeding strategy
- Biomass granulation
- Operating temperature
- Operating pH
- Organic loading rate
- Hydraulic retention time
- Geometric characteristics of the ASBR
- Food-to-microorganism ratio

2.3.1. Mixing strategy

The contents of an ASBR is mixed to promote mass transfer between the sludge and compounds within the liquid being treated (Dague, 1993). Mixing can occur via biogas circulation, liquid circulation or mechanical agitation. Furthermore, the mixing can also occur continuously or intermittently. The mixing required for a specific ASBR is dependent on the type of sludge and ASBR geometric conditions.

Intense mixing can cause granular sludge to rupture (Zaiat *et al.*, 2001). Intense gas recycling has been reported to result in high foam generation (Angenent and Dague, 1996).

Stellenbosch University https://scholar.sun.ac.za

2.3.2. Feeding strategy

The ASBR can be fed in a batch method or fed-batch method (Dague, 1993). In the batch method, the reactor is filled in a short time period. With the fed-batch method, the reactor can be fed over a long period until it is full or have a portion filled quickly and the remainder filled slowly.

Under fed-batch operation, the react phase time is reduced in order for the cycle time to remain constant. A fed-batch system is believed to reduce concentration spikes of certain components which could lead to inhibition of certain groups of bacteria within the biomass. This inhibition would be dependent on the activity of the biomass as well as the substrate composition.

Cheong and Hansen (2008) determined that fed-batch operation allowed for higher OLRs before the ASBR was overloaded resulting in process failure.

2.3.3. Biomass granulation

Biomass granulation occurs when various bacteria groups agglomerate with each other to form a granule. Granulation improves the activity of the sludge as well as improves the settling characteristics of the sludge (Wirtz and Dague, 1996). With granulation, the methanogens sit towards the core of the granule. This improves the methanogens activity by protecting it from pH and temperature variations.

The biggest problem with granulation is that it can take up to 300 days to occur (Sung and Dague, 1995). Intense mixing can contribute to granular sludge disintegrating which leads to sludge floating towards the liquid surface of the ASBR (Du Preez, 2010).

2.3.4. Food-to-microorganism ratio

The food to microorganism ratio (F:M) is a ratio of the substrate (food) to the amount of sludge in the digester. During a batch fed ASBR process, the F:M ratio is high when the ASBR is filled, however, the F:M ratio decreases as the digestion process continues as indicated in Figure 2-4.

Stellenbosch University https://scholar.sun.ac.za

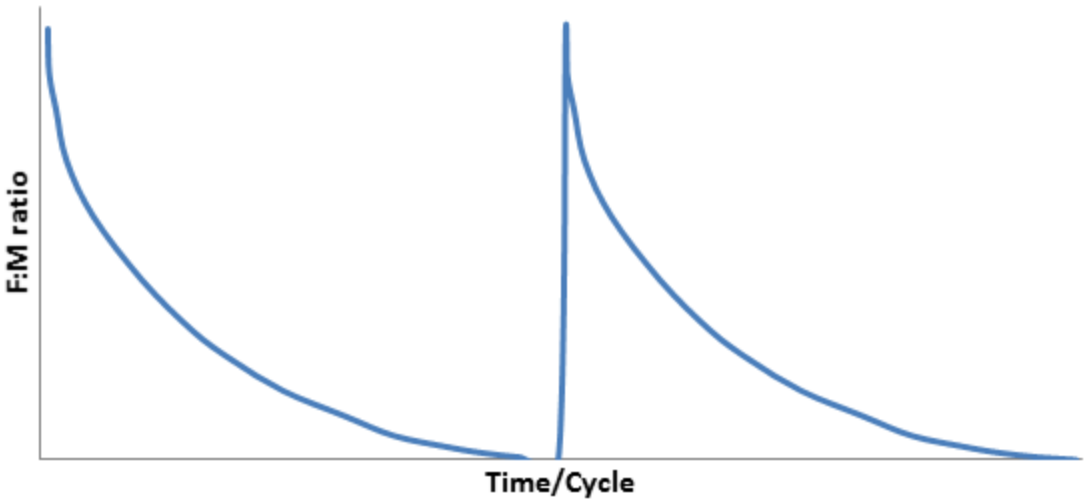

Figure 2-4: Illustration of the effect of batch feeding on F:M ratio throughout the batch

When feeding the ASBR under fed-batch conditions, the initial F:M ratio is lower and prevents inhibition of certain bacteria groups due to excessively high concentrations of certain components. As mentioned earlier, an important concentration to keep low is the propionic acid concentration which can lead to the inhibition of methanogens. If the conditions are such that propionic acid formation is favoured, fed-batch should rather be used.

2.3.5. Summary of studies on ASBRs

Table 2-6 provides a tabulated summary of studies performed on mesophilic ASBR and anaerobic sequencing batch biofilm reactor (ASBBR). Due to the temperature sensitivity of thermophilic digesters, mesophilic digesters were rather investigated. The aim was to consider ASBR systems that treated winery wastewater or wastewater that contained organic components found in winery wastewater.

The studies that used winery and brewery wastewater that lead to the high formation of VFAs indicated that pH good control is needed on the ASBR (Donoso-Bravo *et al*., 2009.; Ruíz *et al*., 2002; Xiangwen *et al*., 2008). While Ruíz *et al.* (2002) experienced a COD reduction of 98%, Farina *et al.* (2004) at times only achieved COD reductions as low as 45%.

The volumetric discharge fraction (VDF) is the quotient of the volume removed with each batch and the total working volume of the ASBR. Archilha *et al*. (2010) and Ramos *et al*. (2003) found that an ASBR can be operated with continuous liquid recirculation for mixing while operating at a volumetric displacement fraction (VDF) of 0.5 and 0.4, respectively.

Stellenbosch University https://scholar.sun.ac.za

Table 2-6: Summary of ASBR studies for methane production on winery or similar wastewater

Substrate and (main COD fraction)	Reactor type	Working Volume [L]	VDF	Mixing	Temperature [C]	OLR g-COD_{feed}. ℓ^{-1}_{ASBR}.day^{-1}	COD reduction [%]	Biogas composition	Methane yield	pH control	Measured dynamic data	Source
Winery wastewater (80% EtOH)	ASBR (batch)	5	0.18	Mechanical mixing	35	8.6	>98	N/A	N/A	25% $NaOH$	Biogas production rate, pH, COD and VFA concentration	Ruíz *et al*. (2002)
Synthetic winery wastewater (Glucose)	ASBR	5	N/A	Mechanical mixing	35	N/A	N/A	N/A	N/A	$NaHCO_3$	N/A	Donoso-Bravo *et al*. (2009)
Brewery wastewater (N/A)	ASBR (Batch)	45	0.33	Mechanical mixing (150 rpm)	33	1 - 6	90%	N/A	N/A	$NaHCO_3$	COD, VFA, Biogas production	Xiangwen *et al.* (2008)
Winery wastewater (N/A)	ASBR	180	0.1	Sludge recycling	35	3 - 4	45 - 95%	50-80% CH_4 20-50% CO_2	0.3-0.35	N/A	N/A	Farina *et al.* (2004)
Olive mill wastewater (N/A)	ASBR	2	N/A	Mechanical mixing	30	5.3	53-83%	N/A	N/A	N/A	N/A	Ammary (2005)
Synthetic domestic wastewater (42% meat extract)	ASBBR (batch)	1.2	0.4	Continuous liquid recirculation (0 - 6.75 $\frac{m^3}{m^2 \cdot h}$)	30	1.25	72 - 87%	55% CH_4, 45% CO_2	N/A	N/A	N/A	Ramos *et al*. (2003)
Synthetic domestic wastewater (42% meat extract)	ASBBR (batch and fed-batch)	1.2	0.5	Continuous liquid recirculation (9.07 $\frac{m^3}{m^2 \cdot h}$)	30	1.5, 4.5	48 - 95%	N/A	N/A	N/A	N/A	Archilha *et al.* (2010)

Stellenbosch University https://scholar.sun.ac.za

2.4. Anaerobic digestion model no.1

The ADM1 is a generalised dynamic representation of the biochemical and physiochemical processes that occur during anaerobic digestion (Batstone *et al.*, 2002). This model was developed by the International Water Association (IWA) anaerobic digestion modelling task group in order to achieve a unified basis for anaerobic digestion modelling. A complete description of the ADM1 can be from published technical report (IWA Task Group for Mathematical Modelling of Anaerobic Digestion Processes, 2002) and only critical functionalities are highlighted here.

The anaerobic digestion pathways that are modelled is the same as that in Figure 2-1. The biochemical processes include:

1. disintegration of particulates and inactive biomass to carbohydrates, proteins and lipids;
2. hydrolysis of those products to monosaccharides, amino acids and LCFA;
3. acidogenesis from monosaccharides and amino acids to form VFAs and hydrogen;
4. acetogenesis of LCFA and VFAs to acetate;
5. methanogenesis from acetate, H_2 and CO_2; and
6. death of various bacteria groups to form particulates.

A generic mass balance for the individual liquid or particulate (biomass) components is presented in Eq. 2-2. As presented here, the differential equation allows for variable liquid volume system to be modelled.

$$\frac{dVS_{liq,i}}{dt} = q_{in}S_{in,i} - q_{out}S_{liq,i} + V\sum_{j=1-19}\rho_j\nu_{i,j} \qquad \textbf{Eq. 2-2}$$

ADM1 can be implemented either as a differential and algebraic equation (DAE) set, or as differential equations (DE) only. In the DAE set, acid-base transfer is modelled with algebraic equations, while DE implementation uses kinetic rate equations for the prediction of acid-base pairs. Along with the acid-base reactions, inorganic cations and anion concentrations can be used to determine the pH of the liquid.

The substrate uptake of bacteria is modelled through Monod-type kinetics while the death of biomass is determined with first order kinetics. Furthermore, the growth of biomass is implicit within the substrate uptake function. Inorganic carbon is used as the carbon source catabolism while allows a carbon balance to be performed with the ADM1.

Stellenbosch University https://scholar.sun.ac.za

Inhibitions functions can easily be added to the kinetic equations. The inhibition functions included in the standard ADM1 are:

- pH inhibition for all bacteria groups;
- hydrogen; and
- free ammonia.

The physiochemical equations describe:

- liquid-liquid reactions – Rapid ion association and dissociation;
- gas-liquid transfers – CH_4, CO_2, H_2 and H_2O; and
- liquid-solid transfer – Precipitation and solubilisation of ions.

Liquid-liquid transfer forms an important part of the model as it is used to determine the pH which is subsequently used for the inhibition functions. Gas-liquid transfer is used to determine pressure and gas flow from the system. Liquid-solid transfer is not always modelled with the ADM1 as it increases the computing power needed, however, it is important for systems with high levels of cations (Mg^{2+} and Ca^{2+}) which readily form carbonate precipitants.

Studies have been performed to add digestion pathways to the standard ADM1 which include:

- ethanol degradation (Batstone *et al.*, 2004);
- sulphate reduction (Barrera *et al.*, 2015);
- phenolic compounds degradation (Fezzani and Cheikh, 2009); and
- nitrate reduction processes (Tugtas *et al.*, 2006).

2.5. Summary

Winery wastewater has a wide COD and pH range. The main components that make up winery wastewater are components that can be consumed by anaerobic digestion bacteria via the acidogenesis, acetogenesis and methanogenesis phases.

Temperature and pH control is important for stable ASBR operation. This needs to be corrected as quickly as possible when it is not at the desired set point. Potassium hydroxide or sodium hydroxide can be used for pH correction of lab scale systems when the pH is too low. The operational conditions of the ASBR should favour the methanogens requirements as they are the most sensitive to environmental changes. Methanogens generally operate in the pH range of 6.6 to 7.4. Acidogens have been found to favour a pH around 6.0 as determined by operating ASBRs for hydrogen production.

Stellenbosch University https://scholar.sun.ac.za

The mixing of the ASBR should not be too intense as to avoid sludge disintegration, however, it should be sufficient to promote mass transfer. Mixing is dependent on the ASBR geometric characteristics as well as the substrate being treated. Intermittent mixing uses less energy per treated batch. Mechanical agitation and liquid recycling are the simpler methods to use for agitation in the ASBR. With liquid recycling it is easier to ensure the system is sealed to avoid gas leaks as compared to mechanical agitation.

The ADM1 sets high demands on available process power and requires a large number of variables to specify conditions of the simulated anaerobic digester. The pH is calculated with a charge balance between cations, anions, ammonium, bicarbonate, acetate, propionate, butyrate, valerate and hydrogen ion. Adjustment of cation and anion concentrations can be used to simulated pH control. The bicarbonate concentration can also be adjusted by the method can become more complex as the bicarbonate itself is a by-product formed in the anaerobic digestion process.

Stellenbosch University https://scholar.sun.ac.za

Chapter 3 - Materials and methods

3.1. Experimental approach

This study was performed in two parts. The first part of the study was done to test whether the mesophilic ASBR can be operated solely on *in-situ* pH control while treating synthetic winery wastewater. During this stage, no alkalinity was added to the ASBR in any way. This part provides an answer for research objective two as stated in Chapter 1.2. A summary of experimental conditions can be seen in Table 3-1. Within, the first part, two different inoculations of the same sludge but different synthetic winery wastewater was used. The type A wastewater recipe, with a concerning high ammonium sulphate concentration, was used as reported by Malandra *et al.* (2003). Type B contained no ammonium sulphate. The ammonium sulphate was removed to reduce the possible inhibition caused by H_2S formed by the sulphate reducing bacteria.

Table 3-1: Summary of long term ASBR operation experiments for part 1

Inoculation	**1**	**2**
Batches	1 - 109	110 - 194
Initial granular sludge volume [ℓ]	2	2
pH dosing solution	2-4 M KOH	4 M KOH
Winery wastewater	Type A (batches 1 – 30) Type B (batches 31– 109)	Type B
Organic Loading Rate $\left[\frac{gCOD}{\ell \cdot day}\right]$	Type A: 1.0 - 2.3 Type B: 1.3 - 3.0	1.2 – 3.0
Volumetric displacement fraction (VDF)	0.5	0.5

The aim of the second part of the study was to evaluate the variation in the dynamic conditions within the ASBR when the pH of the winery wastewater fed to the ASBR was altered and *in-situ* pH control was performed. This was to answer research objective number three as stated in Chapter 1.2. KOH was both used to alter the feed substrate pH as well as for the in-situ pH control system. An additional experimental set was performed to determine the effect that additional alkalinity in the feed substrate had on the *in-situ* pH control and consequent performance of the ASBR. These groups of experiment were all performed with the same sludge. A summary of the difference in pH levels tested can be found in Table 3-2. Experiment sets 1 – 4 formed part of the results of inoculation 2 in part 1. Whereas, the

Stellenbosch University https://scholar.sun.ac.za

results of experiment set 5 was not included in the long term operation results of part 1. The effect of online measured pH, ORP, gas production for part 2 will discussed in Chapter 6.

Table 3-2: The variation in the feed substrate conditions for experiments performed in part 2

Experiment	**1**	**2**	**3**	**4**	**5**
Feed pH	4.3	6.0	7.4	8.5	7.3
Added KOH [mg/ℓ]	0	266	333	377	322
Added $NaHCO_3$ [mg/ℓ]	0	0	0	0	2870
OLR [$g_{COD}.ℓ^{-1}.day^{-1}$]	2.9	2.9	2.9	2.9	2.9

3.2. ASBR setup and operating variables

Figure 3-1 provides a schematic of the ASBR setup used in this study along with a summary of the ASBR specifications in Table 3-3.

Table 3-3: Specifications of the used ASBR in this study

Parameter	**Specification**
Operating temperature	35 °C
Total ASBR volume	14.6 ℓ
Working volume	14.1 ℓ
Gas bag volume	10 ℓ
Reactor height	500 – 530mm (mean height 515mm)
Reactor internal diameter	190 mm
Reactor L/D ratio	2.7
Total equaliser gas bag volume	10 ℓ
Mixing type	Liquid recirculation
Maximum mixing flow rate	8.6 ℓ/min
Calculated upward flux	18.6 $\frac{m^3}{m^2 \cdot h}$

Stellenbosch University https://scholar.sun.ac.za

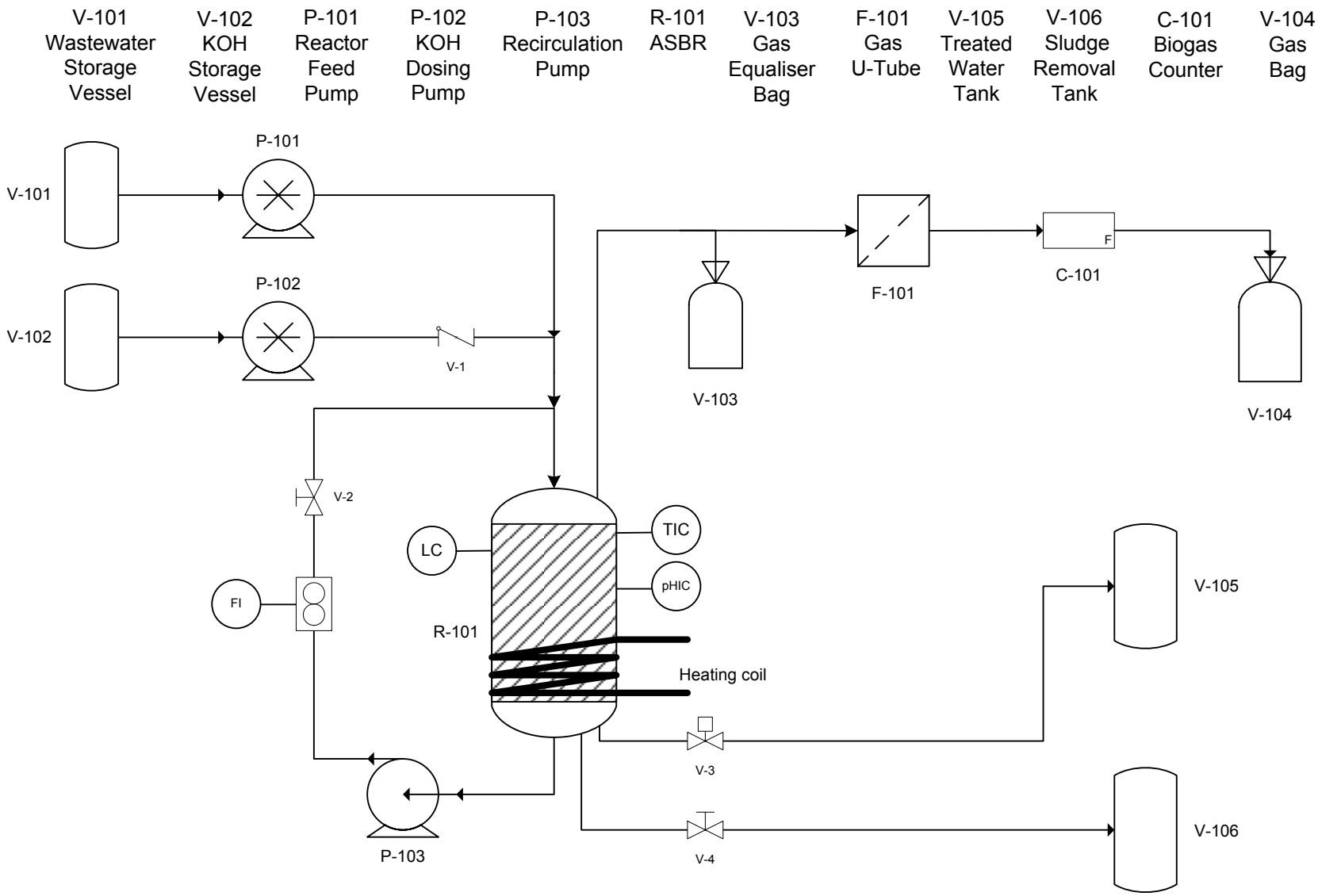

Figure 3-1: Process flow diagram of the experimental lab scale ASBR setup

Stellenbosch University https://scholar.sun.ac.za

The ASBR consisted of a cylindrical glass tube, a HDPE top and conical HDPE base as built by Smit (2013). The system was automated with a custom built and programmed PLC control panel with the assistance of the workshop staff at the Department of Process Engineering at Stellenbosch University. Modifications were made to the original system of Smit (2013). This included the addition of a paddle wheel flow meter, bubble counter, ORP and EC probes, and simplification and improvement of the PLC programming for improved control and data logging capabilities.

Synthetic winery wastewater was fed to the ASBR with a peristaltic pump until the liquid level in the ASBR reached the high level probe. Once the liquid reached the high level probe, the system would move over to the react phase and immediately begin with the first mixing cycle. When the predetermined react phase was over, the settling stage would begin. During the settling phase no mixing and no in-situ pH control occurred. Thereafter, the decant phase would start and the ASBR would drain under gravity until it reaches the required height to achieve a VDF of 0.5.

The approximate times used for each phase of the ASBR operation can be found in Table 3-4. Preliminary investigations determined that biogas was still being produced during the 12 – 24 hour period of a cycle. Therefore, a batch length of 24 h was chosen. A batch feeding regime was used to feed the ASBR, therefore, the feed time was a short a possible. The settling stage was selected to be 60 minutes to ensure as little as possible washout of sludge during the decant phase. The decant time of 5 min ensured that half of the ASBR was drained during every batch.

Table 3-4: Approximate ASBR operation phase times

Feed time	15 min
React time	22h 40 min
Settling time	60 min
Decant time	5 min

The ASBR was operated with a set point temperature of 35°C and a pH of 7.0. As pH dosing could only occur during mixing, the system had to be mixed often to prevent pH gradients and ensure valid pH, ORP and EC data being logged. A preliminary investigation to the pH dosing response conclude that a 60 seconds dead time was measured between the time the ASBR was dosed and a pH change was measured by the pH probe in the ASBR. Therefore, the mixing time had to be longer than the dead time. A cycle of 2 min mixing and 8 min of no mixing was selected to occur during the react stage of the ASBR.

Stellenbosch University https://scholar.sun.ac.za

The temperature of the ASBR was controlled within 0.5°C of the set point. The heating of the ASBR was performed by wrapping heat tracing around the outside of the glass tube. Insulation was added to ensure heat transfer into the ASBR.

The pH control of the system only allows dosing so that the pH is increased to at least 0.1 below the set point pH. *In-situ* dosing was such that it only dosed once every one minute while mixing when required. This is due to the dead time from when the system is dosed until the pH probe recognises a change in pH. The amount dosed was approximately 4 mℓ at a time. The volume of the amount of KOH dosed was determine by dosing from a measuring cylinder. For the first inoculation with type A wastewater, 2 M KOH was used for pH control to avoid high pH levels in the ASBR. For type B wastewater, a 4 M KOH solution was used for all required pH control.

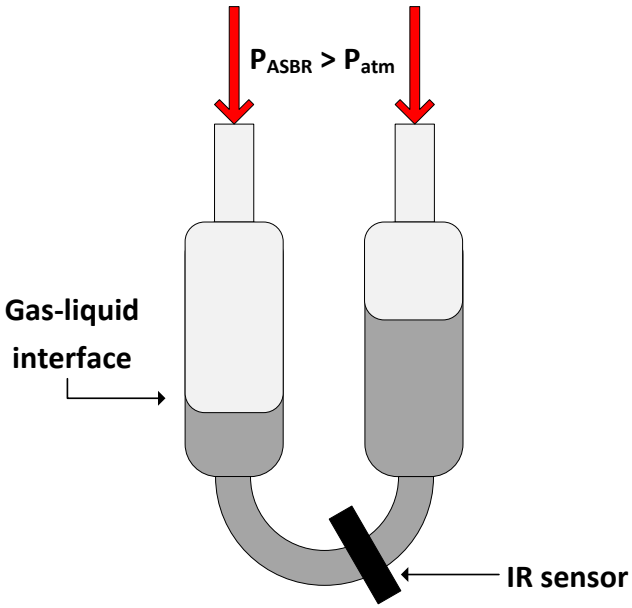

Figure 3-2: A schematic of the working principle of the bubble counter used with the ASBR

A bubble counter, Figure 3-2, was used to determine the biogas production during the anaerobic digestion process. The bubble counter functions uses a moving liquid interface due to a differential pressure caused by biogas production in an ASBR. As the pressure inside the ASBR increased (P_{ASBR}), due to biogas production, the water within the U-tube would be pushed towards the low pressure side (open end to the atmosphere, P_{atm}). When the water passes far enough around the bottom of the U-tube, a bubble is released and the water flows back. The IR sensor reading changes which results in the PLC registering a bubble that passed through. It was assumed that mass and bubble size remained constant when measuring biogas production.

Stellenbosch University https://scholar.sun.ac.za

The pH, ORP and EC probes would be cleaned by rinsing them with distilled water, then soaking them in a 0.1 M HCl and 1% pepsin solution, and finally soaking them in warm soapy water. Calibration of probes were performed every second week. The measured pH, ORP and EC probes would drift a maximum of +0.1, -5 mV and -1 $mS.cm^{-1}$, respectively, from the calibrated values over a two week period.

Mixing of the ASBR was performed via liquid recirculation, which was achieved by pumping the liquid from the outlet port back to the top of the container by means of a small centrifugal. Liquid was drawn from high up in the ASBR and pumped around into the bottom of the ASBR as shown in Figure 3-3. The liquid was pumped against the bottom of the ASBR and spread outwards due to the conical shape. This was to help promote mixing in order to reduce concentration gradients within the ASBR. The mixing pump was operated at its maximum flow rate of 8.6 $\ell.min^{-1}$ which resulted in a calculated upward flux of 18.6 $m^3.m^{-2}.h^{-1}$.

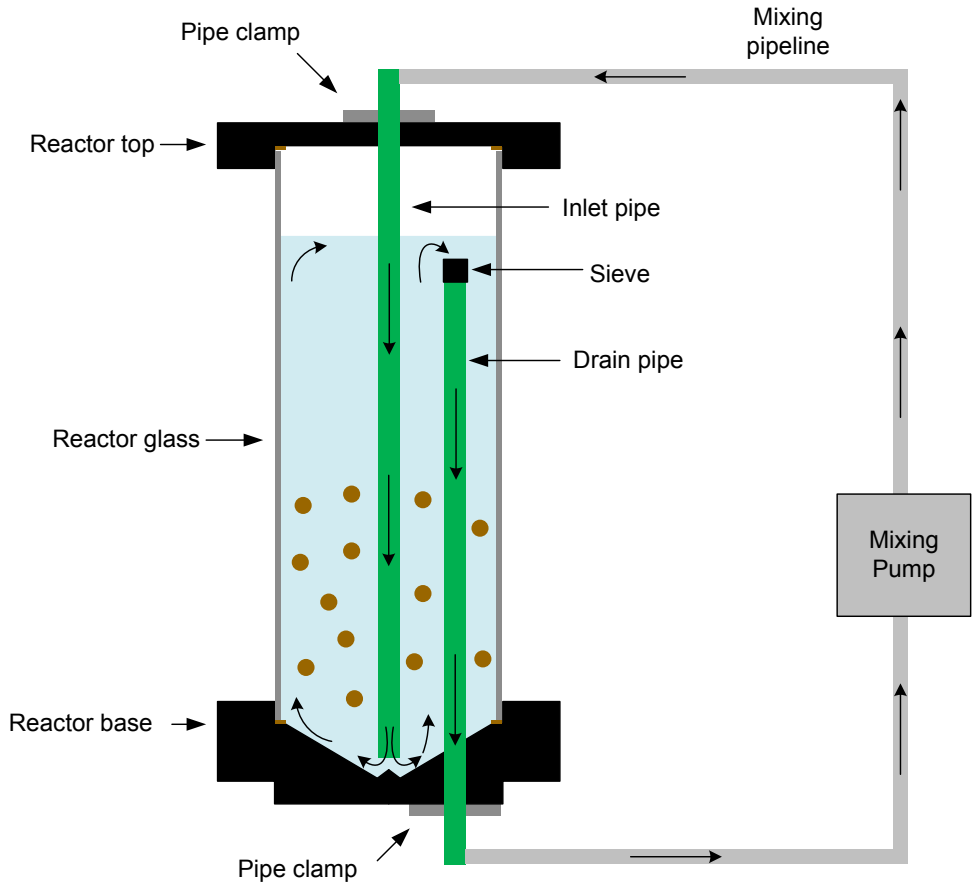

Figure 3-3: Illustration of the experimental ASBR mixing process

The total operating volume of the ASBR, which includes the sludge volume, is 14.1 ℓ. The fill and decant volume of the ASBR was set at 7 ℓ. Therefore, the volumetric discharge fraction (VDF) is 0.5. A high

Stellenbosch University https://scholar.sun.ac.za

VDF was selected to increase the need of possible pH control when a larger amount of VFAs are formed.

3.3. Synthetic winery wastewater

The synthetic winery wastewater recipe used in this study was similar to that of Malandra *et al.* (2003). The "yeast nitrogen base" used by Malandra *et al.* (2003) was switched for yeast extract powder to provide a nitrogen source. The recipe for "type B" synthetic winery wastewater used can be found in Table 3-5. The "type A" wastewater was identical to "type B", however 5000 mg/ℓ ammonium sulphate was added to replicate the recipe provided by Malandra *et al.* (2003). The "type A" wastewater was evaluated with some concern, due to the high ammonium sulphate concentration. Both recipe type A and B was of benefit to the study as it contained high concentrations of monosaccharides which forced the anaerobic digestion process to go through the acidogenesis, acetogenesis and methanogenesis phases. The production procedure of the synthetic winery wastewater can be found in Appendix B.

Table 3-5: The type B synthetic winery wastewater recipe used in the ASBR

Compound	Conc. [mg/ℓ]	Carbon-based components COD [mg/ℓ]
Glucose	1800	1918.3
Fructose	1800	1918.3
Citric acid	1	0.7
Tartaric acid	2	1.1
Malic acid	2	1.4
Lactic acid	2	2.1
Propanol	1.24	3.0
Butanol	1	2.6
i-Amyl alcohol	3.8	10.3
Acetic acid	250	266.4
Ethanol	10	20.8
Ethyl acetate	4	7.3
Propionic acid	8	12.1
Valeric acid	1	2.0
Hexanoic acid	0.5	1.0
Octanoic acid	0.7	1.7
Yeast extract powder	1700	-
Total		4165

The COD presented in Table 3-5 is based on the theoretical calculated amount of the carbon-based components only. When mixing the synthetic winery wastewater, it was noted that the addition of yeast extract powder resulted in an increased COD of 18% to 28% when compared to the calculated

Stellenbosch University https://scholar.sun.ac.za

amount. As a result, the carbon-based components were used as a reference to determine the amount of stock solution required to produce the synthetic winery wastewater.

3.4. Seed sludge

The ASBR was seeded with 2ℓ of granular sludge from a mesophilic UASB obtained from DISTELL in Wellington. The sludge was stored at 4°C before being used. The sludge had a volatile suspended solids (VSS) concentration of 0.1 g-VSS/g-granule.

After the sludge was added to the ASBR, a solution containing urea and dipotassium phosphate (K_2PO_4) at 377 mg/ℓ and 339 mg/ℓ, respectively. The sludge was left overnight in the solution and mixed for 1 min every hour. Additionally, the ASBR was set to heat up to the operating set point of 35°C. The following morning, the ASBR was fed a glucose and acetic acid substrate for three consecutive batches. Thereafter the synthetic winery wastewater solution was fed to the ASBR.

3.5. Sampling

During experiments, only liquid and gas samples were taken and analysed. During the decant phase, about 1ℓ was allowed to decant before a 14 mℓ and 200 mℓ sample was taken from the decant stream. The small sample was used for COD analysis while the large sample was used to determine alkalinity.

Gas samples were taken with 5 ℓ gas bags. Two 5 ℓ gas bags were used as equaliser bags. A third 5 ℓ gas bag was used after the bubble counter to capture product gas. As the start of each batch, the biogas capture bag was vacuumed to reduce the chances of contamination.

3.6. Analytical procedures

The following components of the sampled influent, effluent and biogas was analysed:

- Chemical oxygen demand
- Total, partial and intermediate alkalinity
- Gas composition – N_2, H_2, CO_2, CH_4

The COD of the influent and effluent of the ASBR was measured with COD cell test from Merck. Organic components in the sample were oxidised by potassium dichromate as obtained from Merck COD solution B. Mercury sulphate was added to remove possible chlorine interference in the sample with the use of Merck COD solution A. Both solutions contained sulphuric acid to remove to catalyse the oxidation process. The two solutions were added to a cell along with the sample and allowed to react for 120 min in a thermo reactor. A Spectroquant® NOVA 60 (Merck) spectrophotometer was used to determine the COD of the reacted sample.

Stellenbosch University https://scholar.sun.ac.za

An auto titrator was used to determine the partial and total alkalinity of the effluent. This was achieved by adding a 0.1 M HCl solution to the sample until the two end points of pH 5.75 and pH 4.5 were reached. Following this, the intermediate alkalinity and Ripley's ratio could be calculated.

The biogas compositions of the two equaliser and final capture bag were analysed via gas chromatography (GC) using the TCD detector and Supelco Carbonex 1000 column. Biogas production was low during the settling stage, therefore, the samples were taken for the equaliser bags' analysis during this stage. In the decant phase, the equaliser gas bags had to be connected to the ASBR to prevent a vacuum from occurring. The produced biogas in the capture bag was analysed at the end of the batch. An empty bag was attached to the ASBR during the feed stage to capture the biogas produced during a batch.

Further details of the analytic analysis methods can be found in Appendix B.

3.7. Analysis of measured online data

3.7.1. Overview of Matlab analysis program

Data measured online with the ASBR, was stored onto a flash disk as a 'csv' file. The following data was recorded in two second intervals:

- Date
- Time
- Temperature (Measured value in °C x100)
- pH (Measured value x100)
- Phase (1 – Feed; 2 – React; 3 – Settle; 4 – Decant)
- Dosing I/0 (0 – No dosing; 1 – Dosing pump on)
- Mixing I/0 (0 – No mixing; 1 – Mixing pump on)
- Mixing flow rate (Measured value x100)
- Conductivity (Measured value in mS/m x100)
- Oxidation-reduction potential (mV)
- Bubbles (Counts 0 - 20000 bubbles)
- Bubbles x20000 (Counts group of 20000 bubbles)

Each day the data from the 'csv' file was removed and sorted into number file for each individual batch. A Matlab program was coded to read this 'csv' file and find various bits of information. A brief description of how the data were analysed follows and more details can be found in Appendix B and Appendix D.

Stellenbosch University https://scholar.sun.ac.za

Each variable was imported from the 'csv', adjusted as required and each variable set stored as an array in Matlab. The required smoothing of pH, ORP and EC was performed. The bubble counts were then converted to biogas production. The temperature, pH, ORP, dosing interval and biogas production were presented in graphical format and also saved as sext files to allow easy access via Excel for further analysis.

3.7.2. Data smoothing

Due to signal noise of the 4-20 mA transmitters of the various probes to the PLC, fluctuations were measured. Online measurements for pH, ORP and EC were smoothed with a built in Matlab function named "smooth" and the "rlowess" smoothing technique for that function was selected. The "rlowess" is a local regression model that uses weighted linear least squares to determine the smoothed value. The method assigns zero weight to data outside six mean absolute deviations while determining a value of a function. This method was selected as it performed the best at removing outliers and reducing signal noise compared to other built in methods in Matlab.

3.7.3. Biogas production rate

The produced cumulative biogas measurement is a function of the bubbles counted. At the start of each phase, the bubble counter is reset and bubbles are counted throughout the cycle. The function used to calculate the cumulative biogas produced in mℓ is presented below in Eq. 3-1. The factor of 0.26 is obtained from linear regression while calibrating the bubble counter.

$$V_{biogas} = 0.26 n_{bubbles} \qquad \textbf{Eq. 3-1}$$

The biogas production rate is then calculated from this cumulative biogas volume. Due to the long cycle times relative to the minute time unit, the amount of gas produced per minute was used as the biogas production rate for that specific minute. This was then further smoothed by using the moving average over nine points. Choosing less points resulted in a very jiggered curved and made it difficult to identify key points in the biogas production process.

3.8. Experimental data results

In Chapter 5, the results of repeated experiments are presented such that the OLR is on the x-axis. The OLR was dependent on the COD of the feed solution, batch length and volume added. To keep the OLR identical for each repeated batch was near impossible. Therefore, it was decided to break up the feed COD into nine 500 mg/ℓ intervals when presenting the results of repeat experiments for the same inoculations. This meant that a minimum experimented feed COD of 2000 to 2500 mg/ℓ resulted in an OLR range of 1.01 to 1.26 $g_{COD}.\ell^{-1}.day^{-1}$. This resulted in nine possible OLR ranges that data could fall in

Stellenbosch University https://scholar.sun.ac.za

between with a minimum of 1.01 and a maximum of 3.27 $g_{COD}.\ell^{-1}.day^{-1}$. The average of the repeated batches were calculated for each range along with the standard deviation.

Outliers for various data sets were removed according to the method described in Vining (1997) as a result of experimental or analytical errors. The method used was to determine the first and third quartile of the data set for each variable within one of the nine OLR ranges. Hereafter, a step size was calculated and used determine the “lower inner fence” and the “upper inner fence.” Any value below or above this value was then considered an outlier and removed for further analysis within that data set. The average of the required variable was then determine along with the standard deviation.

For each data set, at least four points and a maximum of eight were used to determine the required information in order to present the results in Chapter 5.

For Chapter 6, the data was grouped together for each experimental set as described in Table 3-2. The same method as described above was followed to determine the average and standard deviation of the various variables presented.

Each data point, for each variable, was measure in 24 hour periods from one another. All error bars presented, represent one standard deviation from the average of that specific data set.

Sample calculations can be found in Appendix B.

Stellenbosch University https://scholar.sun.ac.za

Chapter 4 - Exploratory simulation of an ASBR with the use of ADM1

The first objective of the study was to understand the anaerobic digestion process within an ASBR. To do so, ADM1 was used and programmed with Matlab. As the aim of the ADM1 was to understand the anaerobic digestion process, *in-situ* pH control was not included in the programmed model. The programmed model was tested and modified to ensure that it abided by the law of conservation of mass. A comparison was made of the performance of the programmed model of this study and that used by Batstone *et al*. (2004). Batstone *et al*. (2004) used Aquasim 2.1d as a simulation package for the treatment of winery wastewater within an ASBR. After the comparison was made, the feed substrate was altered to that used in the lab scale unit for this study. The Matlab code can be found in Appendix D.

4.1. Programming of an ADM1 solver for an ASBR

The standard anaerobic digestion model no.1 was used with the addition of the ethanol degradation extension (Batstone *et al*., 2004). This extension was included due the ethanol content of winery wastewater. The model was programmed in MATLAB® R2014b and used the differential equation implementation to include the pH solver function. Solids precipitation, nitrate removal and sulphate reduction were excluded from the model. The ADM1 was programmed using the "ode15s" time step method instead of set time step size to decrease computing power needed for the simulation. Furthermore, "ode15s" handles stiff systems better than other built in differential equation solvers in Matlab.

4.1.1. Differential functions used to describe ADM1

The ADM1 is made up multiple liquid phase equations that describes the state of each component with the following mass balance in Eq. 4-1:

$$\frac{dVS_{liq,i}}{dt} = q_{in}S_{in,i} - q_{out}S_{liq,i} + V\sum_{j=1-19}\rho_j\nu_{i,j} \qquad \textbf{Eq. 4-1}$$

The chain rule has to be applied to Eq. 4-1 when a system with a varying volume is modelled. As the ASBR has two constant and two varying volume phases, a piecewise function had to be incorporated. Eq. 4-2 describes the liquid phase components concentration at any stage of the ASBR process.

$$\frac{dS_{liq,i}}{dt} = \frac{q_{in}S_{in,i} - q_{out}S_{liq,i} + V(t)\sum_{j=1-19}\rho_j\nu_{i,j} - S_{liq,i}\cdot\frac{dV}{dt}}{V(t)} \qquad \textbf{Eq. 4-2}$$

Stellenbosch University https://scholar.sun.ac.za

Where

$$V_{liq}(t) = \begin{cases} V_{min} + q_{in}t, & filling\ phase \\ V_{max} - q_{out}t, & decanting\ phase \end{cases}$$

And

$$\frac{dV}{dt} = \begin{cases} q_{in}, & filling\ phase \\ -q_{out}, & decanting\ phase \end{cases}$$

Through further simplification of Eq. 4-2, the liquid phase concentration state equations can be seen in Table 4-1. The ADM1 model assumes that the reactor works as a CSTR, therefore, concentration gradients are not accounted for. Furthermore, the reacting and settling stages are combined as mixing is not included in the model.

Table 4-1: Liquid phase concentration state equations for various stages of the ASBR process

ASBR Phase	Liquid phase state equation	
Filling	$\frac{dS_{liq,i}}{dt} = \frac{q_{in}(S_{in,i} - S_{liq,i})}{V_{liq}} + \sum_{j=1-19} \rho_j \nu_{i,j}$	**Eq. 4-3**
Reacting and settling	$\frac{dS_{liq,i}}{dt} = \sum_{j=1-19} \rho_j \nu_{i,j}$	**Eq. 4-4**
Decanting	$\frac{dS_{liq,i}}{dt} = \sum_{j=1-19} \rho_j \nu_{i,j}$	**Eq. 4-5**

For further explanation on the kinetic rate, liquid/gas transfer and acid/base transfer rate equations, the ADM1 technical report by the IWA Task Group for Mathematical Modelling of Anaerobic Digestion Processes (2002) can be consulted.

Gas transfer for hydrogen, methane and carbon dioxide was modelled as temperature dependent variables as indicated in the ADM1 technical report (IWA Task Group for Mathematical Modelling of Anaerobic Digestion Processes, 2002). The gas flow rate was modelled while assuming an overhead pressure greater than atmospheric pressure.

With the ADM1, the pH of the liquid phase can be calculated. To calculate the pH, a charge balance was performed with the acid/base concentrations of various components. These acid/base concentrations are either calculated with differential equations or algebraic equations. In this study differential equations were used due to sufficient computational power. Calculating the pH allows the pH-related inhibition of sludge components to be simulated. To reduce the required computation time

Stellenbosch University https://scholar.sun.ac.za

required to determine the pH at a certain point in time, a method suggested by Rosen and Jeppsson (2006) was used for the pH calculation. This consisted of calculating a variable which was the sum of the hydrogen and hydroxide ion, θ, with molar concentrations of the acid/base components as in Eq. 4-6. Thereafter, the molar concentration of the H^+ ion was calculated by finding the root of a hyperbola with Eq. 4-7. That solution was then used to determine the pH with Eq. 4-8.

$$\Theta = S_{cat^+} + S_{nh4^+} - S_{hco3^-} - \frac{S_{ac^-}}{64} - \frac{S_{pro^-}}{112} - \frac{S_{bu^-}}{160} - \frac{S_{va^-}}{208} - S_{an^-} \quad \textbf{Eq. 4-6}$$

$$S_{H^+} = -\frac{\Theta}{2} + \frac{1}{2}\sqrt{\Theta^2 + 4K_W} \quad \textbf{Eq. 4-7}$$

$$pH = -\log_{10}(S_{H^+}) \quad \textbf{Eq. 4-8}$$

4.1.2. Solver methodology

The programmed ADM1 solver was programmed in two separate m-files in MATLAB. This section will provide a brief explanation of how the two fit together.

Figure 4-1 illustrates how the main m-file function works. For the ADM1 solver to be used, the initial conditions of the sludge, liquid and gas concentrations in the ASBR had to be defined. Secondly, the feed component concentrations had to be defined followed by the operating parameters of the ASBR in terms of the volumes, flow rates, operating times and number of batches to be simulated. Due to the stiffness of the model, the initial conditions had to be well selected. Otherwise, aspects like pH calculations and subsequent pH inhibition made the model unstable and results in meaningless predictions.

Figure 4-2 illustrates the ADM1 solver algorithm to calculate various component concentrations at a specific point in time.

Stellenbosch University https://scholar.sun.ac.za

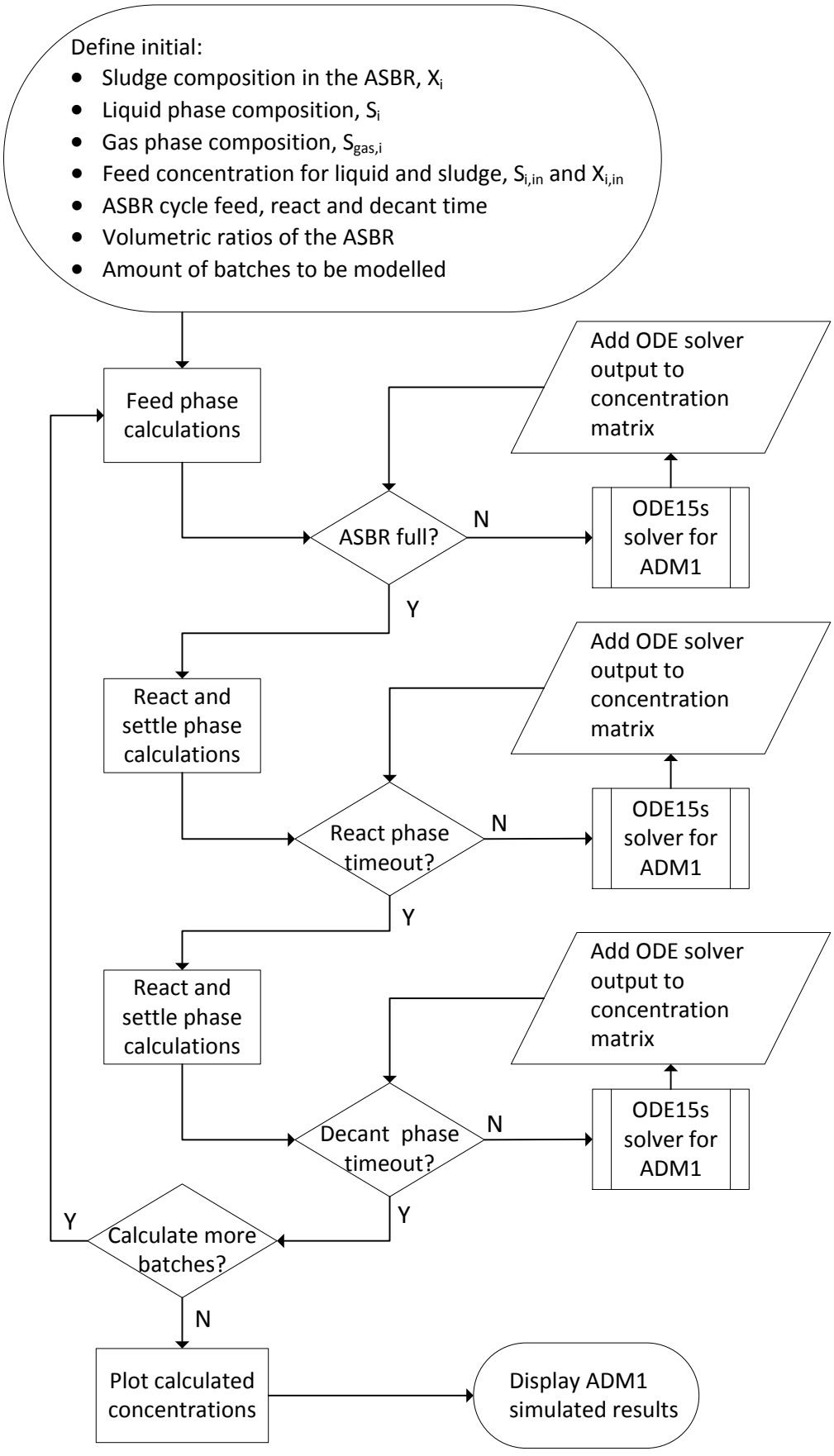

Figure 4-1: Main function methodology for the ADM1 solver

Stellenbosch University https://scholar.sun.ac.za

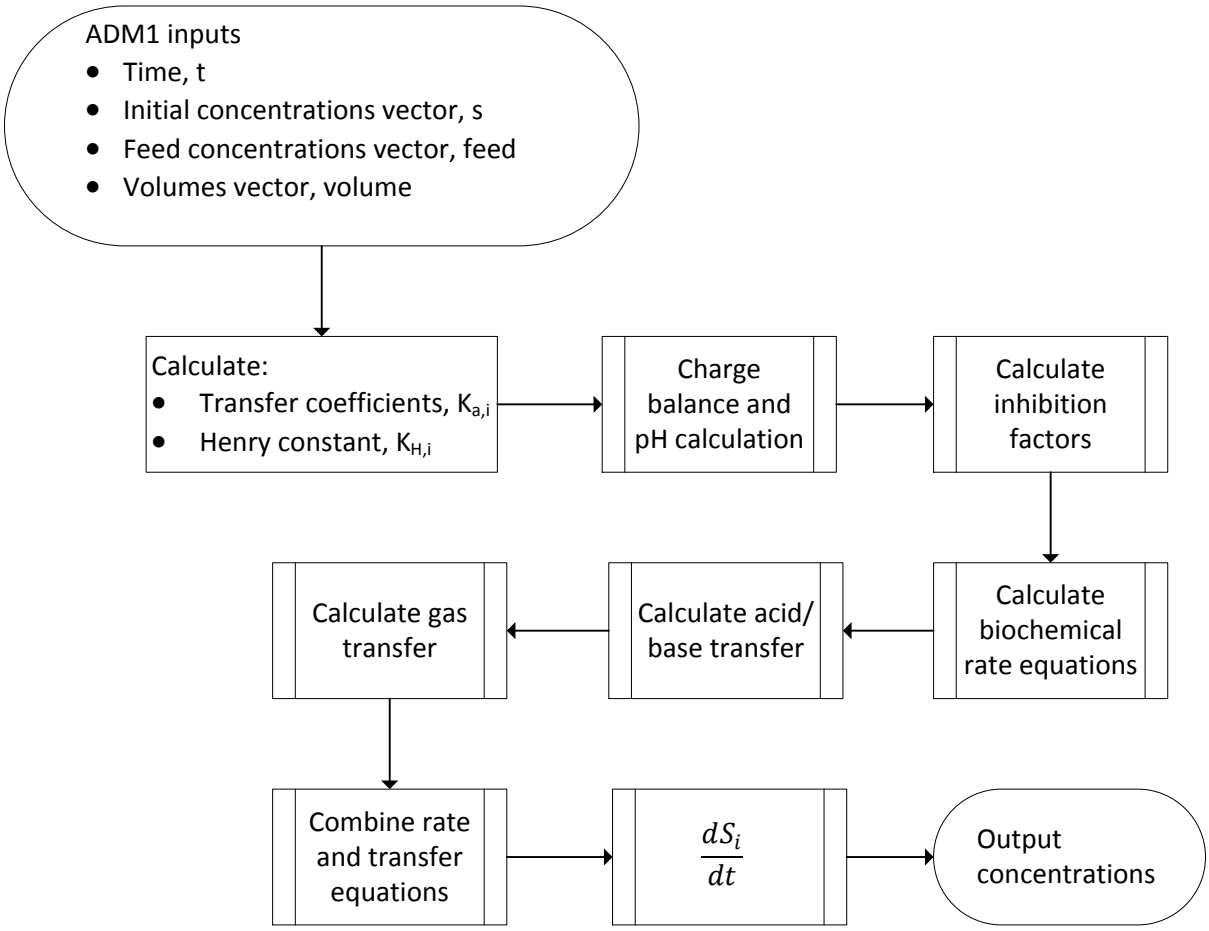

Figure 4-2: ADM1 ODE solver function methodology

4.2. Testing of the ADM1 programming

Several tests we performed to ensure that the ADM1 was correctly programmed. Tests were conducted to ensure that the law of conservation of mass was adhered to during the filling and decanting stage of the ASBR process. These tests were set so that no digestion (biochemical processes), no gas-liquid transfer (physic-chemical processes), no acid-base transfer (conversion processes) and no sludge growth/decay took place. These tests consisted of four consecutive one day long batches. The model was operated to simulate a VDF of 0.5.

4.2.1. Test 1 – Constant concentration

During the first test, the initial concentration of a component in the ASBR was identical to that fed into the ASBR during the feed stage. For the conservation of mass law to be correct, the concentration of that component has to remain constant throughout each stage of the ASBR process. This had to be true irrespective of the liquid volume in the ASBR.

Stellenbosch University https://scholar.sun.ac.za

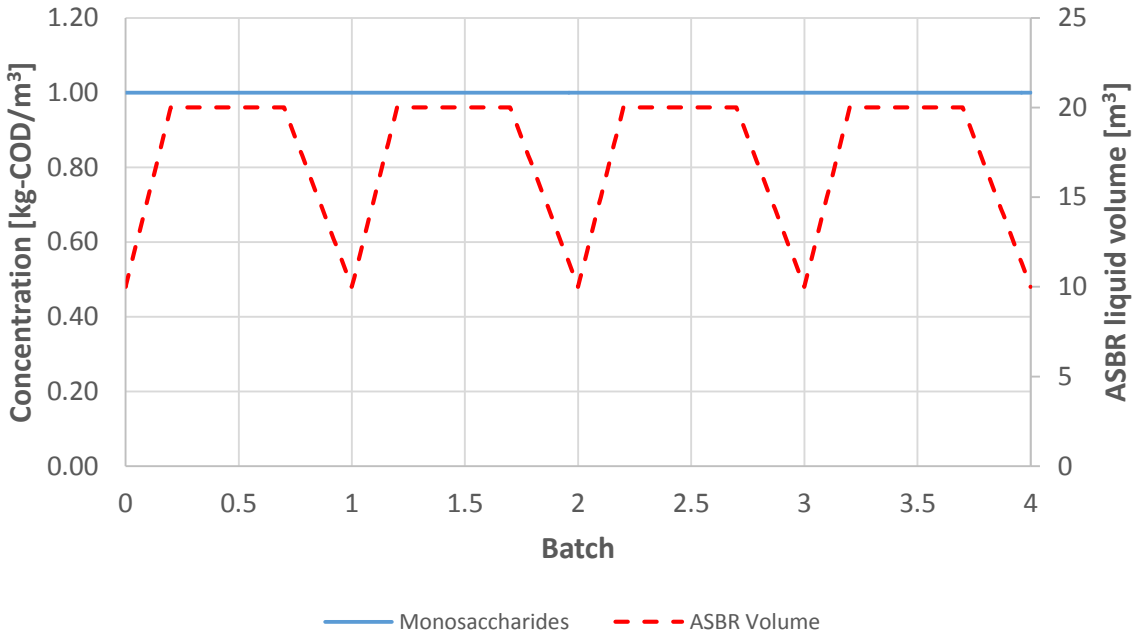

Figure 4-3: Monosaccharides concentration for four simulated batches under test 1 conditions with the programmed ADM1

Figure 4-3 illustrates the concentration of the monosaccharides and ASBR volume for the 4 simulated batches. Each batch was one day long. During the filling stage, when the ASBR volume increased, the monosaccharide concentration remained constant in the ASBR. During the decant stage, when the ASBR volume decreased, the monosaccharide concentration remained constant. Therefore, this test resulted in the programmed ADM1 abiding by the law of conservation of mass.

4.2.2. Test 2 – Dilute and concentrate

The second test was performed to test the effect of feeding one component (monosaccharides) at double the initial ASBR concentration and have the other component (amino acids) not fed at all.

Monosaccharides were fed into the ASBR at 2 kg-COD/m^3 while the initial concentration in the ASBR was 1 kg-COD/m^3. The monosaccharides concentration had to increase with each consecutive batch trying to reach 2 kg-COD/m^3 in the ASBR.

The amino acids had an initial concentration of 1 kg-COD/m^3 in the ASBR, however, the feed concentration of the amino acids was 0 kg-COD/m^3. Between the start and end of each batch, the concentration of the amino acids had to halve as a result of a VDF of 0.5. During this test, the amino acid concentration had to try and reach 0 kg-COD/m^3 after several batches.

Stellenbosch University https://scholar.sun.ac.za

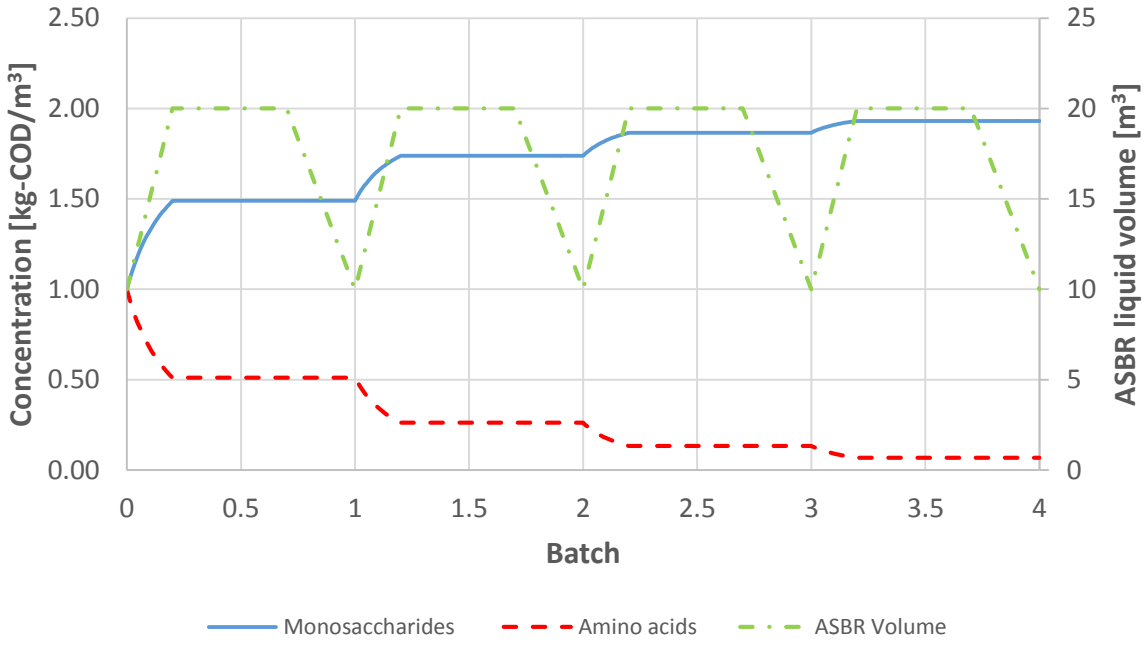

Figure 4-4: Monosaccharide and amino acids concentrations for four simulated batches under test 2 conditions with the programmed ADM1

Four one day long simulated batches are illustrated in Figure 4-4. During the feed stage the volume of the ASBR changes from 10 – 20 m^3. Therefore, when the ASBR was filled with a component which had double the initial concentration of the ASBR, the concentration of that component had to increase by 50% as seen with monosaccharides for the first batch simulated. Thereafter, the concentration of monosaccharides for each batch increases for each cycle as it was trying to reach the feed concentration. When no amino acid was added to the ASBR, the concentration halved with each consecutive batch. Therefore, it could be seen that the law of conservation of mass was abided to in both scenarios.

An advantage of using an ASBR is its sludge retention abilities. Therefore, when an ASBR is decanted, the sludge concentration has to increase in the ASBR to initial concentration at the start of the feeding phase. Sugar degraders were not fed to the ASBR while amino acid degraders were fed into the ASBR at the initial concentration. If no washout is considered, the sugar degraders' concentration should be equivalent at the start and end of a single batch. Furthermore, the sugar degraders concentration should decrease in the feed stage and increase during the decant stage. As the amino acid degraders are fed into the ASBR as the same as the initial ASBR concentration, the concentration had to remain constant during the feed period. Furthermore, the sludge concentration had to increase during the decant phase.

Stellenbosch University https://scholar.sun.ac.za

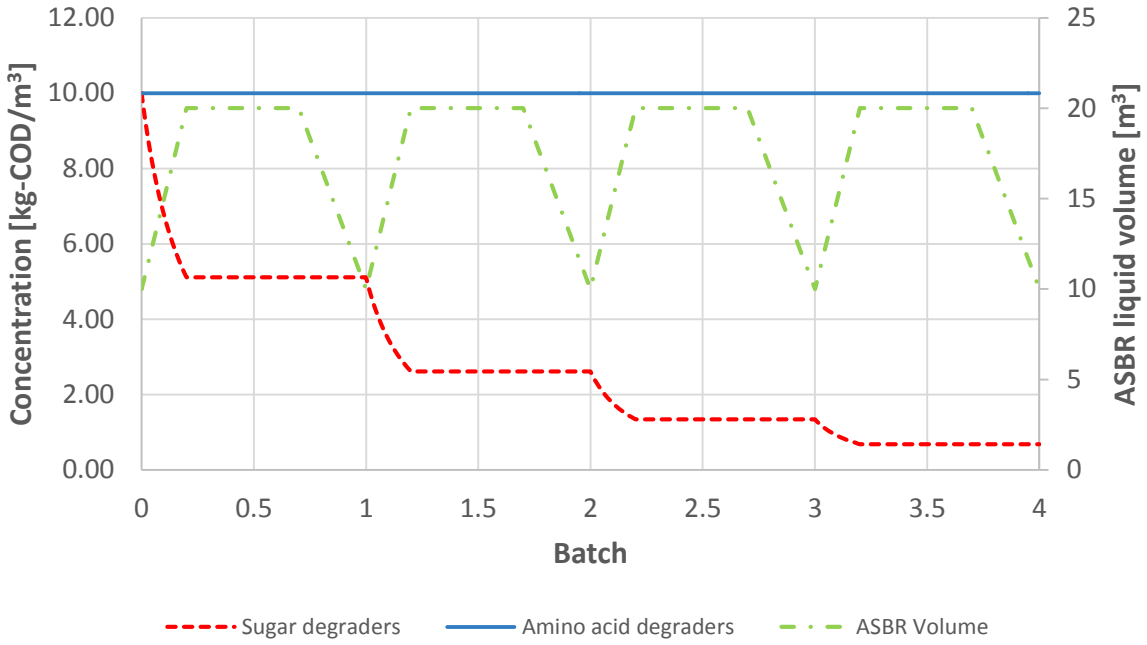

Figure 4-5: Sugar and amino acids degraders concentration simulated for four batches with the programmed ADM1

Figure 4-5 indicates the concentration of the sugar and amino acid degraders that form part of the anaerobic sludge. Both degraders did not perform as required, therefore the programmed model needs to be modified to include sludge retention.

4.2.3. Test 3 – Sludge retention and sludge washout

In high rate digesters, like the ASBR, where the residence time of a solid state components (sludge) was variable, a term was added to model sludge washout with the ADM1 as formulated in Eq. 4-9.

$$\frac{dX_{liq,i}}{dt} = \frac{q_{in}(X_{in,i} - X_{liq,i})}{V_{liq}} - \frac{X_{liq,i}}{\left(t_{res,X} + \frac{V_{liq}}{q_{out}}\right)} + \sum_{j=1-19} \rho_j \nu_{i,j} \qquad \textbf{Eq. 4-9}$$

Eq. 4-9 was designed to predict sludge washout for a continuous system that has a constant volume. However, an ASBR is semi-continuous system which undergoes volume changes during the feed and decant stage. To overcome this, the sludge decanted from the system was modelled to be concentrated and returned to the system. This method was used to model a chemostat with sludge recycling as seen below in Figure 4-6 (Shuler and Kargi, 2010).

Stellenbosch University https://scholar.sun.ac.za

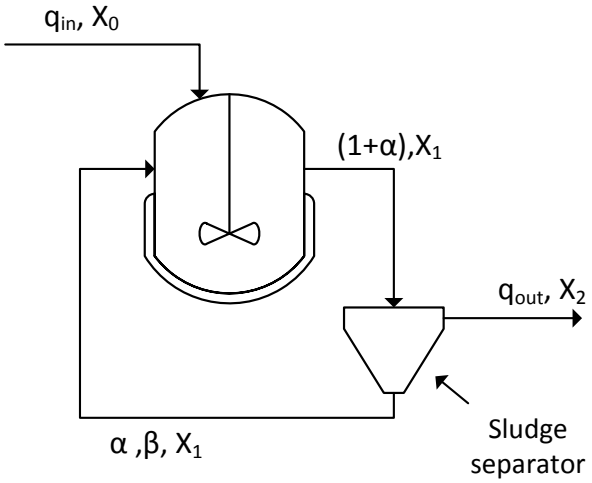

Figure 4-6: Chemostat with sludge recycling. Adapted from Shuler and Kargi (2010).

For a chemostat with sludge recycling, the material balance for the sludge is provided below with Eq. 4-10 (Shuler and Kargi, 2010).

$$V\frac{dX_1}{dt} = q_{in}X_0 + \alpha q_{out}\beta X_1 - (1+\alpha)q_{out}X_1 + V\rho v \qquad \textbf{Eq. 4-10}$$

Where

α is the recycle ratio based on volumetric flow rates.

β is the ratio of sludge concentration in the recycle stream to that in the reactor effluent.

Considering this, the sludge concentration equation, Eq. 4-10, was modified to Eq. 4-11, below.

$$\frac{dX_{liq,i}}{dt} = \frac{q_{in}(X_{in,i} - X_{liq,i})}{V_{liq}} + \frac{\alpha q_{out}\beta X_{liq,i}}{V_{liq}} - \frac{(1+\alpha)q_{out}X_{liq,i}}{V_{liq}} + \sum_{j=1-19}\rho_j\nu_{i,j} \qquad \textbf{Eq. 4-11}$$

The benefit of modelling sludge concentration in the ASBR like this, is that sludge washout can be simulated for a real ASBR. The sludge concentration components of test 2 was used to test the sludge washout/retention in the ASBR. For this test both the initial sugar degraders and amino acids degraders' concentration was 10 kg-COD/m^3. However, the feed substrate contained 0 kg-COD/m^3 sugar degraders and 10 kg-COD/m^3 amino acid degraders. Taking into account that some washout can occur, amino acid degrader's concentration initially in the ASBR had to be less than it at the end of the batch.

Stellenbosch University https://scholar.sun.ac.za

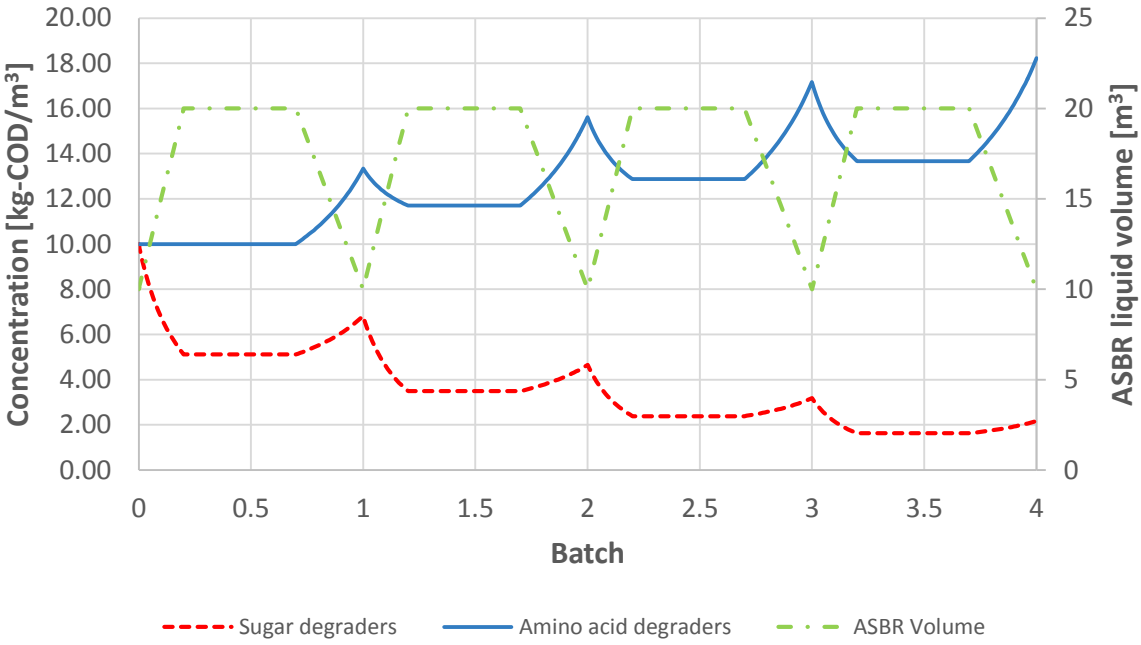

Figure 4-7: Testing sludge retention for an ASBR modelled with the programmed ADM1

The results of the testing of the modified model to incorporate some sludge retention is illustrated in Figure 4-7. As seen during the filling phase, the sugar concentrations decreased initially and the amino acid degraders' concentration remained constant. During the decanting phase, the concentrations of both components increase. The increase was correct as the liquid volume had to be reduced in the ASBR, however, most of the sludge had to remain behind in the ASBR. The sugar degraders did not return to its initial concentration due to some sludge being washed out. Without sludge washout, the amino acid degraders' concentration was supposed to return to 15 kg-COD/m^3 at the end of the first batch. However, the sludge washout resulted in only 13.4 kg-COD/m^3 to remain.

A problem was found with the sludge recycle mass balance during the decanting phase. When the ASBR decant stage was shorter than 0.1 day, the system would under predict the concentration of the particulate components (X_i). With the programmed model, the concentrations of the component at time n+1, was dependent of the value at time n. It seemed that using a using a short time interval (i.e. quick decant phase) combined with "ode15s", the time steps taken were too large, thereby, under predicting the concentrations of components. Notably, this was only found when trying to add the sludge retention into the model during the decant phase.

Even though there was a slight shortfall with regards to the sludge retention, it could still be used to simulate the ASBR process.

Stellenbosch University https://scholar.sun.ac.za

4.3. Simulating the results of a published study with the programmed ADM1 for this study

Batstone *et al*. (2004) suggested that an ASBR can be used for parameter estimation for anaerobic digesters. The model was implemented in Aquasim 2.1d as a CSTR with variable volume linked to a separate gas compartment. An attempt was made to replicate that study to test the performance of the Matlab based ADM1 of this study. However, the study by Batstone *et al*. (2004) did lack in providing information for the initial sludge composition to use for the simulation. Where kinetic rates were not provided by Batstone *et al*. (2004), the standard rates were used as provided in the ADM1 technical report. Missing data for sludge concentrations were sourced from ADM1 models of continuous systems (Cesur and Albertson, 2005; Normak *et al*., 2012; Rosen and Jeppsson, 2006; Schon, 2009). Trial and error was also used to alter some parameters to reduce the chance that the model became unstable. The soluble and particulate concentrations for the initial estimates and the feed concentrations can be found Appendix B. Stoichiometric, biochemical, physiochemical and physical parameter values used can be found in Appendix B.

When modelling continuous systems with the ADM1, the outlet concentrations are typically presented. However, for a batch system like the ASBR, it is more important consider the dynamics of the process. Understanding the dynamics will allow for better control over the ASBR.

The simulation of five 0.33 day long batches were modelled for inputs of the study by Batstone *et al*. (2004). The decant phase time was extended from 14 min to 0.1 day due to the possible inaccuracies that could developed with the sludge retention as discussed in Chapter 4.2.3.

Batstone *et al*. (2004) used algebraic equations to describe the acid-base transfer, whereas, the Matlab based model in this study used differential equations to describe it. The differential based equations are more accurate, but could lead to stability issues.

Batstone *et al*. (2004) included pH control in their study. However, pH control was not included in these preliminary investigations due to a lack of info provided in the study by Batstone *et al*. (2004).

Stellenbosch University https://scholar.sun.ac.za

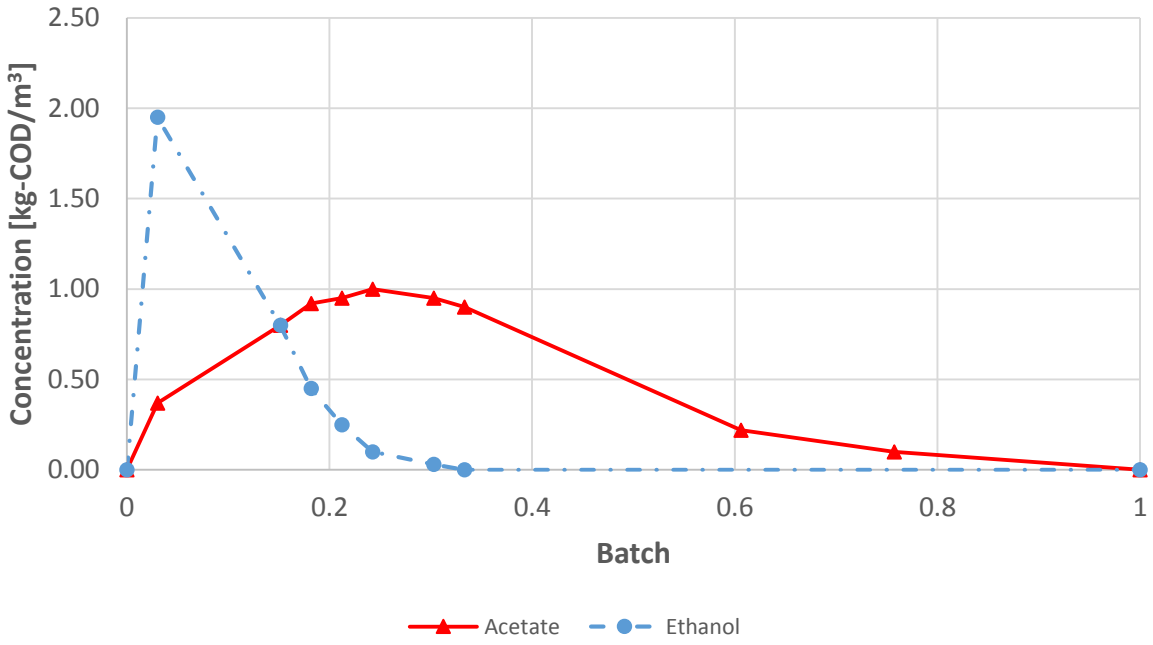

Figure 4-8: Redrawn ADM1 simulation results that were obtained by Batstone *et al*. (2004) for a single 0.33 day long batch

Batstone *et al*. (2004) presented the simulated concentration for ethanol and acetate in their study. Figure 4-8 illustrates the redrawn results for these two components from their study. Figure 4-9 indicates the nearest steady state concentrations obtained.

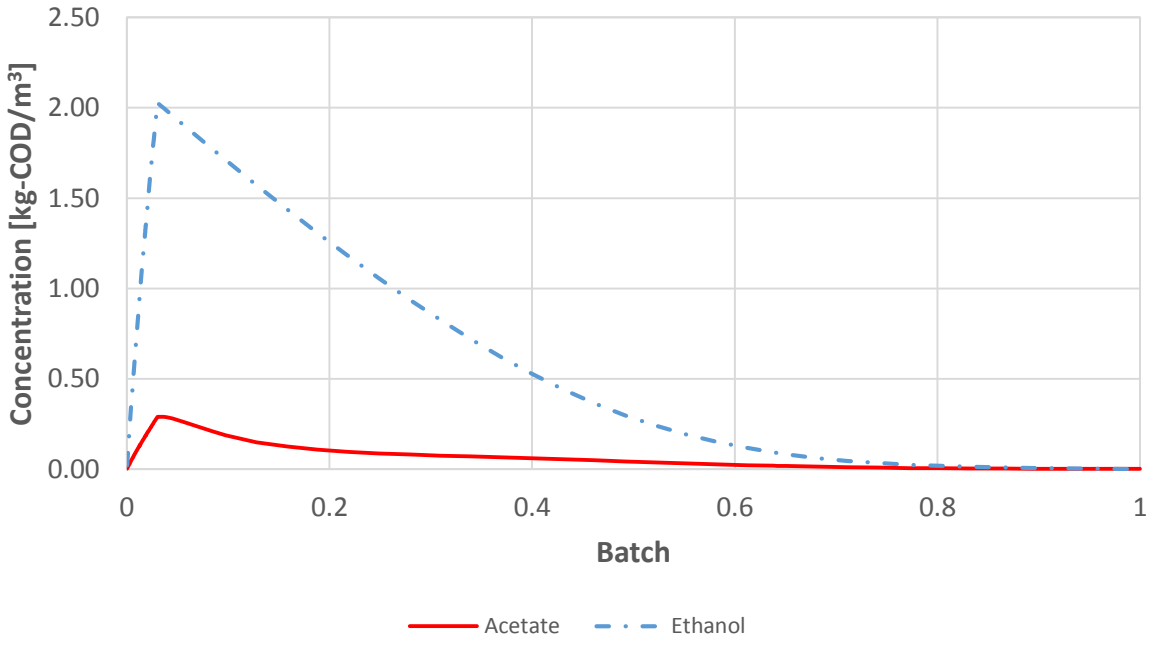

Figure 4-9: Acetate and ethanol simulation from this study's programmed ADM1 in an attempt to replicate the study of Batstone *et al*. (2004)

Stellenbosch University https://scholar.sun.ac.za

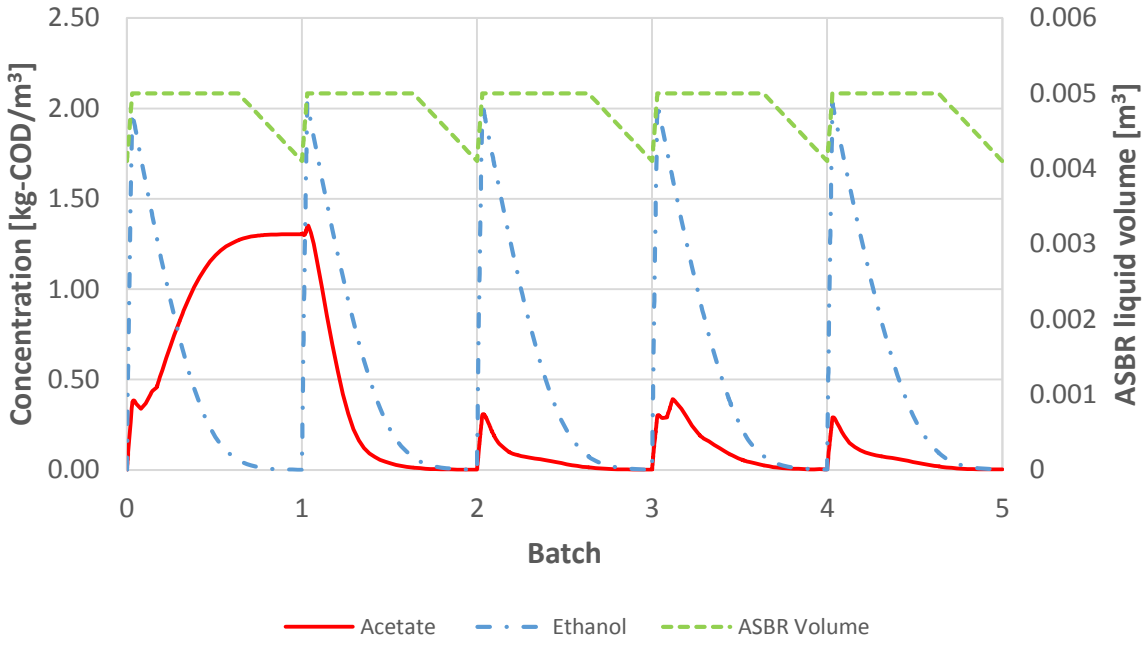

Figure 4-10: Soluble acetate and ethanol concentrations modelled with the programmed ADM1 for five consecutive batches in an attempt to replicate the study of Batstone *et al*. (2004)

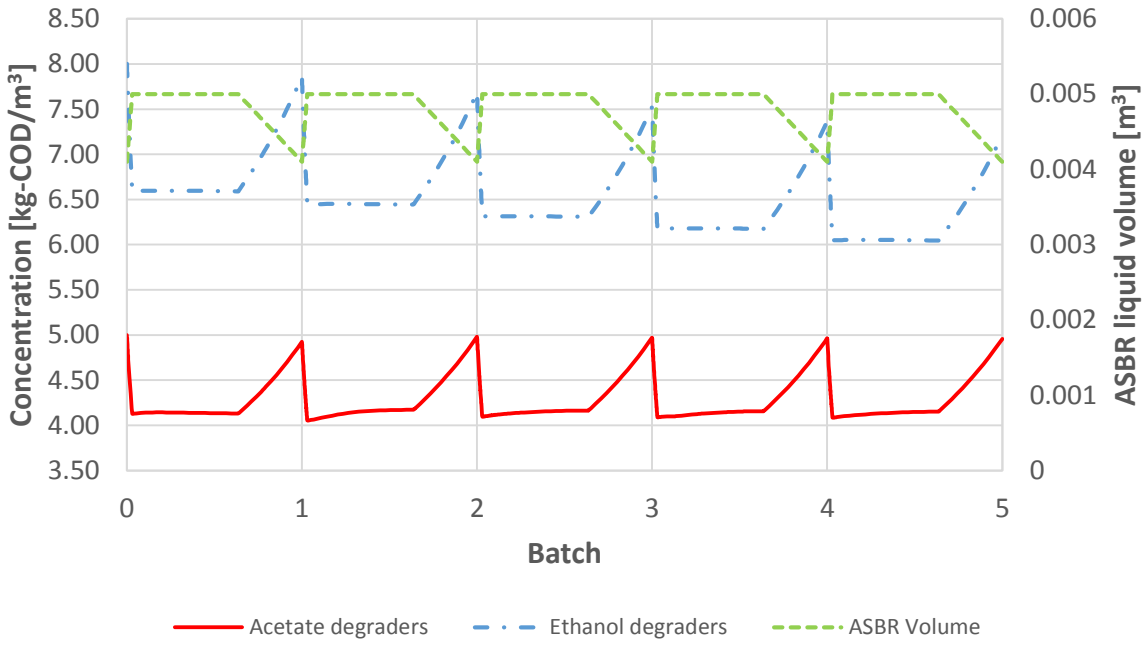

Figure 4-11: Particulate acetate and ethanol degraders' concentrations modelled with the programmed ADM1 for the study by Batstone *et al*. (2004)

Stellenbosch University https://scholar.sun.ac.za

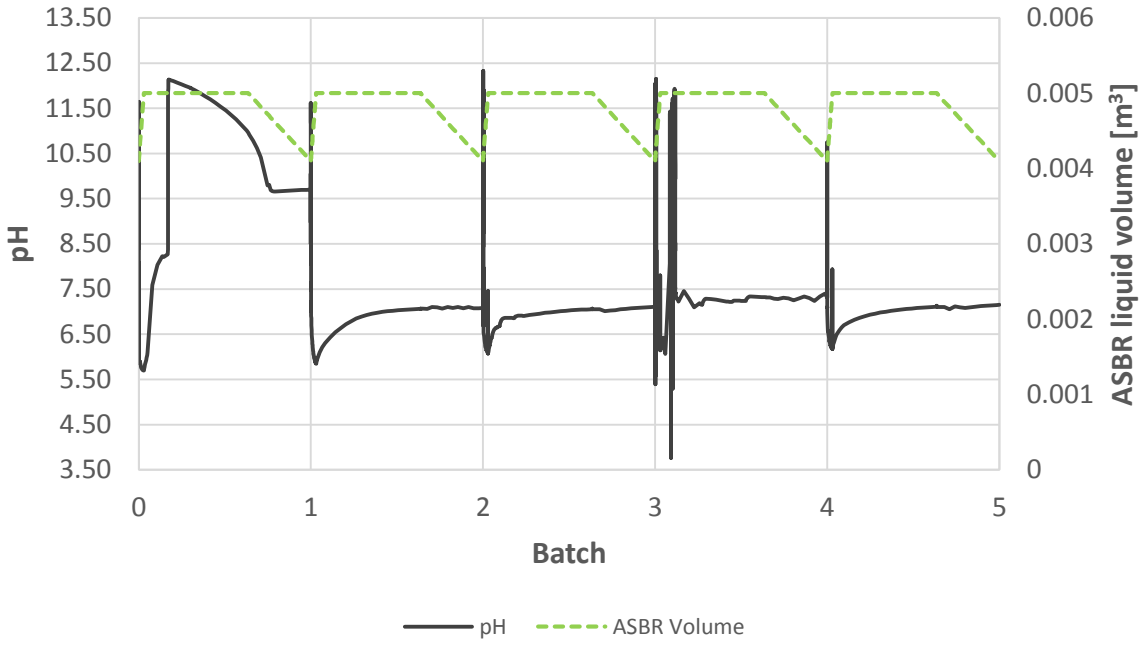

Figure 4-12: Simulated pH by the programmed ADM1 for the study by Batstone *et al*. (2004)

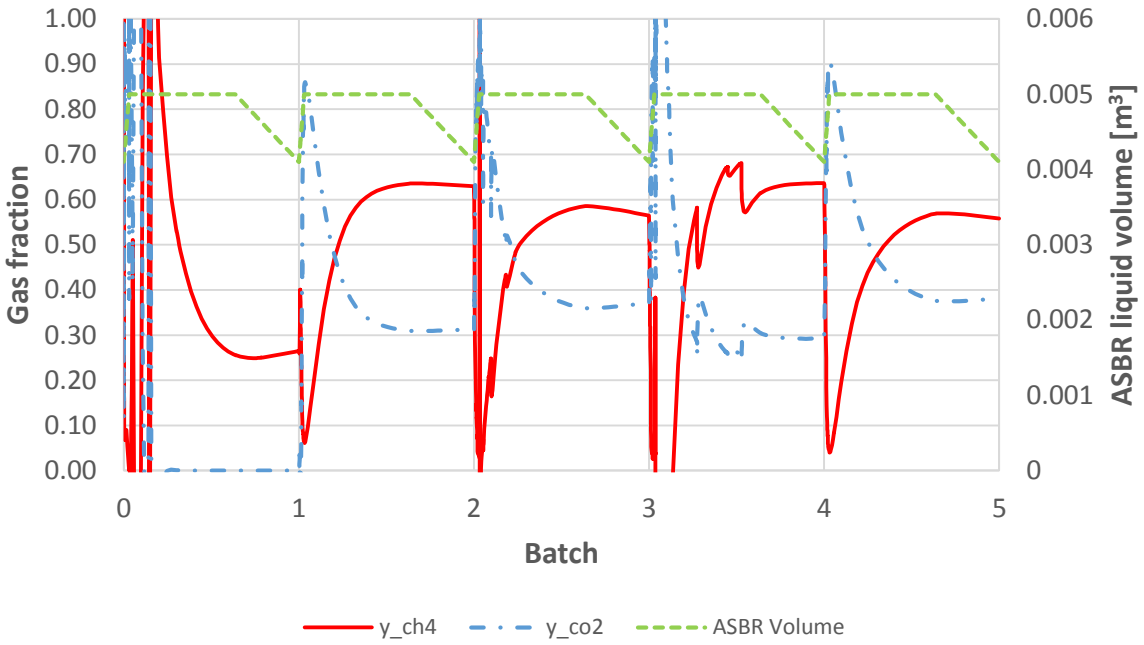

Figure 4-13: Simulated gas fractions by the programmed ADM1 for the study by Batstone *et al*. (2004)

Figure 4-10 presents the first five batches simulated with similar conditions as that provided by Batstone *et al*. (2004) in Figure 4-8. Figure 4-9 represents the fifth batch of Figure 4-10. This was nearest trend that could be obtained similar to that of the study by Batstone *et al*. (2004). The ethanol

Stellenbosch University https://scholar.sun.ac.za

consumption was to slow with this study and the acetic acid did not reach the same peak. At constant volume ethanol degradation is described with Eq. 4-12. The same maximum uptake rate ($k_{m,et}$) and half saturation values ($K_{S,et}$) were used for both studies.

$$\frac{dS_{liq,et}}{dt} = k_{m,et}\frac{S_{et}}{K_{S,et} + S_{et}}X_{et}I_1 \qquad \textbf{Eq. 4-12}$$

To increase the digestion rate of the soluble ethanol, the ethanol degraders in the ASBR could be increased. However, Figure 4-11 indicates that the ethanol degraders were in excess as its concentration was reduced with each consecutive batch.

The inhibition function, I_1, is dependent on the pH of the system. The simulated pH in illustrated in Figure 4-12. From batch 2 onwards, there is a pH drop in the simulated ASBR early in the batch. This would lead to this inhibition function (I_1) having a larger effect on the digestion rate of ethanol. Furthermore, Batstone *et al*. (2004) included pH control while this study excluded it due to a lack of information provided by Batstone *et al*. (2004). Therefore, it is believed that the simulated pH resulted in a slower digestion rate for ethanol than that obtained by Batstone *et al*. (2004).

Sludge growth and decay were included in the Matlab model. The growth and decay of the sludge was slow compared to the digestion process. Figure 4-11 illustrates that the acetate degraders were operated at almost the initial concentration estimate. With the increase in the acetate degrader concentration during the react phase, it made up for the wash out of acetate degraders during the decant phase.

The pH simulation was known as the most sensitive part of the ADM1 (Batstone *et al*., 2002). This was confirmed with the rapid changes in pH in Figure 4-12. It was the easiest to see in the fourth batch. All degraders are modelled for pH inhibition, however, acetate and hydrogen degraders have a more sensitive second pH inhibition term included in the digestion rates. This inhibition terms was set for a predefined pH range. Therefore, when the pH at time n was incorrect, the calculated soluble concentrations and pH at time n+1 can be far from correct. This effect was then transferred to the biogas simulation as seen in Figure 4-13.

The programmed Matlab model performed reasonably well against the result obtained from Batstone *et al*. (2004) under the circumstances. Therefore, it was believed that the model can be used to understand the anaerobic digestion process within an ASBR.

Stellenbosch University https://scholar.sun.ac.za

4.4. Simulating the programmed ADM1 with the experimental ASBR

This section focuses on simulating the ADM1 for the ASBR used in this study. Since Batstone *et al*. (2004) used a different feed substrate as with this study, the sludge composition used for the ADM1 simulation has to be fairly different. Almost all the COD of the feed substrate in this study came from monosaccharides, however, for Batstone *et al*. (2004), the majority of the COD came from ethanol. Therefore, with Batstone *et al*. (2004) the sugars degraders concentration could not be determined. The ADM1 simulation in this section contained the same stoichiometric, biochemical, physiochemical and physical parameter as that used section 4.3. The values for these parameters can be found in Appendix B.

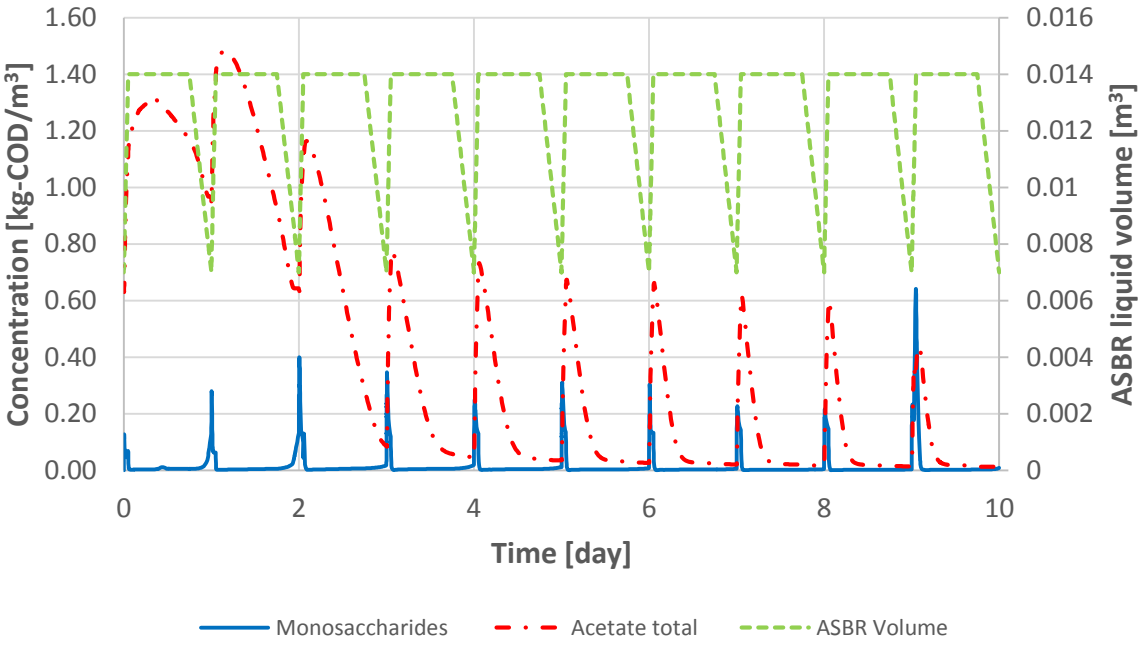

Figure 4-14: Soluble monosaccharides and acetate concentrations modelled with the programmed ADM1 for the synthetic wastewater of this study

Stellenbosch University https://scholar.sun.ac.za

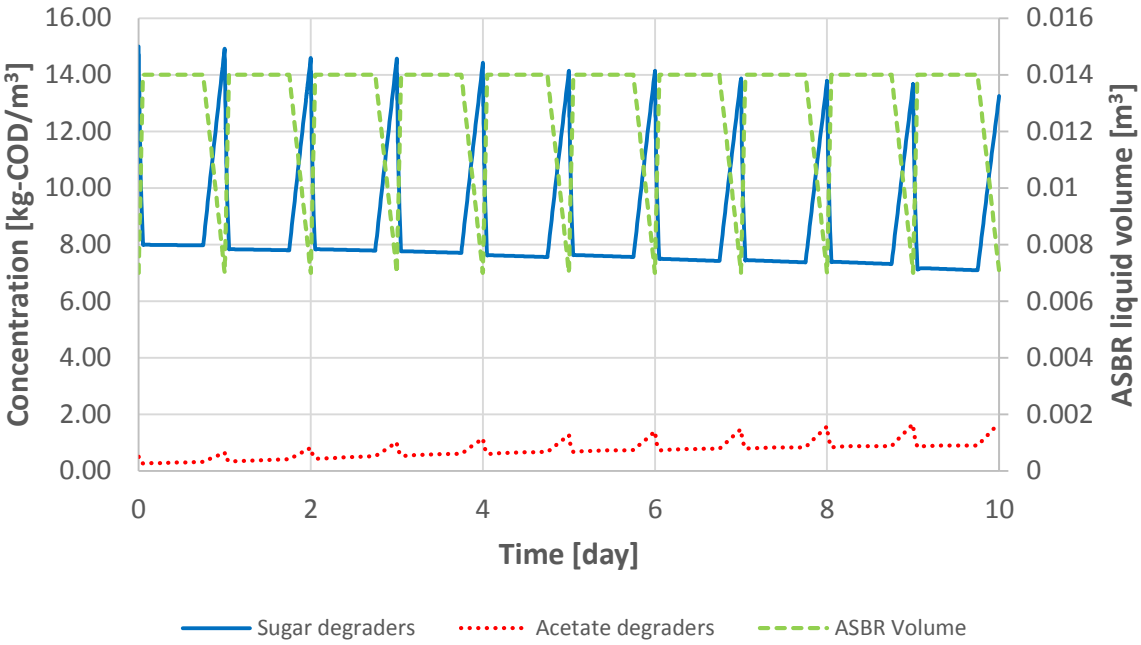

Figure 4-15: Particulate sugar and acetate degraders modelled with the programmed ADM1 for synthetic wastewater of this study

Figure 4-14 and Figure 4-15 provide the simulated concentrations of specific soluble and particulate components for the ASBR used in this study. The feed substrate used for the simulation consisted only of monosaccharides and has an equivalent concentration of the experimental ASBR when it was operated at an OLR of 2.68 g-COD_{feed}.ℓ^{-1}_{ASBR}.day^{-1}. A high OLR was simulated to amplify problems that could occur during the experimental ASBR.

The biggest problem was to guess the sludge (degraders) concentrations so that digestion did not occur to rapidly for some soluble compounds. Sugar degraders' concentration was selected to be high to ensure rapid consumption of monosaccharides as seen in Figure 4-14. However, as seen in Figure 4-15 it was seen that the sugar degraders' concentration was too high and led to a reduction of degraders' concentration within the ASBR for consequent batches.

Acetate degrader's concentration was selected to be low to demonstrate that acetate is not rapidly consumed to form methane. However, the acetate degraders' concentration increases with each batch, which indicates that the growth rate is too large compared to the decay rate for the acetate degraders. With this increase in acetate degraders for each batch, the consumption rate of the acetate increased as seen in Figure 4-14.

From this it could be noted that it is important to determine the concentration of the degraders in the ASBR initially. In Batstone *et al*. (2004), the initial and final sludge concentrations were not provided,

Stellenbosch University https://scholar.sun.ac.za

however, the Monod specific uptake rate ($k_{m,process}$) and the half saturation constant ($K_{S,process}$) was determined with the use of the ADM1. As seen in the simulation, sludge concentration plays an important role to determine the outcome. A better estimate of sludge concentrations can determined using the ASBR as long as there is adequate data. With the use of soluble component concentrations throughout the batch, the initial sludge concentrations can be determined by minimising the simulated results with the experimental results. From the Batstone *et al*. (2004) study, it was concluded that the VFA concentrations can be used to improve this.

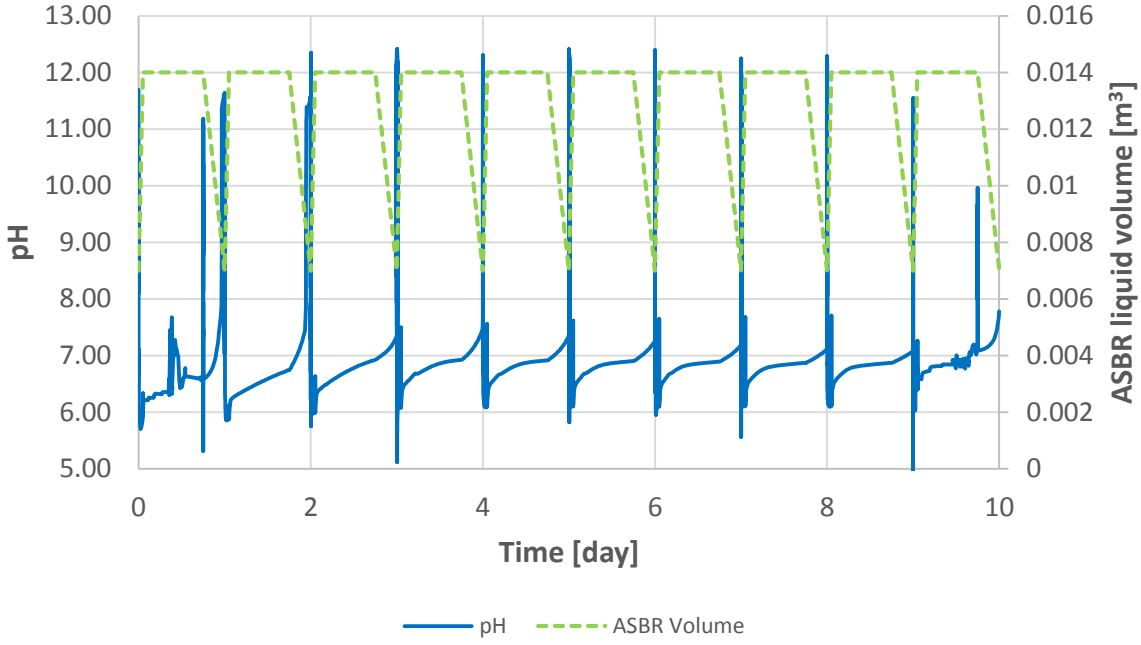

Figure 4-16: Simulated pH with the programmed ADM1 for the synthetic wastewater of this study

Stellenbosch University https://scholar.sun.ac.za

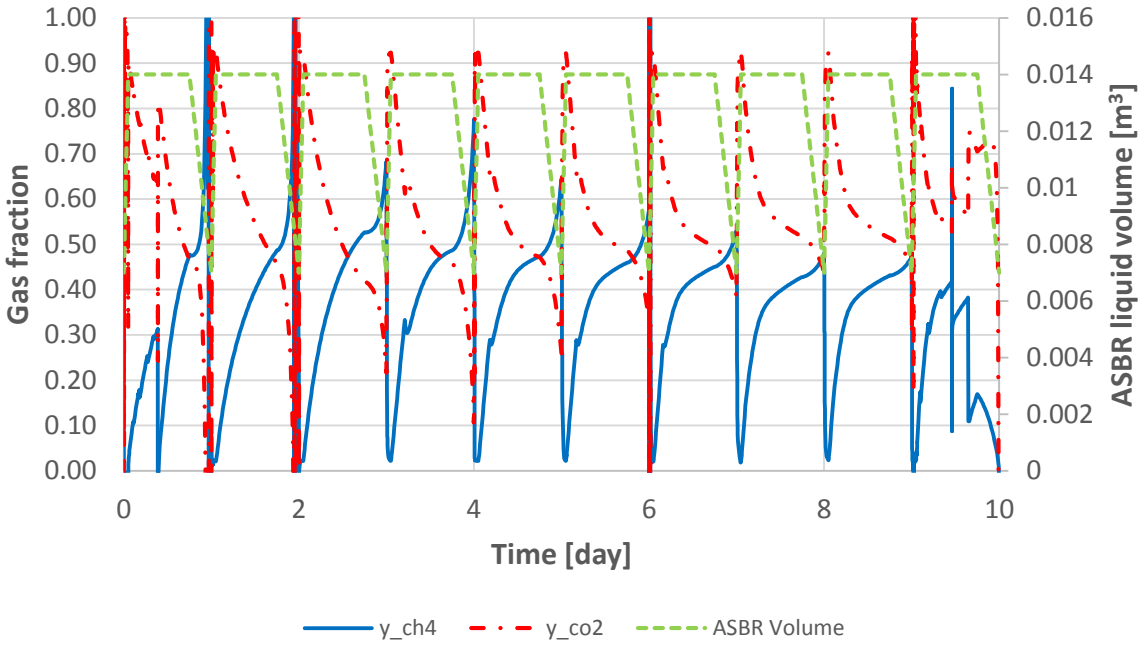

Figure 4-17: Methane and carbon dioxide gas fraction modelled with the programmed ADM1 for the wastewater of this study

As the main aim of the study was to determine whether an ASBR can be operated on in-situ pH control and without additional alkalinity, the simulated pH is presented in Figure 4-16. Due to the high concentration of monosaccharides in the feed substrate and the rapid consumption of these components, the pH in the ASBR seem like is drops quickly. Therefore, it is important to have a quick method to correct the pH of the system for the experimental ASBR. From this is concluded that a strong basic solution should be used for pH to ensure that the pH does not drop too low and possibly damage the anaerobic bacteria. Furthermore, it is noted that the pH of the system increases as the acetate is consumed.

Figure 4-17 illustrates the simulated gas fractions expected in the ASBR. The rapid increase in pH during the decant phase also corresponds to the rapid increase in methane concentration of the biogas. The methane concentration increases from 50 – 75 % at times. This is slightly higher than the methane concentration expected in anaerobic digestion systems of 50 – 70 %.

4.5. Key findings

The Matlab based ADM1 for an ASBR seemed to work. According to the simulation results, a rapid pH drop should occur fairly shorty after feeding the ASBR. Therefore, *in-situ* pH control would be essential during this phase of the process. Sludge concentrations differ from the plant to plant, therefore, the simulated results are only a guideline for what is expected in the ASBR.

Stellenbosch University https://scholar.sun.ac.za

Chapter 5 - Results and discussions I: Long term ASBR operation with *in-situ* pH control

The findings presented in this chapter provides an answer to research objective number two as stated in Chapter 1. The objective was to determine whether an ASBR can be operated without additional alkalinity while relying on *in-situ* pH control. The data obtained and presented in this section was obtained over approximately 230 days of ASBR operation.

5.1. COD reduction and effluent concentration

To determine whether the anaerobic digestion bacteria was functioning under the tested conditions, the COD reduction had to be investigated.

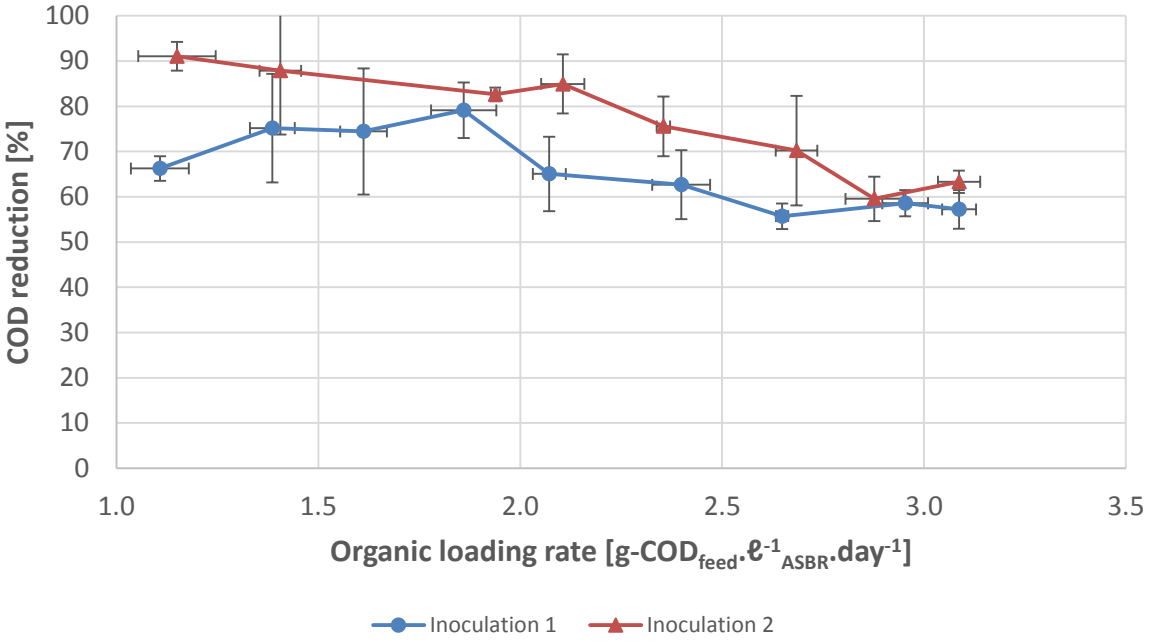

Figure 5-1: COD reduction for various OLRs for two different sludge inoculations for the ASBR treatment of synthetic winery wastewater as presented in Table 3-1. Error bars represent one standard deviation of repeated experiments as described in Chapter 3.8

In Figure 5-1 the COD reduction is presented for various OLRs for two different inoculations as described in Chapter 3. Whereas, in Figure 5-2, the COD removal rate is presented against various OLRs. The COD reduction provides an indicator for how much the COD was reduced between the influent and effluent. The COD removal rate provides an indication of the stability of the ASBR operation.

Stellenbosch University https://scholar.sun.ac.za

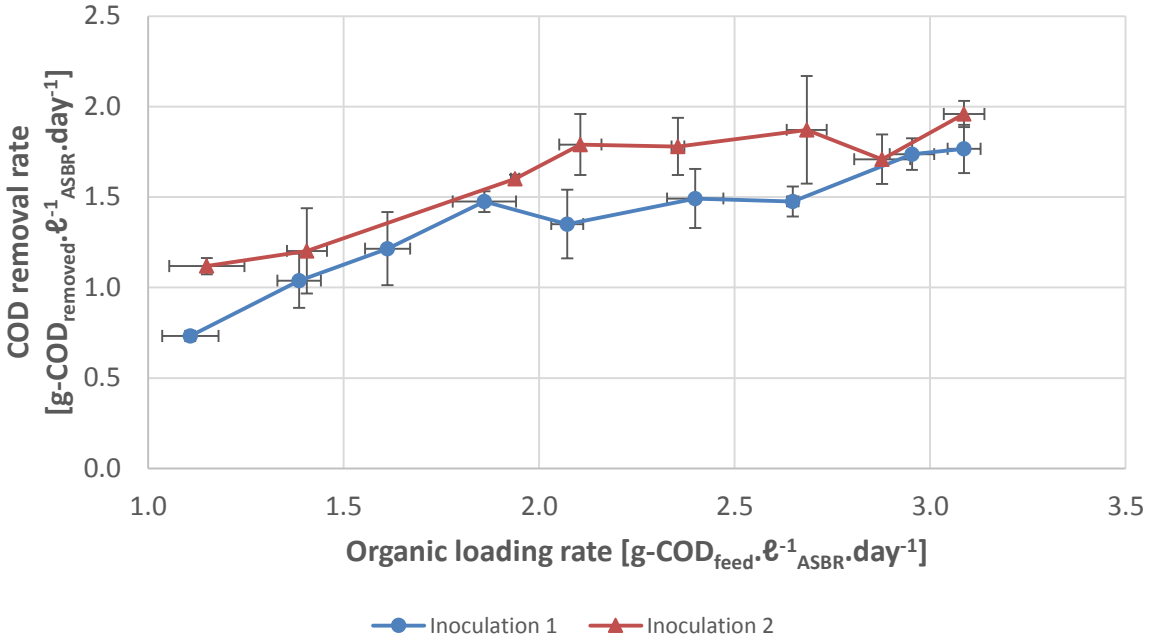

Figure 5-2: COD removal rates for various OLRs of two different sludge inoculations for the ASBR treatment of synthetic winery wastewater as presented in Table 3-1. Error bars represent one standard deviation of repeated experiments as described in Chapter 3.8

The general trend in Figure 5-1 is that the second inoculation had a higher COD reduction when compared with the first inoculation until an OLR of about 2.8 g-COD_{feed}.ℓ^{-1}_{ASBR}.day^{-1} was reached. During the first 30 days of the first inoculation, the feed substrate contained ammonium sulphate while the ASBR was operated with an OLR between 1.1 and 2.1 g-COD_{feed}.ℓ^{-1}_{ASBR}.day^{-1}.

At the set point pH of 7.0, NH_3 was present in the less toxic form of NH_4^+. At a pH of 7.5, NH_4^+ forms about 95% of the total NH_3 present in the solution. The highest OLR of 2.1 g-COD_{feed}.ℓ^{-1}_{ASBR}.day^{-1} at which ammonium sulphate was fed to the ASBR contained a maximum of 1450 mg/ℓ NH_4^+ which would translate to less than 100 mg/ℓ NH_3 in the ASBR at the operating pH of 7.0. According to Gerardi (2003), ammonia concentrations below 200 mg/ℓ can be used as a nitrogen source for the growth of anaerobic bacteria. Therefore, it was believed that reduced COD reduction for inoculation 1 between OLRs of 1.1 and 2.1 g-COD_{feed}.ℓ^{-1}_{ASBR}.day^{-1} was not caused by ammonia toxicity within the ASBR.

From the literature study it is was determined that sulphate reducing bacteria (SRB) has a higher growth rate and higher affinity for acetic acid than acetotrophic methanogens. These two bacteria groups competes for acetic acid and generally results in the formation of hydrogen sulphide gas instead of methane. Sulphate has a low inhibitory effect on methane forming bacteria, however, the H_2S gas

Stellenbosch University https://scholar.sun.ac.za

formed passes through the bacterial cell wall and attacks the enzyme systems which leads to the inhibition of that bacteria (Gerardi, 2003). Therefore, it is believed that the increased sulphate fed with the increased OLR, leads to an increased H_2S formation and resulted in inhibited anaerobic bacteria. Consequently contributing to a reduced COD reduction between the two inoculations. However, the COD reduction increased for inoculation 1 between OLRs of 1.1 and 1.8 g-COD_{feed}.ℓ^{-1}_{ASBR}.day^{-1} which possibly showed an resistance being built up against the H_2S or that gas production was sufficiently high such that the biogas produced scrubbed off the H_2S before it could be absorbed into the other anaerobic bacteria.

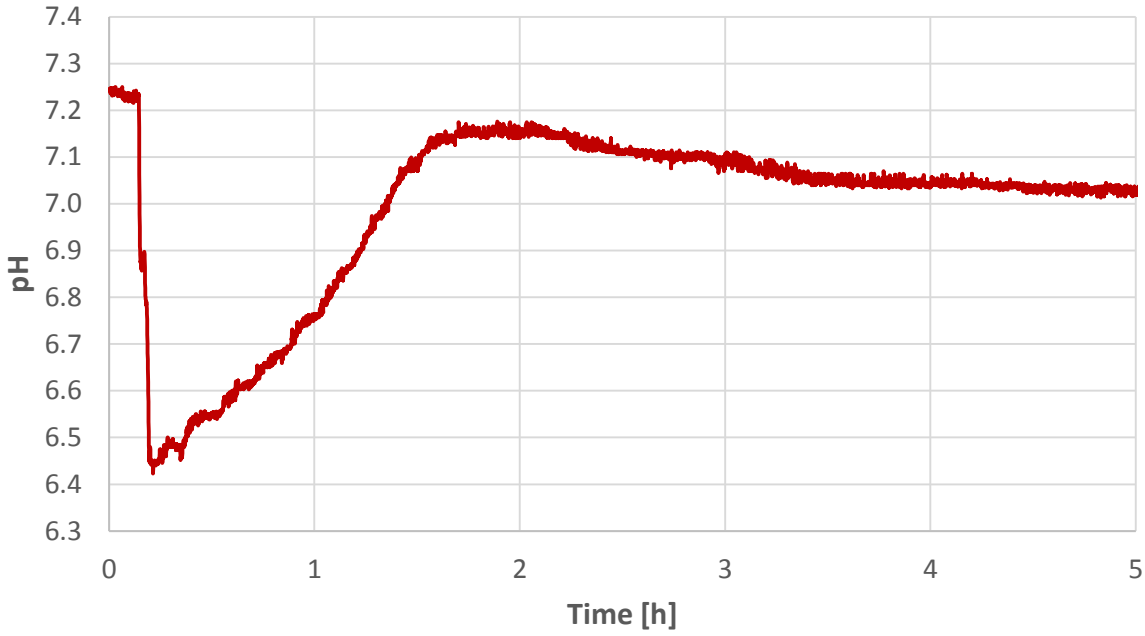

Figure 5-3: Typical pH profile of the first five hours for a batch treated at an OLR of 2.1 g-COD_{feed}.ℓ^{-1}_{ASBR}.day^{-1} (batch 24)

Increasing the OLR for inoculation 1 from 1.8 to 2.1 g-COD_{feed}.ℓ^{-1}_{ASBR}.day^{-1} would increase the amount of ammonium sulphate fed to the ASBR, resulting in an increased amount of H_2S formed. Increasing the OLR also means that more monosaccharides were fed to the ASBR. Due to the rapid consumption of monosaccharides and formation of VFAs via acidogens, the pH of the solution within the ASBR dropped rapidly as shown in Figure 5-3. This was predicted by the ADM1, therefore, *in-situ* pH control was automatically implemented to increase the pH again.

The pH measured during the early stage of the batch was within the optimal range for SRB growth. Additionally, the H_2S which was formed, mostly remains in the toxic form and not in the HS^- form within the solution. At a pH below 6.6, methanogens are generally inhibited, therefore, less biogas was

Stellenbosch University https://scholar.sun.ac.za

produced leading to a reduced scrubbing effect and allows H_2S to absorb into anaerobic bacteria. Thereby, resulting in a reduced COD reduction as seen by the OLR of 2.1 g-COD_{feed}.ℓ^{-1}_{ASBR}.day^{-1}.

After removing the ammonium sulphate from the feed substrate for inoculation 1, the ASBR was allowed to reach a stable COD reduction, which took 14 days, before further COD reduction data was included in Figure 5-1.

Between OLRs of 1.2 and 2.1 g-COD_{feed}.ℓ^{-1}_{ASBR}.day^{-1} for inoculation 2, the COD reduction dropped from 90% to 84%, however, the COD removal rate continued increasing linearly which indicated that ASBR was stable and not overloaded. Increasing the OLR beyond 2.1 to 2.8 g-COD_{feed}.ℓ^{-1}_{ASBR}.day^{-1} showed the removal rate plateaued before slightly increasing and then decreasing again. This plateau stage indicates that the ASBR was operating under unstable and possible overloaded conditions for the amount of sludge in the system. Surprisingly, above an OLR of 2.8 g-COD_{feed}.ℓ^{-1}_{ASBR}.day^{-1}, the COD removal rate increased linearly again indicating that the ASBR operation was stable and not overloaded. The small standard deviation for COD reduction as shown by the error bars at this high OLR provides support that the ASBR is operating under stable conditions. At this stage, it was known that the ASBR can operate with *in-situ* pH control, without additional alkalinity while having a VDF of 0.5. However, it still was not known whether it can produce an effluent with a COD within the legal limitations for disposal via irrigation.

To increase the COD reduction for higher OLRs, more sludge can be added to the ASBR to decrease the F:M ratio at the start of the ASBR cycle. This means that there will be more microorganisms for the same amount of food (substrate). The main aim is to increase the methanogens population, so that acetic acid is converted to biogas at a higher rate, thereby, decreasing the COD within the ASBR faster.

Stellenbosch University https://scholar.sun.ac.za

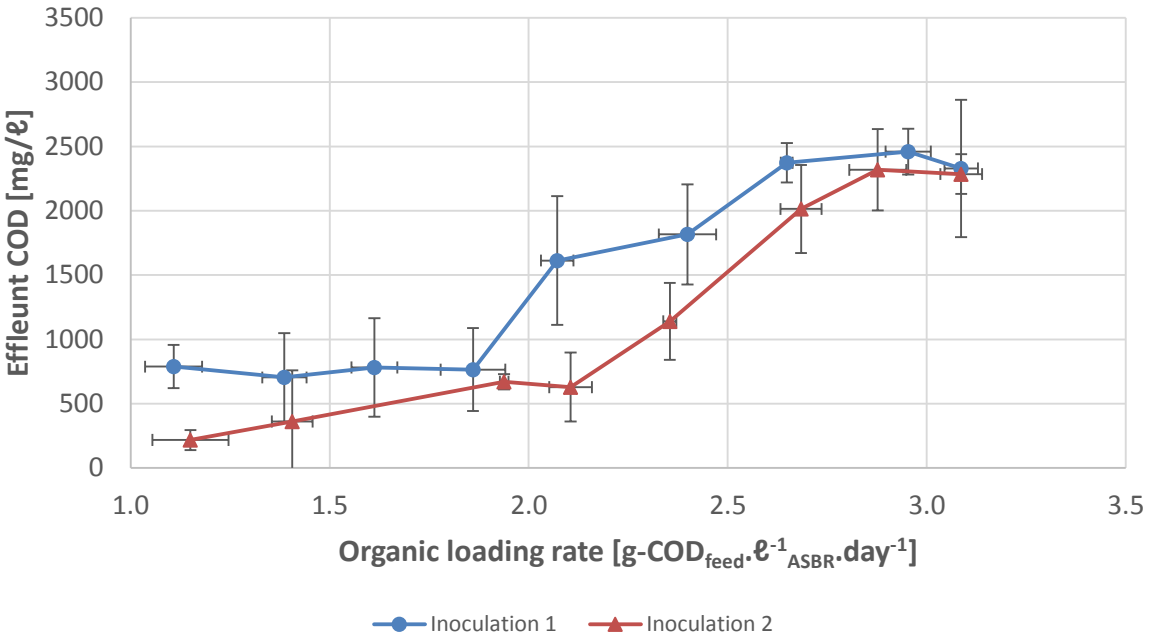

Figure 5-4: Measured COD of the effluent from the ASBR for various OLRs of two different sludge inoculations for the treatment of synthetic winery wastewater as presented in Table 3-1. Error bars represent one standard deviation of repeated experiments as described in Chapter 3.8

Figure 5-4 presents the measured effluent COD from the ASBR after a batch has been treated. To dispose wastewater via irrigation, the COD has to be less than 5000 mg/ℓ when the maximum volume disposed is 50 m^3/day. Furthermore, the maximum COD of wastewater to be irrigated must be below 400 mg/ℓ when the volume irrigated is between 50 and 500 m^3/day (van Schoor, 2005). Therefore, the ASBR effluent from both inoculations can be irrigated when operating between OLRs of 1.1 and 3.1 g-COD$_{feed}$.ℓ$^{-1}$$_{ASBR}$.day^{-1} provided less than 50 m^3/day is disposed. However, if more than 50 m^3/day needs to be disposed, this method with its current operational setup can only work for an OLR of 1.1 g-COD$_{feed}$.ℓ$^{-1}$$_{ASBR}$.day^{-1} if the sludge has not been inhibited or damaged as a result of ammonium sulphate. For higher OLRs, storage tanks can be used to store the treated effluent such that a maximum of 50 m^3/day can be disposed of on other days. However, a feasibility study will need to be performed to determine whether it is feasible to operate a large scale treatment plant in such a manner. In the suggested study, the size of the plant, the amount of wastewater produced and efficiency of the treatment would need to be taken into account.

The compounds which make up the COD of the effluent is very different to that of the feed substrate. The feed substrate's COD was made up of approximately 92% monosaccharides (glucose and fructose). These monosaccharides are quickly digested to form VFAs as indicated with the rapid pH drop in Figure 5-3. These VFAs are further converted to acetic acid, which was further used to produce biogas. As the

Stellenbosch University https://scholar.sun.ac.za

method attempted to analyse the various VFAs within the effluent did not work correctly, the individual concentrations of VFAs could not be determined. However, several samples were taken in the first 5 minutes of the react phase and was tested for monosaccharides with high pressure liquid chromatography (HPLC). However, HPLC could not accurately detect the monosaccharides concentrations below 50 ppm. This indicated that the monosaccharides were rapidly digested. However, it was unsure whether ethanol had been formed during the digestion. Therefore, the COD of the effluent was only considered to be made up of acetic, propionic, butyric and valeric acid.

The general trend for both inoculations was that the effluent COD increases with increasing OLR while operating with a fixed HRT. The F:M ratio increases with increasing OLR. With the digestion rate of the microorganisms remaining constant as well as the time they have to digest, it means that a smaller portion of organic components will be consumed resulting in a reduced COD reduction for increased OLR. This was evident in this study.

To decrease the effluent COD and increase the COD reduction, more sludge per volume of ASBR needs to be added. More sludge will mean there are more methanogens, which is what is actually required to reduce acetic acid to biogas resulting in a reduced COD. However, as winery wastewater is seasonal and not consistent in quality and quantity during that period, there is a risk that some of the sludge might remain dormant and not reduce the COD as required. Some sludge might also remain dormant while operating under low OLRs due to a lack of feed substrate.

5.2. Biogas production and composition

The COD reduction provides an indication that the anaerobic digestion process is occurring, however, it does not provide insight into the biogas production. Therefore, biogas production and composition was investigated to provide an idea of the methanogens activity within the ASBR.

Stellenbosch University https://scholar.sun.ac.za

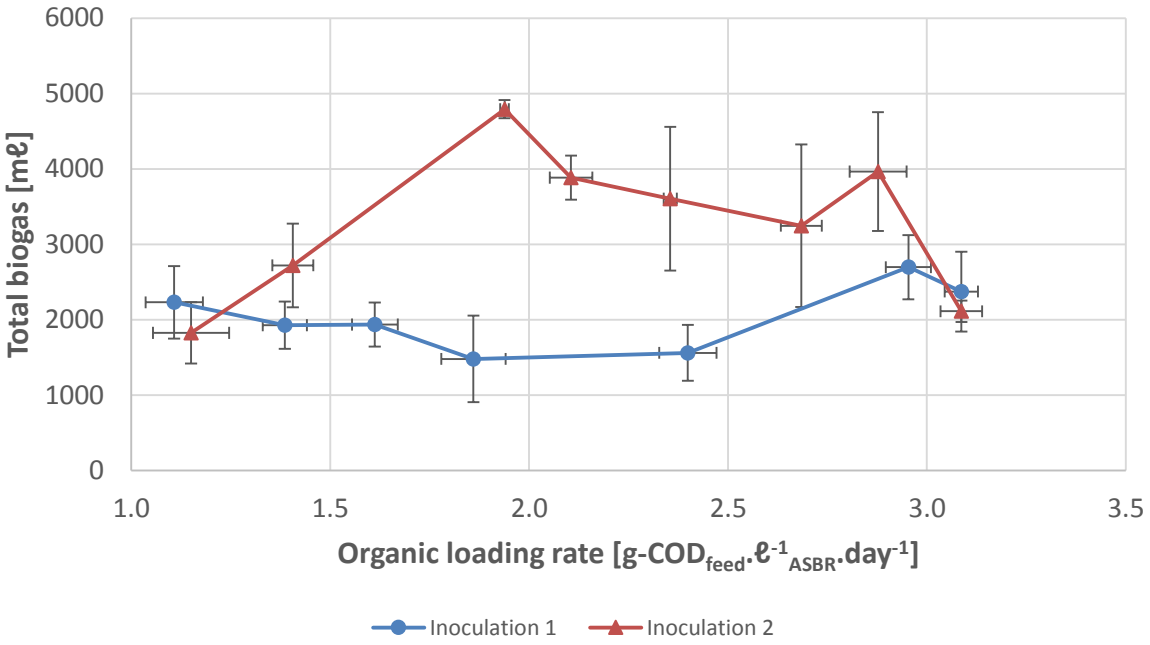

Figure 5-5: Total measured biogas production for two different inoculations while operating at various OLRs for the treatment of synthetic winery wastewater as presented in Table 3-1. Error bars represent one standard deviation of repeated experiments as described in Chapter 3.8

Figure 5-5 presents the total measured biogas production for various OLRs. It needs to be noted that this was gas that has left the ASBR setup and does not include that which dissolved in the water. For inoculation 1, the total biogas produced was generally very low when compared to inoculation two.

Inoculation 1 had ammonium sulphate in the feed between OLRs of 1.1 and 2.1 g-COD$_{feed}$.ℓ$^{-1}_{ASBR}$.day^{-1}. SRB competes with acetotrophic methanogens for acetic acid to produce H_2S gas. The H_2S could not be detected with the GC used for biogas analysis, however, the biogas did have a distinct smell of rotten eggs which was considered to be H_2S. The reduced biogas production of inoculation 1 was to blame on the ammonium sulphate fed to the ASBR. However, after it was removed, the biogas production remained low and it is believed that the methanogens are dormant or dead. The reason that it was considered to be in a dormant state, was that once the feed substrate was changed from type A to B and the OLR was increased to 2.4 g-COD$_{feed}$.ℓ$^{-1}_{ASBR}$.day^{-1}, the biogas production picked up, which indicates more active methanogens. Therefore, it was considered that some methanogens might become dormant rather than die when overdosed with ammonium sulphate.

Inoculation 2, indicates that under the operated conditions and sludge population, an OLR of 1.9 g-COD$_{feed}$.ℓ$^{-1}_{ASBR}$.day^{-1} is the optimal loading to operate this ASBR setup if maximum biogas production is the aim. The total biogas produced increased as the OLR increased from 1.1 to

Stellenbosch University https://scholar.sun.ac.za

1.9 g-COD_{feed}.ℓ^{-1}_{ASBR}.day^{-1}, which is supported by the increasing COD removal rate and constant COD reduction. The drop in biogas and large variation of biogas produced at higher OLRs also coincides with an unsteady state system where the COD removal rate plateaued.

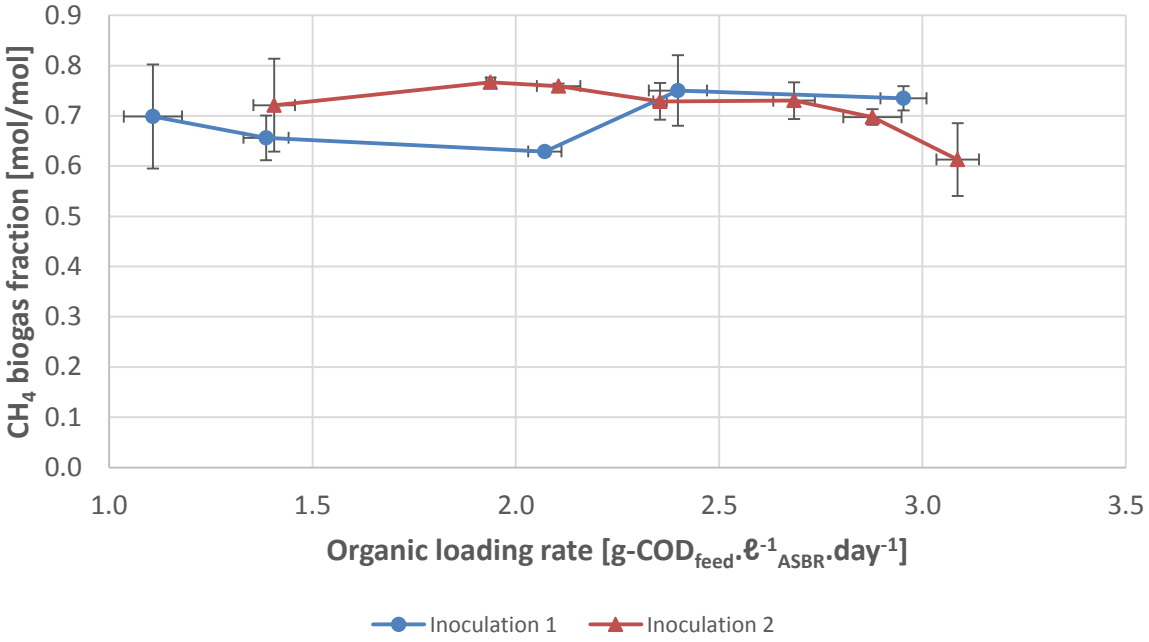

Figure 5-6: Methane fraction of the biogas produced with ASBR of two inoculations while operating at various OLRs as presented in Table 3-1. Error bars represent one standard deviation of repeated experiments as described in Chapter 3.8

The methane fraction of the biogas produced is presented in Figure 5-6, whereas the carbon dioxide and nitrogen fractions are illustrated in Figure 5-7 and Figure 5-8, respectively.

The average methane fraction was lower for inoculation 1 when the feed substrate contained ammonium sulphate between OLRs of 1.1 and 2.1 g-COD_{feed}.ℓ^{-1}_{ASBR}.day^{-1}. This was as a direct result of SRB competing with aceticlastic methanogens for acetic acid as substrate. The SRBs generally have preference for acetic acid consumption, therefore, the amount of produced methane is reduced. However, methane can still be formed during hydrogenotrophic methanogenesis as long as the hydrogen partial pressure remains low. Therefore, methane was evident in the biogas samples.

Inoculation 1 produced a biogas with a higher average methane fraction compared to inoculation 2 at OLRs above 2.4 g-COD_{feed}.ℓ^{-1}_{ASBR}.day^{-1}, however, the total biogas produced was considerably less. This would result in a less energy being recovered from the biogas.

Stellenbosch University https://scholar.sun.ac.za

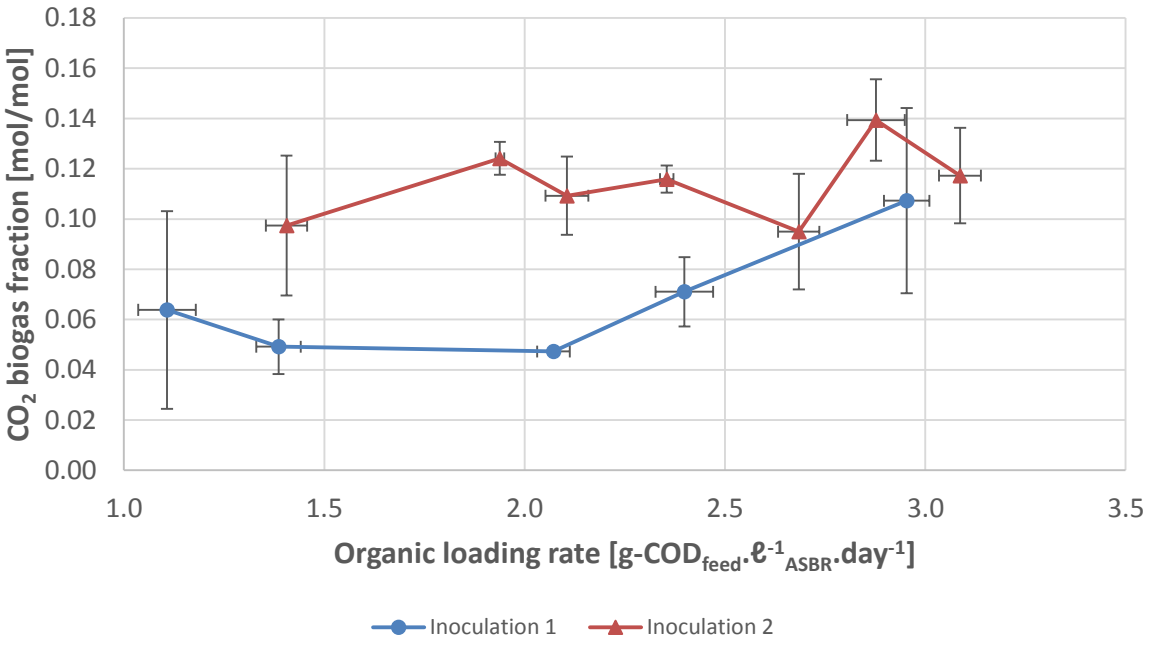

Figure 5-7: Carbon dioxide fraction of the biogas produced with ASBR of two inoculations while operating at various OLRs as presented in Table 3-1. Error bars represent one standard deviation of repeated experiments as described in Chapter 3.8

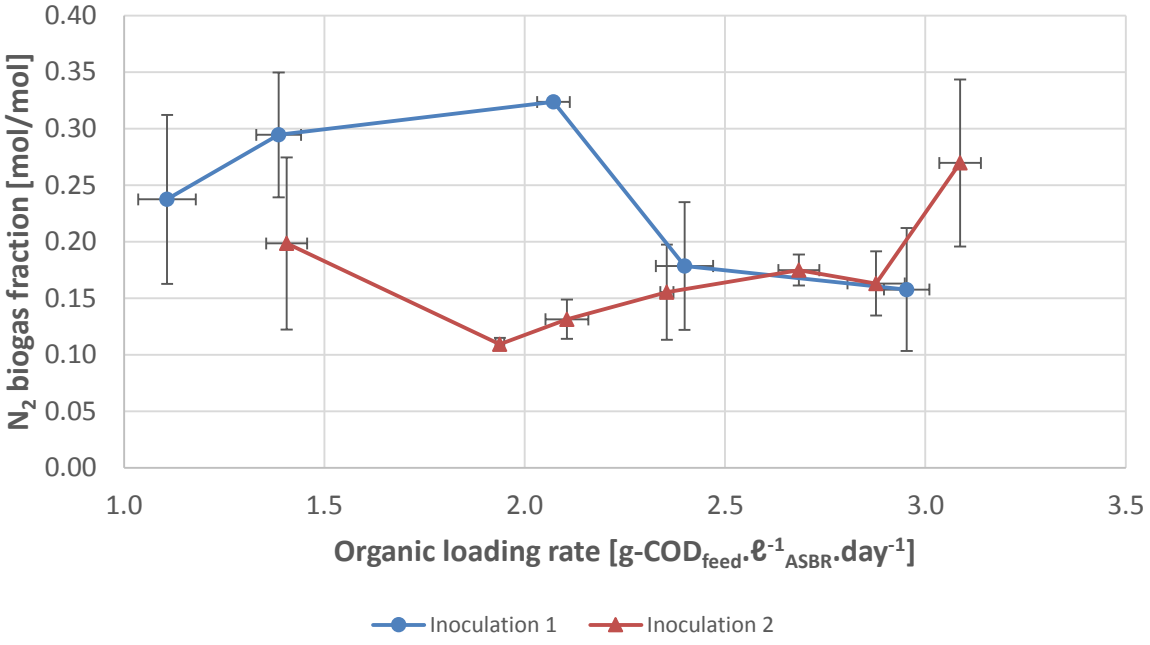

Figure 5-8: Nitrogen fraction of the biogas produced with ASBR of two inoculations while operating at various OLRs as presented in Table 3-1. Error bars represent one standard deviation of repeated experiments as described in Chapter 3.8

Stellenbosch University https://scholar.sun.ac.za

The large variation in biogas composition at the lower OLRs can be as a result of the sludge not settling in long enough. These experiments were performed shortly after the ASBR was inoculated and could indicate that a longer settling in time is required.

The methane fraction of biogas is usually considered about 70% of the gas with the balance being carbon dioxide for anaerobic digestion systems. The methane fraction compares well to this standard, however, the carbon dioxide fraction is considerably less. Due to the VDF of 0.5, more of the produced carbon dioxide was able to dissolve into the solution to form bicarbonate, thereby reducing the amount of biogas produced as well as the carbon dioxide fraction. Essentially this means that the biogas is upgraded in terms of its calorific value due to more carbon dioxide dissolving in the solution. However, this will be discussed later with the alkalinity results in chapter 5.3.

Yeast extract was used as a nitrogen source for the bacteria. The nitrogen was fed in excess and the sludge contained denitrification bacteria which was concluded from the high nitrogen concentration found in the gas analysis. The nitrogen fraction for inoculation 1 while the system was being fed ammonium sulphate was high (0.24 to 0.33 fraction nitrogen) due to the amount of gas being produced being slightly less than that of inoculation 2.

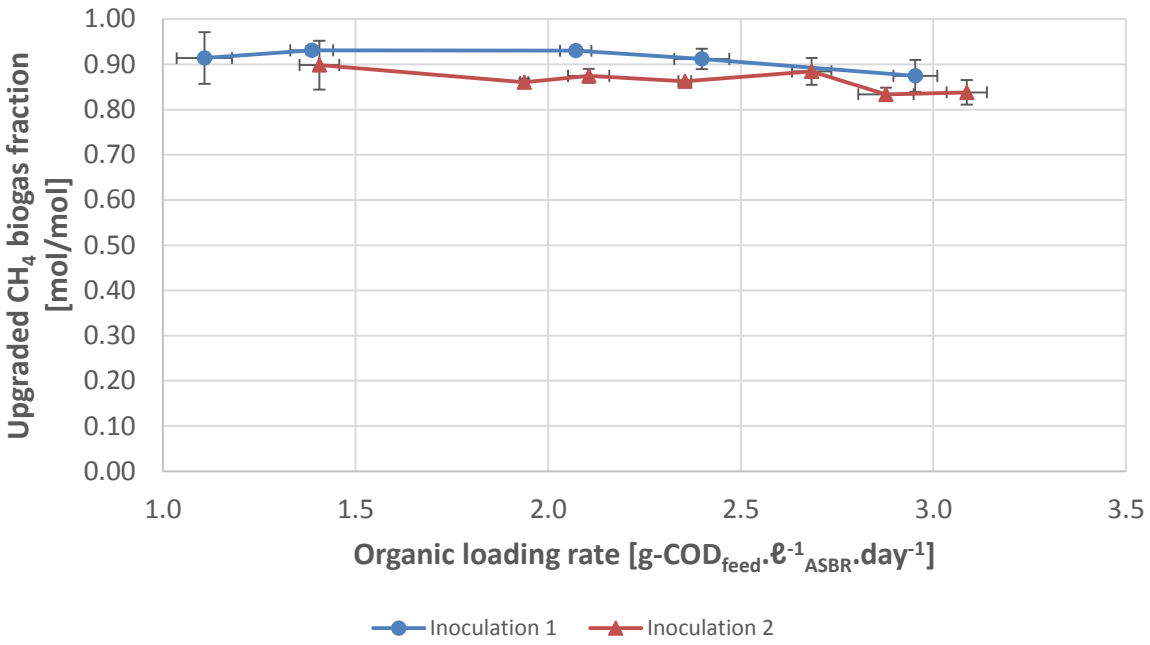

Figure 5-9: Methane biogas fraction when the biogas composition was normalised with only the produced methane and carbon dioxide for two different inoculations as presented in Table 3-1. Error bars represent one standard deviation of repeated experiments as described in Chapter 3.8

Stellenbosch University https://scholar.sun.ac.za

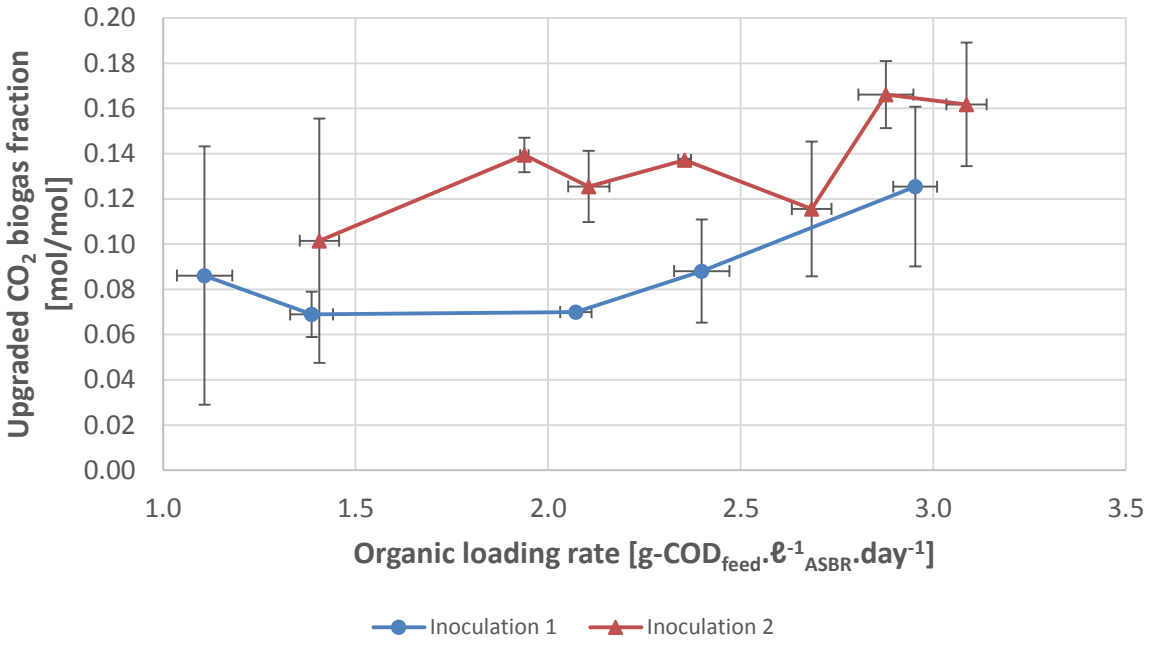

Figure 5-10: Carbon dioxide biogas fraction when the biogas composition was normalised with only the produced methane and carbon dioxide for two different inoculations as presented in Table 3-1. Error bars represent one standard deviation of repeated experiments as described in Chapter 3.8

If the ASBR were to operate without excess nitrogen for bacteria growth, there should almost be zero nitrogen in the biogas. Therefore, the so called upgraded biogas fraction between methane and carbon dioxide and the exclusion of nitrogen is presented in Figure 5-9 and Figure 5-10, respectively.

Upgrading the biogas, allows the methane to fraction to increase above 80%, thereby making it more economical to use the biogas for reheating purposes. For inoculation 1, the methane fraction was in excess of 90% during the OLRs of 1.1 and 2.1 g-COD_{feed}.ℓ^{-1}_{ASBR}.day^{-1}. This was due to the methanogens inhibition and resulted in less carbon dioxide being formed (from aceticlastic methanogens). The carbon dioxide would go to the biogas phase instead of being used for bicarbonate. Therefore, if the ASBR was allowed to treat the batch longer, more carbon dioxide would have formed which would have resulted in the methane fraction being reduced.

Stellenbosch University https://scholar.sun.ac.za

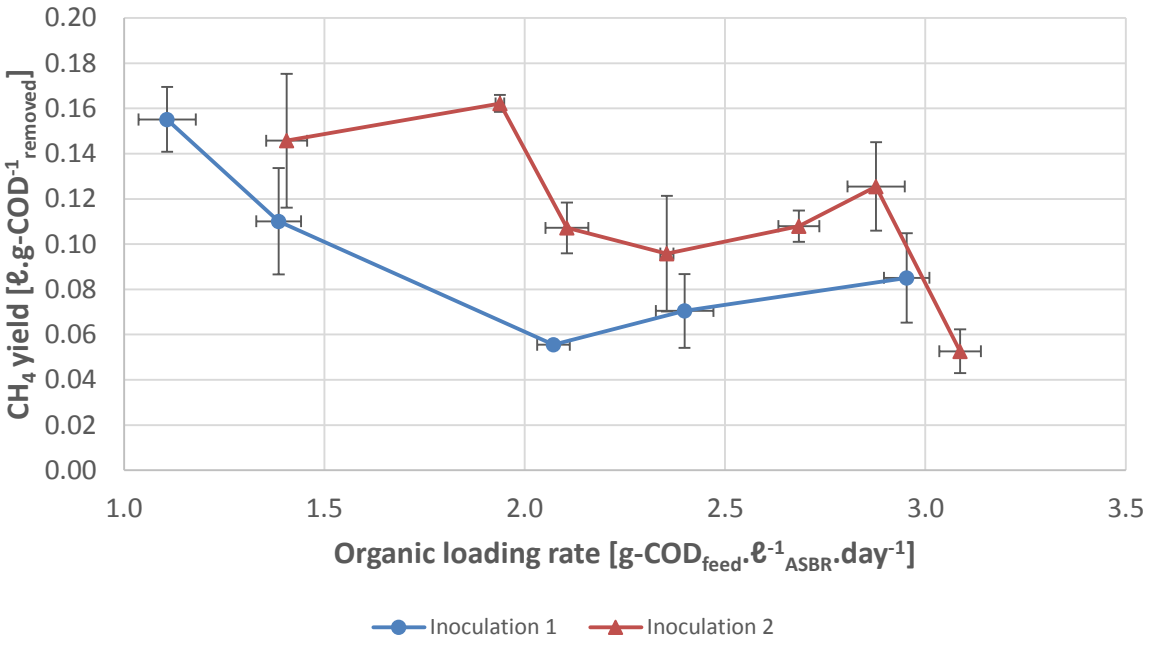

Figure 5-11: Methane yield of the produced biogas for both inoculations while operating at various OLRs as presented in Table 3-1. Error bars represent one standard deviation of repeated experiments as described in Chapter 3.8

The methane yield and productivity forms a normalised unit of measure to compare the performance of one anaerobic digestion type system with another. The methane yield was used to determine how well organic compounds was converted to methane. The theoretical maximum methane yield from glucose consumption is 0.35 ℓ.g-$COD^{-1}_{removed}$. As seen in Figure 5-11, the methane yield is rather poor throughout all the OLRs when compared to the theoretical maximum. The optimum methane yield for inoculation 2 was obtained at an OLR of 1.9 g-COD_{feed}.$ℓ^{-1}_{ASBR}$.day^{-1}. This indicates the ASBR contained the correct amount of sludge for that specific OLR and the type of substrate fed to the ASBR. The sudden drop of methane yield for inoculation 2 at the OLR 3.1 g-COD_{feed}.$ℓ^{-1}_{ASBR}$.day^{-1} indicates that the ASBR could possibly be overloaded.

For inoculation 1, the inhibition of the aceticlastic methanogens can be seen between OLRs of 1.1 and 2.1 g-COD_{feed}.$ℓ^{-1}_{ASBR}$.day^{-1} due to the reduction of methane yield. The methane yield increased again when the feed substrate did not contain ammonium sulphate, therefore, less inhibition occurred. However, as the methane yield never returned to that of the inoculation 2, it is thought that some methanogens died.

Stellenbosch University https://scholar.sun.ac.za

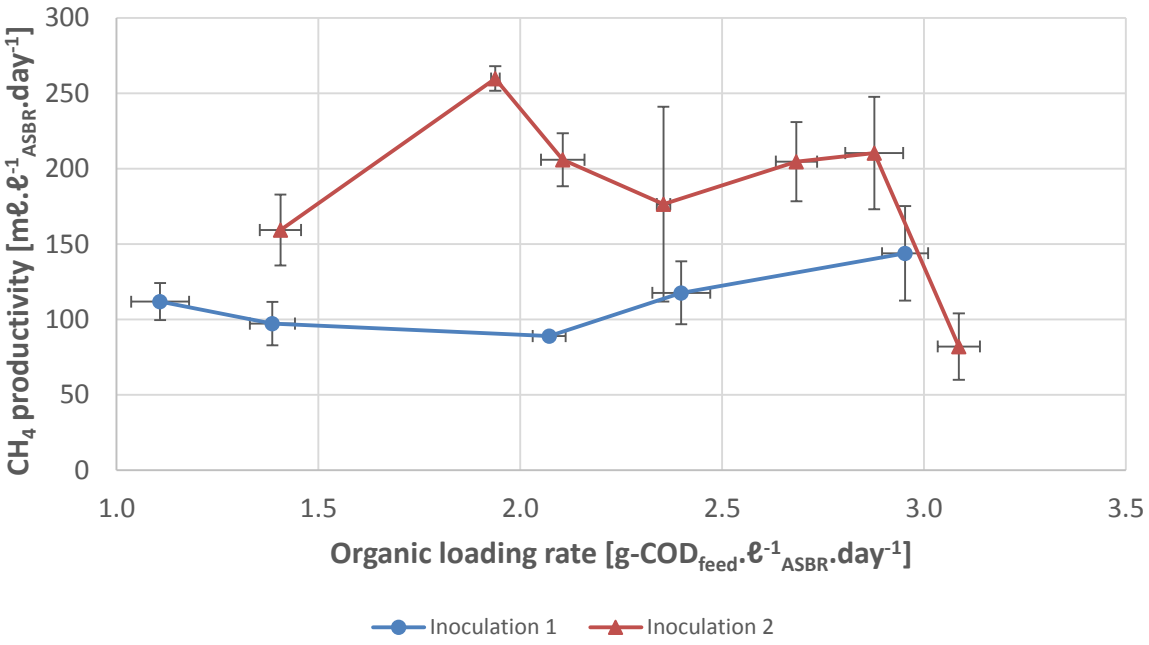

Figure 5-12: Methane productivity for two inoculations while operating at various OLRs as presented in Table 3-1. Error bars represent one standard deviation of repeated experiments as described in Chapter 3.8

Methane productivity provides a useful way to normalise digester size and treatment time. As noted above, the methane productivity was low for inoculation 1 due to the damaged and inhibited methanogens as seen in Figure 5-12. The peak methane productivity for inoculation 2 occurred at an OLR of 1.9 g-COD_{feed}.ℓ^{-1}_{ASBR}.day^{-1} and supports the statement that it was the optimum point to operate this ASBR at, given the feed substrate and sludge amount.

5.3. Alkalinity of the effluent

Alkalinity forms an important aspect with regards to evaluating the stability of an anaerobic digester. For this study, total, partial and intermediate alkalinity were determined for the effluent of the ASBR and can be found below in Figure 5-13, Figure 5-14 and Figure 5-15, respectively. The calculated Ripley ratio (IA/PA) of the effluent, which provides a ratio of VFAs to bicarbonate, is shown Figure 5-16.

Stellenbosch University https://scholar.sun.ac.za

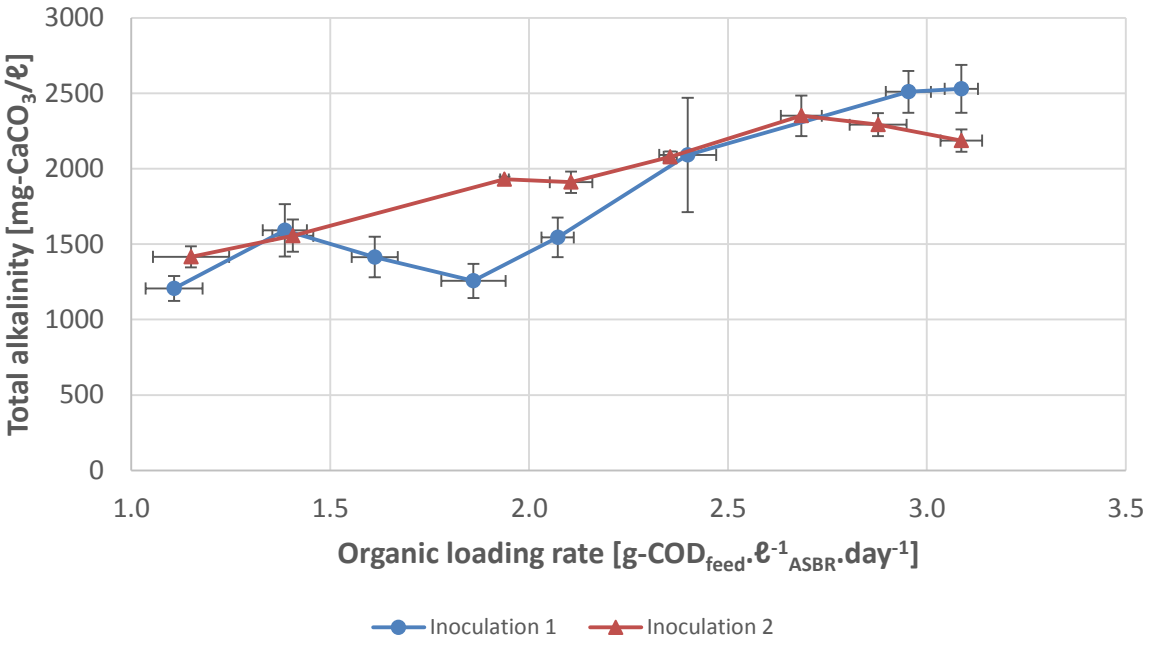

Figure 5-13: Measured total alkalinity (TA) of the effluent from the ASBR for various OLRs for two inoculations while treating synthetic winery wastewater as presented in Table 3-1. Error bars represent one standard deviation of repeated experiments as described in Chapter 3.8

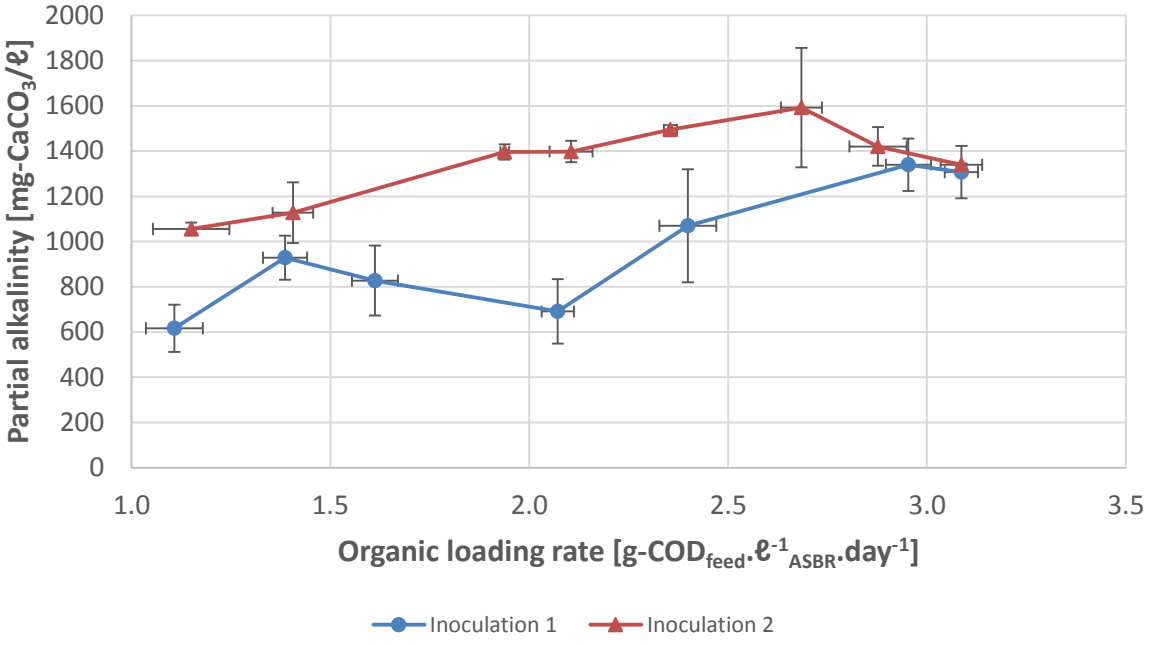

Figure 5-14: Measured partial alkalinity (PA) of the effluent from the ASBR for various OLRs for two inoculations while treating synthetic winery wastewater as presented in Table 3-1. Error bars represent one standard deviation of repeated experiments as described in Chapter 3.8

Stellenbosch University https://scholar.sun.ac.za

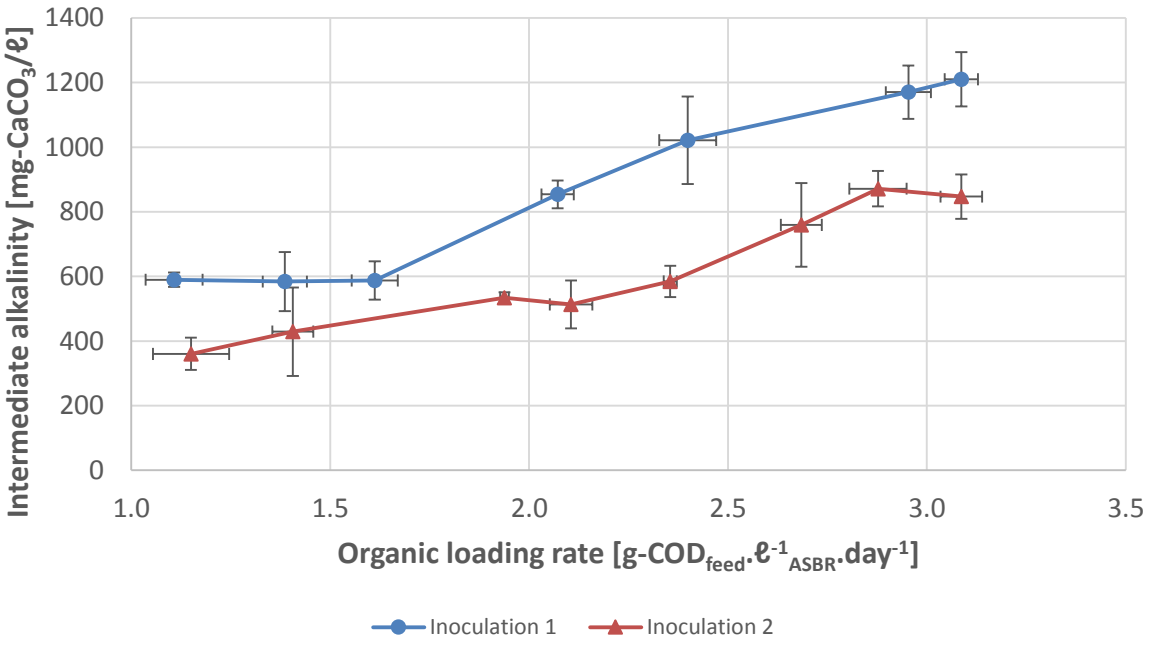

Figure 5-15: Measured intermediate alkalinity (IA) of the effluent from the ASBR for various OLRs for two inoculations while treating synthetic winery wastewater as presented in Table 3-1. Error bars represent one standard deviation of repeated experiments as described in Chapter 3.8

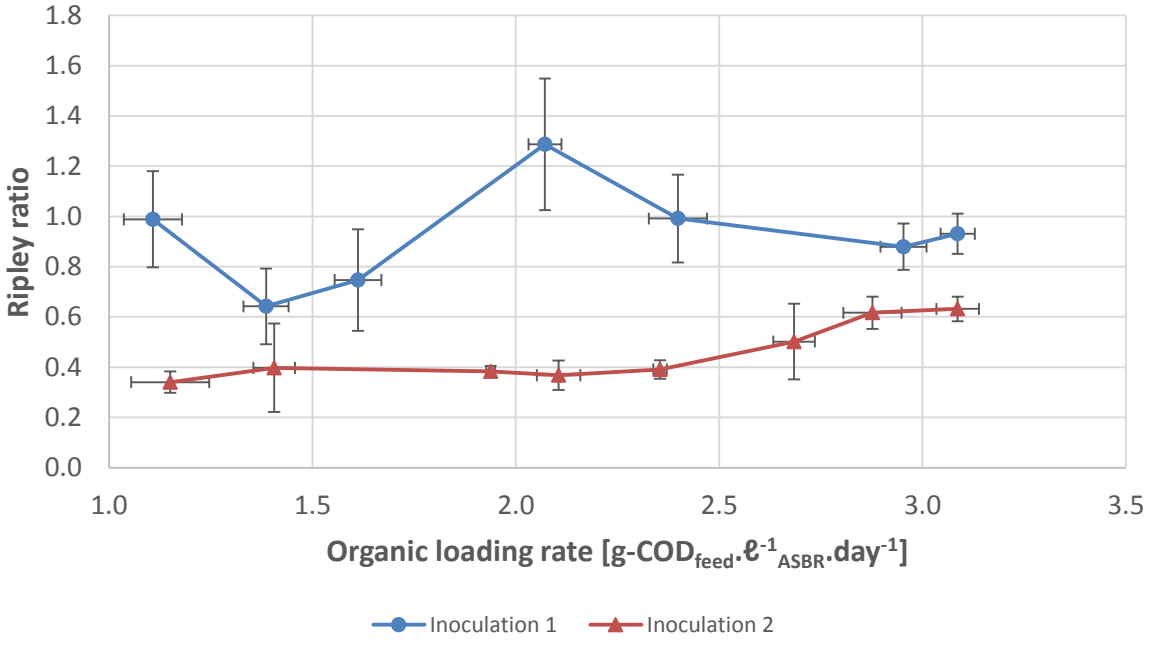

Figure 5-16: Calculated Ripley ratio (IA/PA) of the effluent from the ASBR for various OLRs for two inoculations while treating synthetic winery wastewater as presented in Table 3-1. Error bars represent one standard deviation of repeated experiments as described in Chapter 3.8

Stellenbosch University https://scholar.sun.ac.za

The substrate fed to the ASBR contained no added alkalinity. The bicarbonate alkalinity formed in the ASBR came from the digestion process of the organic compounds. Due to the VDF of 0.5, when the ASBR is decanted at the end of a batch, the quantity of alkalinity is halved when the ASBR is filled up for the next batch. The drop in pH presented in Figure 5-3 occurs due to two key operating aspects. With the large amount of monosaccharides fed into the ASBR, rapid formation of VFAs occur which leads to a drop in pH as there is a lack of alkalinity due to a VDF of 0.5.

The general trend for total and intermediate alkalinity was that it increases for increasing OLRs. This was more notable for inoculation 2. The total alkalinity is the sum of the partial and intermediate alkalinity, where the partial alkalinity was an indication of the bicarbonate and carbonates, and the intermediate alkalinity provides an indication of the VFAs. As previously stated, with increasing OLR, the COD reduction decreases due to more VFAs being left in the ASBR resulting from a constant digestion rate over a fixed time period. Therefore, the intermediate alkalinity has to increase resulting in the increase of total alkalinity of the effluent from the ASBR.

The formation of bicarbonate to make up the partial alkalinity comes from the anaerobic digestion process. During the anaerobic digestion process, CO_2 was formed from the acidogenesis of monosaccharides and methanogenesis of acetic acid. As the sludge was generally at the bottom of the ASBR, this CO_2 formed has to pass through the liquid into the headspace of the ASBR. An undetermined amount of CO_2 dissolved in water and forms carbonic acid, which further dissociates into bicarbonate and carbonate depending on the pH of the solution. With the pH correction to near 7.0, most of it would be in the bicarbonate form in the ASBR. With inoculation 2, the partial alkalinity remains fairly constant between 1100 and 1600 mg-$CaCO_3$/ℓ for all OLRs evaluated. This can provide an indication the ASBR was operating such that the solubility limit of CO_2 is reached under the given operating environment.

For inoculation 1, the partial alkalinity dropped from 950 to 800 mg-$CaCO_3$/ℓ when increasing the OLR from 1.4 to 1.6 g-COD_{feed}.$ℓ^{-1}_{ASBR}$.day^{-1} which coincides with the period that the ASBR feed substrate contained ammonia sulphate. This decrease in partial alkalinity provides an early indicator for the inhibition of anaerobic bacteria in the ASBR for inoculation 1. Bicarbonate still had to be produced during these batches for the partial alkalinity to remain constant as the OLR increased further to 2.4 g-COD_{feed}.$ℓ^{-1}_{ASBR}$.day^{-1}. As the intermediate alkalinity increased and the COD was reduced, it meant that VFAs were being formed along with CO_2 as a by-product. This CO_2 can then dissolve into the water and form bicarbonate which maintains the partial alkalinity at the measured level. Therefore, it was the methanogens that had the first signs of inhibition occurring in the ASBR.

Stellenbosch University https://scholar.sun.ac.za

The Ripley ratio was used to provide a ratio between the intermediate and partial alkalinity and provide insight into the stability of the digester. According to Drosg (2013), the Ripley ratio is not comparable between various plants, but a Ripley ratio in stable anaerobic digesters is regarded as anything below 0.3, however, stable operation has been reported for ratios of up to 0.8. According to this, inoculation 1 was operating under unstable conditions which has been previously attributed to the OLRs of 1.1 to 2.1 g-COD_{feed}.ℓ^{-1}_{ASBR}.day^{-1} containing ammonium sulphate. At OLRs of 2.9 to 3.1 g-COD_{feed}.ℓ^{-1}_{ASBR}.day^{-1} for inoculation 1, the Ripley ratio reduced to 0.9 and seemed like the ASBR was operating stably again. At the same OLRs, inoculation 2, had a Ripley ratio of 0.6 which indicates that the Ripley ratio was not comparable for systems that operated under different conditions, i.e. different substrate composition, and possibly resulting in different anaerobic bacteria populations.

Inoculation 2 operated under stable conditions between two different ranges of OLRs if the COD removal rate (Figure 5-2) is considered. The first OLR range being from 1.4 to 2.1 g-COD_{feed}.ℓ^{-1}_{ASBR}.day^{-1}, and the second being between 2.8 and 3.1 g-COD_{feed}.ℓ^{-1}_{ASBR}.day^{-1}. This range also coincides with the region where the Ripley ratio remains relatively constant. The first section being approximately 0.4 and the second section 0.65. The Ripley ratio varies in the OLR range between these two sections, which is also the region that the COD removal rate plateaus. This suggests that the sludge was adapting to changing conditions, namely the change in OLR, so that it can settle at a new pseudo-steady state environment.

5.4. Required KOH dosing for *in-situ* pH control

The lab scale ASBR unit used in this study was operated with pH control. The pH control only allows *in-situ* dosing such that the pH was increased to 0.1 below the set point pH. This was to prevent the pH controller from overshooting the set point. As indicated from the literature study, pH plays an important part of the anaerobic digestion process. As seen in Figure 5-3, the rapid consumption of monosaccharides by acidogens rapidly reduces the pH of the system due to a lack of alkalinity at the start of a batch. As pH dropped to almost 6.4, it has to be corrected to at least above 6.6 (preferably near 7.0) so that the pH sensitive methanogens can consume acetic acid to produce biogas and reduce the COD.

The KOH dosed in this study was presented as a mass per ASBR working volume in Figure 5-17 below. For inoculation 2, the general trend was that more KOH had to be dosed with increasing OLR. The fed monosaccharide quantity increased with increasing OLR, however, the bicarbonate alkalinity almost remained constant. This meant that more VFAs could be formed, however, with the bicarbonate

Stellenbosch University https://scholar.sun.ac.za

alkalinity remaining constant, more KOH had to be dosed for pH control. This data is useful to help predict operating costs of a large scale ASBR that will operate under similar conditions.

For inoculation 1, the average amount of the KOH added drops significantly at OLRs of 1.4 to 1.8 g-COD_{feed}.ℓ^{-1}_{ASBR}.day^{-1}. From OLRs 2.1 to 3.1 g-COD_{feed}.ℓ^{-1}_{ASBR}.day^{-1}, more KOH is dosed in comparison to inoculation 2. Inoculation 1 had a lower partial alkalinity during this period compared to inoculation 2, which means that it had a lowered buffering capacity to prevent a pH drop due to VFA formation, therefore, required more KOH to be dosed.

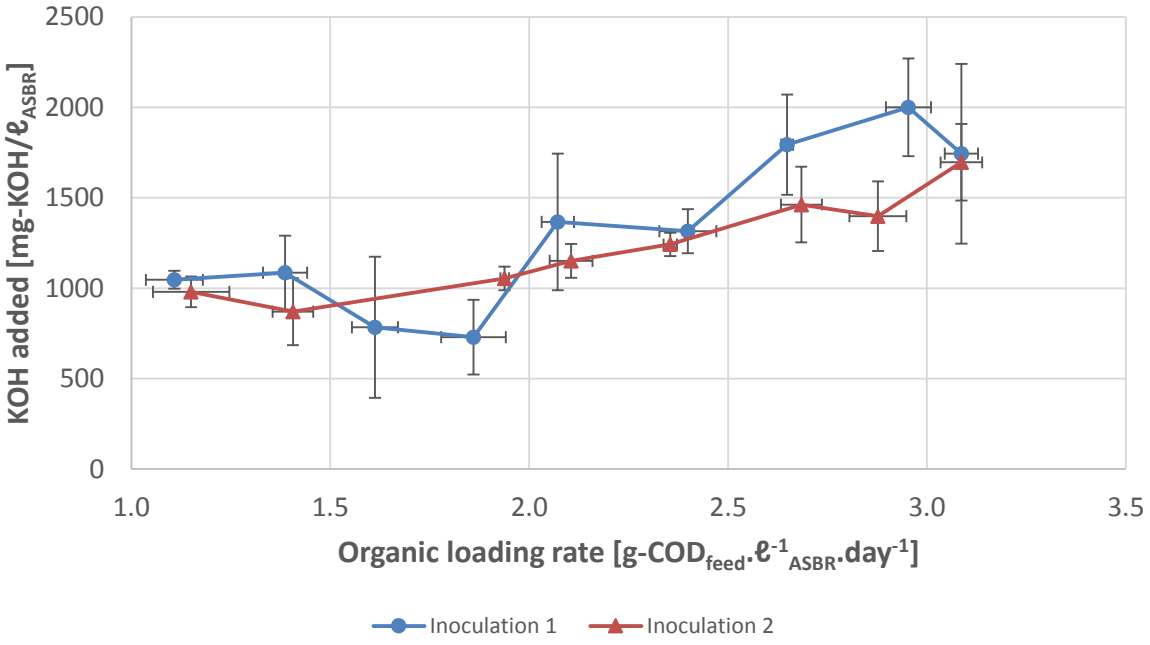

Figure 5-17: Specific mass of KOH added for *in-situ* pH control while operating the ASBR at various OLRs for two different inoculations while treating synthetic winery wastewater as presented in Table 3-1. Error bars represent one standard deviation of repeated experiments as described in Chapter 3.8

Stellenbosch University https://scholar.sun.ac.za

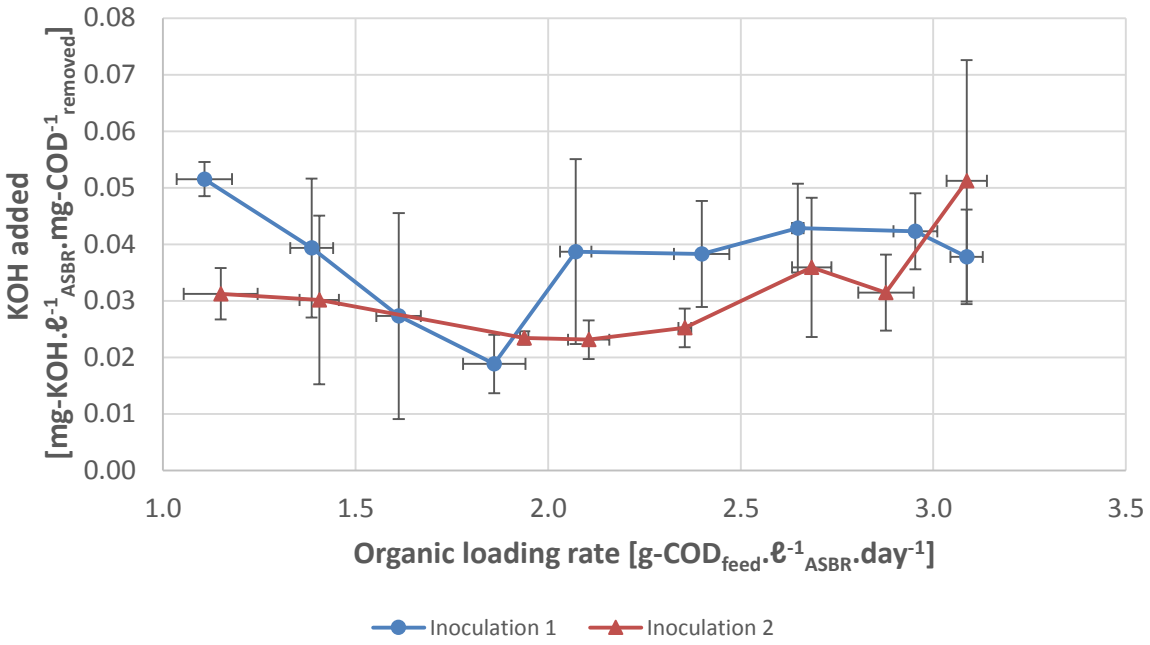

Figure 5-18: Total dosed KOH in relation to the COD removed for various OLRs while treating synthetic winery wastewater with two different inoculations as presented in Table 3-1. Error bars represent one standard deviation of repeated experiments as described in Chapter 3.8

Even though it was known how much KOH is dosed for the ASBR, the dosed amount is related to the amount of COD removed in the ASBR. Therefore, Figure 5-18 is presented which relates the KOH dosed with the working volume of the ASBR and the COD removed. Inoculation 1 generally had required more KOH to be dosed for each mg-COD removed than when compared to inoculation 2. This was due to the fact that inoculation 1 did not reduce the COD as far as inoculation 2 had a lower buffering capacity (partial alkalinity). Secondly, inoculation 2 could have consumed acetic faster due to the methanogens not being effected from the ammonium sulphate.

Inoculation 2 indicates that a factor of 0.035 mg-KOH.ℓ^{-1}_{ASBR}.mg-$COD^{-1}_{removed}$ can be used for determine whether operating the ASBR is financially feasible to operate at OLRs under 2.9 g-COD_{feed}.ℓ^{-1}_{ASBR}.day^{-1}.

Stellenbosch University https://scholar.sun.ac.za

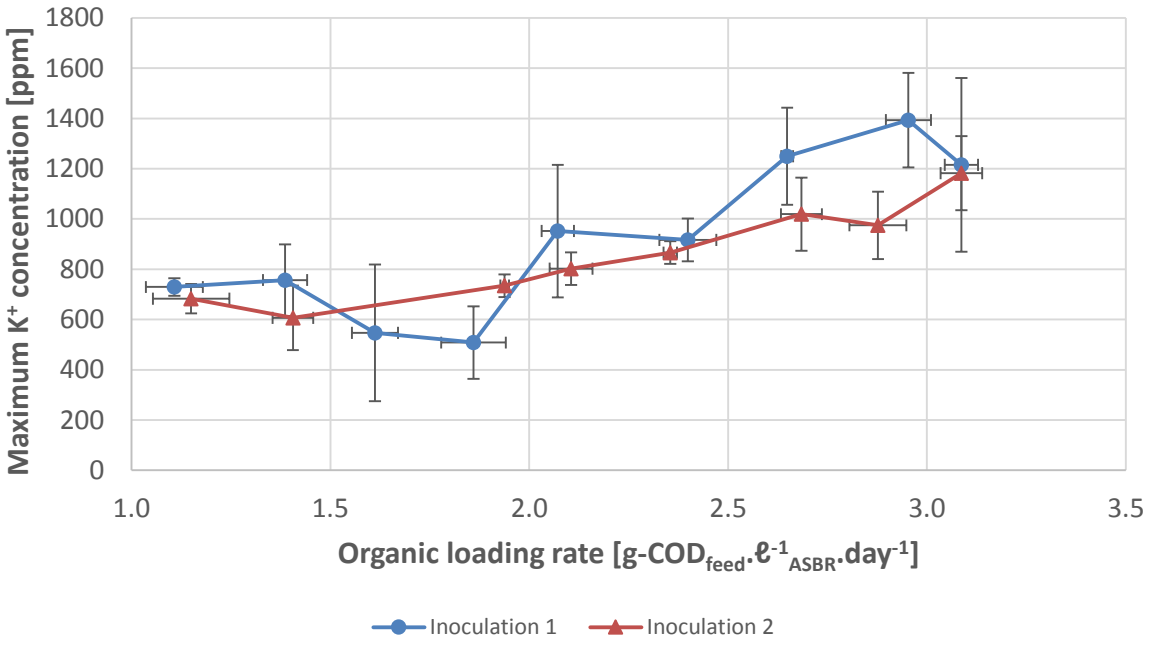

Figure 5-19: Maximum K^+ concentration in the ASBR due to the addition of KOH for *in-situ* pH control for two inoculations at various OLRs while treating synthetic winery wastewater as presented in Table 3-1. Error bars represent one standard deviation of repeated experiments as described in Chapter 3.8

As there is a possibility that the effluent from an ASBR can be used for irrigation, the maximum K^+ concentration is presented in Figure 5-19. This concentration is important for a viticulturist or soil scientist. It is important to note that the potassium indicated here comes solely from the dosing of KOH for pH control as the synthetic wastewater did not contain any. However, real winery wastewater will contain either K^+ or Na^+ from caustic washes and needs to be taken into concentration with Figure 5-19. Further evaluation will be required to determine whether it is feasible to irrigate this water back into the vineyards.

5.5. Key findings and observations

The biggest key finding and answer to the second research objective, was that these experiments indicated that an ASBR can be operated without additional alkalinity and only with *in-situ* pH control. Partial alkalinity remains fairly constant throughout the OLRs tested which leads to more KOH being required for pH control. Therefore, it was beneficial to investigate the online dynamic variables at a higher OLR, so that the effect of various aspects of the anaerobic digestion process can be magnified.

From this investigation it was noted that *in-situ* pH control was mainly only required in the first five hours of operation of an individual batch. As the major components of the feed substrate was glucose

Stellenbosch University https://scholar.sun.ac.za

and fructose, the anaerobic digestion process first requires VFAs to be formed as an intermediate product for biogas production.

During the treatment of a batch, it was noted that the finer sludge particles would rise in the ASBR and float on the surface. Against the glass surface of the ASBR, small bubbles could be seen between the particles. During the first few hours of a batch it was noted that this layer was the greatest. As the batch progresses, the layer would reduce with the particles settling to the bottom of the ASBR again. Once the settling stage started almost no particles were on the surface. It is believed that as biogas was produced, these particles attached to the bubble and floated to the top surface.

When the biogas production was high during the first few hours of the process, small bubbles could be seen rising from the sludge at the bottom in the ASBR to the top. Furthermore, once the ASBR was mixed a lot more bubbles were released. This was easy to seen when a light was shined into the ASBR.

At the end of inoculation 1, the temperature probe broke, which allowed the ASBR to heat up in excess of 50°C. The temperature was brought back down again and it was attempted to get the process going again. Biogas was produced, however, no methane was detected. Therefore, it is important to ensure that the mesophilic sludge is not over heated and results in the death of the methanogens.

Stellenbosch University https://scholar.sun.ac.za

Chapter 6 - Results and discussions II: The effect of feed substrate pH on the performance of an ASBR

The findings from Chapter 5 indicated that an ASBR can be operated without additional alkalinity but rather with *in-situ* pH control. The findings presented in this chapter provides an answer to research objective number 3 as stated in Chapter 1.

From the literature review, it was determined that winery wastewater is found in a pH range of 3.5 - 8.0 while the ASBR needs to be operated at a pH of approximately 7.0. To keep the ASBR simple, winery wastewater would be fed straight to the ASBR and allow the *in-situ* pH controller to adjust the pH when required. This was tested in Chapter 5. However, this chapter discusses the effect that the feed substrate's pH has on the performance of an ASBR as indicated in Table 3-2.

6.1. Measured online variables

The measured online variables are presented here. To reduce redundancy, only the measured online variables of one batch (batch 182) will be discussed in detail. Along with this, a comparison of key points for the different experimental sets will be discussed.

6.1.1. Temperature

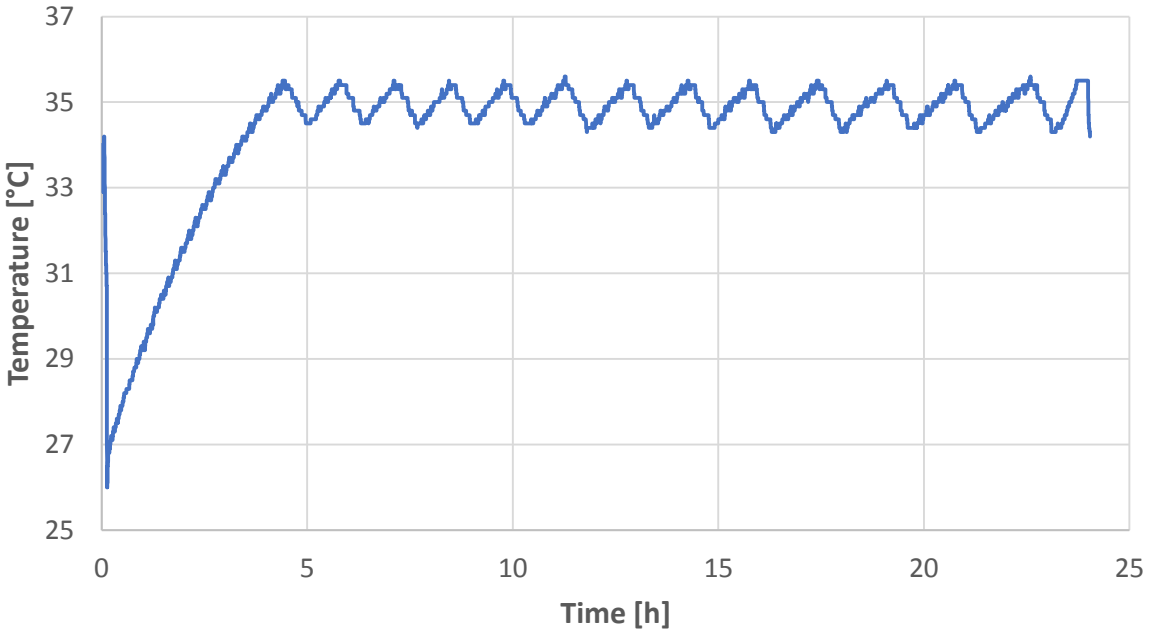

Figure 6-1: Measured temperature within the ASBR for batch 182

Stellenbosch University https://scholar.sun.ac.za

Figure 6-1 shows the temperature profile within the ASBR for batch 182. From the literature review in Chapter 2, it is known that the kinetic rates for the various groups of anaerobic bacteria is temperature and pH dependent. The feed substrate is fed to the ASBR at room temperature resulting in a sudden temperature drop at around the 0.2 h mark. This drop occurs at the end of the feeding stage when the system moves to the react stage. The react stage starts with a mixing cycle, thereby reducing temperature gradients in the system.

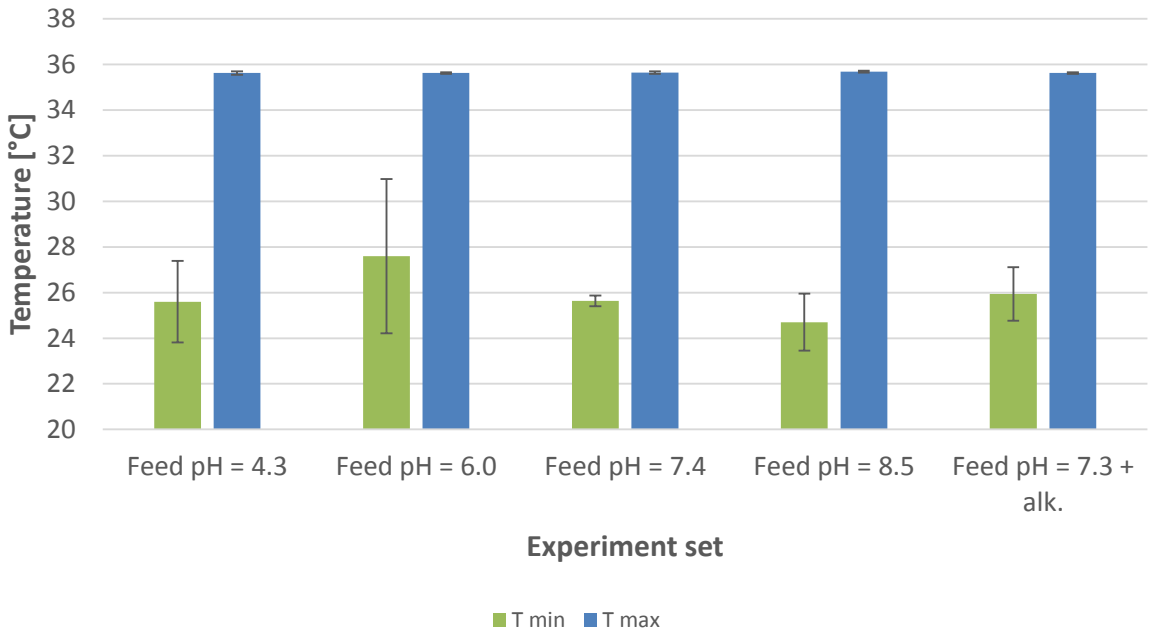

Figure 6-2: Comparison of the average minimum and maximum temperature reached in the ASBR for the experiments described in Table 3-2. Error bars represent one standard deviation of repeated experiments as described in Chapter 3.8

The minimum and maximum temperature measured within the ASBR is compared for each experimental set in Figure 6-2. The maximum temperatures of each experimental set was identical as the temperature control of the ASBR was set to heat 0.5 °C above the set point of 35 °C. The minimum temperature was dependent on the environmental temperature at the time of the experiments. A maximum difference of about 3 °C was obtained between experiment sets. Experimental set 2 had the highest minimum temperature, however, it had the largest standard deviation as seen with error bars.

Stellenbosch University https://scholar.sun.ac.za

6.1.2. ORP

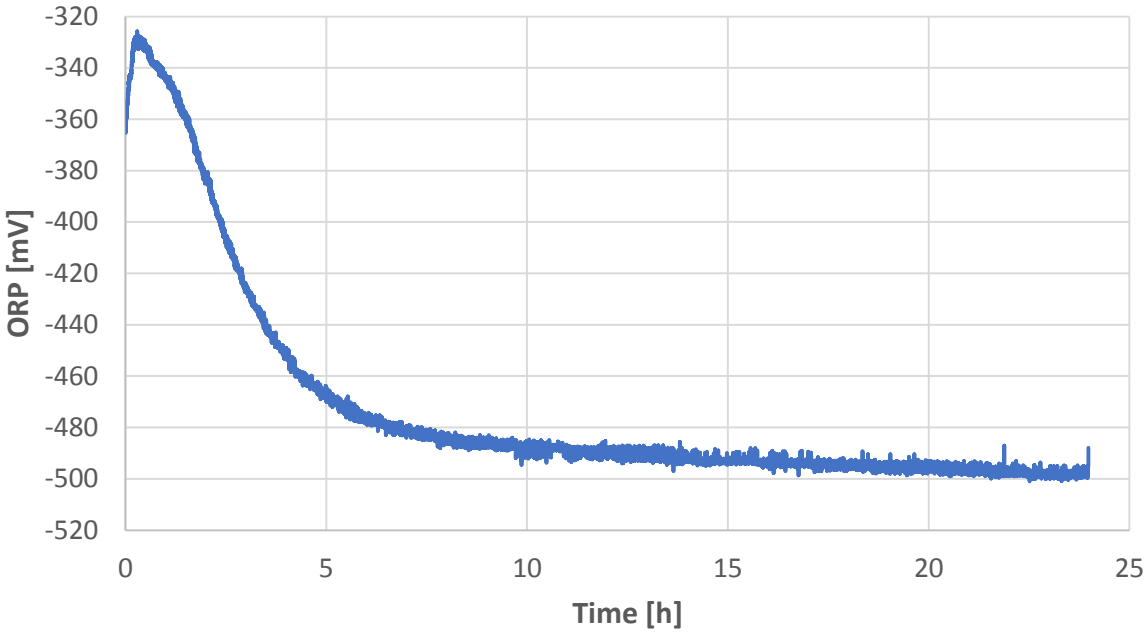

Figure 6-3: Measured ORP within the ASBR for batch 182

Figure 6-3 shows the ORP profile within the ASBR for batch 182. According to the summary of cellular activity in Table 2-5, ORP measurements below -300 mV indicates an environment within the ASBR that favours anaerobic conditions via the fermentation and methane production processes. This means that the environment favours the consumption of monosaccharides to form VFAs and methane was produced by methanogens. It is important to note that the ORP does not indicate how active a bacteria group is, but rather provides a method of determining which bacteria group is more active than another. Under anaerobic conditions, VFA formation is dominant when the ORP is measured between -300 and -100 mV (Gerardi, 2003).

In the instance of batch 182, the increase of ORP in the first hour indicated that the fermentation bacteria (acidogens and acetogens) is more active than when compared to the methanogens. However, feeding at a pH of 4.3 resulted in a slight ORP drop at 0.2 h which indicated that the methanogens were more active relative to the fermentation bacteria. In both cases it was unclear whether the aceticlastic or hydrogenotrophic methanogens were the more active of the two. From Chapter 5 it was known that the COD was not completely removed and the intermediate alkalinity indicated the presence of VFAs at the end of each batch within the ASBR. Furthermore, the feed substrate contained an insignificant 0.25 mg/ℓ of acetic acid. Both of these were sources for methane production from aceticlastic methanogens. However, there was dissolved hydrogen and carbon

Stellenbosch University https://scholar.sun.ac.za

dioxide in the ASBR which could be used by the hydrogenotrophic methanogens. Consequently, it was unclear which methanogenic group has a greater responsibility for the decrease in ORP at 0.2 – 0.8 h. However, it was known that hydrogenotrophic methanogens were less sensitive to temperature, and as the first hour was below the set point temperate, it was most likely that they were the more active group of methanogens.

The ORP in the ASBR reaches a maximum turning point where it begins to drop sharply before tapering off at around the 5 h mark, before it slowly reduces towards about -500 mV. The turning point occurs between 0.5 – 1.5 h for all batches. At this point it was safe to say that the monosaccharides have all been consumed to form various VFAs as determined with HPLC. At this stage, the methanogens became more active relative to the other bacteria groups which resulted in the ORP drop after 1.5 h.

No relation was found to the stages at which KOH was added to the ASBR and the ORP profile recorded.

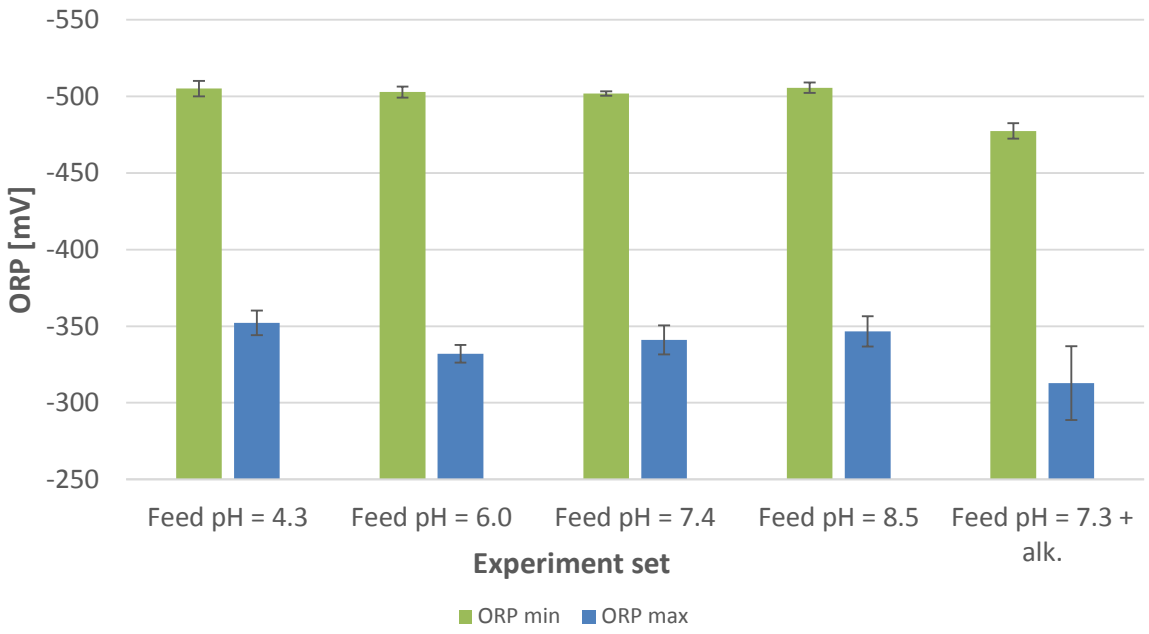

Figure 6-4: Comparison of the average minimum and maximum ORP reached in the ASBR for the experiments described in Table 3-2. Error bars represent one standard deviation of repeated experiments as described in Chapter 3.8

A comparison of the average minimum and maximum ORP measured for each experimental set is illustrated in Figure 6-4. The maximum ORP compares the peak ORP measured in the first 1.5 h of each batch. Essentially it provides a comparison of the relative activity between the fermentation bacteria

Stellenbosch University https://scholar.sun.ac.za

and methanogens. The higher the ORP was, the greater the activity of the fermentation bacteria relative to the methanogens.

It was evident from experiment set 1 that the methanogens were the most active relative to the fermentation bacteria when the feed substrate was fed at a pH of 4.3. During the feed stage, the feed substrate was pumped through the sludge in the ASBR. Due to the granular nature of the sludge, it could be that the fermentation bacteria protected the methanogens from the low pH during the feed stage of the process. This would make the methanogens more active relative to the fermentation bacteria.

For experiment set 3 and 4, the maximum ORP measured was only marginally worse than that of experiment set 1. In both these case, it seemed that fermentation bacteria experienced more inhibition or that the methanogens were just digesting better.

It was evident that the under the experimental conditions, the ASBR would reach about the same ORP of -500 mV when using a feed substrate without additional alkalinity. Adding alkalinity to the ASBR both increased the minimum and maximum ORP measured in the ASBR. $NaHCO_3$ was used as for additional alkalinity to the feed substrate. $NaOH$ solution is used in wineries for caustic washes. It was unclear with the lack of experiments, but the added Na^+ could be the cause of the increased ORP. Therefore, it was suspected that the source of the wastewater will also change the ORP profile of the ASBR. However, more experiments will need to be performed with different composition of winery wastewaters.

Stellenbosch University https://scholar.sun.ac.za

6.1.3. pH

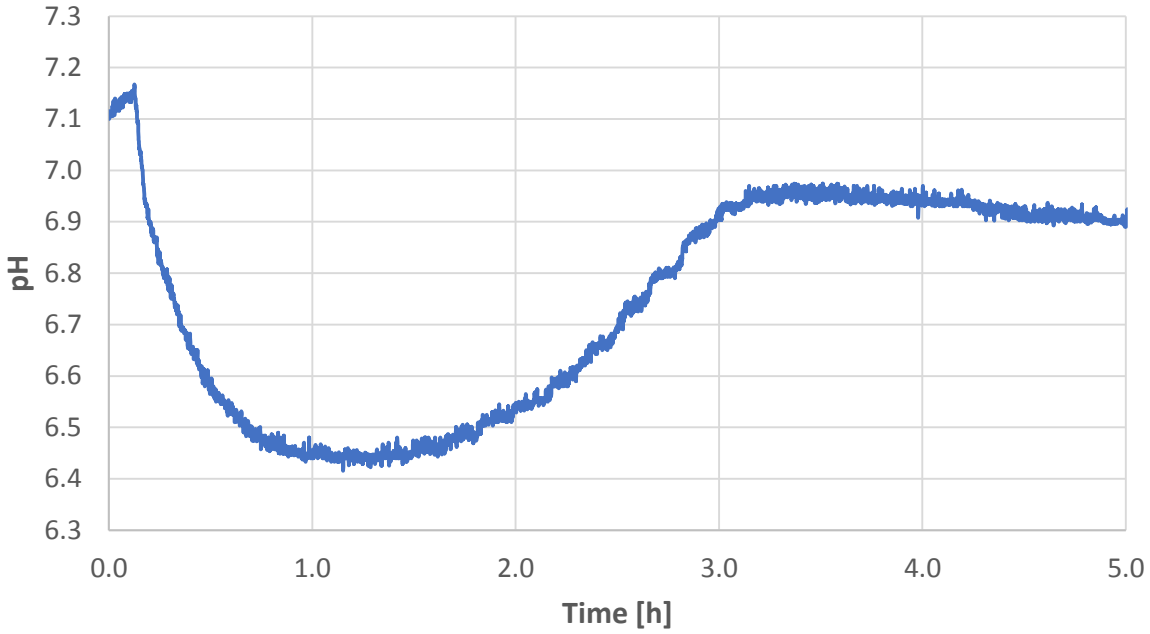

Figure 6-5: First 5h of the measure pH within the ASBR for batch 182

Only the first 5 hours of the measured pH is presented in Figure 6-5 in order to amplify the pH profile in the ASBR during this time period. In the first 0.1 h of the batch, the pH could not be taken as accurate. This is part of the feeding stage and the pH probe was not in contact with the liquid in the ASBR all the time.

The first thing noted in Figure 6-5, was the sudden drop in the pH after the ASBR was filled and the first mixing occurs at 0.15 h. When the feed substrate was fed to the ASBR, it was pumped so that the feed substrate flows through the settled granular sludge which was at the bottom of the ASBR. During this stage, monosaccharides (glucose and fructose), which also forms the largest portion of the fed COD, was consumed rapidly by acidogens resulting in the formation of various VFAs. Thereby, causing a pH drop due to having insufficient buffering capacity.

From literature it was known that methanogens are pH sensitive and generally inhibited when the pH was below 6.6. However, Won *et al*. (2013) found methane production for an ASBR operating at a pH of 5.5 and OLR below 7 g-COD_{feed}.ℓ^{-1}_{ASBR}.day^{-1}, therefore, there could be a methanogen species that was not as inhibited in the sludge at low pHs. Combining the idea of the ORP in Figure 6-3 and pH in Figure 6-5, there is a possibility that methane formation was occurring during the period that has the lowest pH measurement.

Stellenbosch University https://scholar.sun.ac.za

The consumption of monosaccharides was promoted by bringing the feed substrate into contact with the sludge when the ASBR was fed. If the substrate had been fed in at the liquid surface in the ASBR, the contact will be dependent on diffusion during the feed stage due to the lack of mixing during this stage of the ASBR process. This could cause the gradient of the pH drop to be reduced and the quantity that that drop to be less at around 0.2h in the process. However, for these experiments the feed stage was very short (15 min). Mixing would occur quickly which would promote digestion resulting in a rapid pH drop. If the ASBR were to be operated in a fed-batch way, pH control would need to occur during the feed stage as well. The fed-batch feed method can be used to reduce the pH drop by preventing rapid formation of a high concentration of VFAs.

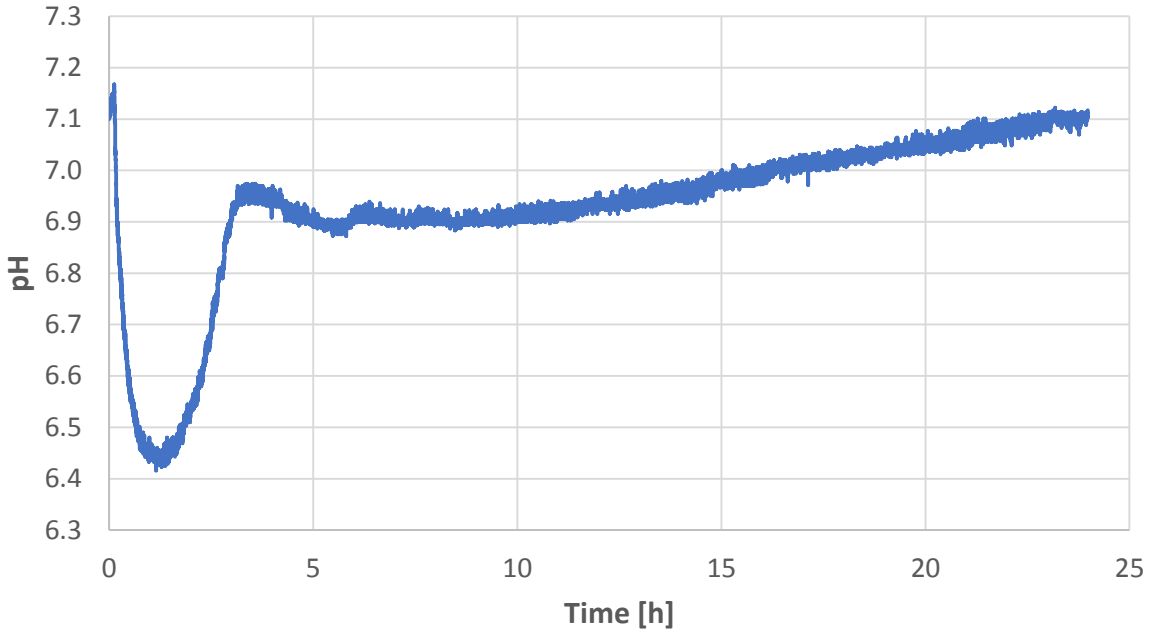

Figure 6-6: Measured pH within the ASBR for batch 182

Figure 6-6 provides an illustration of the measure pH within the ASBR for the complete cycle of batch 182. Around the 3 – 4 h mark, the batch typically reached their minimum pH compared to the set point. For batch 182, this was at about 3 h. The pH further increased due to extra KOH dosing during the mixing cycle. After this, the pH reached a local maximum at 6 hours, before it dropped again. This was then corrected at about the 6 h mark. This "saw tooth" pattern was commonly noted for other batches. The pH reduction in the 3 – 8 h mark occurred at a slower rate than that at the start of the batch. This drop was caused by a lack of alkalinity and further formation of VFAs.

Sample of the liquid in the ASBR were taken for several batches were taken within the first five minutes of the react stage. These samples were tested for monosaccharides with HPLC that could accurately

Stellenbosch University https://scholar.sun.ac.za

test to a minimum of 50ppm. Monosaccharides were not detected so it was safe to say that there were no monosaccharides at the 3 h mark. Therefore, it was believed that it was acetic acid being formed from the other VFA sources during acidogenesis that caused the pH reduction. The reduction of propionic, butyric and valeric acid to acetic acid, resulted in H^+ ion being set free. The excess H^+ cannot be countered by the alkalinity and results in the pH drop. Therefore, this "saw tooth" pattern was a result of the lack of alkalinity, acetic acid formation and *in-situ* pH controller.

At around the 8 h mark, no more pH control was required in any of the experiments performed. From the pH profile in Figure 6-6, a new *in-situ* pH controller system could be developed and experimented with. A piece-wise type *in-situ* pH controller is proposed to keep the system simple. In the first 3 h, the greatest amount of pH control is required and can be done by dosing larger amounts of KOH in the ASBR. However, from the 3 – 8 h, finer pH control is required which can be done with dosing smaller amounts at a time. The controller can be made more complicated to include the operating OLR.

While making the pH control more aggressive in the first 3 h period, it must be noted that the not all the KOH required be dosed into the ASBR. This could increase the pH to above 8.0 and inhibit all the bacteria. This would deem the ASBR treatment useless and cause a loss of production time trying to get the ASBR up to steady state condition again.

From around the 8 – 10 h mark, the measured pH increases. This increase was caused by the production of methane from acetic acid by the aceticlastic methanogens. With the removal of acetic acid in the system, the pH can only remain constant or increase.

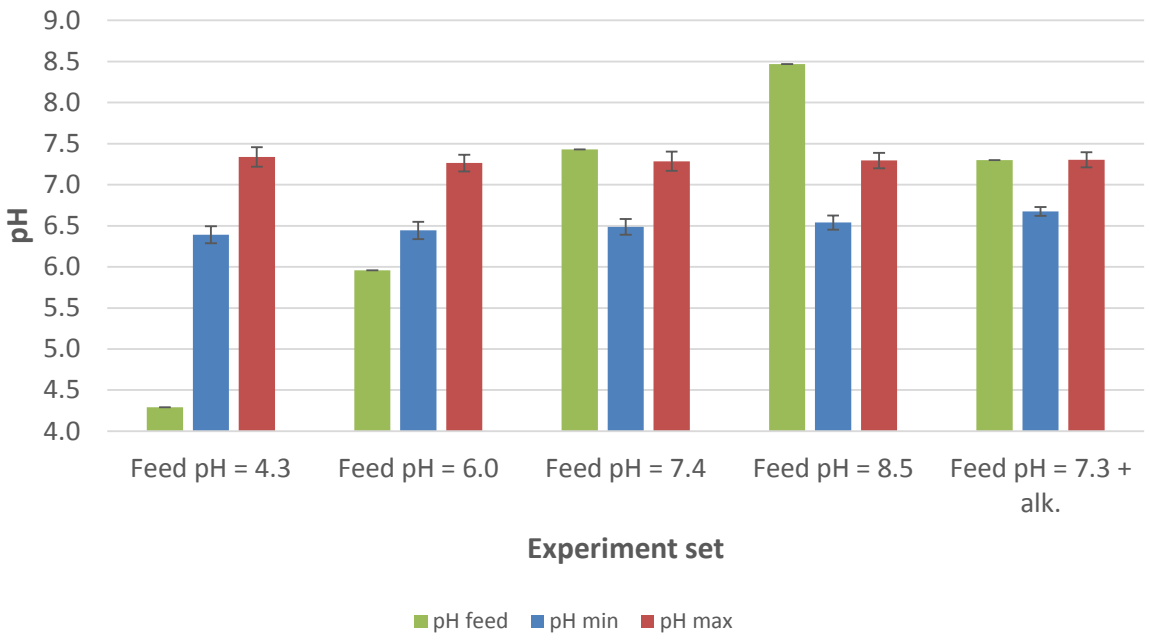

Stellenbosch University https://scholar.sun.ac.za

Figure 6-7: Comparison of the feed pH, minimum pH measured and maximum pH measured for each experimental set as described in Table 3-2. Error bars represent one standard deviation of repeated experiments as described in Chapter 3.8

Figure 6-7 provides a comparison of the various pH measurements. The maximum pH measured in the ASBR occurred at the end of the batch.

The minimum pH measured in the system occurred during the first 2 h of the process. For experiment sets 1 – 4 it is noted that the minimum pH measured, increased as the feed substrates pH increased. However, the difference between the various minimum pH levels were not as great as the difference in feed substrate pH. This was an indication that the *in-situ* pH controller functioned as required.

Adding alkalinity, as seen experiment set 5, increased the minimum pH measured when compared to the other experiment sets.

6.1.4. Biogas production

Biogas production provides an easy online indicator for the performance of an anaerobic digester.

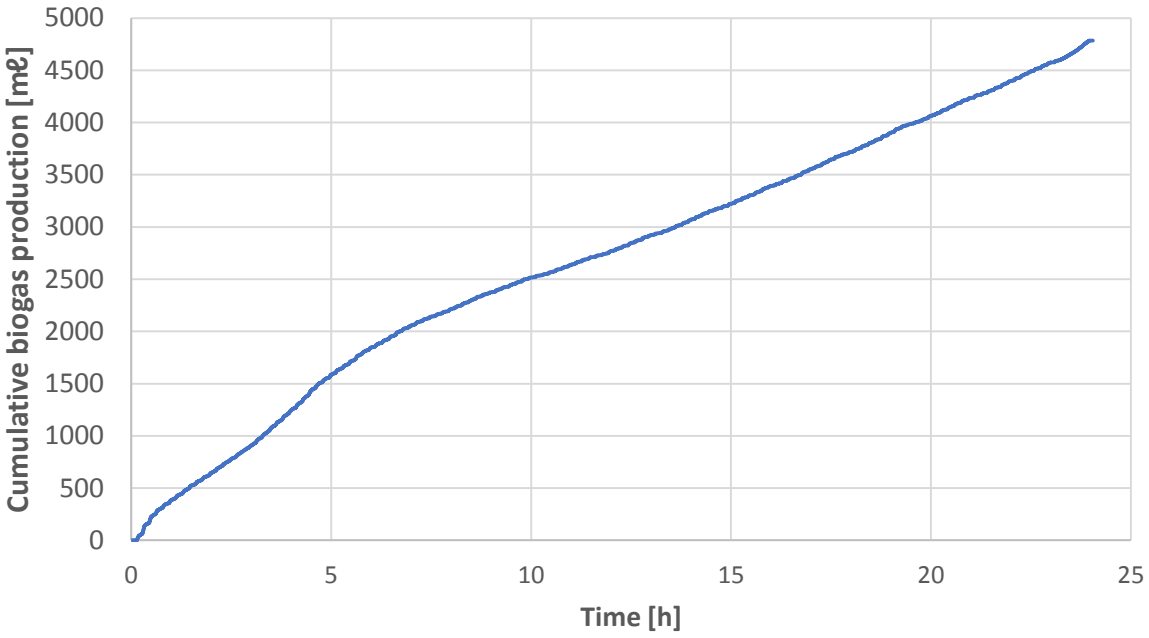

Figure 6-8: Measured cumulative biogas from the ASBR for batch 182

Stellenbosch University https://scholar.sun.ac.za

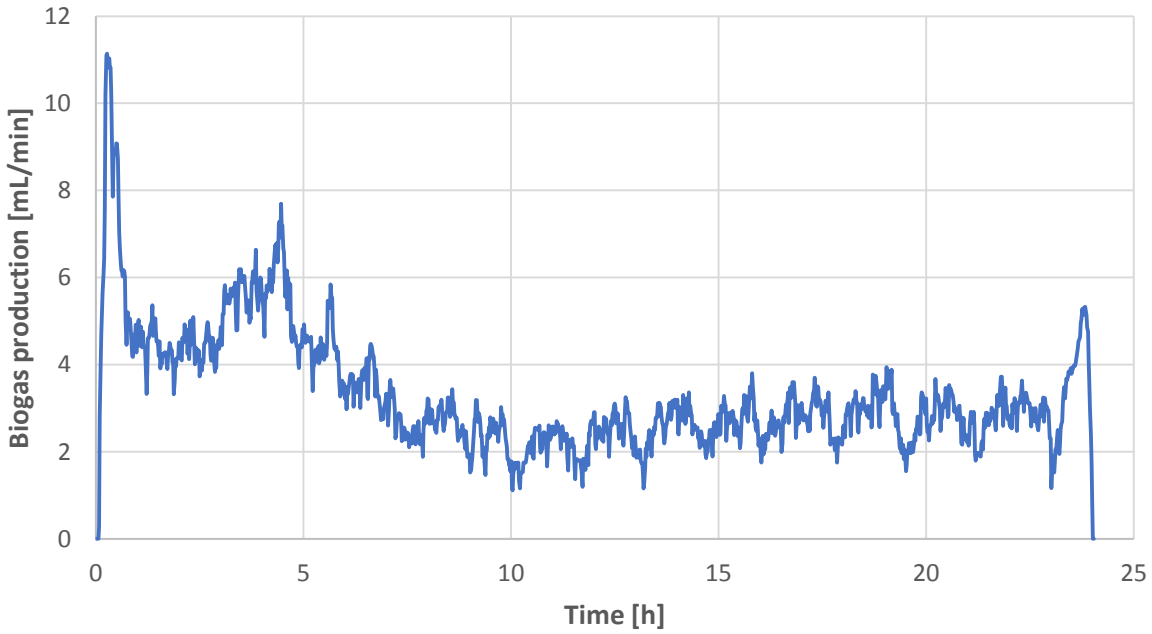

Figure 6-9: Calculated biogas production rate for batch 182

Figure 6-8 provides an illustration of the cumulative biogas production for batch 182. This was a combination of all the biogas produced as measured with the bubble counter. However, not much can be told from the cumulative biogas production. Therefore, the calculated biogas production rate is illustrated in Figure 6-9.

Not clearly evident in Figure 6-8, is the small stepwise increase that the biogas undergoes. These steps coincide with the periods that the ASBR was mixed. When the ASBR was not mixed, some of the biogas that was formed was trapped between the settled sludge. With the mixing of the ASBR, granules were shaken greatly and assists with biogas being releasing from the surface of the sludge which allowed it to leave the ASBR through the gas line. This caused small bursts biogas being measured and in turn created a step wise increase when plotted.

The first 0.2 h of the batch indicates no gas production. However, this was not true. Biogas comprising of CO_2 and H_2 is formed when monosaccharides are digested during the feeding of the process. With the automation of the filling stage being determined with a level probe, the ASBR could be filled up to different volumes. Though these heights were seen to differ by about 3mm over long term operating and could have a significant difference in the measured volume of biogas produced during that period. Therefore, to standardise it, the bubbles counted from the start of the react phase was considered biogas produced. This assumption was considered valid as the feeding time was under 15 min.

Stellenbosch University https://scholar.sun.ac.za

During the filling stage, the granular sludge in ASBR was only slightly fluidised and made it difficult for the biogas to escape to the headspace in the ASBR. As soon as the ASBR was filled and the react stage starts, the ASBR was mixed for the first time. When the ASBR was mixed, the then fluidised bed of the ASBR expands and the granules were “shaken”. This allows the small biogas bubbles on the sludge to release to the headspace. The headspace was then pressurised further to a point where it could overcome the hydrostatic pressure within the bubble counter and allow biogas out. Due to this sudden release of biogas from the sludge, a high biogas production rate is calculated initially as seen with the spike in Figure 6-9 for all the batches.

A second important point with the biogas production rate was the dip at the 1 – 3 h mark. This drop in biogas production rate also coincides with the measured pH dip in Figure 6-6. This helps further validate that the main biogas forming bacteria, the methanogens, are being inhibited.

Around the 5 h mark, the third important point occurs. This is a localised peak in the biogas production rate. This occurs when the pH was near the set point then. It was thought that the propionic acid concentration was low and led to less inhibition of methanogens, thereby, increasing the biogas production rate. Secondly, the temperature of the ASBR was at operating temperature which also improves the digestion rates of the methanogens.

The biogas production rate then dropped towards the 10 h mark. For some batches, the biogas production rate reached zero, whereas others reduced to just above zero. At the 10 h mark, the ORP was also almost at its lowest. Therefore, it was believed that only methane and carbon dioxide was formed from methanogens.

Stellenbosch University https://scholar.sun.ac.za

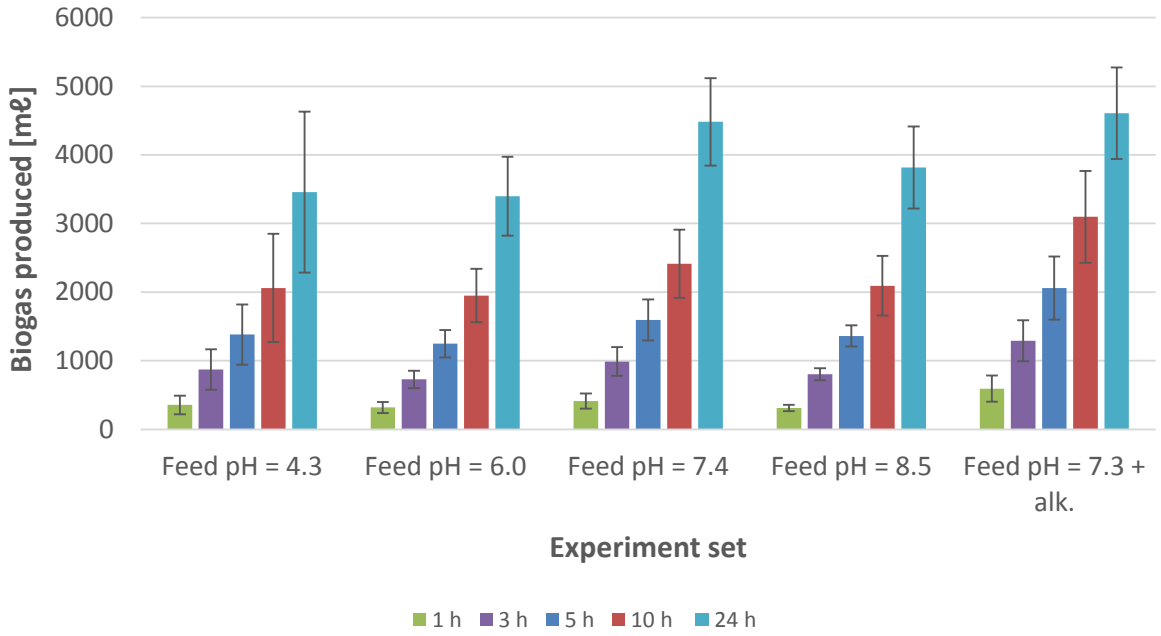

Figure 6-10: Comparison of cumulative biogas production at various time points throughout a batch for different experimental sets as described in Table 3-2. Error bars represent one standard deviation of repeated experiments as described in Chapter 3.8

Figure 6-10 provides a comparison of the biogas produced at different instances. Due to the variation of the spike in the biogas production rate at the 0.2 h mark, the total biogas produced was compared at the 1 h mark.

The addition of alkalinity resulted in experiment set 5 outperforming all other experiments with biogas production throughout the time intervals. With the added alkalinity, a smaller amount of CO_2 dissolved into the water to form bicarbonate. Therefore, more biogas was expelled and led to a high biogas production rate. To really indicate whether it was better, the composition of the biogas had to be determined. This will be discussed in section 6.2.2.

Between the other experiments, feeding at a pH of 7.4 (experiment set 3) produced the largest amount of biogas throughout a batch. All the other experiments seemed dependent on the pH at a certain stage. For experiment set 1, it seemed that the low feed pH of 4.3 has little effect on the shielded methanogens in the first 3 h. However, at the 10 h mark, experiments 1, 2 and 4 are almost equivalent on biogas produced. Conditions for experiment 4 seemed to be correct between the 10 - 24 h mark with the amount that the biogas increased when compared to the experiment sets 1 and 2. The increased amount of biogas produced at the 1 and 3 hour mark for experiment 3 provides an indication that the pH of the feed substrate being correct to 7.4 is advantageous. It was though that this pH was

Stellenbosch University https://scholar.sun.ac.za

favourable for the methanogens during the feed stage and resulted in less inhibition through the remainder of the batch.

6.2. A comparison of analytical analysis for feed substrates with varying pH

This section of the results focuses on the analysis of the effluent and biogas at the end of each batch where the substrate pH was altered, as well as the one experiment set with added alkalinity in substrate.

6.2.1. COD reduction

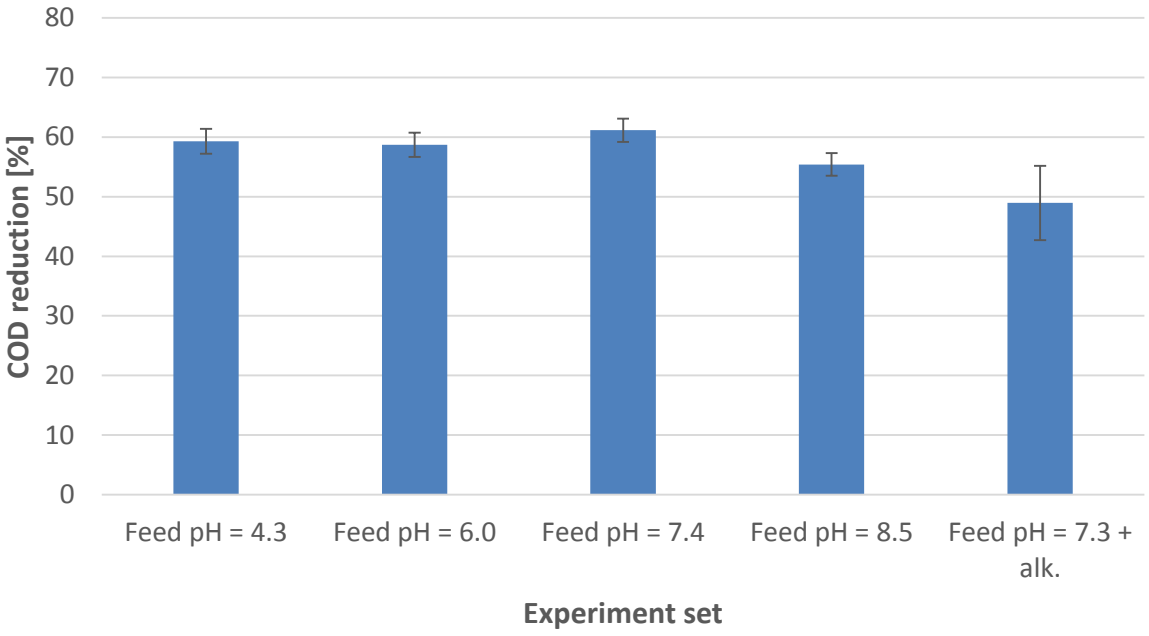

Figure 6-11: Comparison of COD reduction for the experiments described in Table 3-2. Error bars represent one standard deviation of repeated experiments as described in Chapter 3.8

Figure 6-11 provides a summary of the COD reduction for the various experiments. While operating at an OLR of 2.9 g-COD_{feed}.ℓ^{-1}_{ASBR}.day^{-1}, the experiments performed with the feed substrate at a pH of 7.4 (Experiment set 3), had a 61% in COD reduction. Since this experimental set was performed in the preferred pH range for methanogens, the methanogens had less inhibition initially, which is backed up with the measured ORP, pH and biogas production data previously discussed.

However, experiment 3 (feed substrate pH 7.4) performed only marginally better than experiment 1 and 2. This provides an indicator that feed substrate's pH can be between 4.3 and 7.4, and the ASBR

Stellenbosch University https://scholar.sun.ac.za

can still reach an approximate COD reduction of 60% while operating at an OLR of 2.9 g-COD_{feed}.ℓ^{-1}_{ASBR}.day^{-1} while getting the pH to operation set point within 4 h.

Since winery wastewater can be caustic due to caustic washes of wine making equipment, there is a possibility of feeding the ASBR at a higher pH. It was found that feeding the ASBR at a pH of 8.5 (experiment 4), reduced the COD reduction to 55%. Operating at higher pH values, resulted in the methanogens as well as the acidogens experiencing some sort of inhibition. Thereby, this effected the overall performance of the ASBR. The inhibition was however more severe than that experienced when feeding at a pH of 4.3.

In experiment 5, the addition of alkalinity reduced the pH drop and showed that the methanogens were more active from the ORP measurements during the first 5 h of the batch. However, as seen with the reduced COD reduction, the additionally bicarbonate negatively affected the performance of the process.

From this, it can be deduced that and ASBR operating at VDF of 0.5 with pH control can obtain an COD reduction of at least 55% while operating at an OLR of 2.9 g-COD_{feed}.ℓ^{-1}_{ASBR}.day^{-1} with a substrate's pH varying between 4.3 and 8.5, and containing 92% of the COD in the monosaccharide form. To increase this reduction, more sludge can be added to the ASBR or the batch time can be extended, however, that would reduce the OLR of the system.

Stellenbosch University https://scholar.sun.ac.za

6.2.2. Biogas production

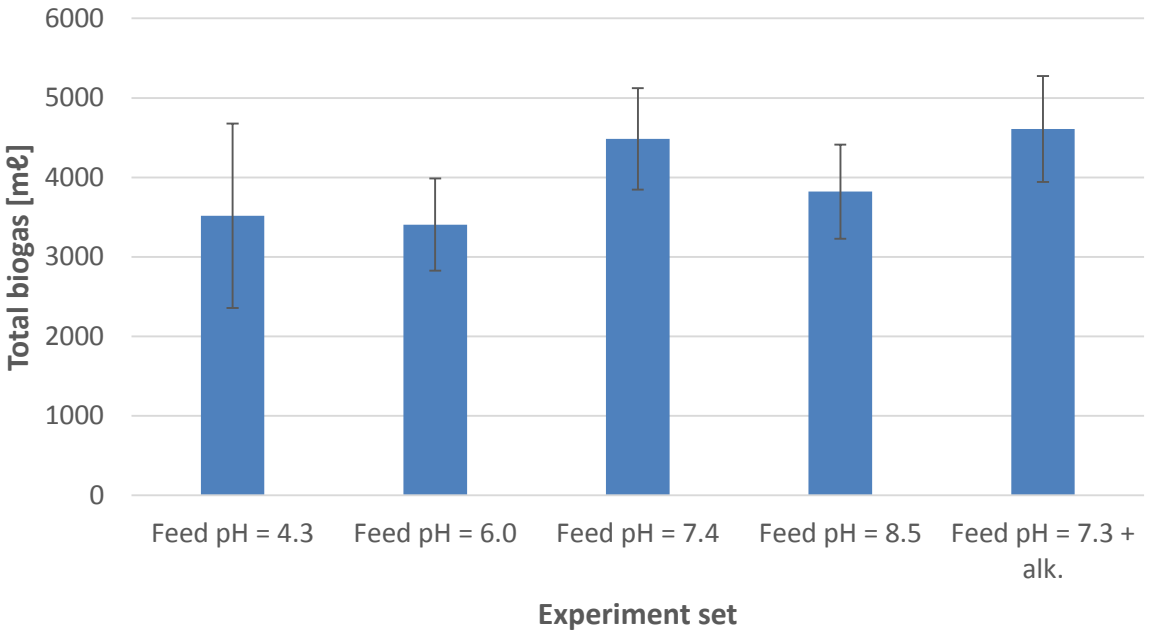

Figure 6-12: Comparison of total biogas produced for the experiments described in Table 3-2. Error bars represent one standard deviation of repeated experiments as described in Chapter 3.8

Figure 6-12 provides a comparison of the difference in total biogas produced with the ASBR process. As experiment 3 had the highest COD reduction, it was expected to the have the highest amount of biogas produced. Surprisingly, experiment 4, which had a lower COD reduction compared to 1 and 2, had a higher amount of biogas produced. To determine why this is the case, a look at the biogas composition is required. Experiment 5 had a rather high biogas production, considering the rather poor COD reduction.

Stellenbosch University https://scholar.sun.ac.za

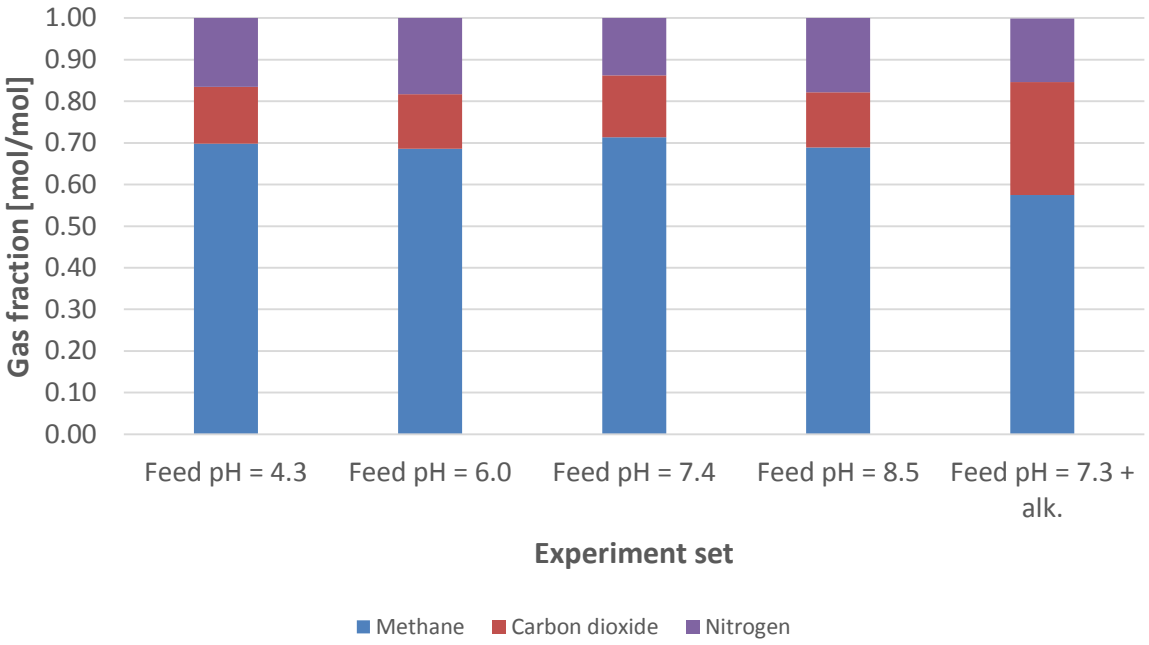

Figure 6-13: Comparison of biogas composition for the experiments described in Table 3-2. Error bars represent one standard deviation of repeated experiments as described in Chapter 3.8

Figure 6-13, above, provides a comparison of the gas fraction between CH_4, CO_2 and N_2. Comparing the methane fraction between the experiments where the pH was altered, the biogas generally obtains a methane fraction of 68 - 72 %. Experiment 3 had the highest methane fraction as it had the highest COD reduction and experienced the least methanogenic inhibition during the early stages of the batch treatment.

Experiment 5 had a high carbon dioxide fraction. This was expected due to the missing bicarbonate in the liquid phase of the ASBR did not have to be made up with dissolved carbon dioxide. Compared to experiment 3, approximately 14% more CO_2 was produced.

All the batches produced N_2 biogas. Yeast extract powder was used as a nitrogen source in the feed substrate and as a result nitrogen gas was formed, meaning that it had to be fed in excess. However, in excess the denitrification can occur and results in the formation of N_2 in the biogas. If the nitrogen was not added in excess, the biogas produced during the process can be upgraded and a new composition can be seen in Figure 6-14, below.

Stellenbosch University https://scholar.sun.ac.za

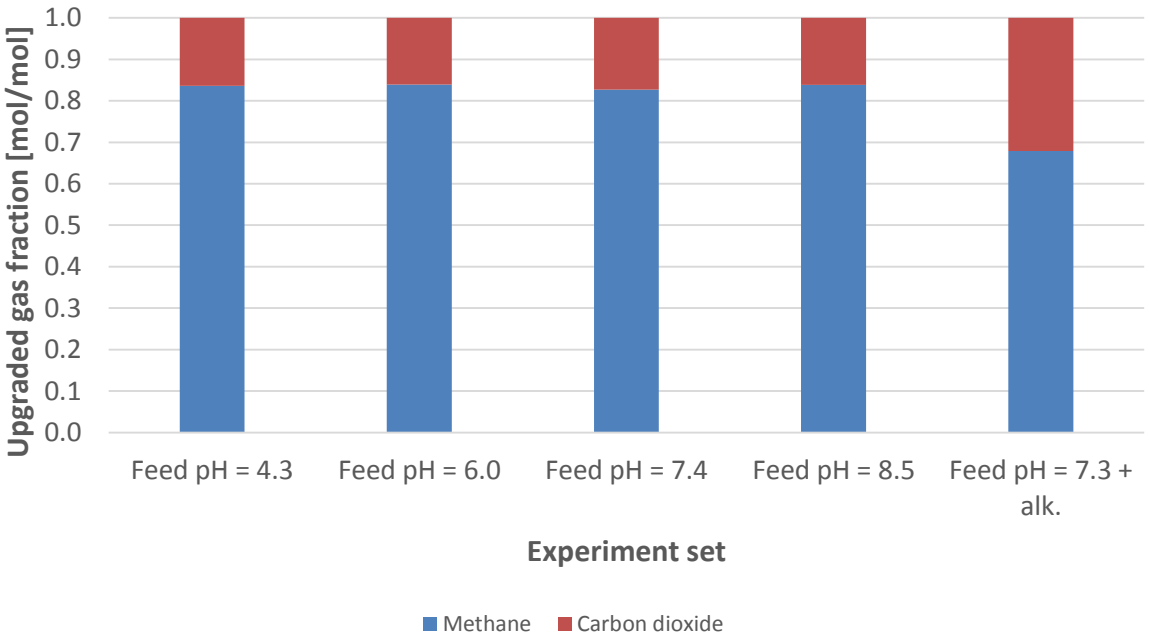

Figure 6-14: Comparison of the theoretical upgraded biogas composition for the experiments described in Table 3-2. Error bars represent one standard deviation of repeated experiments as described in Chapter 3.8

If the nitrogen could be removed from the biogas, a methane fraction in excess of 82% could be obtained. The removal of nitrogen in the biogas was never performed in this study. However, its removal allows the biogas to be compared to other studies which only report carbon dioxide and methane.

For experiment 3, the biogas produced with a composition of 71% CH_4, 15% CO_2 and 14% N_2 was then upgraded to 82% CH_4 and 18% CO_2 which resulted in an increased HHV from 26.83 MJ/m^3 to 31.00 MJ/m^3. Whereas for experiment 5, the biogas was upgraded from 58% CH_4, 27% CO_2 and 15% N_2 to 68% CH_4 and 32% CO_2, consequently increasing the HHV from 21.92 MJ/m^3 to 25.72 MJ/m^3. The upgraded biogas composition was almost identical to that with which anaerobic digesters get designed for. Therefore, operating an ASBR with a with a feed substrate pH of 7.4 without additional bicarbonate and at a VDF of 0.5, an increase in HHV of 5.32 MJ/m^3 could be obtained. Experiments 1, 2 and 4 have the ability to achieve a slightly higher HHV for the upgraded biogas of experiment 3, however, these produced less biogas, consequently leading to a smaller amount of total energy that could be harvested.

To compare this setup to other anaerobic digestion processes, the methane yield and methane productivity is provided below in Figure 6-15 and Figure 6-16, respectively. The theoretical maximum methane yield from glucose consumption is 0.35 ℓ.g-COD$^{-1}_{removed}$ to which the level of performance of

Stellenbosch University https://scholar.sun.ac.za

the system was rated. Compared to this standard, the ASBR performed rather poorly with the best yield at 0.15 ℓ.g-$COD^{-1}_{removed}$ for experiment 5. Whereas, the worst methane yield of 0.115 ℓ.g-$COD^{-1}_{removed}$ was obtained for experiment 1 and 2. Experiment 5 had the highest methane yield since as it had the smallest COD reduction, however, it produced the most biogas. Furthermore, experiment 5 had the lowest HVV for the upgraded biogas produced, therefore, it should be the option that must be avoided when operating a similar ASBR as it was less effective at treating winery wastewater.

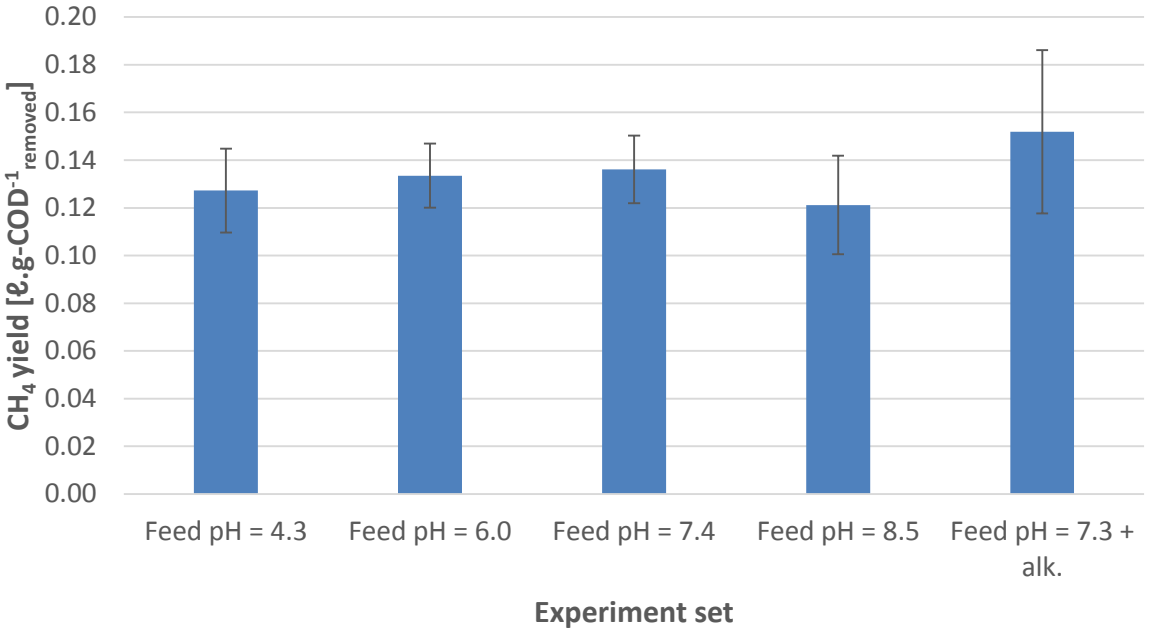

Figure 6-15: Comparison of methane yield for the experiments described in Table 3-2. Error bars represent one standard deviation of repeated experiments as described in Chapter 3.8

The highest methane yield was obtained when feeding the ASBR at a pH of 7.4 and without additional alkalinity where a productivity of 240 mℓ.$ℓ^{-1}_{ASBR}$.day^{-1} was achieved. The other pH experiments obtained a methane productivity of approximately 190 mℓ.$ℓ^{-1}_{ASBR}$.day^{-1} which was only slightly less than the 205 mℓ.$ℓ^{-1}_{ASBR}$.day^{-1} obtained when operating with additional alkalinity. The methane productivity can be increased by increasing the amount of sludge in the ASBR.

Stellenbosch University https://scholar.sun.ac.za

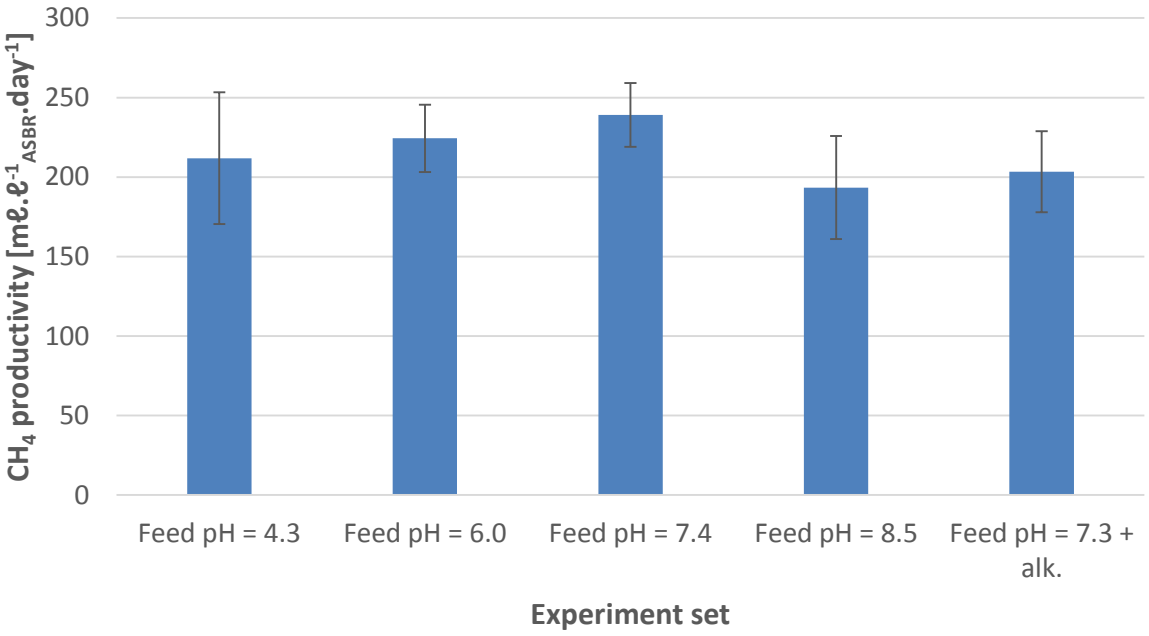

Figure 6-16: Comparison of methane productivity for the experiments described in Table 3-2. Error bars represent one standard deviation of repeated experiments as described in Chapter 3.8

Winery wastewater pH can vary between 3.5 and 8.0 depending on the source of the wastewater. Even though these experiments were only performed at one OLR, the drastic difference in the performance can be seen by just correcting the pH to near where the ASBR needs to operated. Therefore, it is important to correct the pH of the substrate being fed before it enters the system.

Secondly, the partial and intermediate alkalinity should be used as easy and cheap indicators for the performance of the ASBR. This would be unique for each system due to varying bacteria populations and analysis methods. Logging this data can be helpful in building up a log book of the performance of the system and in future be used to correct bicarbonate of VFA concentrations in the ASBR if the system where to malfunction.

Stellenbosch University https://scholar.sun.ac.za

6.2.3. Alkalinity

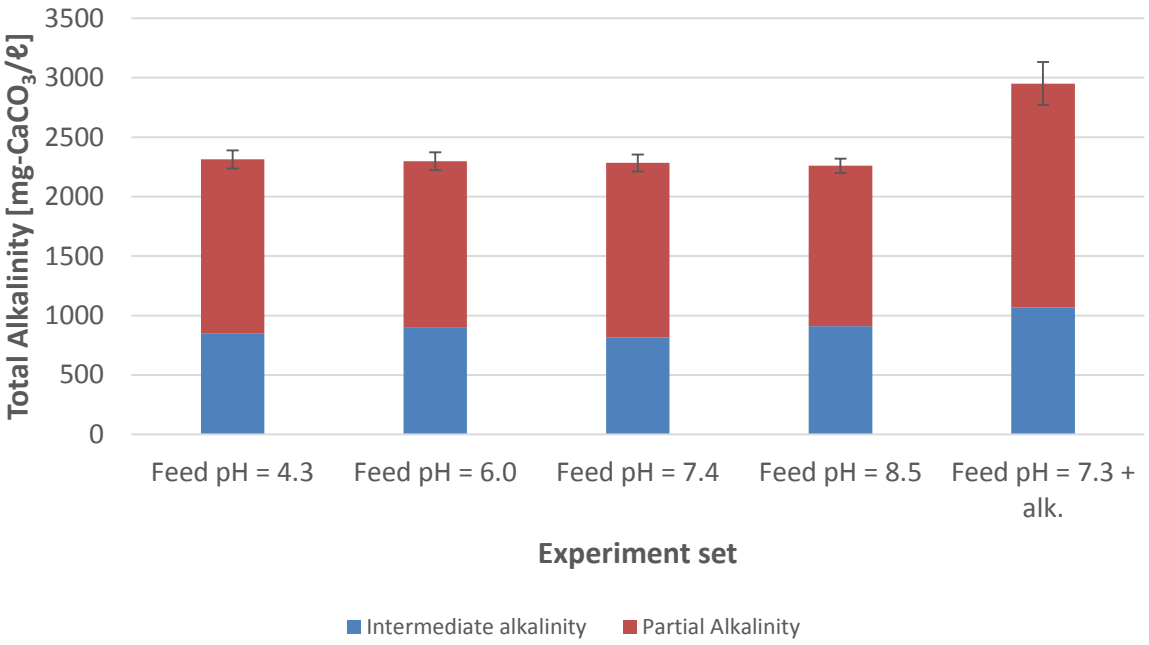

Figure 6-17: Comparison of total, intermediate and partial alkalinity for the experiments described in Table 3-2. Error bars represent one standard deviation of repeated experiments as described in Chapter 3.8

Figure 6-17, above, indicates the total alkalinity, as well as the portion made up of intermediate and partial alkalinity. For the set of experiments, where only the pH was altered, the various forms of alkalinity remained fairly constant throughout. Experiment 3, pH 7.4, has the lowest intermediate alkalinity which is the indicator for the amount of VFAs. This is correct as it was the set with the highest COD reduction. Experiment set 5 which contained the added alkalinity, had the highest total alkalinity, which was due to the increased partial alkalinity. As partial alkalinity is the bicarbonate alkalinity in anaerobic digesters, the increase comes from the added feed.

The partial alkalinity of experiment 5 was an average of 500 mg-$CaCO_3$/ℓ higher than that of the other experiments, however, 2870 mg-$NaHCO_3$/ℓ was added to the feed which correlates to 3420 mg-$CaCO_3$/ℓ. Assuming the same amount of carbonate was produced for experiment 5 as with the others, 75.4% of the fed bicarbonate was absent and could have been consumed or expelled via other means within or from the ASBR. Bicarbonate could be used a carbon source for anaerobic sludge growth (Bitton, 2005; Gerardi, 2003). The reverse reaction of the dissolving carbon dioxide to form bicarbonate can also occur, thereby, the amount of carbon dioxide in the biogas released from the ASBR should increase.

Stellenbosch University https://scholar.sun.ac.za

6.2.4. In-situ KOH dosed for pH control

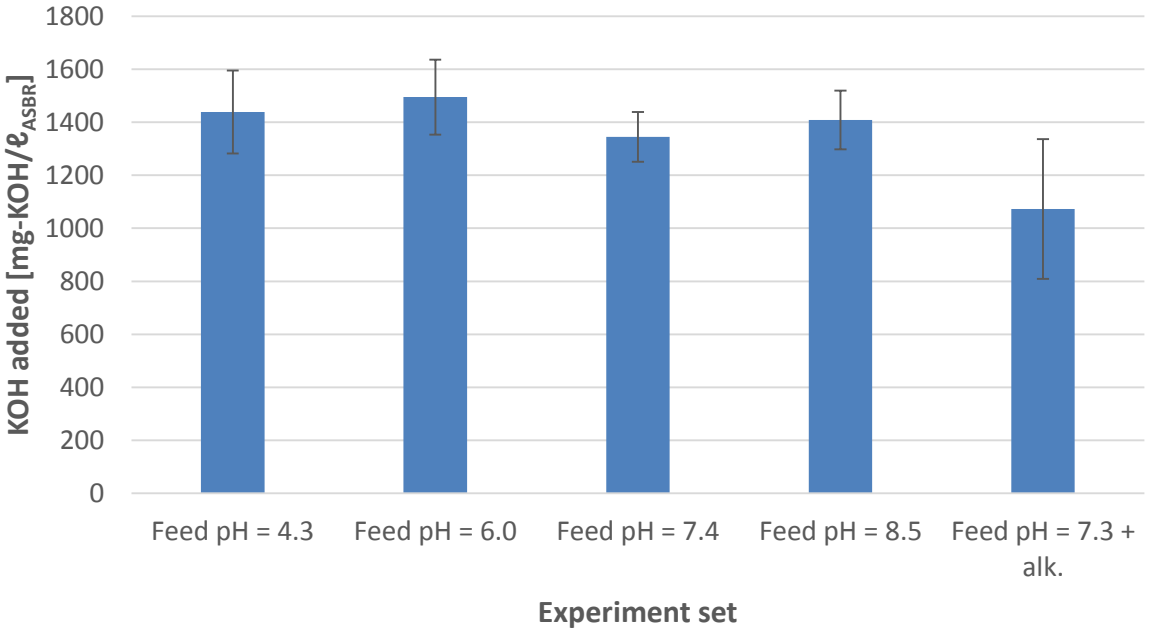

Figure 6-18: Comparison of total KOH added for the experiments described in Table 3-2. Error bars represent one standard deviation of repeated experiments as described in Chapter 3.8

Above in Figure 6-18, the total amount of KOH added to the ASBR is indicated. It is important to note that amount included the KOH that was fed into the ASBR with the substrate as well as the amount dosed for pH control. This concentration indicated was also the calculated concentration of KOH that was in the effluent from the ASBR. The KOH concentration in the feed substrate needs to be halved when determining the fraction that it forms of the total KOH dosed due to the ASBR operating with a VDF of 0.5.

As experiment set 5 had the lowest pH drop due to the increase bicarbonate, it required the least amount of KOH dosed for pH control in the ASBR.

The effect of inhibition due to the feed pH can be seen with the amount of KOH that was dosed. Experiment 3 required the least amount of KOH dosed compared when compared to experiment 1, 2 and 4. As experiment 3 was fed at a pH where the methanogens are within the optimal operating range, VFAs were consumed quickly as they were produced in the ASBR. This meant that less VFAs had to be neutralised to get the pH back to the set point. Therefore, if only varying the substrate pH to the ASBR, the feed substrate should be correct to 7.4 so that the lowest operating cost can be achieved in terms of dosing.

Stellenbosch University https://scholar.sun.ac.za

With experiment 1, the ASBR was fed at the lowest pH of 4.3. Comparing this to experiment 2, the acidogens in experiments 1, would have received some inhibition as less VFAs had to be neutralised in terms of KOH dosing. Experiment 2 was fed such that there were inhibitory effects on the methanogens, however, it favoured VFA production with the acidogens. Therefore, experiment 2 required more KOH for pH control.

Experiment 4 was fed at such a pH that both the methanogens and acidogens experienced inhibition. In terms of KOH dosed, approximately the same amount was dosed for this as when compared to that at a pH of 4.3. However, at a pH of 4.29, the ASBR had a higher COD reduction which is essentially the aim of the ASBR treatment process.

6.3. Key findings

In order to keep an ASBR simple, the feed substrate could be fed straight to the ASBR without pH correction. However, from the above experiments, it was beneficial to correct the pH of the feed substrate to at least 7.4 while operating the ASBR with *in-situ* pH control. Feeding at this pH resulted in the COD reduction and gas production being maximised. It is believed that feeding at this level results in less inhibition during the earlier stages of the batch during the treatment process. Furthermore, approximately 8 – 12% less KOH can be dosed when feeding in a pH of 7.4. This can decrease the operating of cost of the treatment plant.

Stellenbosch University https://scholar.sun.ac.za

Chapter 7 - Conclusions and Recommendations

The primary objective of this study was to evaluate the behaviour and efficiency of operation of an ASBR during the treatment of synthetic winery effluent while performing *in-situ* pH adjustment during mixing, and without the addition of alkalinity.

7.1. ADM1 simulation of an ASBR and related pH predictions

Although the modelling of the ADM1 gave a better understanding of the anaerobic digestion process, it had some limitations. Problems were experienced with the modelling of sludge retention and biogas production.

The normal ADM1 model does not incorporate sludge retention into its mass balance differentials. To overcome this, the sludge retention was modelled as if the sludge was separated with a clarifier and returned to the ASBR. However, the modelling of this showed that the decant phase cannot be too short, or else it won't simulate sludge retention successfully.

When poorly selected soluble and particulate concentrations are specified, the model can become unstable. It seemed that when the sludge concentrations were not known, over-specifying the sludge concentration and notably under-specifying the initial soluble component concentrations of the ASBR, prevented the simulation from becoming unstable. However, during the feed stage of the batch when a component is rapidly added to the ASBR, the ADM1 simulation can become unstable.

The simulation of the ADM1, when considering the synthetic wastewater treated in this study, predicted a rapid reduction of pH early in the process. This was as a result of rapid consumption of monosaccharides and formation of VFAs. From this, it was clear that *in-situ* pH control would be required. This pH behaviour was proven with the lab scale ASBR used in this study.

7.2. Operating an ASBR with *in-situ* pH control

An ASBR could be operated successfully with *in-situ* pH control and at a VDF of 0.5, while the feed substrate typically consisted of 75% monosaccharides. This followed while operating the ASBR with OLRs between 1.1 and 3.1 g-COD_{feed}.ℓ^{-1}_{ASBR}.day^{-1}. Furthermore, this was achieved when only 15% of the ASBR was filled with sludge. Additionally, the ASBR could be operated under a lower VDF if the wastewater composition remained the same. However, if the wastewater composition were to change, further research would be required to determine how the ASBR would react.

Stellenbosch University https://scholar.sun.ac.za

With the current ASBR setup, ammonium sulphate concentrations of 5000 mg/ℓ within winery wastewater can be treated between OLR of 1.1 and 1.8 g-COD_{feed}.ℓ^{-1}_{ASBR}.day^{-1} while achieving a COD reduction of at least 65%.

When ammonium sulphate is excluded from the feed substrate, a COD reduction in excess of 80% can be obtained between OLRs of 1.1 and 2.1 g-COD_{feed}.ℓ^{-1}_{ASBR}.day^{-1}. Additionally, this effluent from the ASBR is clean enough so that less than 50 m^3/day can be irrigated legally.

A factor of 0.035 mg-KOH.ℓ^{-1}_{ASBR}.mg-$COD^{-1}_{removed}$ can be used to determine the requirements for KOH dosing while the ASBR is operated between OLRs of 1.1 and 2.9 g-COD_{feed}.ℓ^{-1}_{ASBR}.day^{-1}. This factor can be used to determine the expected chemical cost of operating an up-scaled ASBR.

Under the experimental operating conditions, an OLR of 1.9 g-COD_{feed}.ℓ^{-1}_{ASBR}.day^{-1} produced the most biogas and highest methane yield of 0.16 ℓ.g-$COD^{-1}_{removed}$. Furthermore, the ASBR was the most stable under these conditions as the least variation in terms of COD reduction and COD removal rate was measured.

The biogas produced with the ASBR contained nitrogen. If the nitrogen were to be removed by feeding at a higher COD:N ratio, an upgraded biogas can be formed. With this study, upgrading the biogas resulted in a methane fraction of about 80%. This means that through the upgrading of biogas, the HHV would be increased by 5.32 MJ/m^3 when compared to the typical biogas production of 70% methane and 30% carbon dioxide.

The investigation concluded that *in-situ* pH control was most important during the first five hours of batch operation. However, very rarely, it was required for eight hours. It is recommended that a two phase in-situ pH controller be investigated to maintain the pH closer to the set point throughout the batch. During the first five hours, the amount of KOH dosed should be greater for faster pH correction. After this, the correction should only be allowed by dosing small amounts of KOH. This should help maintain the pH closer to 7 and hopefully reduce inhibition experienced by the methanogens.

For large scale operations it is recommended that the intermediate and partial alkalinity also be measured. If the intermediate alkalinity suddenly increases, it indicates an accumulation of VFAs. When the partial alkalinity decreases, it indicates that less bicarbonate is being produced, consequently indicating that the methanogens are less active as less carbon dioxide is being formed. Keeping a record of these two parameters can help ensure correct operation of an ASBR

Stellenbosch University https://scholar.sun.ac.za

A further recommendation in terms of equipment is to pre-heat the feed substrate into the ASBR. This could help with reducing methanogens inhibition in the early stages of the treated batch. However, increasing the temperature could lead to increased acidogens and acetogens activity. Furthermore, increasing the feed temperature would also add to the cost of the treatment. This would result in a faster pH reduction. Therefore, the *in-situ* pH controller setup should then also be adapted to add more KOH for each dose.

7.3. Adjusting the pH of the feed substrate along with *in-situ* pH control

Part of this study aimed to keep the ASBR as simple as possible and only use *in-situ* pH control. However, it was determined that adjusting the pH of the feed substrate to 7.4, was beneficial for the performance of the ASBR. Feeding at this pH maximised the COD reduction and gas production. Furthermore, 8 – 12% less KOH was required in total for *in-situ* and feed pH adjustments for the treatment of the synthetic winery wastewater.

Adding alkalinity to the feed substrate resulted in using the least amount of KOH per batch, however, the produced biogas contained less methane resulting in a lowered HHV.

Stellenbosch University https://scholar.sun.ac.za

Chapter 8 - References

Ammary, B.Y., 2005. Treatment of Olive mill wastewater using an anaerobic sequencing batch reactor. Desalination 177, 131–137.

Angenent, L.T., Dague, R.R., 1996. A laboratory-scale comparison of the UASB and ASBR processes. Ann Arbor Press, Inc., Chelsea, MI (United States).

Archer, D.B., Hilton, M.G., Adams, P., Wiecko, H., 1986. Hydrogen as a process control index in pilot scale anaerobic digester. Biotechnol. Lett. 8, 197–202.

Archilha, N.C., Canto, C.S.A., Ratusznei, S.M., Rodrigues, J.A.D., Zaiat, M., Foresti, E., 2010. Effect of feeding strategy and COD/sulfate ratio on the removal of sulfate in an AnSBBR with recirculation of the liquid phase. J. Environ. Manage. 91, 1756–1765. doi:10.1016/j.jenvman.2010.03.016

Barrera, E.L., Spanjers, H., Solon, K., Amerlinck, Y., Nopens, I., Dewulf, J., 2015. Modeling the anaerobic digestion of cane-molasses vinasse: Extension of the Anaerobic Digestion Model No. 1 (ADM1) with sulfate reduction for a very high strength and sulfate rich wastewater. Water Res. 71, 42–54. doi:10.1016/j.watres.2014.12.026

Batstone, D.J., Keller, J., Angelidaki, I., Kalyuzhnyi, S.V., Pavlostathis, S.G., Rozzi, A., Sanders, W.T.M., Siegrist, H., Vavilin, V.A., 2002. The IWA Anaerobic Digestion Model No 1 (ADM1). Water Sci. Technol. 45, 65–73.

Batstone, D.J., Torrijos, M., Ruiz, C., Schmidt, J.E., 2004. Use of an anaerobic sequencing batch reactor for parameter estimation in modelling of anaerobic digestion. Water Sci. Technol. J. Int. Assoc. Water Pollut. Res. 50, 295–303.

Bitton, G., 2005. Wastewater microbiology, 3rd ed.. ed. Wiley-Liss, John Wiley & Sons, Hoboken, NJ.

Cesur, D., Albertson, M.L., 2005. Modification of anaerobic digestion model no. 1 for accumulation and biomass recycling, in: AGU Hydrology Days. Presented at the Hydrology Days 2005, Colorado State University, pp. 1–30.

Chen, J.L., Ortiz, R., Steele, T.W.J., Stuckey, D.C., 2014. Toxicants inhibiting anaerobic digestion: A review. Biotechnol. Adv. doi:10.1016/j.biotechadv.2014.10.005

Stellenbosch University https://scholar.sun.ac.za

Chen, W.-H., Sung, S., Chen, S.-Y., 2009. Biological hydrogen production in an anaerobic sequencing batch reactor: pH and cyclic duration effects. Int. J. Hydrog. Energy 34, 227–234. doi:10.1016/j.ijhydene.2008.09.061

Cheong, D.-Y., Hansen, C.L., 2008. Effect of feeding strategy on the stability of anaerobic sequencing batch reactor responses to organic loading conditions. Bioresour. Technol., Exploring Horizons in Biotechnology: A Global Venture 99, 5058–5068. doi:10.1016/j.biortech.2007.08.084

Chernicharo, C.A. de L., 2007. Anaerobic reactors. IWA Publishing, London.

Colmenarejo, M.F., Sánchez, E., Bustos, A., García, G., Borja, R., 2004. A pilot-scale study of total volatile fatty acids production by anaerobic fermentation of sewage in fixed-bed and suspended biomass reactors. Process Biochem. 39, 1257–1267. doi:10.1016/S0032-9592(03)00253-X

Conradie, A., Sigge, G.O., Cloete, T.E., 2014. Influence of winemaking practices on the characteristics of winery wastewater and water usage of wineries. South Afr. J. Enol. Vitic. 35, 10–19.

Dague, R.R., 1993. Anaerobic sequencing batch reactor. US5185079 A.

Degrémont, s a, 2007. Water treatment handbook., 7th [English] ed.. ed. Degrémont ; Cachan, France: Distributed by Lavoisier, Rueil-Malmaison, France.

Donoso-Bravo, A., Rosenkranz, F., Valdivia, V., Torrijos, M., Ruiz-Filippi, G., Chamy, R., n.d. Anaerobic sequencing batch reactor as an alternative for the biological treatment of wine distillery effluents. Water Sci. Technol. 60, 1155–1160.

Drosg, B., 2013. Process monitoring in biogas plants. IEA Bioenergy.

Du Preez, J., 2010. Treatment of typical South African milking parlour wastewater by means of anaerobic sequencing batch reactor technology. (Thesis). Stellenbosch : University of Stellenbosch.

Farina, R., Cellamare, C.M., Stante, L., Giodarno, A., 2004. Pilot scale anaerobic sequencing batch reactor for distillery wastewater [WWW Document]. URL http://www.bologna.enea.it/ambtd/articoli/04-09-27-montreal-ASBR.pdf (accessed 5.1.16).

Fezzani, B., Cheikh, R.B., 2009. Extension of the anaerobic digestion model No. 1 (ADM1) to include phenolic compounds biodegradation processes for the simulation of anaerobic co-digestion of olive mill wastes at thermophilic temperature. J. Hazard. Mater. 162, 1563–1570. doi:10.1016/j.jhazmat.2008.06.127

Stellenbosch University https://scholar.sun.ac.za

Fillaudeau, L., Bories, A., Decloux, M., 2008. Brewing, winemaking and distilling: An overview of wastewater treatment and utilisation schemes., Handbook of water and energy management in food processing.

Gerardi, M.H., 2003. The Microbiology of Anaerobic Digesters. John Wiley & Sons.

IWA Task Group for Mathematical Modelling of Anaerobic Digestion Processes, 2002. Anaerobic digestion model no. 1. IWA, London.

Khanal, S.K., Huang, J.-C., 2003. ORP-based oxygenation for sulfide control in anaerobic treatment of high-sulfate wastewater. Water Res. 37, 2053–2062. doi:10.1016/S0043-1354(02)00618-8

Lee, S.J., 2008. Relationship between Oxidation Reduction Potential (ORP) and Volatile Fatty Acid (VFA) Production in the Acid-Phase Anaerobic Digestion Process (Thesis). University of Canterbury, New Zealand.

Liu, C.-M., Wu, S.-Y., Chu, C.-Y., Chou, Y.-P., 2014. Biohydrogen production from rice straw hydrolyzate in a continuously external circulating bioreactor. Int. J. Hydrog. Energy 39, 19317–19322. doi:10.1016/j.ijhydene.2014.05.175

Malandra, L., Wolfaardt, G., Zietsman, A., Viljoen-Bloom, M., 2003. Microbiology of a biological contactor for winery wastewater treatment. Water Res. 37, 4125–4134. doi:10.1016/S0043-1354(03)00339-7

Metcalf & Eddy, 2003. Wastewater engineering : treatment and reuse, 4th ed. / revised by George Tchobanoglous, Franklin L. Burton, H. David Stensel.. ed. McGraw-Hill, Boston.

Mosey, F.E., Fernades, X.A., 1989. Paterns of hydrogen in biogas from the anaerobic digestion of milk sugars. Water Sci. Technol. 21, 187–196.

Mosse, K. p. m., Patti, A. f., Christen, E. w., Cavagnaro, T. r., 2011. Review: Winery wastewater quality and treatment options in Australia. Aust. J. Grape Wine Res. 17, 111–122. doi:10.1111/j.1755-0238.2011.00132.x

Mulidzi, R., Laker, G., Wooldridge, J., van Schoor, L., 2002. Composition of effluents from wineries in the Western and Northern Cape provinces (Part 1): Seasonal variation and differences between wineries. Wynboer Tegnies.

Normak, A., Suurpere, K., Orupold, K., Kokin, E., 2012. Simulation of anaerobic digestion of cattle manure. Agron. Res. 167–174.

Stellenbosch University https://scholar.sun.ac.za

Parawira, W., 2004. Anaerobic Treatment of Agricultural Residues and Wastewater - Application of High-Rate Reactors (Dissertation (Composite)). Lund University, Department iof Biotechnology.

Parawira, W., Murto, M., Read, J.S., Mattiasson, B., 2007. A Study of Two-Stage Anaerobic Digestion of Solid Potato Waste using Reactors under Mesophilic and Thermophilic Conditions. Environ. Technol. 28, 1205–1216. doi:10.1080/09593332808618881

Parawira, W., Murto, M., Read, J.S., Mattiasson, B., 2004. Volatile fatty acid production during anaerobic mesophilic digestion of solid potato waste. J. Chem. Technol. Biotechnol. 79, 673–677. doi:10.1002/jctb.1012

Pinho, S.C., Ratusznei, S.M., Rodrigues, J.A.D., Foresti, E., Zaiat, M., 2005. Feasibility of treating partially soluble wastewater in anaerobic sequencing batch biofilm reactor (ASBBR) with mechanical stirring. Bioresour. Technol. 96, 517–519. doi:10.1016/j.biortech.2004.05.027

Pinho, S.C., Ratusznei, S.M., Rodrigues, J.A.D., Foresti, E., Zaiat, M., 2004. Influence of the agitation rate on the treatment of partially soluble wastewater in anaerobic sequencing batch biofilm reactor. Water Res. 38, 4117–4124. doi:10.1016/j.watres.2004.08.015

Ramos, A.C.T., Ratusznei, S.M., Rodrigues, J.A.D., Zaiat, M., 2003. Mass Transfer Improvement of a Fixed-Bed Anaerobic Sequencing Batch Reactor with Liquid-Phase Circulation. Interciencia 28, 214–219.

Ripley, L.E., Boyle, W.C., Converse, J.C., 1986. Improved Alkalimetric Monitoring for Anaerobic Digestion of High-Strength Wastes. J. Water Pollut. Control Fed. 58, 406–411.

Rosen, C., Jeppsson, U., 2006. Aspects on ADM1 implementation within the BSM2 framework. Lund University: Department of Industrial Electrical Engineering and Automation.

Ruíz, C., Torrijos, M., Sousbie, P., Lebrato Martínez, J., Moletta, R., Delgenès, J.P., 2002. Treatment of winery wastewater by an anaerobic sequencing batch reactor. Water Sci. Technol. J. Int. Assoc. Water Pollut. Res. 45, 219–224.

Schon, M., 2009. Numerical modelling of anaerobic digestion processes in agricultural biogas plants (Dissertation). University of Innsbruck, Austria.

Shuler, M.L., Kargi, F., 2010. Bioprocess Engineering: Basic concepts, second edition. ed. Prentice Hall PTR.

Stellenbosch University https://scholar.sun.ac.za

Sigge, G.O., 2005. Integration of anaerobic biological and advanced chemical oxidation processes to facilitate biodegradation of fruit canning and winery wastewaters (Thesis). Stellenbosch : Stellenbosch University.

Smit, J., 2013. The construction and preliminary evaluation of an anaerobic sequential batch reactor for the treatment of winery effluent. Stellenbosch University, Process Engineering.

Solera, R., Romero, L.I., Sales, D., 2002. The evolution of biomass in a two-phase anaerobic treatment preocess during start-up. Chem. Biochem. Eng. Q. 16, 25–29.

Sung, S., Dague, R.R., 1995. Laboratory Studies on the Anaerobic Sequencing Batch Reactor. Water Environ. Res. 67, 294–301.

Tugtas, A.E., Tezel, U., Pavlostathis, S.G., 2006. An extension of the Anaerobic Digestion Model No. 1 to include the effect of nitrate reduction processes. Water Sci. Technol. J. Int. Assoc. Water Pollut. Res. 54, 41–49.

van Schoor, L.H., 2005. Guidelines for the management of wastewater and solid waste at existing wineries.

Vining, G.G., 1997. Statistical methods for engineers. International Thomson Publishing Company, University of Florida.

Wang, L., Zhou, Q., Li, F.T., 2006. Avoiding propionic acid accumulation in the anaerobic process for biohydrogen production. Biomass Bioenergy 30, 177–182. doi:10.1016/j.biombioe.2005.11.010

Wang, Y., Zhang, Y., Wang, J., Meng, L., 2009. Effects of volatile fatty acid concentrations on methane yield and methanogenic bacteria. Biomass Bioenergy 33, 848–853. doi:10.1016/j.biombioe.2009.01.007

Wirtz, R.A., Dague, R.R., 1996. Enhancement of Granulation and Start-Up in the Anaerobic Sequencing Batch Reactor. Water Environ. Res. 68, 883–892.

Won, S.G., Baldwin, S.A., Lau, A.K., Rezadehbashi, M., 2013. Optimal operational conditions for biohydrogen production from sugar refinery wastewater in an ASBR. Int. J. Hydrog. Energy 38, 13895–13906. doi:10.1016/j.ijhydene.2013.08.071

Wu, X., Yao, W., Zhu, J., 2010. Effect of pH on continuous biohydrogen production from liquid swine manure with glucose supplement using an anaerobic sequencing batch reactor. Int. J. Hydrog. Energy,

Stellenbosch University https://scholar.sun.ac.za

ISMF-09 International Symposium on Multiphase Flow, Heat Mass Transfer and Energy Conversion 35, 6592–6599. doi:10.1016/j.ijhydene.2010.03.097

Xiangwen, S., Dangcong, P., Zhaohua, T., Xinghua, J., 2008. Treatment of brewery wastewater using anaerobic sequencing batch reactor (ASBR). Bioresour. Technol. 99, 3182–3186. doi:10.1016/j.biortech.2007.05.050

Yu, H., Zhu, Z., Hu, W., Zhang, H., 2002. Hydrogen production from rice winery wastewater in an upflow anaerobic reactor by using mixed anaerobic cultures. Int. J. Hydrog. Energy, BIOHYDROGEN 2002 27, 1359–1365. doi:10.1016/S0360-3199(02)00073-3

Zaiat, M., Rodrigues, J.A., Ratusznei, S.M., de Camargo, E.F., Borzani, W., 2001. Anaerobic sequencing batch reactors for wastewater treatment: a developing technology. Appl. Microbiol. Biotechnol. 55, 29–35.

Zhu, J., Li, Y., Wu, X., Miller, C., Chen, P., Ruan, R., 2009. Swine manure fermentation for hydrogen production. Bioresour. Technol., OECD Workshop: Livestock Waste Treatment Systems of the Future: A Challenge to Environmental Quality, Food Safety, and Sustainability 100, 5472–5477. doi:10.1016/j.biortech.2008.11.045

Stellenbosch University https://scholar.sun.ac.za

Appendix A - ASBR long term operation results

A.1. Chemical oxygen demand

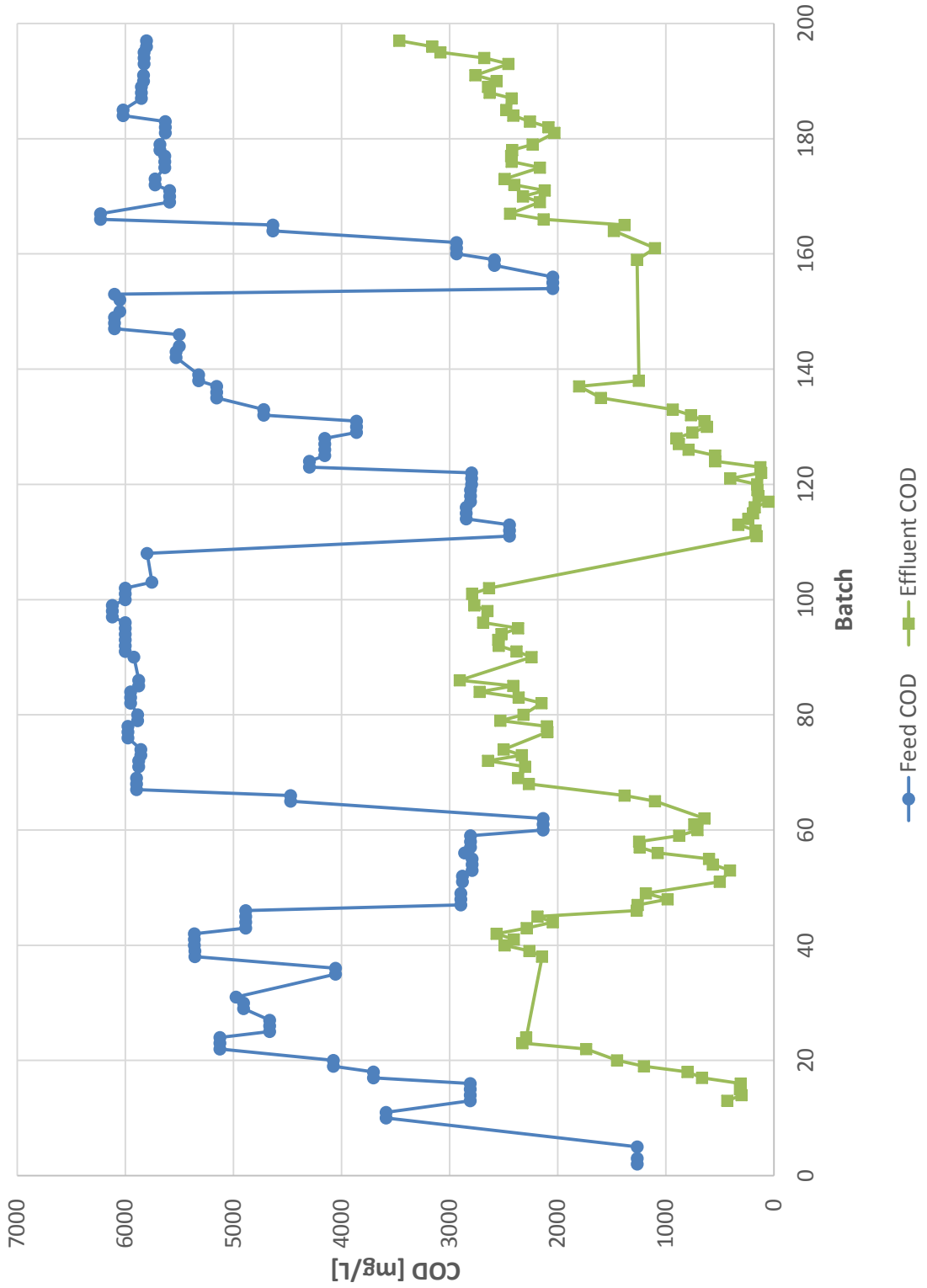

Stellenbosch University https://scholar.sun.ac.za

A.2. Alkalinity

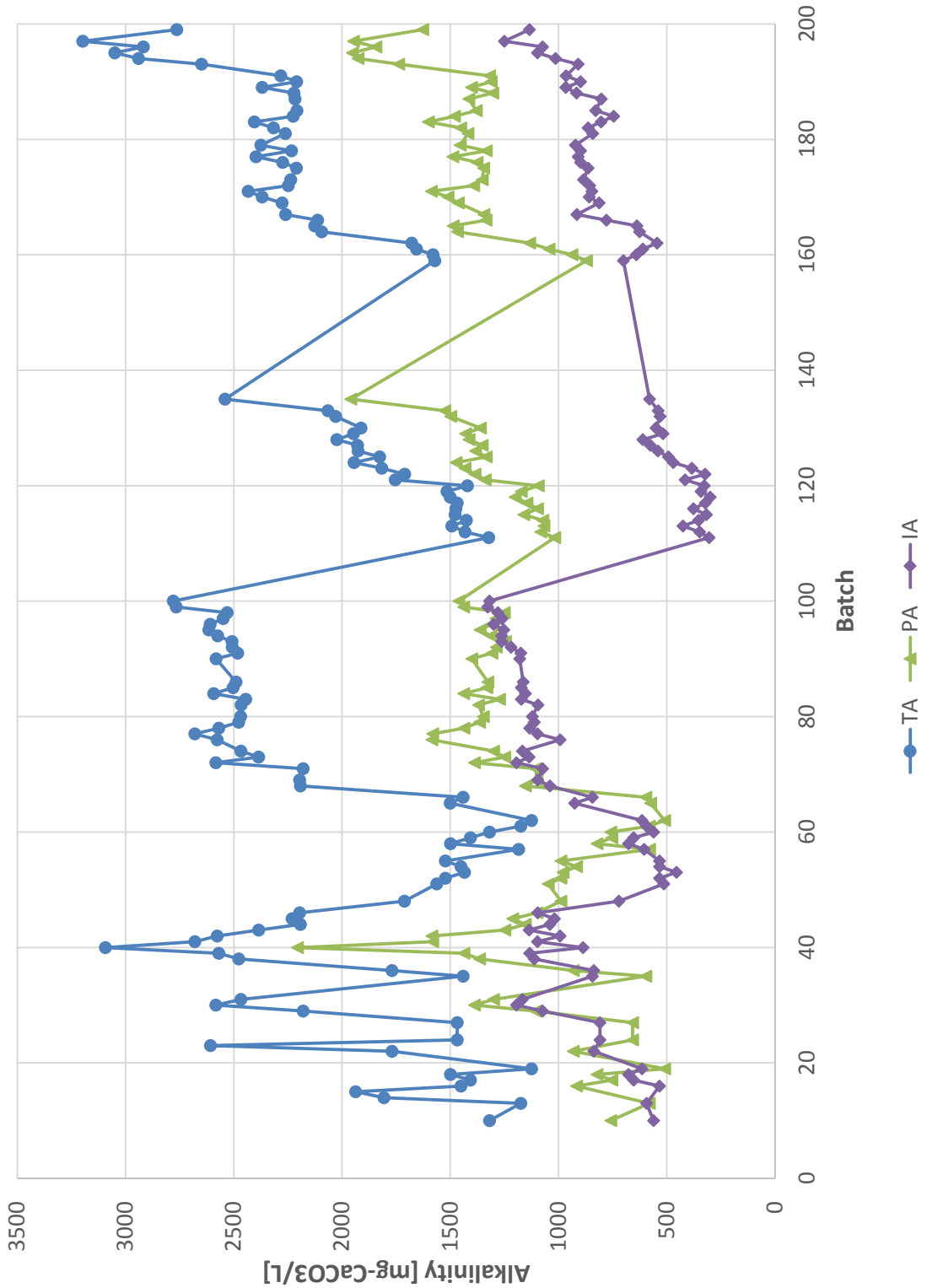

Stellenbosch University https://scholar.sun.ac.za

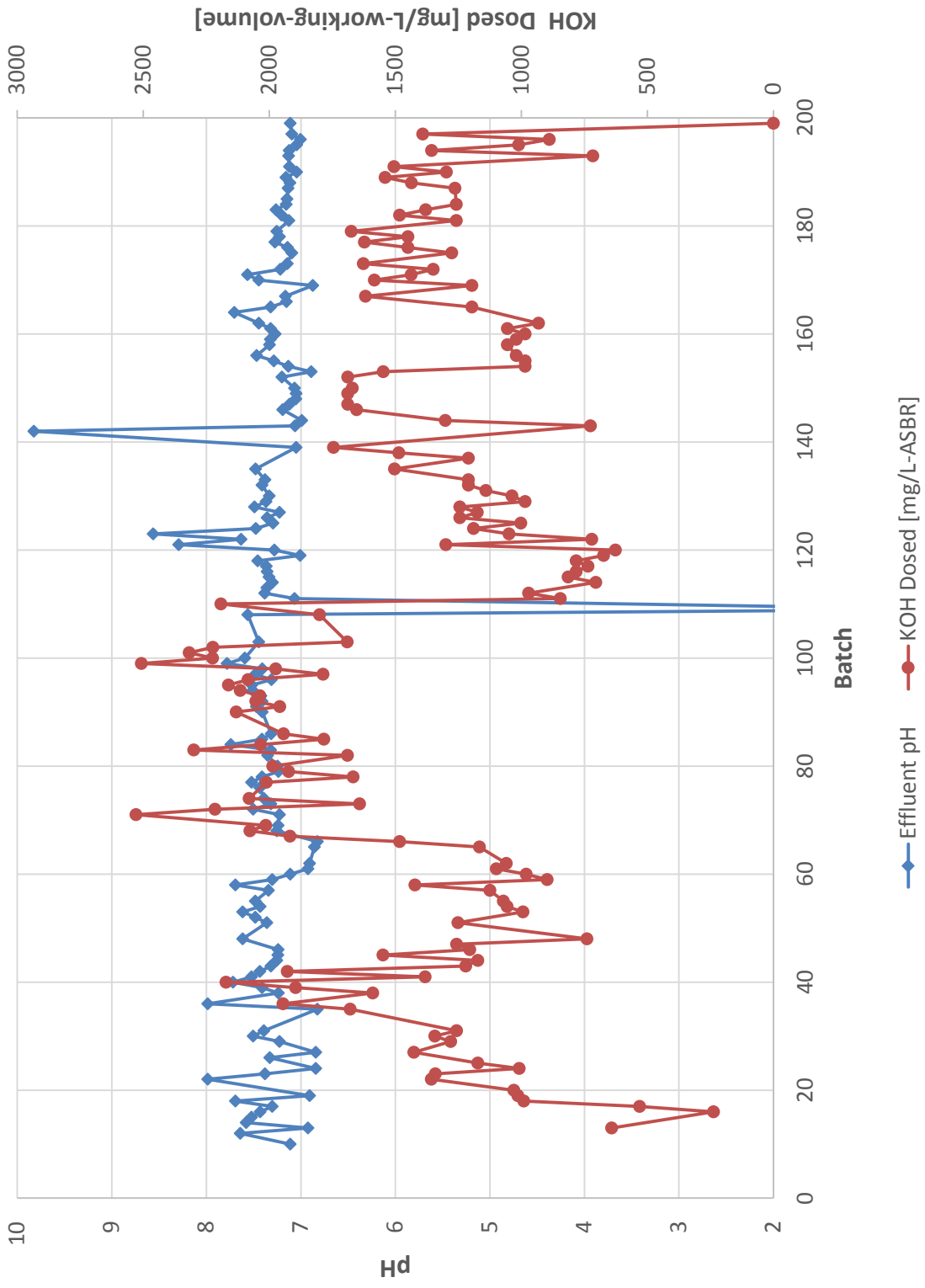

Stellenbosch University https://scholar.sun.ac.za

A.3. Biogas production

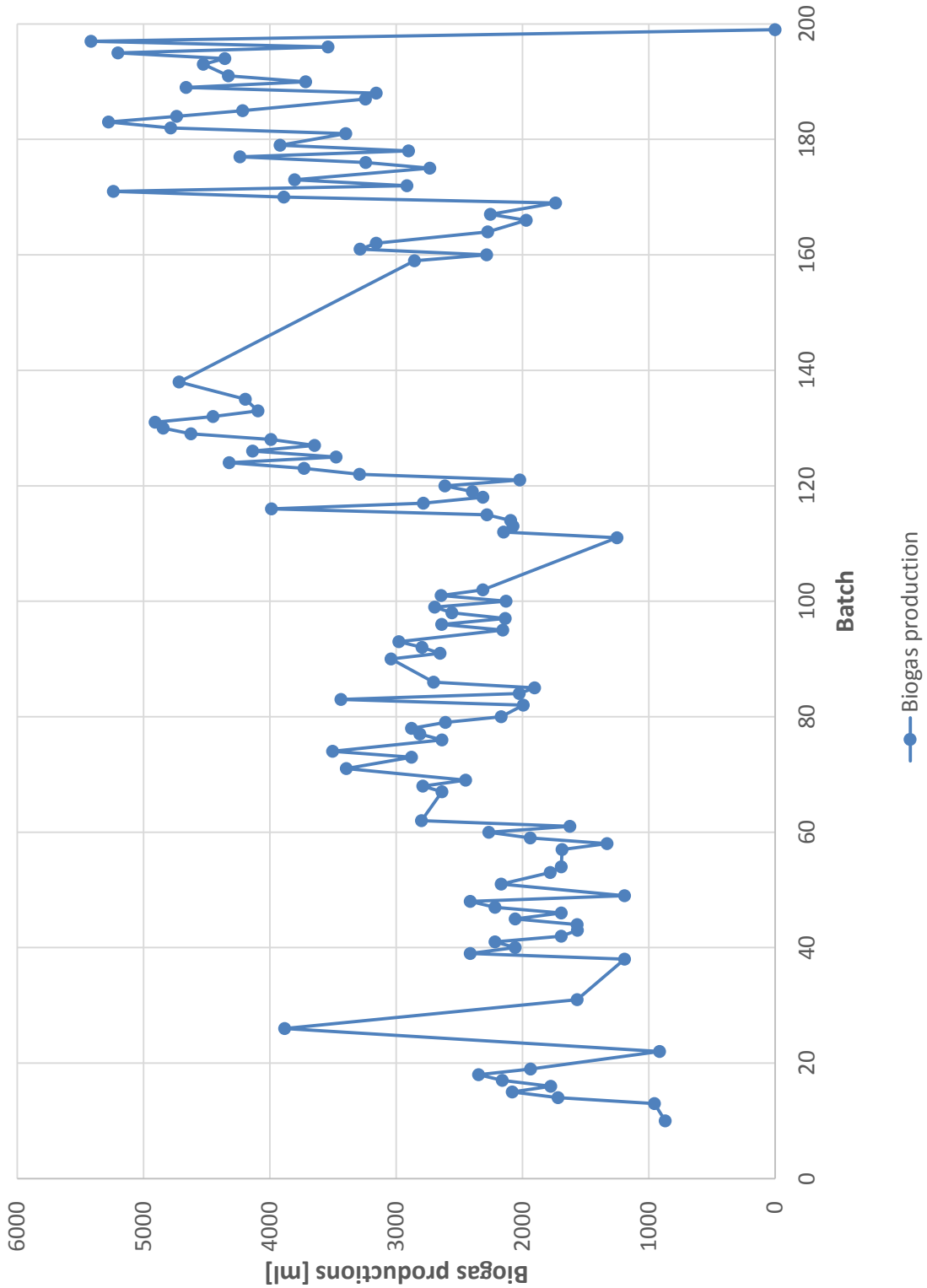

Stellenbosch University https://scholar.sun.ac.za

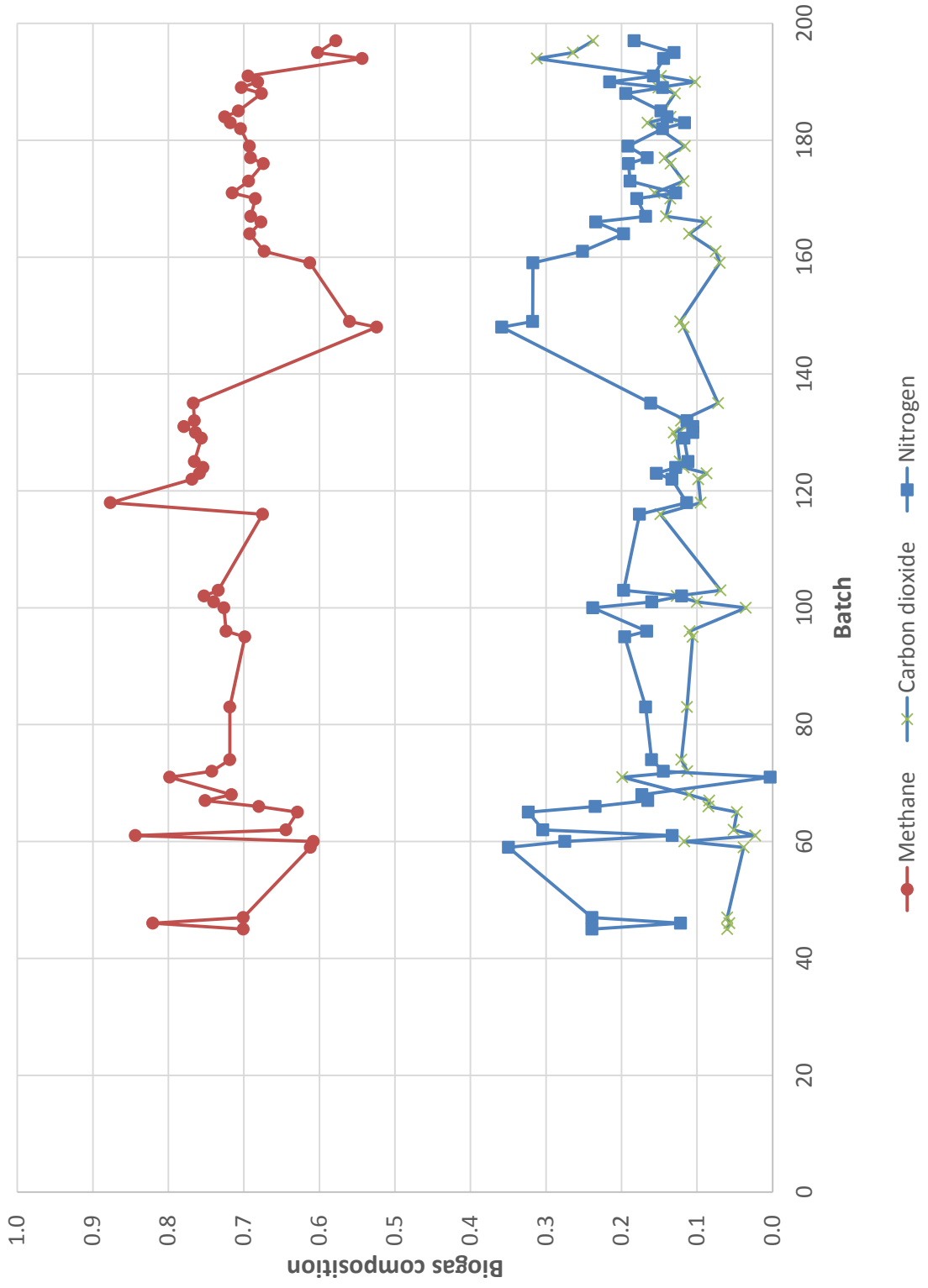

Stellenbosch University https://scholar.sun.ac.za

Appendix B - Analytical procedures and data analysis

B.1. COD analysis

a. Determining COD

The procedure below describes the method followed to determine the COD of the wastewater in the influent and effluent streams.

1. The 14 mℓ sample was spun in a centrifuge at 6000rpm for 10 minutes to obtain a particle free supernatant.
2. Pipette the required solution A and B in a clean test cell and mix with the vortex mixer. Required solution A and B volumes according to Table B-1.
3. Pipette the required sample into the test cell from the supernatant and close tightly before mixing it in the vortex mixer.
4. Place the test cells into the preheated Thermoreaktor TR300 (Merck) at 148°C for 120 min.
5. After the two reaction time, remove the cell to cool down to room temperature.
6. Place the test cell into the Spectroquant® NOVA 60 (Merck) and select the correct method according to the COD range.
7. Note the measured value.
8. Dispose of cell test solution as advised by the head of the laboratory.

Table B-1: Volume of solution A and B for COD analyses

COD range [mg/L]	Solution A [mL]	Solution B [mL]	Sample volume [mL]	Spec. method
10 – 150	0.3	2.85	3	014
100 – 1500	0.3	2.3	3	023
500 – 15000	2.2	1.8	1	024

b. Calculating COD removal efficiency, COD removal rate and OLR.

COD removal efficiency

$$\varepsilon_{COD} = \frac{COD_{in} - COD_{eff}}{COD_{in}} \times 100$$

Stellenbosch University https://scholar.sun.ac.za

COD removal rate

$$COD\ removal\ rate = \frac{COD_{removed}[g_{COD}]}{V_{ASBR}[\ell] \times t_{batch}[day]}$$

Organic loading rate

$$OLR = \frac{COD_{fed}[g_{COD}]}{V_{ASBR}[\ell] \times t_{batch}[day]}$$

B.2. Alkalinity analysis

a. pH, partial alkalinity and total alkalinity

The final pH, partial alkalinity and total alkalinity was determined with the use of an auto titrator with the following procedure:

1. Switch on the auto titrator.
2. Select “pH and alkalinity” mode.
3. Rinse the probes with distilled water and pat dry.
4. Calibrate the pH probe for pH 10 and then pH 4. Clean and dry pH probe between different calibration points.
5. Add 40 mℓ of the sample into a beaker along with a stirring magnet.
6. Place the underneath the probes and measure the pH.
7. Let the auto titrator to two end points of pH 5.75 and pH 4.5 with a 0.1 M HCl solution.
8. Once the titration is complete, note down the alkalinity of PA (pH 5.75) and TA (pH 4.5) in mg/ℓ-$CaCO_3$.
9. Clean the probes with distilled water.
10. If the analysis of more probes is required, repeat steps 4-8.
11. If the analysis is complete, place the pH probe in a solution of KCl.

b. Calculating intermediate alkalinity and Ripleys ratio

Intermediate alkalinity is the difference between total and partial alkalinity:

$$IA = TA - PA$$

Ripleys ratio:

$$IA{:}\ PA = \frac{IA}{PA}$$

Stellenbosch University https://scholar.sun.ac.za

B.3. Biogas composition analysis

a. Determining biogas composition

The composition of the biogas produced in the ASBR was determined with the use of a GC while following the following procedure:

1. Switch on the GC and set specifications according to Table B-2.
2. Ensure all components are at the desired temperature before switching on the detector.
3. Connect the gas bag to the GC and purged the gas to be analysed through the sample loop.
4. Open the valve and allow the carrier gas to flow through the sample loop.
5. Close it after 10 seconds and start the detector.
6. Once the gas is analysed, select the peaks of the GC output.
7. Take the area under the peak and use that along with calibrations curves to determine the composition of the gas in the sample.
8. Repeat for the analyses for both equaliser bags and the final gas capture bag.
9. Determine the complete gas composition and volume (bubble counter) for the current cycle.
10. Remove the initial composition in the two equaliser bags as determined to be the composition at the end of the previous batch.

Table B-2: GC specifications

Column Type	**Supelco Carbonex 1000**
Column Oven Temperature [°C]	120
Hold Time [min]	6
Ramp Temperature [°C]	225
Heating rate [°C/min]	20
Hold Time [min]	2
Detector	TCD
TCD Temperature [°C]	160
Filament Temperature [°C]	250
Filament current [mA]	102
Range	0.05
Injector Temperature [°C]	120
Carrier Gas	Argon
Carrier Gas flow rate [mℓ/min]	26.8

Stellenbosch University https://scholar.sun.ac.za

Reference Gas flow rate [mℓ/min]	26.9
Sample loop [µℓ]	1255

b. Gas chromatography calibrations

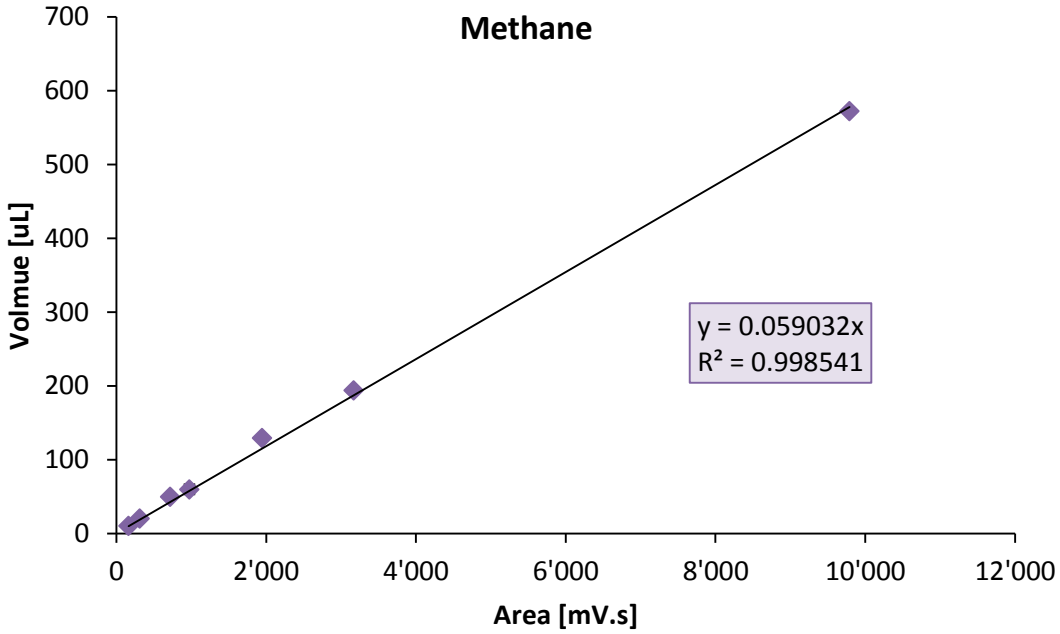

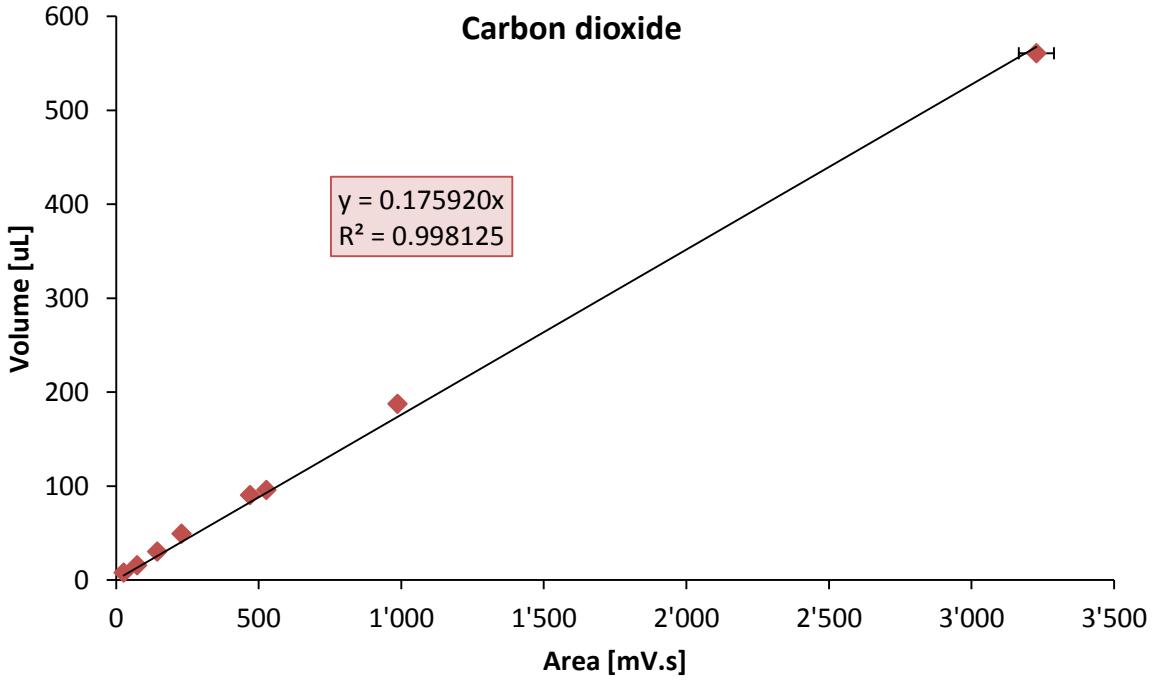

Stellenbosch University https://scholar.sun.ac.za

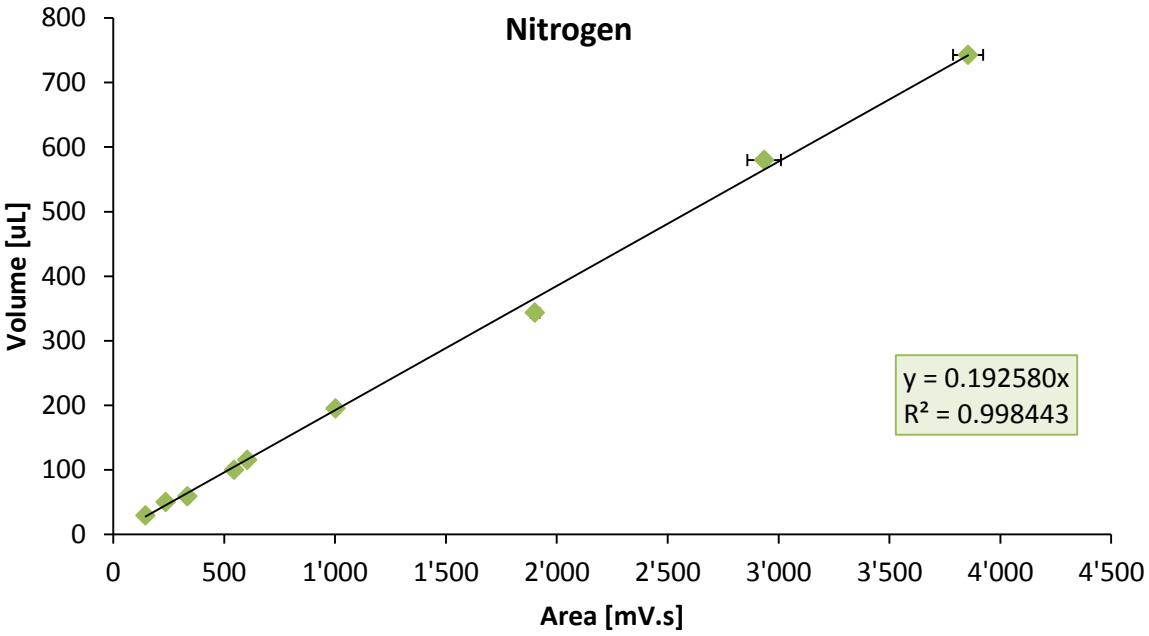

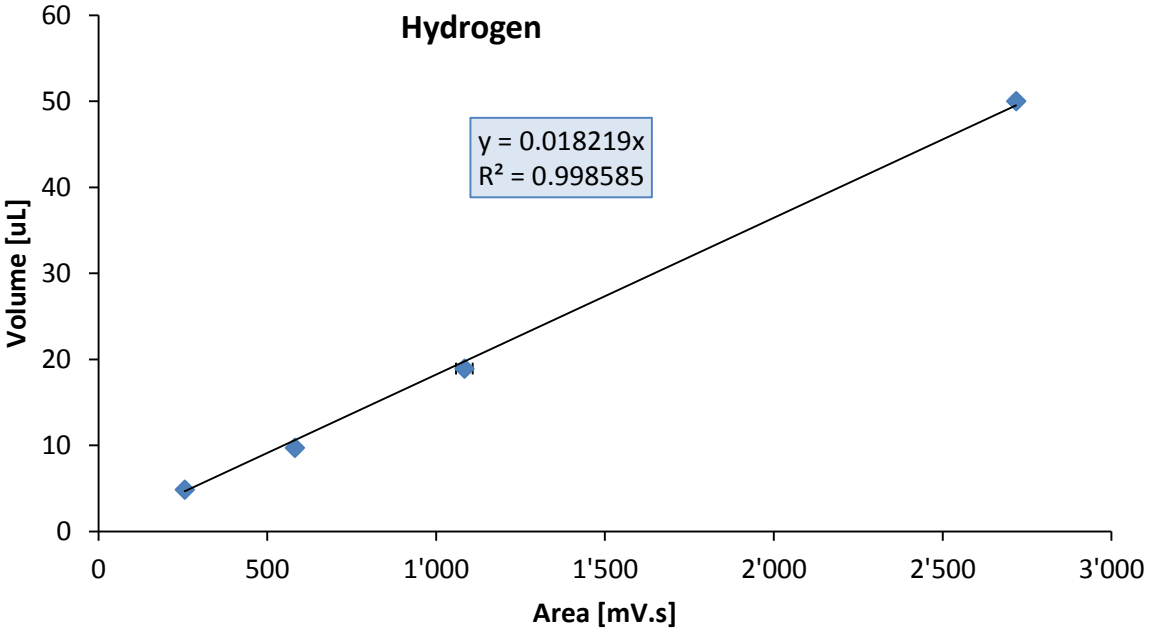

c. Calculating methane yield and methane productivity

Methane yield:

$$Yield = \frac{V_{gas\ produced}[m\ell]}{COD_{removed}[g_{COD}]}$$

Methane productivity:

Stellenbosch University https://scholar.sun.ac.za

$$Productivity = \frac{V_{gas\ produced}[m\ell]}{V_{ASBR}[\ell] \times t_{batch}[day]}$$

B.4. Online measured data analysis

a. Smoothing of data and removing outliers

The data measured online with the ASBR was saved onto a flash drive and saved as a "csv" file. A Matlab file was created to read this file and do the necessary calculations to obtain the required data. The code can be found in Appendix D.

Signal noise from the 4-20 mA transmitter of the various probes to the PLC caused fluctuations and small changes to be measured. As a result, the logged data had to be smoothed out to present. It has to be noted that every 2 seconds a data point was logged and no smoothing of data was performed on the PLC during ASBR operation.

A Matlab program was written to analyse the data which was recorded online and can be found in Appendix E.3. The raw data was read and the length of each ASBR stage was calculated and presented on screen. The bubble counter measurement was converted to cumulative biogas production with a constant multiplication factor. Due to no signal noise presented with the temperature readings, it was not smoothed out. Online measurements for pH, ORP and EC were smoothed with a built in Matlab function named "smooth" and the "rlowess" method for that function was selected. The "rlowess" is a local regression model that uses weighted linear least squares to determine the smoothed value. The method assigns zero weight to data outside six mean absolute deviations while determining a value of a function. This method was selected as it performed the best at removing outliers and reducing signal noise compared to other built in method for Matlab.

Below in Figure B-8-1 and Figure B-8-2, examples of data for pH and ORP measurements are presented before and after data smoothing was performed on the data set.

In Figure B-8-1 the stored data before smoothing shows occasional outliers and generally a wide band of pH variations measured. After the smoothing operation, the pH band is slightly reduced and most outliers removed. Just before 7h in Figure B-8-1, the smoothed data presents 4 points which look like outliers compared to the remainder of the pH around that time. This outlier is created due to the multiple points measured as outlier at that time increment.

Stellenbosch University https://scholar.sun.ac.za

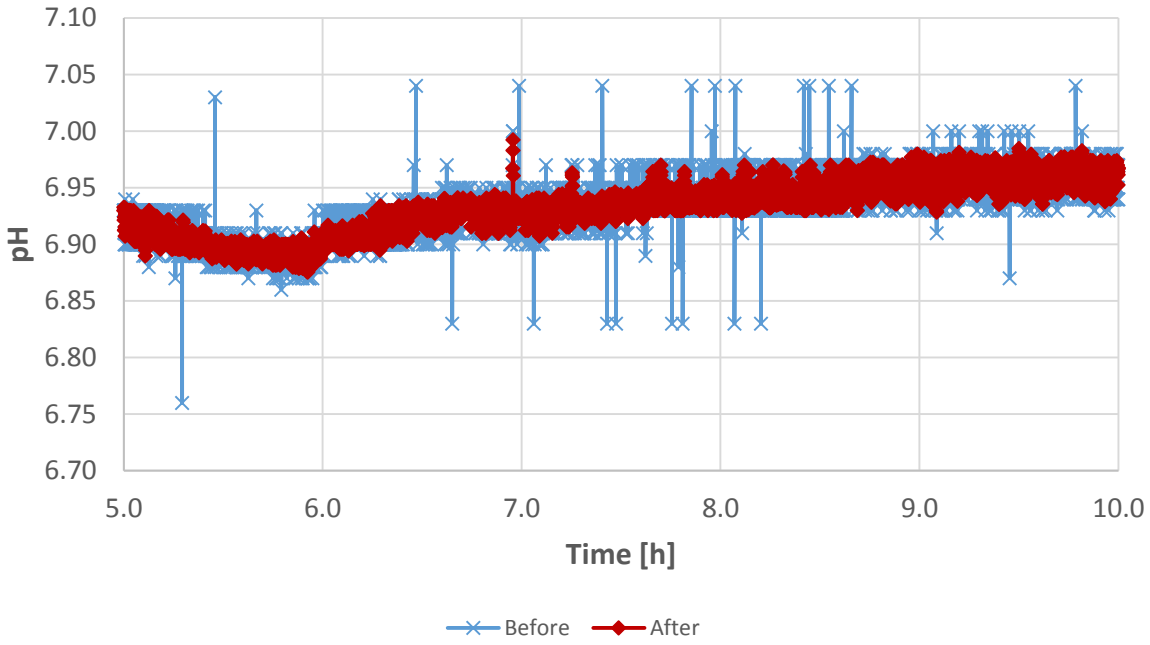

Figure B-8-1: An example of before and after smoothing online measured data due to signal noise

In Figure B-8-2, the stored data before and after smoothing for and ORP sample is presented. Several outliers laying far from the general operating measurements are removed to present the smooth curve after smoothing has been performed.

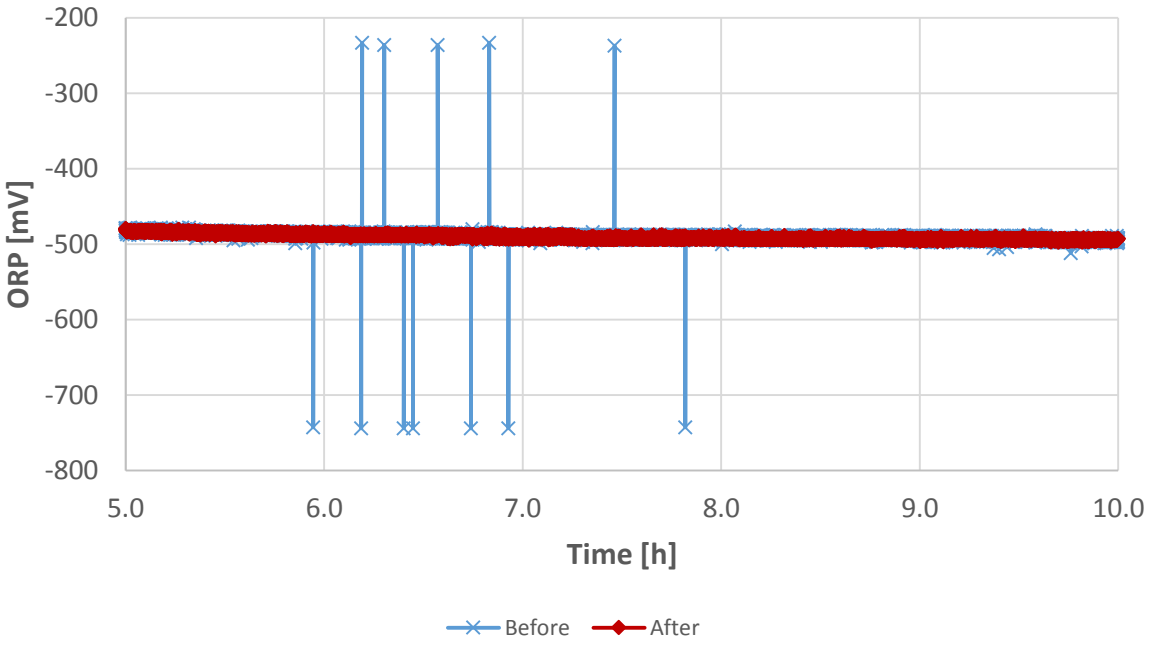

Figure B-8-2: An example of before and after smoothing online measured data to remove outliers

Stellenbosch University https://scholar.sun.ac.za

B.5. Synthetic winery wastewater production

A 5ℓ synthetic winery wastewater stock solution with a COD of 1000 g/ℓ was produced as required. This stock solution was then diluted as required for experiments.

1. Dissolve components 1 – 6 in a Schott bottle with distilled water.
2. Dissolve the yeast extract powder in another Schott bottle with distilled water.
3. Add 3ℓ of distilled water in another Schott bottle.
4. Autoclave the three Schott bottles for 20 minutes.
5. Add components 7 – 16 with a pipette into a small flask with some distilled water.
6. Add all the components into the Schott bottle containing the monosaccharides.
7. Top up the Schott bottle to 5ℓ with the autoclaved water.
8. Flame the top of the Schott bottle before closing it.
9. Store solution in the fridge and dilute as required.

Table C-4 Winery wastewater stock solution recipe

ID	Compound	conc. [mg/L]	Carbon based components COD [mg/L]	mg	uL
1	Glucose	43174	46010.92	21587	14017.6
2	Fructose	43174	46010.92	21587	12773.4
3	Citric acid	24	17.98	12	7.2
4	Tartaric acid	48	25.57	24	13.4
5	Malic acid	48	34.34	24	14.9
6	Lactic acid	48	51.12	24	19.8
7	Propanol	30	71.27	15	18.5
8	Butanol	24	62.13	12	14.8
9	i-Amyl alcohol	91	248.15	46	55.9
10	Acetic acid	5996	6390.51	2998	2855.4
11	Ethanol	240	499.81	120	152.0
12	Ethyl acetate	96	174.22	48	53.5
13	Propionic acid	192	290.10	96	96.9
14	Valeric acid	24	48.85	12	12.9
15	Hexanoic acid	12	23.13	6	6.4
16	Octanoic acid	17	40.98	8	9.2
17	Yeast Extract powder	40776		20388	
	COD Theory	100000	100000		

Stellenbosch University https://scholar.sun.ac.za

B.6. Sample calculations

a. COD

COD reduction for batch 165 which contributes a datum point in Figure 5-1 between OLRs of 2.27 and 2.52 g-COD_{feed}.ℓ^{-1}_{ASBR}.day^{-1}. COD measurements were obtained from the spectrophotometer.

$$\varepsilon_{COD} = \frac{COD_{in} - COD_{eff}}{COD_{in}} \times 100 = \frac{4635 - 1380}{4635} \times 100 = 70.23\%$$

OLR for batch 165

$$OLR = \frac{COD_{fed}[g_{COD}]}{V_{ASBR}[\ell] \times t_{batch}[day]} = \frac{4635}{14.1 \times 0.99} = 2.37 \frac{g_{COD}}{\ell . day}$$

b. Alkalinity

Alkalinity calculations for batch 165 which contributes a datum point in Figure 5-1 between OLRs of 2.27 and 2.52 g-COD_{feed}.ℓ^{-1}_{ASBR}.day^{-1}

Total alkalinity (TA) from the titration analysis for batch 165: 2126 $\frac{mg_{CaCO_3}}{\ell}$

Partial alkalinity (PA) from the titration analysis for batch 165: 1487 $\frac{mg_{CaCO_3}}{\ell}$

Intermediate alkalinity (IA): $IA = TA - PA = 2146 - 1487 = 639$ $\frac{mg_{CaCO_3}}{\ell}$

Ripley ratio: $\frac{IA}{PA} = \frac{639}{1487} = 0.43$

c. Biogas

The section focuses on the determination of the moles of biogas produced for each component.

Biogas signal area size in the 10 ℓ equalisation bags at the end of batch 166 as determined with GC. This composition represented the initial biogas in the ASBR at the start of batch 167.

	H_2	N_2	CH_4	CO_2
Signal area [mV.s]	0.991	1782.648	15439.41	696.407
Sample loop volume [µℓ]	0.018055	343.3024	911.4193	122.5119
Mole of gas [mol]	2.111841	40155.02	106605.9	14329.84

The signal area was determined with GC. The signal area is then converted to a volume within the sample through the calibration curve as indicated with methane:

Stellenbosch University https://scholar.sun.ac.za

$$volume\ CH_4 = 0.059023 \times area = 0.059023 \times 15439.41 = 911\ \mu\ell$$

The sample loop composition was then determined by the fraction of each gas in the sample loop. This composition was considered identical to that in the gas bag analysed. From here, the total biogas volume was used to determine the mole of each gas in the gas bag.

These steps are repeated for the equalisation bag and the final capture bag for batch 167 to determine the total amount of gas at the end of batch 167. The difference between the gas at the start and end of the batch, is what was produced within that batch.

	H_2	N_2	CH_4	CO_2
Start of batch 167 [mol]	2.11	40155	106605	14329
Total gas end of 167 [mol]	6.82	59555	186408	30630
Gas produced [mol]	4.71	19400	79803	16300

The amount of hydrogen gas was considered insignificant relative to the other three, therefore, it was excluded for further analysis.

d. Standard deviation – error bars

All error bars presented in any figure, represents one standard deviation of the average for the specific variable. The calculation of the average COD reduction [%] and standard deviation for inoculation two between OLR 2.01 and 2.27 g-COD_{feed}.ℓ^{-1}_{ASBR}.day^{-1} for Figure 5-1 is indicated here.

Experimental COD reduction [%] data for Figure 5-1: 81.03; 86.96; 78.34; 78.87; 87.38; 97.14

Identify Q1 and Q3 in the data set: Q_1 = 79.41 %; Q_3 = 87.27 %

Step size for outlier identification: $step\ size = 1.5(Q_3 - Q_1) = 1.5(87.27 - 79.41) = 11.79$

Outlier boundary limits: $LIF = Q_1 - step\ size = 67.62\ \%$ $\quad$ $UIF = Q_3 + step\ size = 99.06\ \%$

Therefore, all the data falls within the outlier boundary limits.

$$mean = \bar{x} = \frac{81.03 + 86.96 + 78.34 + 78.87 + 87.38 + 97.14}{6} = 84.95\ \%$$

$$\sigma = \sqrt{\frac{1}{n}\sum_{i=1}^{n}(x_i - \bar{x})^2} = \sqrt{\frac{254.4}{6}} = 6.512\ \%$$

Stellenbosch University https://scholar.sun.ac.za

Appendix C - ADM1 parameters

C.1. ADM1 equation set – constant volume

Soluble components mass balance for constant volume:

Monosaccharides	$\boldsymbol{\frac{dS_{su}}{dt} = \rho_2 + (1 - f_{fa,li})\rho_4 - \rho_5}$
Amino acids	$\frac{dS_{aa}}{dt} = \rho_3 - \rho_6$
Long chain fatty acids	$\frac{dS_{fa}}{dt} = f_{fa,li}\rho_4 - \rho_7$
Total valerate	$\frac{dS_{va}}{dt} = (1 - Y_{aa})f_{va,aa}\rho_6 - \rho_8$
Total butyrate	$\frac{dS_{bu}}{dt} = (1 - Y_{su})f_{bu,su}\rho_5 + (1 - Y_{aa})f_{bu,aa}\rho_6 - \rho_9$
Total propionate	$\frac{dS_{pro}}{dt} = (1 - Y_{su})f_{pro,su}\rho_5 + (1 - Y_{aa})f_{pro,aa}\rho_6 + (1 - Y_{c4})f_{pro,va}\rho_8 - \rho_{10}$
Total acetate	$\frac{dS_{ac}}{dt} = (1 - Y_{su})f_{ac,su}\rho_5 + (1 - Y_{aa})f_{ac,aa}\rho_6 + \left(1 - Y_{fa}\right)f_{ac,fa}\rho_7 + (1 - Y_{c4})f_{ac,va}\rho_8 + (1 - Y_{c4})f_{ac,bu}\rho_9 + \left(1 - Y_{pro}\right)f_{ac,pro}\rho_{10} - \rho_{11} + (1 - Y_{et})f_{ac,et}\rho_{13}$
Hydrogen gas	$\frac{dS_{h2}}{dt} = (1 - Y_{su})f_{h2,su}\rho_5 + (1 - Y_{aa})f_{h2,aa}\rho_6 + \left(1 - Y_{fa}\right)f_{h2,fa}\rho_7 + (1 - Y_{c4})f_{h2,va}\rho_8 + (1 - Y_{c4})f_{h2,bu}\rho_9 + \left(1 - Y_{pro}\right)f_{h2,pro}\rho_{10} - \rho_{12} + (1 - Y_{et})f_{h2,et}\rho_{13} - \rho_{T,h2}$
Methane gas	$\frac{dS_{ch4}}{dt} = (1 - Y_{ac})\rho_{11} + (1 - Y_{h2})\rho_{12} - \rho_{T,ch4}$
Inorganic carbon	$\frac{dS_{IC}}{dt} = \nu_{10,5}\rho_5 + \nu_{10,6}\rho_6 + \nu_{10,10}\rho_{10} + \nu_{10,11}\rho_{11} + \nu_{10,12}\rho_{12} - \rho_{T,co2}$

$$\nu_{10,5} = -\sum_{i=1-9,11-24} C_i\nu_{i,5}$$
$$= -\left[-C_{su} + (1 - Y_{su})f_{bu,su}C_{bu} + (1 - Y_{su})f_{pro,aa}C_{pro} + (1 - Y_{su})f_{ac,su}C_{ac} + Y_{su}C_{biom}\right]$$

Stellenbosch University https://scholar.sun.ac.za

$$\nu_{10,6} = -\sum_{i=1-9,11-24} C_i \nu_{i,6}$$
$$= -\left[-C_{aa} + (1 - Y_{aa}) f_{va,aa} C_{va} + (1 - Y_{aa}) f_{bu,aa} C_{bu} + (1 - Y_{aa}) f_{pro,aa} C_{pro} + (1 - Y_{aa}) f_{ac,aa} C_{ac} + Y_{aa} C_{biom}\right]$$

$$\nu_{10,7} = -\sum_{i=1-9,11-24} C_i \nu_{i,7} = -\left[-C_{fa} + (1 - Y_{fa}) f_{ac,fa} C_{ac} + Y_{fa} C_{biom}\right]$$

$$\nu_{10,8} = -\sum_{i=1-9,11-24} C_i \nu_{i,8}$$
$$= -\left[-C_{va} + (1 - Y_{c4}) f_{pro,va} C_{pro} + (1 - Y_{c4}) f_{ac,va} C_{ac} + Y_{c4} C_{biom}\right]$$

$$\nu_{10,9} = -\sum_{i=1-9,11-24} C_i \nu_{i,9}$$
$$= -\left[-C_{bu} + (1 - Y_{c4}) f_{ac,bu} C_{pro} + (1 - Y_{c4}) f_{ac,va} C_{ac} + Y_{c4} C_{biom}\right]$$

$$\nu_{10,10} = -\sum_{i=1-9,11-24} C_i \nu_{i,10}$$
$$= -\left[-C_{pro} + (1 - Y_{pro}) f_{ac,pro} C_{ac} + Y_{pro} C_{biom}\right]$$

$$\nu_{10,11} = -\sum_{i=1-9,11-24} C_i \nu_{i,11} = -\left[-C_{ac} + (1 - Y_{ac}) f_{ch4,ac} C_{ch4} + Y_{ac} C_{biom}\right]$$

$$\nu_{10,12} = -\sum_{i=1-9,11-24} C_i \nu_{i,11} = -Y_{h2} C_{biom}$$

Inorganic nitrogen

$$\frac{dS_{IN}}{dt} = -Y_{su} N_{bac} \rho_5 - (N_{aa} - Y_{aa} N_{bac}) \rho_6 - Y_{fa} N_{bac} \rho_7 - Y_{c4} N_{bac} \rho_8 - Y_{c4} N_{bac} \rho_9 - Y_{pro} N_{bac} \rho_{10} - Y_{ac} N_{bac} \rho_{11} - Y_{h2} N_{bac} \rho_{12} - Y_{et} N_{bac} \rho_{13}$$

Soluble inerts

$$\frac{dS_I}{dt} = f_{sI,xc} \rho_1$$

Ethanol

$$\frac{dS_{et}}{dt} = -\rho_{13}$$

Stellenbosch University https://scholar.sun.ac.za

Particulate components mass balance for constant volume:

Composites	$\boldsymbol{\frac{dX_c}{dt} = -\rho_1 + \rho_{13} + \rho_{14} + \rho_{15} + \rho_{16} + \rho_{17} + \rho_{18} + \rho_{19}}$
Carbohydrates	$\frac{dX_{ch}}{dt} = f_{ch,xc}\rho_1 - \rho_2$
Proteins	$\frac{dX_{pr}}{dt} = f_{pr,xc}\rho_1 - \rho_3$
Lipids	$\frac{dX_{li}}{dt} = f_{li,xc}\rho_1 - \rho_4$
Sugar degraders	$\frac{dX_{su}}{dt} = Y_{su}\rho_5 - \rho_{13}$
Amino acid degraders	$\frac{dX_{aa}}{dt} = Y_{aa}\rho_6 - \rho_{14}$
LCFA degraders	$\frac{dX_{fa}}{dt} = Y_{fa}\rho_7 - \rho_{15}$
C4 degraders	$\frac{dX_{c4}}{dt} = Y_{c4}\rho_8 + Y_{c4}\rho_9 + \rho_{16}$
Propionate degraders	$\frac{dX_{pro}}{dt} = Y_{pro}\rho_{10} - \rho_{17}$
Acetate degraders	$\frac{dX_{ac}}{dt} = Y_{ac}\rho_{11} - \rho_{18}$
Hydrogen degraders	$\frac{dX_{h2}}{dt} = Y_{h2}\rho_{12} - \rho_{19}$
Particulate inerts	$\frac{dX_I}{dt} = f_{xI,xc}\rho_1$
Ethanol degraders	$\frac{dX_{et}}{dt} = Y_{et}\rho_{13} - \rho_{21}$

Stellenbosch University https://scholar.sun.ac.za

Digestion kinetic rate

Disintegration	$\boldsymbol{\rho_1 = k_{dis} X_c}$
Hydrolysis of carbohydrates	$\rho_2 = k_{hyd,ch} X_{ch}$
Hydrolysis of proteins	$\rho_3 = k_{hyd,pr} X_{pr}$
Hydrolysis of lipids	$\rho_4 = k_{hyd,li} X_{li}$
Uptake of sugars	$\rho_5 = k_{m,su} \frac{S_{su}}{K_{S,su} + S_{su}} X_{su} I_5$
Uptake of amino acids	$\rho_6 = k_{m,aa} \frac{S_{aa}}{K_{S,aa} + S_{aa}} X_{aa} I_6$
Uptake of LCFA	$\rho_7 = k_{m,fa} \frac{S_{fa}}{K_{S,fa} + S_{fa}} X_{fa} I_7$
Uptake of valerate	$\rho_8 = k_{m,c4} \frac{S_{va}}{K_{S,va} + S_{va}} X_{c4} \frac{1}{1 + \frac{S_{bu}}{S_{va}}} I_8$
Uptake of butyrate	$\rho_9 = k_{m,c4} \frac{S_{bu}}{K_{S,bu} + S_{bu}} X_{c4} \frac{1}{1 + \frac{S_{va}}{S_{bu}}} I_9$
Uptake of propionate	$\rho_{10} = k_{m,pro} \frac{S_{pro}}{K_{S,pro} + S_{pro}} X_{pro} I_{10}$
Uptake of acetate	$\rho_{11} = k_{m,ac} \frac{S_{ac}}{K_{S,ac} + S_{ac}} X_{ac} I_{11}$
Uptake of hydrogen	$\rho_{12} = k_{m,h2} \frac{S_{h2}}{K_{S,h2} + S_{h2}} X_{h2} I_{12}$
Uptake of ethanol	$\rho_{13} = k_{m,et} \frac{S_{et}}{K_{S,et} + S_{et}} X_{et}$
Decay of sugar degraders	$\rho_{14} = k_{dec,X_{su}} X_{su}$
Decay of amino acid degraders	$\rho_{15} = k_{dec,X_{aa}} X_{aa}$
Decay of LCFA degraders	$\rho_{16} = k_{dec,X_{fa}} X_{fa}$
Decay of C4 degraders	$\rho_{17} = k_{(c4,X_{c4})} X_{c4}$
Decay of propionate degraders	$\rho_{18} = k_{dec,X_{pro}} X_{pro}$
Decay of acetate degraders	$\rho_{19} = k_{dec,X_{ac}} X_{ac}$
Decay of hydrogen degraders	$\rho_{20} = k_{dec,X_{h2}} X_{h2}$
Decay of ethanol degraders	$\rho_{21} = k_{dec,X_{et}} X_{et}$

Stellenbosch University https://scholar.sun.ac.za

Acid base transfer state equations

Valerate anion	$\boldsymbol{\frac{dS_{vaac}}{dt} = -\rho_{A,va}}$
Butyrate anion	$\frac{dS_{buac}}{dt} = -\rho_{A,bu}$
Propionate anion	$\frac{dS_{proac}}{dt} = -\rho_{A,pro}$
Acetate anion	$\frac{dS_{acac}}{dt} = -\rho_{A,ac}$
HCO_3^- anion	$\frac{dS_{ICac}}{dt} = -\rho_{A,co2}$
NH_4^+ anion	$\frac{dS_{INac}}{dt} = -\rho_{A,IN}$

Acid base transfer rates:

Valerate/valeric acid	$\boldsymbol{\rho_{A,va} = k_{A,Bva}(S_{vaac}(K_{a,va} + S_H) - K_{a,va}S_{va})}$
Butyrate/butyric acid	$\rho_{A,bu} = k_{A,Bbu}(S_{buac}(K_{a,bu} + S_H) - K_{a,bu}S_{bu})$
Propionate/propionic acid	$\rho_{A,pro} = k_{A,Bpro}(S_{proac}(K_{a,pro} + S_H) - K_{a,pro}S_{pro})$
Acetate/acetic acid	$\rho_{A,ac} = k_{A,Bac}(S_{acac}(K_{a,ac} + S_H) - K_{a,ac}S_{ac})$
CO_2/inorganic carbon	$\rho_{A,co2} = k_{A,Bco2}(S_{ICac}(K_{a,co2} + S_H) - K_{a,co2}S_{IC})$
NH_3/NH_4^+	$\rho_{A,IN} = k_{A,BIN}(S_{INac}(K_{a,IN} + S_H) - K_{a,IN}S_{IN})$

pH calculations:

Charge balance	$\boldsymbol{\Theta = S_{cat^+} + S_{nh4^+} - S_{hco3^-} - \frac{S_{ac^-}}{64} - \frac{S_{pro^-}}{112} - \frac{S_{bu^-}}{160} - \frac{S_{va^-}}{208} - S_{an^-}}$
Soluble proton concentration	$S_{H^+} = -\frac{\Theta}{2} + \frac{1}{2}\sqrt{\Theta^2 + 4K_W}$
pH calculation	$pH = -\log_{10}(S_{H^+})$

Inhibition functions:

pH based BAC inhibition	$\boldsymbol{I_{pH,bac} = \frac{1 + 2 \times 10^{0.5(pH_{LL,bac} - pH_{UL,bac})}}{1 + 10^{(pH - pH_{UL,bac})} + 10^{pH_{LL,bac} - pH}}}$

Stellenbosch University https://scholar.sun.ac.za

pH based acetate inhibition	$\boldsymbol{I_{pH,ac} = \frac{1 + 2 \times 10^{0.5(pH_{LL,ac} - pH_{UL,ac})}}{1 + 10^{(pH - pH_{UL,ac})} + 10^{pH_{LL,ac} - pH}}}$
pH bases H_2 inhibition	$\boldsymbol{I_{pH,h2} = \frac{1 + 2 \times 10^{0.5(pH_{LL,h2} - pH_{UL,h2})}}{1 + 10^{(pH - pH_{UL,h2})} + 10^{pH_{LL,h2} - pH}}}$
Secondary substrate inhibition	$I_{IN} = \begin{cases} 0, & S_{IN} \leq 0 \\ \frac{1}{1 + \frac{K_{S,IN}}{S_{IN}}}, & S_{IN} > 0 \end{cases}$
Free NH_3 inhibition	$I_{nh3} = \frac{1}{1 + \frac{S_{INac}}{K_{I,nh3}}}$
Hydrogen inhibition LCFA	$I_{h2,fa} = \frac{1}{1 + \frac{S_{h2}}{K_{I,h2,fa}}}$
Hydrogen inhibition c4	$I_{h2,c4} = \frac{1}{1 + \frac{S_{h2}}{K_{I,h2,c4}}}$
Hydrogen inhibition propionate	$I_{h2,pro} = \frac{1}{1 + \frac{S_{h2}}{K_{I,h2,pro}}}$
Inhibition functions	$I_5 = I_{pH,bac} I_{IN}$ $I_6 = I_{pH,bac} I_{IN}$ $I_7 = I_{pH,bac} I_{IN} I_{h2,fa}$ $I_8 = I_{pH,bac} I_{IN} I_{h2,c4}$ $I_9 = I_{pH,bac} I_{IN} I_{h2,c4}$ $I_{10} = I_{pH,bac} I_{IN} I_{h2,pro}$ $I_{11} = I_{pH,ac} I_{IN} I_{nh3}$ $I_{10} = I_{pH,h2} I_{IN}$

Gas transfer

Hydrogen transfer rate	$\boldsymbol{\rho_{T,h2} = k_L a(S_{h2} - 16 K_{H,h2} P_{gas,h2})}$
Methane transfer rate	$\rho_{T,ch4} = k_L a(S_{ch4} - 64 K_{H,ch4} P_{gas,ch4})$
Carbon dioxide transfer rate	$\rho_{T,co2} = k_L a(S_{co2} - K_{H,co2} P_{gas,co2})$
Hydrogen gas	$\frac{dS_{gas,h2}}{dt} = -S_{gas,h2} \frac{q_{gas}}{V_{gas}} + \rho_{T,h2} \frac{V_{liq}}{V_{gas}}$
Methane gas	$\frac{dS_{gas,ch4}}{dt} = -S_{gas,ch4} \frac{q_{gas}}{V_{gas}} + \rho_{T,ch4} \frac{V_{liq}}{V_{gas}}$

Stellenbosch University https://scholar.sun.ac.za

Carbon dioxide gas	$\frac{dS_{gas,co2}}{dt} = -S_{gas,co2}\frac{q_{gas}}{V_{gas}} + \rho_{T,co2}\frac{V_{liq}}{V_{gas}}$

Gas composition

Hydrogen partial pressure	$\boldsymbol{P_{h2} = S_{gas,h2} R \frac{T_{op}}{16}}$
Methane partial pressure	$P_{ch4} = S_{gas,ch4} R \frac{T_{op}}{64}$
Carbon dioxide partial pressure	$P_{co2} = S_{gas,co2} R T_{op}$
Water vapour partial pressure	$P_{h2o} = 0.0313 e^{5290\left(\frac{1}{298} - \frac{1}{T_{op}}\right)}$
Total gas pressure	$P_{tot} = P_{h2} + P_{ch4} + P_{co2} + P_{h2o}$

Stellenbosch University https://scholar.sun.ac.za

C.2. Stoichiometric, biochemical, physiochemical and physical parameters

Table C-1: Stoichiometric parameter values

Parameter	Value	Unit
$f_{sI,xc}$	0.1	-
$f_{xI,xc}$	0.2	-
$f_{ch,xc}$	0.2	-
$f_{pr,xc}$	0.2	-
$f_{li,xc}$	0.3	-
N_{xc}	0.0376/14	kmol-N/kg-COD
N_I	0.06/14	kmol-N/kg-COD
N_{aa}	0.007	kmol-N/kg-COD
C_{xc}	0.02786	kmol-C/kg-COD
C_{sI}	0.03	kmol-C/kg-COD
C_{ch}	0.0313	kmol-C/kg-COD
C_{pr}	0.03	kmol-C/kg-COD
C_{li}	0.022	kmol-C/kg-COD
C_{xI}	0.03	kmol-C/kg-COD
C_{su}	0.0313	kmol-C/kg-COD
C_{aa}	0.03	kmol-C/kg-COD
$f_{fa,li}$	0.95	-
C_{fa}	0.0217	kmol-C/kg-COD
$f_{h2,su}$	0.19	-
$f_{bu,su}$	0.13	-
$f_{pro,su}$	0.27	-
$f_{ac,su}$	0.41	-
N_{bac}	0.08/14	kmol-N/kg-COD
C_{bu}	0.025	kmol-C/kg-COD
C_{pro}	0.0268	kmol-C/kg-COD
C_{ac}	0.0313	kmol-C/kg-COD
C_{bac}	0.0313	kmol-C/kg-COD
Y_{su}	0.1	-
$f_{h2,aa}$	0.06	-
$f_{va,aa}$	0.23	-
$f_{bu,aa}$	0.26	-
$f_{pro,aa}$	0.05	-
$f_{ac,aa}$	0.40	-
C_{va}	0.024	kmol-C/kg-COD
Y_{aa}	0.08	-
Y_{fa}	0.06	-
Y_{c4}	0.06	-

Stellenbosch University https://scholar.sun.ac.za

Y_{pro}	0.04	-
C_{ch4}	0.0156	kmol-C/kg-COD
Y_{ac}	0.05	-
Y_{h2}	0.06	-
Y_{et}	0.01	

Table C-2: Biochemical parameter values

Parameter	Value	Unit
k_{dis}	0.4	d^{-1}
$k_{hyd,ch}$	0.25	d^{-1}
$k_{hyd,pr}$	0.2	d^{-1}
$k_{hyd,li}$	0.1	d^{-1}
$K_{S,IN}$	1e-4	M
$k_{m,su}$	30	d^{-1}
$K_{S,su}$	0.1	kg-COD/m^3
$pH_{UL,aa}$	5.5	-
$pH_{LL,aa}$	4.0	-
$k_{m,aa}$	50	d^{-1}
$K_{S,aa}$	0.3	kg-COD/m^3
$k_{m,fa}$	6	d^{-1}
$K_{S,fa}$	0.4	kg-COD/m^3
$K_{Ih2,fa}$	5e-6	M
$k_{m,c4}$	20	d^{-1}
$K_{S,c4}$	0.3	kg-COD/m^3
$K_{Ih2,c4}$	1e-5	M
$k_{m,pro}$	13	d^{-1}
$K_{S,pro}$	0.1	kg-COD/m^3
$K_{Ih2,pro}$	3.5e-6	M
$k_{m,ac}$	8	d^{-1}
$K_{S,ac}$	0.15	kg-COD/m^3
$K_{I,nh3}$	0.0018	M
$pH_{UL,ac}$	7.5	-
$pH_{LL,ac}$	5.8	-
$k_{m,h2}$	35	d^{-1}
$K_{S,h2}$	7e-6	kg-COD/m^3
$pH_{UL,h2}$	6.5	-
$pH_{LL,h2}$	5	-
$k_{m,et}$	3	d^{-1}
$K_{S,et}$	0.5	kg-COD/m^3
$k_{dec,Xsu}$	0.02	d^{-1}
$k_{dec,Xaa}$	0.02	d^{-1}

Stellenbosch University https://scholar.sun.ac.za

$k_{dec,Xfa}$	0.02	d^{-1}
$k_{dec,Xc4}$	0.02	d^{-1}
$k_{dec,Xpro}$	0.02	d^{-1}
$k_{dec,Xac}$	0.02	d^{-1}
$k_{dec,Xh2}$	0.02	d^{-1}
$k_{dec,Xet}$	0.02	d^{-1}

Table C-3: Physiochemical parameter values

Parameter	Value	Unit
R	0.083145	$bar.M^{-1}.K^{-1}$
T_{op}	308.15	K
K_w	$10^{-14}\exp\left(\frac{55900}{100R}\times\left(\frac{1}{298.5}-\frac{1}{T_{op}}\right)\right)$	M
$K_{a,va}$	$10^{-4.86}$	M
$K_{a,bu}$	$10^{-4.82}$	M
$K_{a,pro}$	$10^{-4.88}$	M
$K_{a,ac}$	$10^{-4.76}$	M
$K_{a,co2}$	$10^{-6.35}\exp\left(\frac{7646}{100R}\times\left(\frac{1}{298.5}-\frac{1}{T_{op}}\right)\right)$	M
$K_{a,IN}$	$10^{-9.25}\exp\left(\frac{51965}{100R}\times\left(\frac{1}{298.5}-\frac{1}{T_{op}}\right)\right)$	M
$k_{A,Bva}$	1e10	$M^{-1}.d^{-1}$
$k_{A,Bbu}$	1e10	$M^{-1}.d^{-1}$
$k_{A,Bpro}$	1e10	$M^{-1}.d^{-1}$
$k_{A,Bac}$	1e10	$M^{-1}.d^{-1}$
$k_{A,Bco2}$	1e10	$M^{-1}.d^{-1}$
$k_{A,BIN}$	1e10	$M^{-1}.d^{-1}$
P_{atm}	1.013	bar
k_p	5e4	$m^3d^{-1}bar^{-1}$
k_La	200	d^{-1}
$K_{H,co2}$	$0.035\exp\left(\frac{-19410}{100R}\times\left(\frac{1}{298.5}-\frac{1}{T_{op}}\right)\right)$	$M_{liq}.bar^{-1}$
$K_{H,ch4}$	$0.0014\exp\left(\frac{-14240}{100R}\times\left(\frac{1}{298.5}-\frac{1}{T_{op}}\right)\right)$	$M_{liq}.bar^{-1}$
$K_{H,h2}$	$7.8(10)^{-4}\exp\left(\frac{-4180}{100R}\times\left(\frac{1}{298.5}-\frac{1}{T_{op}}\right)\right)$	$M_{liq}.bar^{-1}$

Stellenbosch University https://scholar.sun.ac.za

Table C-4: Physical parameters

Parameter	Value	Unit
t_{feed}	0.05	d
t_{react}	0.7	d
t_{decant}	0.25	d
$V_{ASBR,min}$	0.007	m^3
$V_{ASBR,max}$	0.014	m^3
$V_{headspace}$	0.01	m^3

Stellenbosch University https://scholar.sun.ac.za

C.3. Batstone *et al*. (2004) simulation concentrations

Initial state variable	Provided value by Batstone *et al*. (2004)	Used value	Unit
Monosaccharides, $S_{su,in}$	-	1e-6	kg-COD.m^{-3}
Amino acids, $S_{aa,in}$	-	1e-6	kg-COD.m^{-3}
LCFA, $S_{fa,in}$	-	1e-6	kg-COD.m^{-3}
Total valerate, $S_{va,in}$	-	1e-6	kg-COD.m^{-3}
Total butyrate, $S_{bu,in}$	-	1e-6	kg-COD.m^{-3}
Total propionate, $S_{pro,in}$	-	1e-6	kg-COD.m^{-3}
Total acetate, $S_{ac,in}$	-	1e-6	kg-COD.m^{-3}
Hydrogen gas, $S_{h2,in}$	-	1e-10	kg-COD.m^{-3}
Methane gas, $S_{ch4,in}$	-	1e-7	kg-COD.m^{-3}
Inorganic carbon, $S_{IC,in}$	-	0.1	kmol-C.m^{-3}
Inorganic nitrogen, $S_{IN,in}$	-	0.01	kmol-N.m^{-3}
Soluble inerts, $S_{I,in}$	-	0.02	kg-COD.m^{-3}
Ethanol, $S_{et,in}$	-	1e-6	kg-COD.m^{-3}
Composites, $X_{c,in}$	-	0	kg-COD.m^{-3}
Carbohydrates, $X_{ch,in}$	-	0	kg-COD.m^{-3}
Proteins, $X_{pr,in}$	-	0	kg-COD.m^{-3}
Lipids, $X_{li,in}$	-	0	kg-COD.m^{-3}
Sugar degraders, $X_{su,in}$	-	10	kg-COD.m^{-3}
Amino acid degraders, $X_{aa,in}$	-	10	kg-COD.m^{-3}
LCFA degraders, $X_{fa,in}$	-	10	kg-COD.m^{-3}
Valerate and butyrate degraders, $X_{c4,in}$	-	10	kg-COD.m^{-3}
Propionate degraders, $X_{pro,in}$	-	10	kg-COD.m^{-3}
Acetate degraders, $X_{ac,in}$	-	5	kg-COD.m^{-3}
Hydrogen degraders, $X_{h2,in}$	-	10	kg-COD.m^{-3}
Particulate inerts, $X_{I,in}$	-	10	kg-COD.m^{-3}
Ethanol degraders, $X_{et,in}$	-	8	kg-COD.m^{-3}
Cations, $S_{cat,in}$	-	0.12	kmol.m^{-3}
Anions, $S_{an,in}$	-	0.1	kmol.m^{-3}

Stellenbosch University https://scholar.sun.ac.za

Feed state variable	Provided value by Batstone *et al*. (2004)	Used value	Unit
Monosaccharides, $S_{su,f}$	0	0	kg-COD.m^{-3}
Amino acids, $S_{aa,f}$	-	0	kg-COD.m^{-3}
LCFA, $S_{fa,f}$	-	0	kg-COD.m^{-3}
Total valerate, $S_{va,f}$	-	0	kg-COD.m^{-3}
Total butyrate, $S_{bu,f}$	0.6	0.6	kg-COD.m^{-3}
Total propionate, $S_{pro,f}$	1	1	kg-COD.m^{-3}
Total acetate, $S_{ac,f}$	1.5	1.5	kg-COD.m^{-3}
Hydrogen gas, $S_{h2,f}$	-	0	kg-COD.m^{-3}
Methane gas, $S_{ch4,f}$	-	0	kg-COD.m^{-3}
Inorganic carbon, $S_{IC,f}$	-	0.71231	kmol-C.m^{-3}
Inorganic nitrogen, $S_{IN,f}$	0.03	0.03	kmol-N.m^{-3}
Soluble inerts, $S_{I,f}$	-	0	kg-COD.m^{-3}
Ethanol, $S_{et,f}$	12	12	kg-COD.m^{-3}
Composites, $X_{c,f}$	-	0	kg-COD.m^{-3}
Carbohydrates, $X_{ch,f}$	2	2	kg-COD.m^{-3}
Proteins, $X_{pr,f}$	-	0	kg-COD.m^{-3}
Lipids, $X_{li,f}$	-	0	kg-COD.m^{-3}
Sugar degraders, $X_{su,f}$	-	0	kg-COD.m^{-3}
Amino acid degraders, $X_{aa,f}$	-	0	kg-COD.m^{-3}
LCFA degraders, $X_{fa,f}$	-	0	kg-COD.m^{-3}
Valerate and butyrate degraders, $X_{c4,f}$	-	0	kg-COD.m^{-3}
Propionate degraders, $X_{pro,f}$	-	0	kg-COD.m^{-3}
Acetate degraders, $X_{ac,f}$	-	0	kg-COD.m^{-3}
Hydrogen degraders, $X_{h2,f}$	-	0	kg-COD.m^{-3}
Particulate inerts, $X_{I,f}$	-	0	kg-COD.m^{-3}
Ethanol degraders, $X_{et,f}$	-	0	kg-COD.m^{-3}
Cations, $S_{cat,f}$	-	0.12	kmol.m^{-3}
Anions, $S_{an,f}$	0.03	0.1	kmol.m^{-3}

Stellenbosch University https://scholar.sun.ac.za

C.4. This study's simulation concentrations

Initial state variable	Used value	Unit
Monosaccharides, $S_{su,in}$	1e-6	kg-COD.m^{-3}
Amino acids, $S_{aa,in}$	1e-6	kg-COD.m^{-3}
LCFA, $S_{fa,in}$	1e-6	kg-COD.m^{-3}
Total valerate, $S_{va,in}$	1e-6	kg-COD.m^{-3}
Total butyrate, $S_{bu,in}$	1e-6	kg-COD.m^{-3}
Total propionate, $S_{pro,in}$	1e-6	kg-COD.m^{-3}
Total acetate, $S_{ac,in}$	0.642	kg-COD.m^{-3}
Hydrogen gas, $S_{h2,in}$	1e-10	kg-COD.m^{-3}
Methane gas, $S_{ch4,in}$	1e-7	kg-COD.m^{-3}
Inorganic carbon, $S_{IC,in}$	0.1	kmol-C.m^{-3}
Inorganic nitrogen, $S_{IN,in}$	0.01	kmol-N.m^{-3}
Soluble inerts, $S_{I,in}$	0.02	kg-COD.m^{-3}
Ethanol, $S_{et,in}$	1e-6	kg-COD.m^{-3}
Composites, $X_{c,in}$	10	kg-COD.m^{-3}
Carbohydrates, $X_{ch,in}$	10	kg-COD.m^{-3}
Proteins, $X_{pr,in}$	10	kg-COD.m^{-3}
Lipids, $X_{li,in}$	10	kg-COD.m^{-3}
Sugar degraders, $X_{su,in}$	15	kg-COD.m^{-3}
Amino acid degraders, $X_{aa,in}$	10	kg-COD.m^{-3}
LCFA degraders, $X_{fa,in}$	10	kg-COD.m^{-3}
Valerate and butyrate degraders, $X_{c4,in}$	5	kg-COD.m^{-3}
Propionate degraders, $X_{pro,in}$	2	kg-COD.m^{-3}
Acetate degraders, $X_{ac,in}$	0.5	kg-COD.m^{-3}
Hydrogen degraders, $X_{h2,in}$	5	kg-COD.m^{-3}
Particulate inerts, $X_{I,in}$	10	kg-COD.m^{-3}
Ethanol degraders, $X_{et,in}$	5	kg-COD.m^{-3}
Cations, $S_{cat,in}$	0.12	kmol.m^{-3}
Anions, $S_{an,in}$	0.1	kmol.m^{-3}

Stellenbosch University https://scholar.sun.ac.za

Feed state variable	Used value	Unit
Monosaccharides, $S_{su,f}$	3.564	kg-COD.m^{-3}
Amino acids, $S_{aa,f}$	0	kg-COD.m^{-3}
LCFA, $S_{fa,f}$	1e-8	kg-COD.m^{-3}
Total valerate, $S_{va,f}$	1e-8	kg-COD.m^{-3}
Total butyrate, $S_{bu,f}$	0	kg-COD.m^{-3}
Total propionate, $S_{pro,f}$	1e-8	kg-COD.m^{-3}
Total acetate, $S_{ac,f}$	1e-8	kg-COD.m^{-3}
Hydrogen gas, $S_{h2,f}$	0	kg-COD.m^{-3}
Methane gas, $S_{ch4,f}$	0	kg-COD.m^{-3}
Inorganic carbon, $S_{IC,f}$	0.71231	kmol-C.m^{-3}
Inorganic nitrogen, $S_{IN,f}$	0.03	kmol-N.m^{-3}
Soluble inerts, $S_{I,f}$	0	kg-COD.m^{-3}
Ethanol, $S_{et,f}$	1e-8	kg-COD.m^{-3}
Composites, $X_{c,f}$	1e-8	kg-COD.m^{-3}
Carbohydrates, $X_{ch,f}$	0	kg-COD.m^{-3}
Proteins, $X_{pr,f}$	0	kg-COD.m^{-3}
Lipids, $X_{li,f}$	0	kg-COD.m^{-3}
Sugar degraders, $X_{su,f}$	0	kg-COD.m^{-3}
Amino acid degraders, $X_{aa,f}$	0	kg-COD.m^{-3}
LCFA degraders, $X_{fa,f}$	0	kg-COD.m^{-3}
Valerate and butyrate degraders, $X_{c4,f}$	0	kg-COD.m^{-3}
Propionate degraders, $X_{pro,f}$	0	kg-COD.m^{-3}
Acetate degraders, $X_{ac,f}$	0	kg-COD.m^{-3}
Hydrogen degraders, $X_{h2,f}$	0	kg-COD.m^{-3}
Particulate inerts, $X_{I,f}$	0	kg-COD.m^{-3}
Ethanol degraders, $X_{et,f}$	0	kg-COD.m^{-3}
Cations, $S_{cat,f}$	0.12	kmol.m^{-3}
Anions, $S_{an,f}$	0.1	kmol.m^{-3}

Stellenbosch University https://scholar.sun.ac.za

Appendix D - Online measured data results for Chapter 6 results

D.1. Experiment set 1

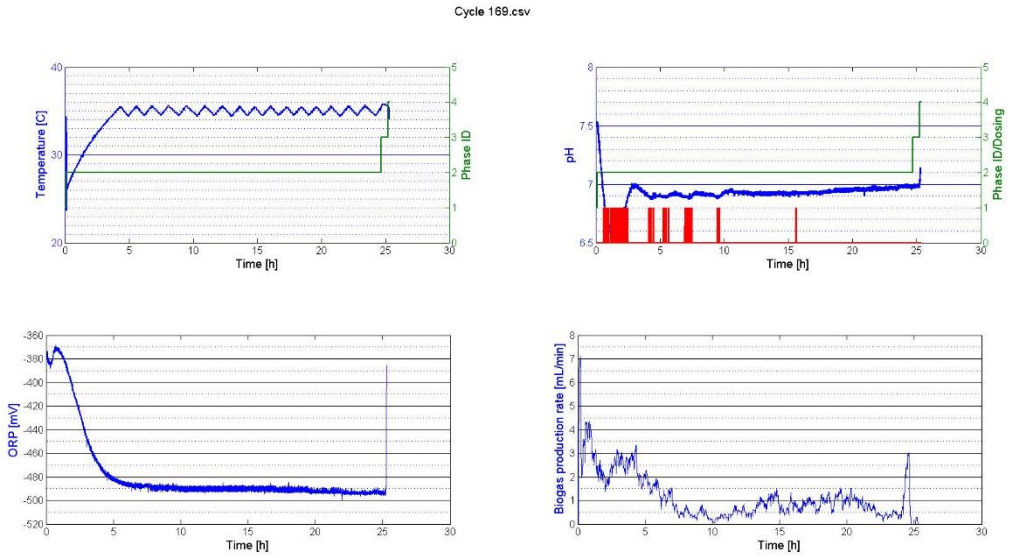

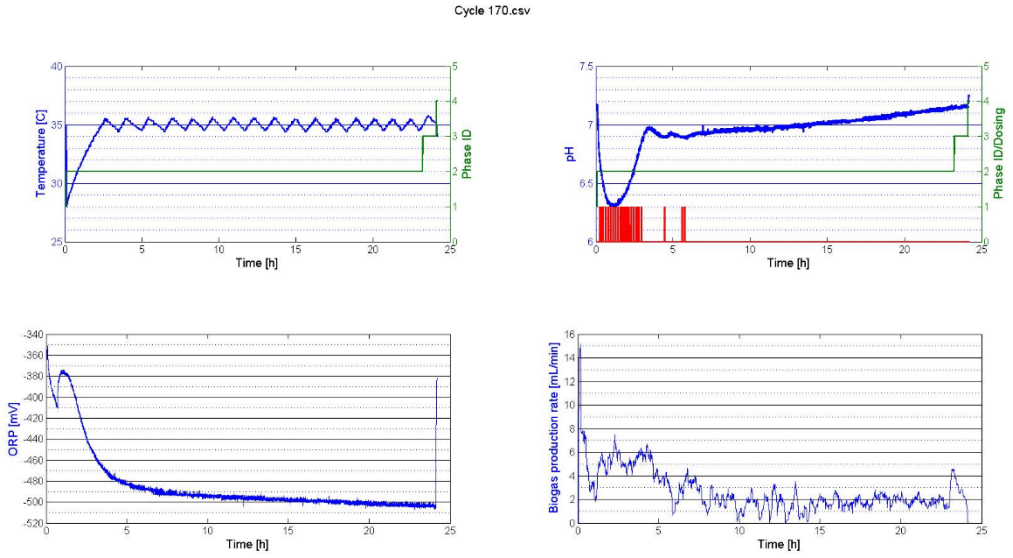

Stellenbosch University https://scholar.sun.ac.za

Cycle 171.csv

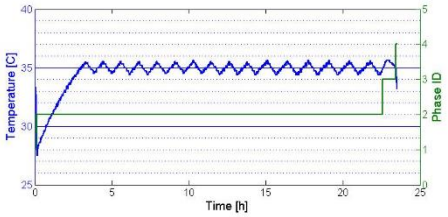

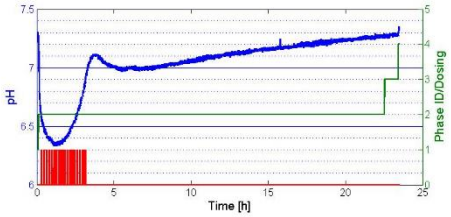

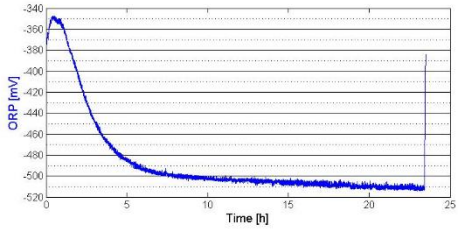

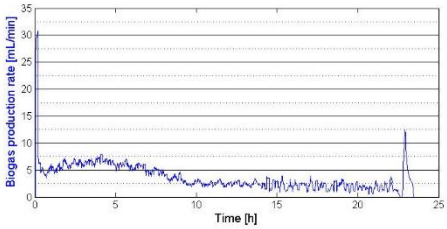

Cycle 172.csv

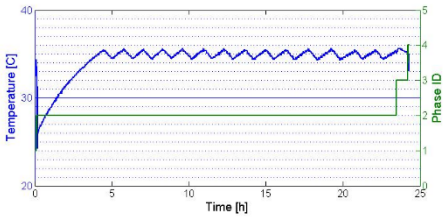

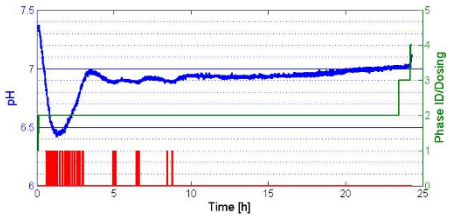

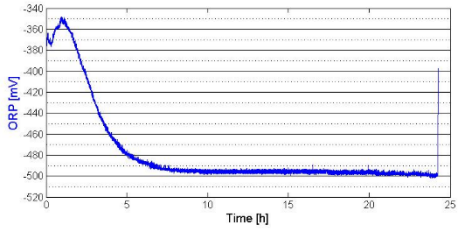

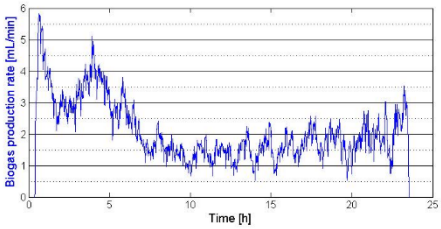

Stellenbosch University https://scholar.sun.ac.za

Cycle 173.csv

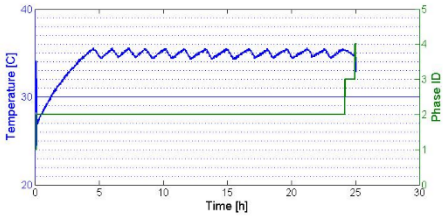

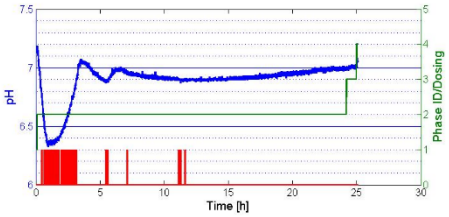

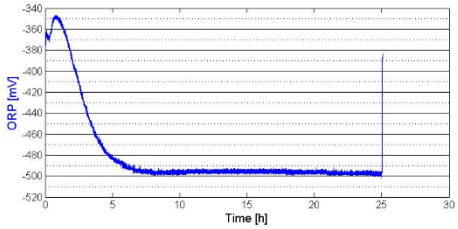

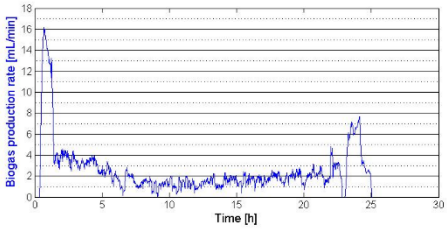

Stellenbosch University https://scholar.sun.ac.za

D.2. Experiment set 2

Cycle 175.csv

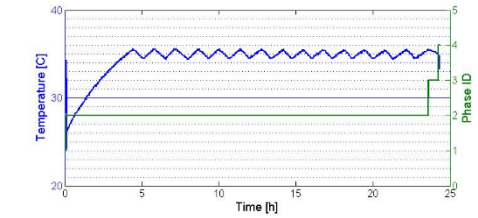

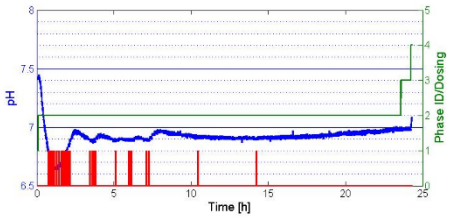

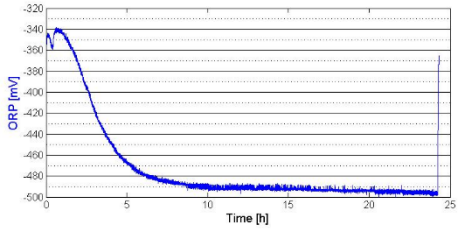

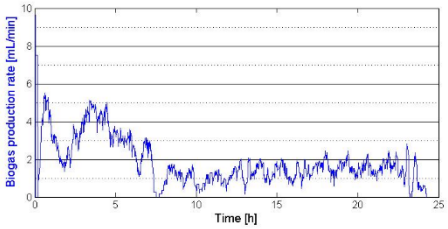

Cycle 176.csv

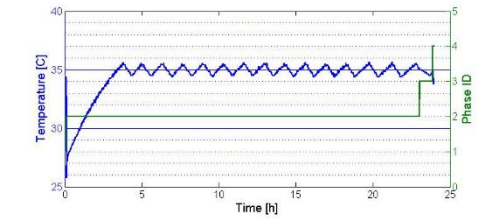

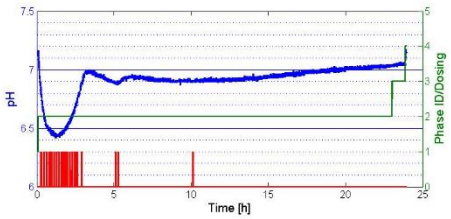

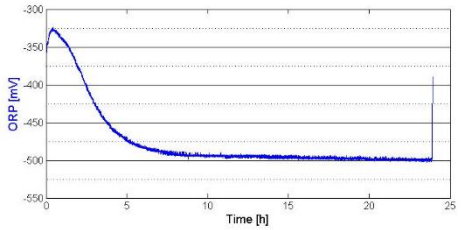

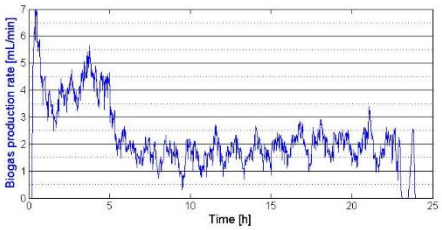

Stellenbosch University https://scholar.sun.ac.za

Cycle 177.csv

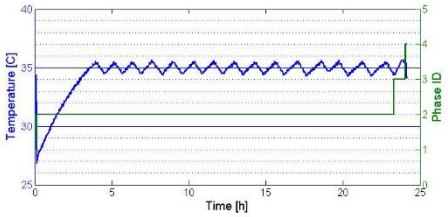

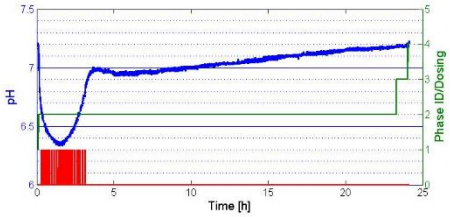

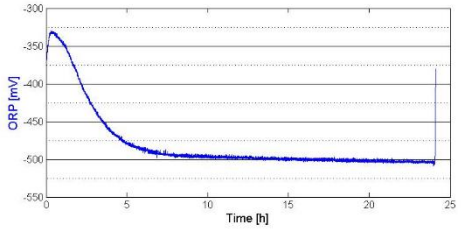

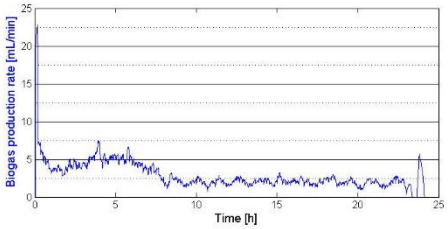

Cycle 178.csv

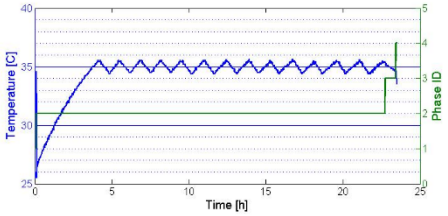

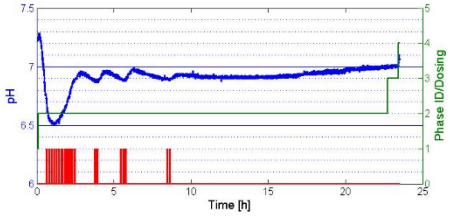

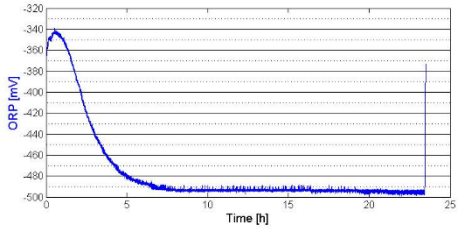

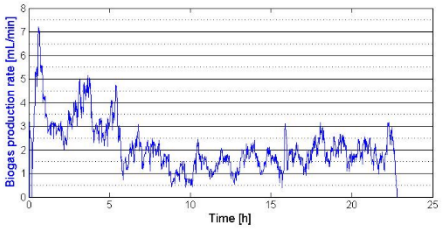

Stellenbosch University https://scholar.sun.ac.za

Cycle 179.csv

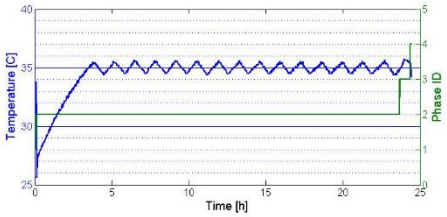

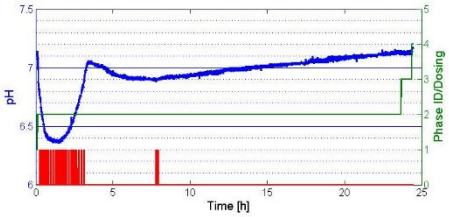

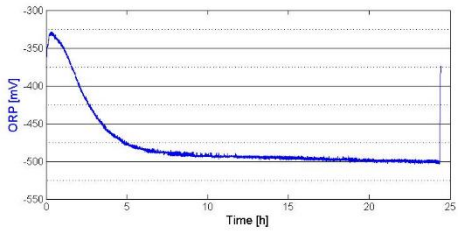

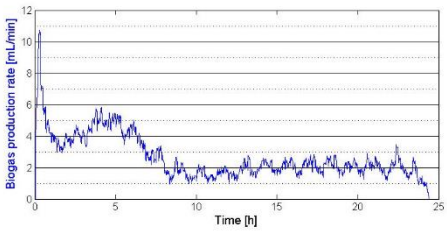

Stellenbosch University https://scholar.sun.ac.za

D.3. Experiment set 3

Cycle 180.csv

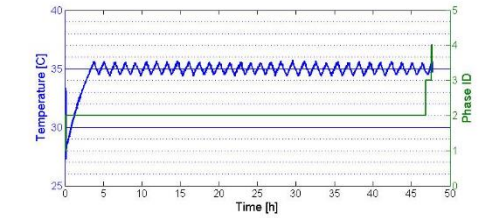

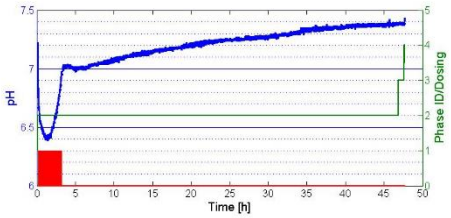

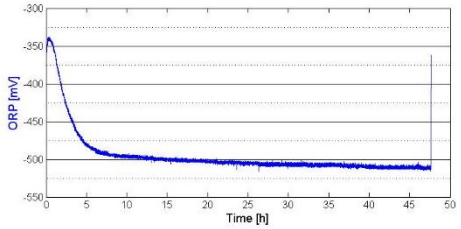

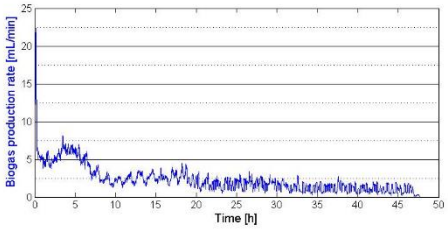

Cycle 181.csv

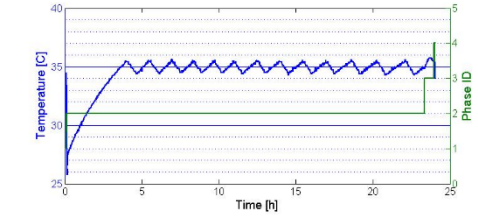

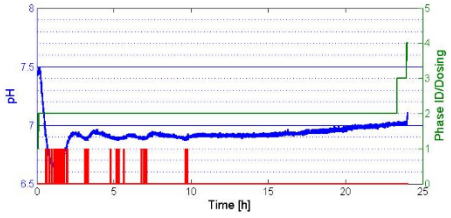

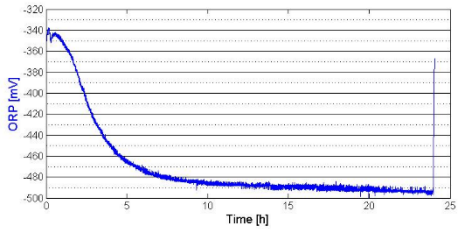

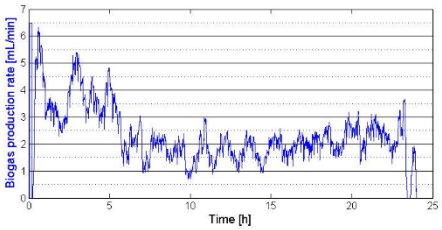

Stellenbosch University https://scholar.sun.ac.za

Cycle 182.csv

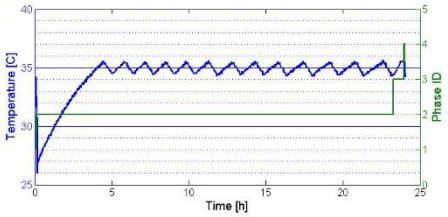

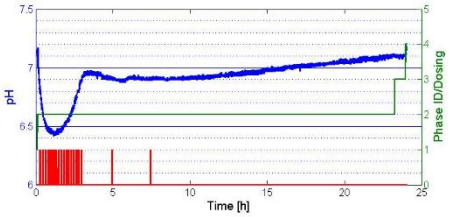

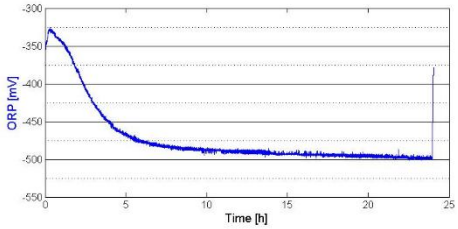

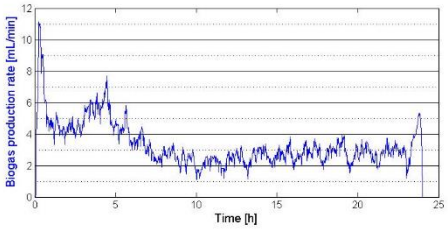

Cycle 183.csv

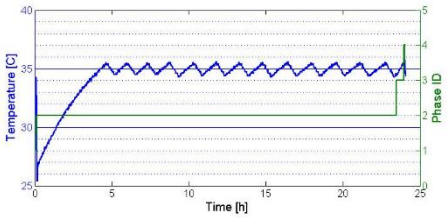

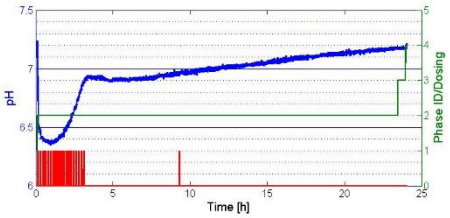

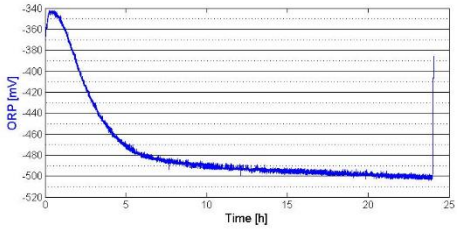

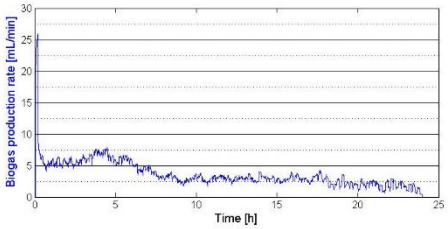

Stellenbosch University https://scholar.sun.ac.za

Cycle 184.csv

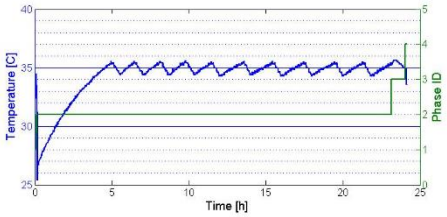

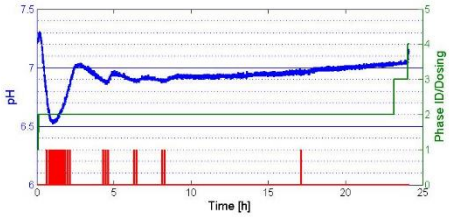

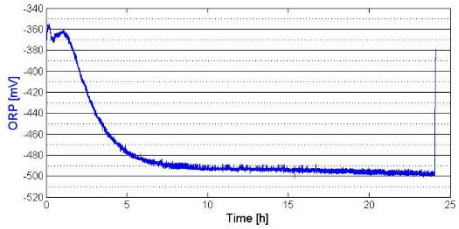

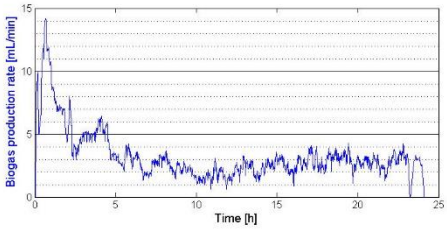

Cycle 185.csv

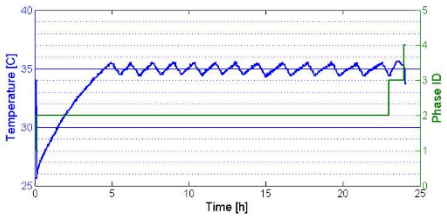

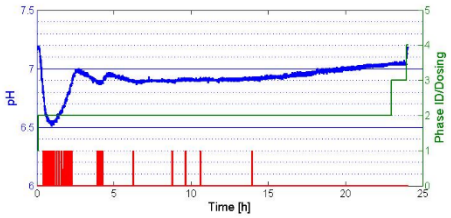

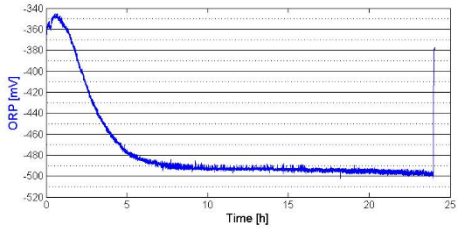

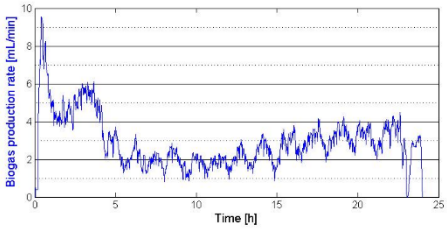

Stellenbosch University https://scholar.sun.ac.za

D.4. Experiment set 4

Cycle 187.csv

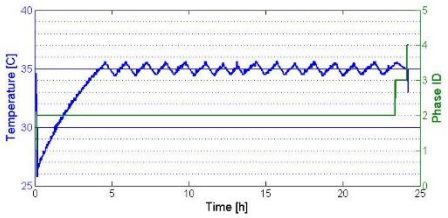

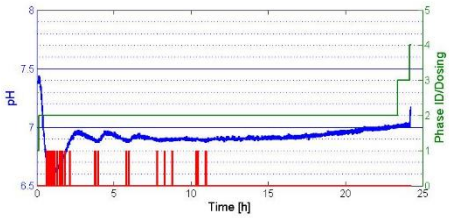

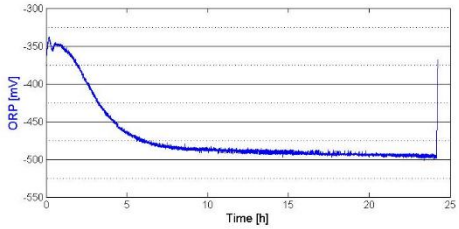

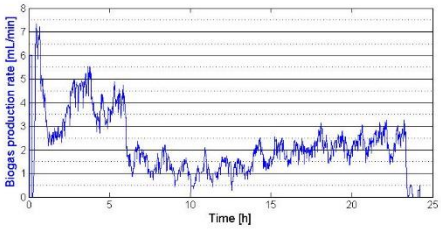

Cycle 188.csv

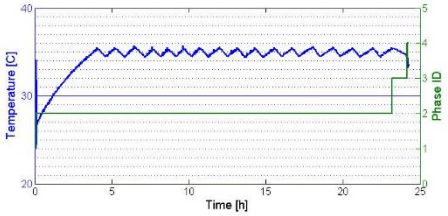

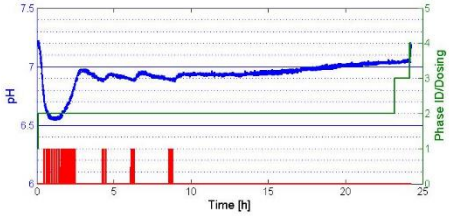

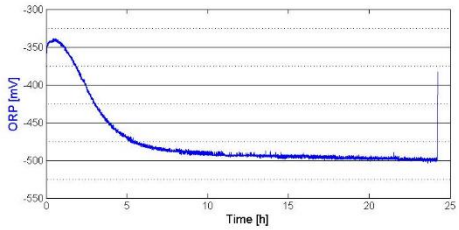

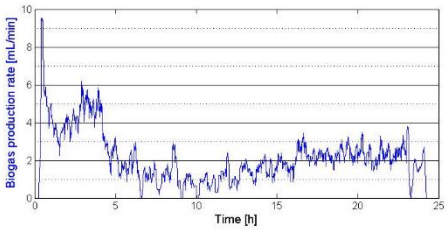

Stellenbosch University https://scholar.sun.ac.za

Cycle 189.csv

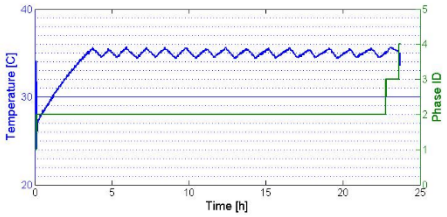

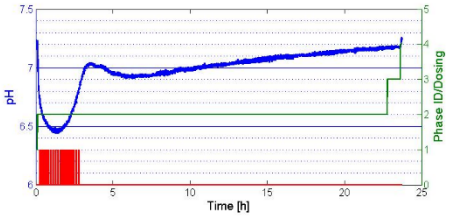

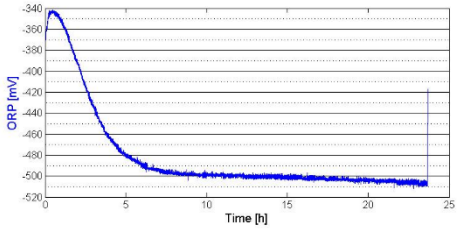

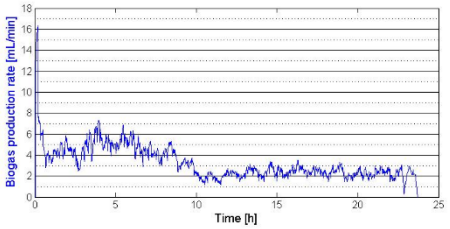

Cycle 190.csv

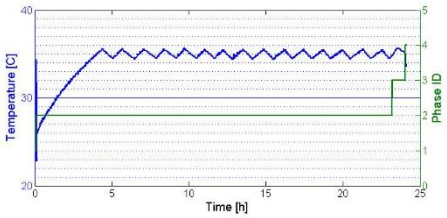

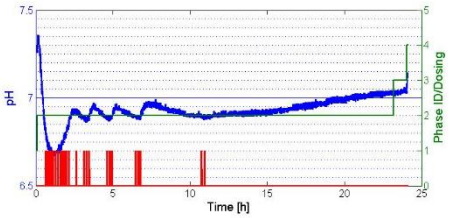

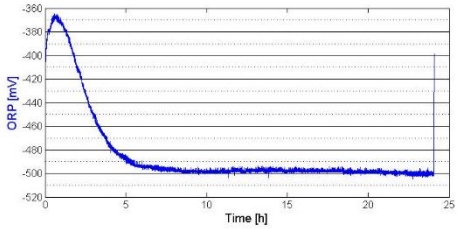

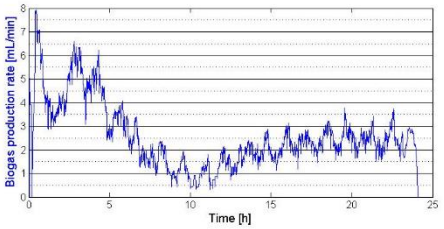

Stellenbosch University https://scholar.sun.ac.za

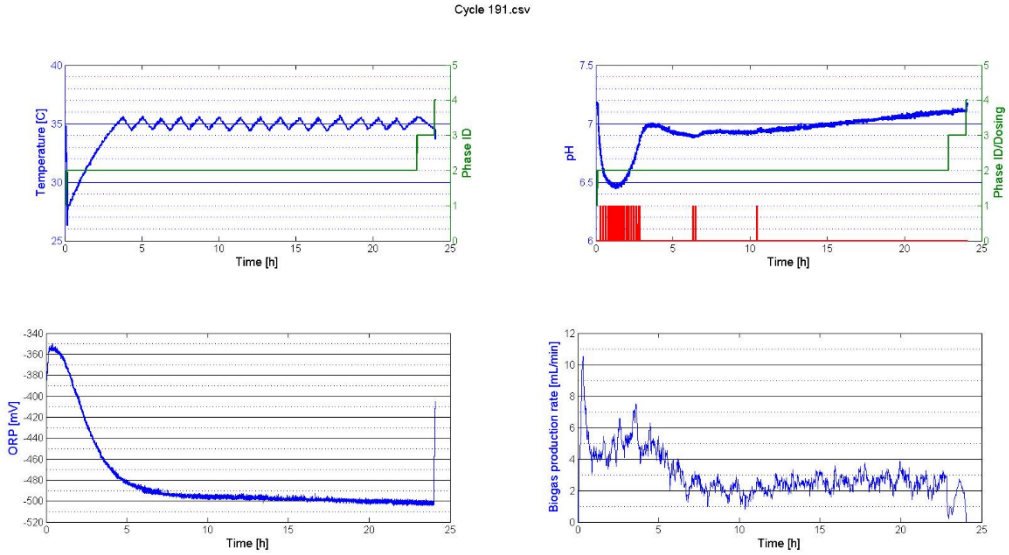

Stellenbosch University https://scholar.sun.ac.za

D.5. Experiment set 5

Cycle 193.csv

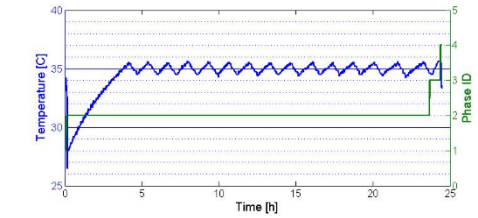

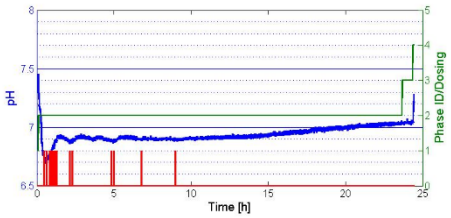

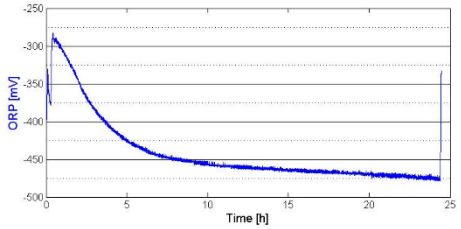

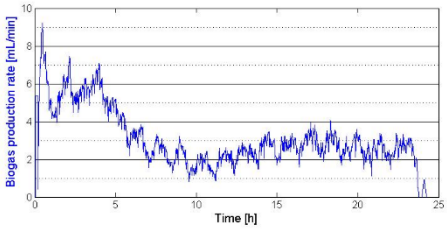

Cycle 194.csv

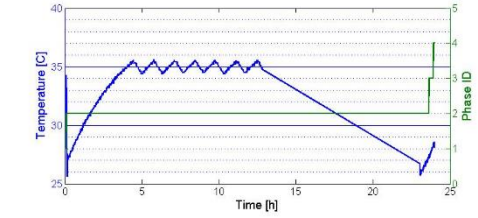

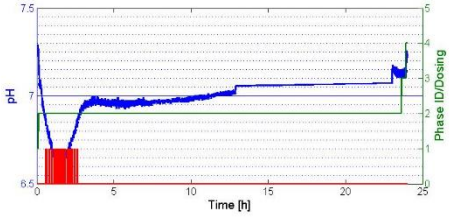

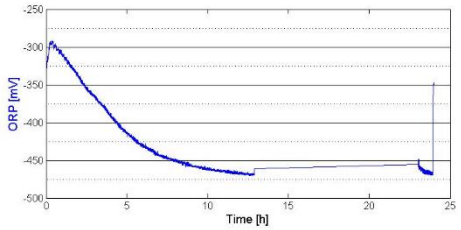

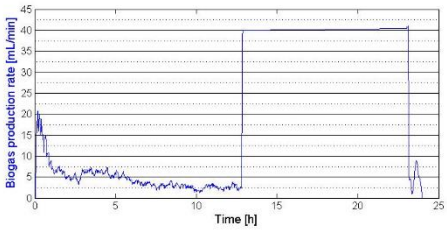

Stellenbosch University https://scholar.sun.ac.za

Cycle 195.csv

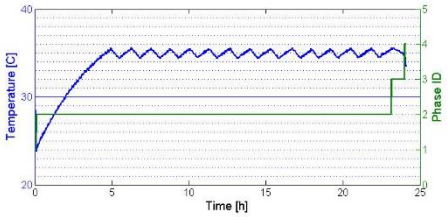

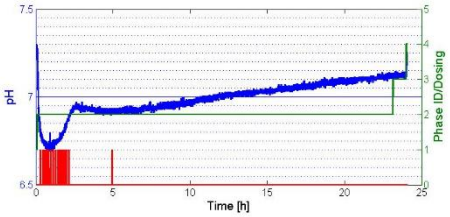

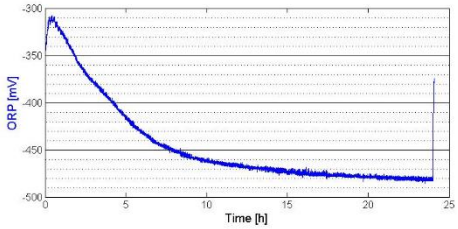

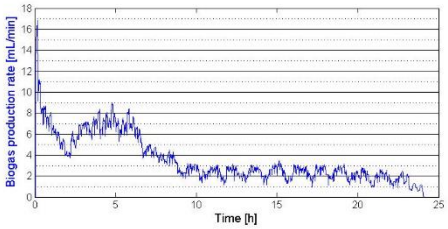

Cycle 196.csv

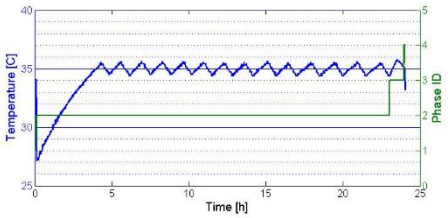

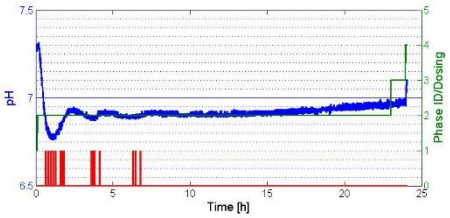

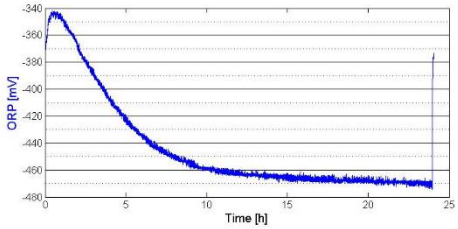

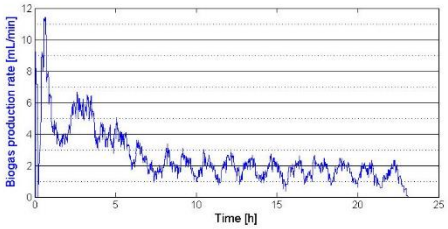

Stellenbosch University https://scholar.sun.ac.za

Cycle 197.csv

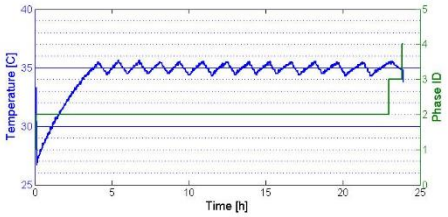

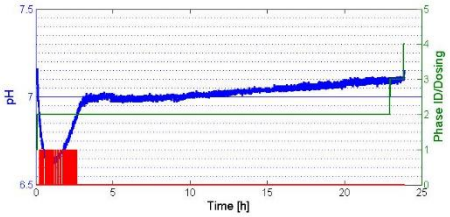

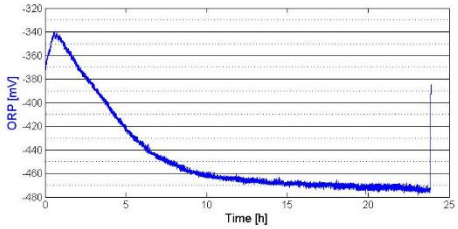

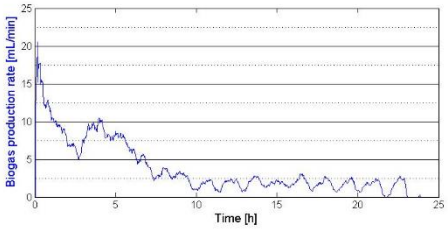

Stellenbosch University https://scholar.sun.ac.za

Appendix E - Matlab code

E.1. ADM 1 - main

```
%{
    Jason Smit
    Stellenbosch University
    Process Engineering
    MEng
    ADM1 modelling
    Ode15s used for reduced number of iterations
%}

% ========= ========= TIME CALCULATIONS ============================

tic;

% ================ Initial values ================
% These are values of the liquid in the ASBR at the start of a cycle
S_su = 0.000000001;
S_aa = 0.0000000001;
S_fa = 0.0000000001;
S_va = 0.0000000001;
S_bu = 0.00000000001;
S_pro = 0.0000000001;
S_ac = 0.642;
S_h2 = 1e-10;
S_ch4 = 1e-7;
S_IC = 0.01;

S_IN = 0.01;
S_I = 0.02;
S_et = 0.0000001;
X_c = 10;
X_ch = 10;
X_pr = 10;
X_li = 10;
X_su = 15;
X_aa = 10;
X_fa = 10;

X_c4 = 5;
X_pro = 2;
X_ac = 0.5;
X_h2 = 5;
X_I = 10;
X_et = 5;

S_cat = 0.12;
S_an = 0.1;

% Make ions equal to concentration of respective acid
% Values in
S_va_an = S_va/208;
S_bu_an = S_bu/160;
S_pro_an = S_pro/112;
S_ac_an = S_ac/64;
```

Stellenbosch University https://scholar.sun.ac.za

```
S_hco3_an = S_IC;
S_nh3 = S_IN;

S_gas_h2 = 1.02e-5;
S_gas_ch4 = 1.99872;
S_gas_co2 = 0.013385;

P_h2 = 0;
P_ch4 = 0;
P_co2 = 0;
P_h2o = 0;
q_gas = 0;
pH = 7;
S_H_cat = 10^(-pH);

theta_in    =    S_cat-S_an+S_IN-S_hco3_an-(S_ac/64)-(S_pro/112)-(S_bu/160)-
(S_va/208);
S_H_in = -theta_in*0.5 + 0.5*sqrt((theta_in^2)+4*2.08e-14);
pH_in = -log10(S_H_in);

in = [S_su S_aa S_fa S_va S_bu S_pro S_ac S_h2 S_ch4 S_IC S_IN S_I S_et X_c
X_ch X_pr X_li X_su X_aa X_fa X_c4 X_pro X_ac X_h2 X_I X_et S_cat S_an S_va_an
S_bu_an S_pro_an S_ac_an S_hco3_an S_nh3 S_gas_h2 S_gas_ch4 S_gas_co2 pH_in];
% intial conditions of reactor


% ================ Feed concentrations ================
S_su_f = 3.564;
S_aa_f = 0;
S_fa_f = 1e-8;
S_va_f = 1e-8;
S_bu_f = 0;
S_pro_f = 1e-8;
S_ac_f = 1e-8;
S_h2_f = 0;
S_ch4_f = 0;
S_IC_f = 0.71231;

S_IN_f = 0.03;
S_I_f = 0;
S_et_f = 1e-8;
X_c_f = 1e-8;
X_ch_f = 0;
X_pr_f = 0;
X_li_f = 0;
X_su_f = 0;
X_aa_f = 0;
X_fa_f = 0;

X_c4_f = 0;
X_pro_f = 0;
X_ac_f = 0;
X_h2_f = 0;
X_I_f = 0;
X_et_f = 0;
S_cat_f = 0.12; % 0.12093
S_an_f = 0.1;

S_va_an_f = S_va_f/208;
```

Stellenbosch University https://scholar.sun.ac.za

```
S_bu_an_f = S_bu_f/160;
S_pro_an_f = S_pro_f/112;
S_ac_an_f = S_ac_f/64;
S_hco3_an_f = S_IC_f;
S_nh3_f = S_IN_f;

S_gas_h2_f = 0;
S_gas_ch4_f = 0;
S_gas_co2_f = 0;
P_h2_f = 0;
P_ch4_f = 0;
P_co2_f = 0;

theta_f = S_cat_f-S_an_f+S_IN-S_IC_f-(S_ac_f/64)-(S_pro_f/112)-(S_bu_f/160)-
(S_va_f/208);
S_H_f = -theta_f*0.5 + 0.5*sqrt((theta_f^2)+4*2.08e-14);
pH_f = -log10(S_H_f);

feed = [S_su_f S_aa_f S_fa_f S_va_f S_bu_f S_pro_f S_ac_f S_h2_f S_ch4_f
S_IC_f S_IN_f S_I_f S_et_f X_c_f X_ch_f X_pr_f X_li_f X_su_f X_aa_f X_fa_f
X_c4_f X_pro_f X_ac_f X_h2_f X_I_f X_et_f S_cat_f S_an_f S_va_an_f S_bu_an_f
S_pro_an_f S_ac_an_f S_hco3_an_f S_nh3_f S_gas_h2_f S_gas_ch4_f S_gas_co2_f
pH_f];

% ========== Volumes and flow rates ==========
timeFill = 0.05;    % Time to fill reactor in days
timeReact = 0.7;     % Time to react and settle reactor in days. Assuming
system operates like a CSTR during react and settle phase.
timeDecant = 0.25; % Time to decant reactor in days
reactTimeEnd = timeFill+timeReact;
decantTimeEnd = timeFill+timeReact+timeDecant;

V_reactor_min = 0.007;  % Volume of minimum working volume in reactor
V_reactor_max = 0.014; % Volume of maximum working volume in reactor
q_in_set = (V_reactor_max - V_reactor_min)/timeFill;     % Volumetric flow
rate in such that the reactor is fed the correct volume in timeFill
q_out_set = (V_reactor_max - V_reactor_min)/timeDecant; % Volumetric flow
rate in such that the reactor is fed the correct volume in timeDecant
V_headspace = 0.01; % Volume of headspace in the reactor. Assumes the
headspace is constant and the buffering is from buffering bags. Like my ASBR.

volumes = [0 0 0 0];    % Vector to store: 1-q_in, 2-q_out, 3-V_reactor, 4-
V_headspace

options                                                                 =
odeset('NonNegative',1:35,'Reltol',6,'InitialStep',[],'Refine',1,'MaxOrder'
,[],'BDF','on','MaxStep',0.01);
in = in.';
feed = feed.';
tv_prev = 0;
sv_prev = in.';
vol_prev = V_reactor_min;
batchEnd_prev = sv_prev;

cycles = 20;
for loop=1:cycles

    % Solver to determine what is happening in the reactor during the filling
phase
```

Stellenbosch University https://scholar.sun.ac.za

```
    volumes = [q_in_set 0 V_reactor_min V_headspace];
    [tFill, sFill] = ode15s(@ADM1_ASBR_solver, [0 timeFill], in, options,
feed, volumes);

    ASBR_volumeFill = V_reactor_min + q_in_set*tFill;

    % Solver to determine what is happening in the reactor during the react
and settle phase
    in = sFill(end,:);  % Last row of array 's' becomes the initial guess
for liquid concentrations in during the react and settle phase
    volumes(1) = 0; % Feed flow rate to ASBR is zero
    volumes(2) = 0; % Decant flow rate to ASBR is zero
    volumes(3) = V_reactor_max; % During react and settle phase ASBR is at
the maximum volume
    [tReact, sReact] = ode15s(@ADM1_ASBR_solver, [timeFill reactTimeEnd], in,
options, feed, volumes);

    reactLength = length(tReact);
    for i = 1:reactLength
        ASBR_volumeReact(i) = V_reactor_max;
    end

    % determine is matrix needs to be transposed to column or not
    testColumn = iscolumn(ASBR_volumeReact);
    if testColumn == 0
        ASBR_volumeReact = ASBR_volumeReact.';
    end

    % Solver to determine the decant phase
    in = sReact(end,:);  % Last row of array 's' becomes the initial guess
for liquid concentrations in during the react and settle phase
    volumes(1) = 0; % Feed flow rate to ASBR is zero
    volumes(2) = q_out_set; % Decant flow rate to ASBR is zero
    volumes(3) = V_reactor_max; % During react and settle phase ASBR is at
the maximum volume
    [tDecant,    sDecant]    =    ode15s(@ADM1_ASBR_solver,    [reactTimeEnd
decantTimeEnd], in, options, feed, volumes);

    ASBR_volumeDecant = V_reactor_max - q_out_set*(tDecant-reactTimeEnd);

    % Added each phase to vector/marix of current cycle
    tv_current_cycle  =  vertcat(tFill,tReact,tDecant);     %  concatenate
different phase time vectors to form one large time vector
    sv_current = vertcat(sFill,sReact,sDecant);
    vol_current                                                          =
vertcat(ASBR_volumeFill,ASBR_volumeReact,ASBR_volumeDecant);  % Concatenate
volume throughout the ASBR process

    tv_current = tv_current_cycle + tv_prev(end);

    % Add current cycle to previous cycle
    tv = vertcat(tv_prev, tv_current);
    sv = vertcat(sv_prev, sv_current);
    ASBR_volume = vertcat(vol_prev, vol_current);

    % Make current cycle, new cycle for the next cycle to be calculated
    tv_prev = tv;
    sv_prev = sv;
    vol_prev = ASBR_volume;
```

Stellenbosch University https://scholar.sun.ac.za

```
    % Need to make final conc of previous batch in ASBR, the initial conc
for
    % the next batch
    in = sv(end,:);

    batchEnd = vertcat(batchEnd_prev,in);
    batchEnd_prev = batchEnd;

    % Empty vectors to prevent over writing of data
    clear ASBR_volumeFill;
    clear ASBR_volumeReact;
    clear ASBR_volumeDecant;
end

% pH calculation
n = length(tv);
for i = 1:n
    theta   =   sv(i,27)-sv(i,28)+(sv(i,11)-sv(i,34))-sv(i,33)-(sv(i,32)/64)-
(sv(i,31)/112)-(sv(i,30)/160)-(sv(i,29)/208);
    S_H(i) = -theta*0.5+0.5*sqrt((theta^2)+4*2e-14);
    pH(i) = -log10(S_H(i));
end
pH = pH.';

P_gas_h2o_cal = 0.0313*exp(5290*(1/298 - 1/308));
P_gas_h2_cal = sv(:,35)*0.083145*308/16;
P_gas_ch4_cal = sv(:,36)*0.083145*308/64;
P_gas_co2_cal = sv(:,37)*0.083145*308;
kp = 5e4;
P_atm = 1.013;
P_gas_cal = P_gas_h2o_cal+P_gas_h2_cal+P_gas_ch4_cal+P_gas_co2_cal;

for i = 1:n
    q_gas(i) = kp*(P_gas_cal(i)-P_atm);
    if q_gas(i) < 0;
        q_gas(i) = 0;
    end
end
q_gas = q_gas.';

x_h2 = P_gas_h2_cal./P_gas_cal;
x_ch4 = P_gas_ch4_cal./P_gas_cal;
x_co2 = P_gas_co2_cal./P_gas_cal;
x_total = x_h2 + x_ch4 + x_co2;

% ================================ LARGE 5x5 graph ====================

figure
subplot(5,5,1);
plot(tv, sv(:,1));
title('Monosaccharides');
xlabel('time [days]');
ylabel('S_s_u [kgCOD/m^3]');

subplot(5,5,2);
plot(tv, sv(:,2));
title('Amino acids');
xlabel('time [days]');
```

Stellenbosch University https://scholar.sun.ac.za

```
ylabel('S_a_a [kgCOD/m^3]');

subplot(5,5,3);
plot(tv, sv(:,3));
title('LCFA');
xlabel('time [days]');
ylabel('S_f_a [kgCOD/m^3]');

subplot(5,5,4);
plot(tv, sv(:,4));
title('Total valerate');
xlabel('time [days]');
ylabel('S_v_a [kgCOD/m^3]');

subplot(5,5,5);
plot(tv, sv(:,5));
title('Total butyrate');
xlabel('time [days]');
ylabel('S_b_u [kgCOD/m^3]');

subplot(5,5,6);
plot(tv, sv(:,6));
title('Total propionate');
xlabel('time [days]');
ylabel('S_p_r_o [kgCOD/m^3]');

subplot(5,5,7);
plot(tv, sv(:,7));
title('Total acetate');
xlabel('time [days]');
ylabel('S_a_c [kgCOD/m^3]');

subplot(5,5,8);
plot(tv, sv(:,8));
title('Dissolved hydrogen');
xlabel('time [days]');
ylabel('S_h_2 [kgCOD/m^3]');

subplot(5,5,9);
plot(tv, sv(:,9));
title('Dissolved Methane');
xlabel('time [days]');
ylabel('S_c_h_4 [kgCOD/m^3]');

subplot(5,5,10);
plot(tv, sv(:,10));
title('Inorganic carbon');
xlabel('time [days]');
ylabel('S_I_C [kgCOD/m^3]');

subplot(5,5,11);
plot(tv, sv(:,11));
title('Inorganic nitrogen');
xlabel('time [days]');
ylabel('S_I_N [kgCOD/m^3]');

subplot(5,5,12);
plot(tv, sv(:,12));
title('Soluble inerts');
```

Stellenbosch University https://scholar.sun.ac.za

```
xlabel('time [days]');
ylabel('S_I [kgCOD/m^3]');

subplot(5,5,13);
plot(tv, sv(:,13));
title('Ethanol');
xlabel('time [days]');
ylabel('S_e_t [kgCOD/m^3]');

subplot(5,5,14);
plot(tv, sv(:,14));
title('Composites');
xlabel('time [days]');
ylabel('S_c [kgCOD/m^3]');

subplot(5,5,15);
plot(tv, sv(:,15));
title('Carbohydrates');
xlabel('time [days]');
ylabel('S_c_h [kgCOD/m^3]');

subplot(5,5,16);
plot(tv, sv(:,16));
title('Proteins');
xlabel('time [days]');
ylabel('X_p_r [kgCOD/m^3]');

subplot(5,5,17);
plot(tv, sv(:,17));
title('Lipids');
xlabel('time [days]');
ylabel('X_l_i [kgCOD/m^3]');

subplot(5,5,18);
plot(tv, sv(:,18));
title('Sugar degraders');
xlabel('time [days]');
ylabel('X_s_u [kgCOD/m^3]');

subplot(5,5,19);
plot(tv, sv(:,19));
title('Amino acids degraders');
xlabel('time [days]');
ylabel('X_a_a [kgCOD/m^3]');

subplot(5,5,20);
plot(tv, sv(:,20));
title('LCFA degraders');
xlabel('time [days]');
ylabel('X_f_a [kgCOD/m^3]');

subplot(5,5,21);
plot(tv, sv(:,21));
title('C4 degraders');
xlabel('time [days]');
ylabel('X_c_4[kgCOD/m^3]');

subplot(5,5,22);
plot(tv, sv(:,22));
```

Stellenbosch University https://scholar.sun.ac.za

```
title('Propionate degraders');
xlabel('time [days]');
ylabel('X_p_r_o [kgCOD/m^3]');

subplot(5,5,23);
plot(tv, sv(:,23));
title('Acetate degraders');
xlabel('time [days]');
ylabel('X_a_c [kgCOD/m^3]');

subplot(5,5,24);
plot(tv, sv(:,24));
title('Hydrogen degraders');
xlabel('time [days]');
ylabel('X_h_2 [kgCOD/m^3]');

subplot(5,5,25);
plot(tv, sv(:,26));
title('Ethanol degraders');
xlabel('time [days]');
ylabel('X_e_t [kgCOD/m^3]');



% ==================== 2nd large 5x5 figure

figure
subplot(5,5,1);
plot(tv, sv(:,27));
title('Cations');
xlabel('time [days]');
ylabel('S_c_a_t [kgCOD/m^3]');

subplot(5,5,2);
plot(tv, sv(:,28));
title('Anions');
xlabel('time [days]');
ylabel('S_a_n [kgCOD/m^3]');

subplot(5,5,3);
plot(tv, sv(:,29));
title('Valerate anion');
xlabel('time [days]');
ylabel('S_v_a_a_c [kgCOD/m^3]');

subplot(5,5,4);
plot(tv, sv(:,30));
title('Butyrate anion');
xlabel('time [days]');
ylabel('S_b_u_a_c [kgCOD/m^3]');

subplot(5,5,5);
plot(tv, sv(:,31));
title('Propoinate ions');
xlabel('time [days]');
ylabel('S_p_r_o_a_c [kgCOD/m^3]');

subplot(5,5,6);
```

Stellenbosch University https://scholar.sun.ac.za

```
plot(tv, sv(:,32));
title('Acetate ions');
xlabel('time [days]');
ylabel('S_a_c_a_c [kgCOD/m^3]');

subplot(5,5,7);
plot(tv, sv(:,33));
title('HCO_3 anion');
xlabel('time [days]');
ylabel('S_h_c_o_3_a_n [kgCOD/m^3]');

subplot(5,5,8);
plot(tv, sv(:,34));
title('NH_4 anion (NH_3)');
xlabel('time [days]');
ylabel('S_N_H_4_a_c [kgCOD/m^3]');

subplot(5,5,9);
plot(tv, sv(:,35));
title('Gas H2');
xlabel('time [days]');
ylabel('S_h_2 [kgCOD/m^3]');

subplot(5,5,10);
plot(tv, sv(:,36));
title('Gas ch4');
xlabel('time [days]');
ylabel('S_c_h_4 [kgCOD/m^3]');

subplot(5,5,11);
plot(tv, sv(:,37));
title('Gas co2');
xlabel('time [days]');
ylabel('S_c_o_2 [kgCOD/m^3]');

subplot(5,5,12);
plot(tv, q_gas);
title('Q gas');
xlabel('time [days]');
ylabel('q_o_u_t [m^3/d]');

subplot(5,5,13);
plot(tv, x_ch4,'b');
title('y ch4');
xlabel('time [days]');
ylabel('Gas fraction');

subplot(5,5,14);
plot(tv, x_co2,'b');
title('y co2');
xlabel('time [days]');
ylabel('Gas fraction');

subplot(5,5,15);
plot(tv, x_h2,'b');
title('y h2');
xlabel('time [days]');
ylabel('Gas fraction');
```

Stellenbosch University https://scholar.sun.ac.za

```
subplot(5,5,16);
plot(tv, pH);
title('pH');
xlabel('time [days]');
ylabel('pH');

subplot(5,5,17);
plot(tv, sv(:,38));
title('pH Solver');
xlabel('time [days]');
ylabel('pH');

subplot(5,5,18);
plot(tv, ASBR_volume);
title('ASBR Volume');
xlabel('time [days]');
ylabel('Liquid volume [m^3]');

subplot(5,5,19);
plot(tv, S_H,'o');
title('S_H proton');
xlabel('time [days]');
ylabel('S_H [kmol/m^3]');

subplot(5,5,20);
plot(tv, P_gas_cal,'o');
title('P_g_a_s');
xlabel('time [days]');
ylabel('P_g_a_s [bar]');

clear;
toc;
```

Stellenbosch University https://scholar.sun.ac.za

E.2. ADM 1 - solver

```
function dS = ADM1_ASBR_solver(t,s,feed,volumes)

% Initial conditions in reactor. state variables
S_su = s(1); % sugar state variable
S_aa = s(2); % amino acid state variable
S_fa = s(3); % LCFA state variable
S_va = s(4); % S_va kg-COD/m3
S_bu = s(5); % S_bu kg-COD/m3
S_pro = s(6); % S_pro kg-COD/m3
S_ac = s(7); % S_ac kg-COD/m3
S_h2 = s(8); % S_h2 kg-COD/m3
S_ch4 = s(9); % S_ch4 kg-COD/m3
S_IC = s(10); % S_IC kmol/m3
S_IN = s(11); % S_IN kmol/m3
S_I = s(12); % S_I kg-COD/m3
S_et = s(13);

X_c = s(14); % X_c kg-COD/m3
X_ch = s(15); % X_ch kg-COD/m3
X_pr = s(16); % X_pr kg-COD/m3
X_li = s(17); % X_li kg-COD/m3
X_su = s(18); % X_su kg-COD/m3
X_aa = s(19); % X_aa kg-COD/m3
X_fa = s(20); % X_fa kg-COD/m3
X_c4 = s(21); % X_c4 kg-COD/m3
X_pro = s(22); % X_pro kg-COD/m3
X_ac = s(23); % X_ac kg-COD/m3
X_h2 = s(24); % X_h2 kg-COD/m3
X_I = s(25); % X_I kg-COD/m3
X_et = s(26);

% Unit are kmol/m3
S_cat = s(27);
S_an = s(28);
S_vaac = s(29);
S_buac = s(30);
S_proac = s(31);
S_acac = s(32);
S_ICac = s(33);
S_INac = s(34);

% Units
S_gas_h2 = s(35);
S_gas_ch4 = s(36);
S_gas_co2 = s(37);

S_co2 = S_IC - S_ICac;  % CO2 in liquid phase. kmol/m3

pH_in = s(38);

q_in = volumes(1); % volumetric flow rate in
q_out = volumes(2); % volumetric flow rate out
V_liq = volumes(3) + q_in*t - q_out*t; % Liquid volume
V_gas = volumes(4); % Gas/headspace volume
t_resX = 10;   % Solids retention time in days. Degraders retention time in
the ASBR
```

Stellenbosch University https://scholar.sun.ac.za

```
% ================== ADM1 benchmark parameters ============================
% All values from Batstone et al 2002
% Values adjusted to that of Jeppson and Ulfson
% Stiochiometric parameter values
f_sI_xc = 0.1;
f_xI_xc = 0.2;
f_ch_xc = 0.2;
f_pr_xc = 0.2;
f_li_xc = 0.3;

N_xc = 0.0376/14;
N_I = 0.06/14;
N_aa = 0.007;

C_xc = 0.02786;
C_sI = 0.03;
C_ch = 0.0313;
C_pr = 0.03;
C_li = 0.022;
C_xI = 0.03;
C_su = 0.0313;
C_aa = 0.03;
f_fa_li = 0.95;
C_fa = 0.0217;

f_h2_su = 0.19;
f_bu_su = 0.13;
f_pro_su = 0.27;
f_ac_su = 0.41;
N_bac = 0.08/14;
C_bu = 0.025;
C_pro = 0.0268;
C_ac = 0.0313;
C_bac = 0.0313;
Y_su = 0.1;

f_h2_aa = 0.06;
f_va_aa = 0.23;
f_bu_aa = 0.26;
f_pro_aa = 0.05;
f_ac_aa = 0.4;
C_va = 0.024;

Y_aa = 0.08;
Y_fa = 0.06;
Y_c4 = 0.06;
Y_pro = 0.04;
C_ch4 = 0.0156;
Y_ac = 0.05;
Y_h2 = 0.06;
Y_et = 0.01;

% Biochemical parameter values
k_dis = 0.4;
k_hyd_ch = 0.25;
k_hyd_pr = 0.2;
k_hyd_li = 0.1;
```

Stellenbosch University https://scholar.sun.ac.za

```
k_m_su = 30;
k_m_aa = 50;
k_m_fa = 6;
k_m_c4 = 20;
k_m_pro = 13;
k_m_ac = 8; % Problem when 0.5 as Batstone 2004
k_m_h2 = 35;
k_m_et = 3;

% All decay variables are 0.02 as by Batstone et al 2002
k_dec_Xsu = 0.02;
k_dec_Xaa = 0.02;
k_dec_Xfa = 0.02;
k_dec_Xc4 = 0.02;
k_dec_Xpro = 0.02;
k_dec_Xac = 0.02;
k_dec_Xh2 = 0.02;
k_dec_Xet = 0.02;

% Half saturation values
K_s_su = 0.1;
K_s_aa = 0.3;
K_s_fa = 0.4;
K_s_c4 = 0.3;
K_s_pro = 0.1;
K_s_ac = 0.15;
K_s_h2 = 7e-6;
K_s_et = 0.5;
% K_s_IN = 1e-4;
%
% Operating parameters
T_op = 273.15+35; % Operating temperature
P_atm = 1.013;  % Atmospheric pressure in bar
R = 0.083145;    %Gas constant [bar/(M.K)]
k_p = 5e4;

% Physicochemical parameters
pKa_ac = 4.76;
pKa_bu = 4.82;
pKa_co2 = 6.35;
pKa_h2o = 14;
pKa_nh3 = 9.25;
pKa_pro = 4.88;
pKa_va = 4.86;

dH0_Ka_co2 = 7646;
dH0_Ka_h2o = 55900;
dH0_Ka_nh4 = 51965;
dH0_KH_ch4 = -14240;
dH0_KH_co2 = -19410;
dH0_KH_h2 = -4180;

k_A_Bva = 1e10; % 1/M/d
k_A_Bbu = 1e10; % 1/M/d
k_A_Bpro = 1e10;    % 1/M/d
k_A_Bac = 1e10; % 1/M/d
k_A_Bco2 = 1e10;    % 1/M/d
k_A_BIN = 1e10; % 1/M/d
```

Stellenbosch University https://scholar.sun.ac.za

```
K_a_va = 10^(-pKa_va);
K_a_bu = 10^(-pKa_bu);
K_a_pro = 10^(-pKa_pro);
K_a_ac = 10^(-pKa_ac);
K_a_co2 = 10^(-pKa_co2)*exp(dH0_Ka_co2/(R*100)*(1/298 - 1/T_op));
K_a_IN = 10^(-pKa_nh3)*exp(dH0_Ka_nh4/(R*100)*(1/298 - 1/T_op));
K_W = 10^(-pKa_h2o)*exp(dH0_Ka_h2o/(R*100)*(1/298 - 1/T_op));
%K_W = 1e-14;

K_H_h2 = 0.00078*exp(dH0_KH_h2/R/100*(1/298-1/T_op));
K_H_ch4 = 0.0014*exp(dH0_KH_ch4/R/100*(1/298-1/T_op));
K_H_co2 = 0.035*exp(dH0_KH_co2/R/100*(1/298-1/T_op));
kLa = 200;

% ======== pH calculations ===============
theta = S_cat-S_an+(S_IN-S_INac)-S_ICac-(S_acac/64)-(S_proac/112)-
(S_buac/160)-(S_vaac/208);
S_H = -theta*0.5 + 0.5*sqrt((theta^2)+4*K_W);
pH = -log10(S_H);
S_cat_new = S_cat;
S_an_new = S_an;

% if pH < 7
%     S_H_new = 10^(-7);
%     S_cat_new = S_an +
K_W/S_H_new+(S_vaac/208)+(S_buac/160)+(S_proac/112)+(S_acac/64)+S_ICac-
S_H_new-(S_IN-S_INac);
%     S_H = S_H_new;
%
% % elseif pH > 7
% %     S_H_new = 10^(-7);
% %     S_an_new = S_cat+(S_IN-S_INac)+S_H_new-S_ICac-(S_acac/64)-
(S_proac/112)-(S_buac/160)-(S_vaac/208)-K_W/S_H_new;
% %     S_H = S_H_new;
% end

dS_Cat_add = S_cat_new - S_cat;
dS_An_add = S_an_new - S_an;


% ============== Gas transfer ==================
P_gas_h2 = S_gas_h2*R*T_op/16;  % Partial pressure of hydrogen
P_gas_ch4 = S_gas_ch4*R*T_op/64; % Partial pressure of methane
P_gas_co2 = S_gas_co2*R*T_op;    % Partial pressure of CO2
P_gas_h2o = 0.0313*exp(5290*(1/298-1/T_op));    % Pratial pressure of H2O
P_gas = P_gas_h2 + P_gas_ch4 + P_gas_co2 + P_gas_h2o;

q_gas = k_p*(P_gas - P_atm)*(P_gas/P_atm);
if q_gas < 0;
    q_gas = 0;
end


% ========== Inihibition ==========
% pH inhibition upper and lower limits
pH_UL_bac = 5.5;
pH_LL_bac = 4;

pH_UL_ac = 7.5;
```

Stellenbosch University https://scholar.sun.ac.za

```
pH_LL_ac = 5.8;

pH_UL_h2 = 6.5;
pH_LL_h2 = 5;

K_S_IN = 0.0001;
K_I_NH3 = 0.0018;
K_I_h2_fa = 5e-6;
K_I_h2_c4 = 1e-5;
K_I_h2_pro = 3.5e-6;

% ========================== Inhibition ==============================
% pH inhibition
I_pH_bac = (1 + 2*10^(0.5*(pH_LL_bac - pH_UL_bac)))/(1 + 10^(pH-
pH_UL_bac)+10^(pH_LL_bac-pH));
I_pH_ac = (1 + 2*10^(0.5*(pH_LL_ac - pH_UL_ac)))/(1 + 10^(pH-
pH_UL_ac)+10^(pH_LL_ac-pH));
I_pH_h2 = (1 + 2*10^(0.5*(pH_LL_h2 - pH_UL_h2)))/(1 + 10^(pH-
pH_UL_h2)+10^(pH_LL_h2-pH));

% Secondary substrate inhibition
if S_IN<0
    I_IN = 0;
else
    I_IN = 1/(1+K_S_IN/S_IN);
end

% Free NH3 inhibition
I_NH3 = 1/(1+S_INac/K_I_NH3);

% Hydrogen inhibtion
I_h2_fa = 1/(1+S_h2/K_I_h2_fa);
I_h2_c4 = 1/(1+S_h2/K_I_h2_c4);
I_h2_pro = 1/(1+S_h2/K_I_h2_pro);

I_5 = I_pH_bac*I_IN;
I_6 = I_pH_bac*I_IN;
I_7 = I_pH_bac*I_IN*I_h2_fa;
I_8 = I_pH_bac*I_IN*I_h2_c4;
I_9 = I_pH_bac*I_IN*I_h2_c4;
I_10 = I_pH_bac*I_IN*I_h2_pro;
I_11 = I_pH_ac*I_IN*I_NH3;
I_12 = I_pH_h2*I_IN;

% ==================== Kinetic rate equations ======================
% Only calculate each value as required. Do not need to know the change in
% kinetic parameters.

% Biochemical process rate equations
p1 = k_dis*X_c;
p2 = k_hyd_ch*X_ch;
p3 = k_hyd_pr*X_pr;
p4 = k_hyd_li*X_li;
p5 = k_m_su*S_su/(K_s_su + S_su)*X_su*I_5;
p6 = k_m_aa*S_aa/(K_s_aa + S_aa)*X_aa*I_6;
p7 = k_m_fa*S_fa/(K_s_fa + S_fa)*X_fa*I_7;
p8 = k_m_c4*S_va/(K_s_c4 + S_va)*X_c4*1/(1 + S_bu/S_va)*I_8;
p9 = k_m_c4*S_bu/(K_s_c4 + S_bu)*X_c4*1/(1 + S_va/S_bu)*I_9;
p10 = k_m_pro*S_pro/(K_s_pro + S_pro)*X_pro*I_10;
```

Stellenbosch University https://scholar.sun.ac.za

```
p11 = k_m_ac*S_ac/(K_s_ac + S_ac)*X_ac*I_11;
p12 = k_m_h2*S_h2/(K_s_h2 + S_h2)*X_h2*I_12;
p13 = k_m_et*S_et/(K_s_et + S_et)*X_et;
p14 = k_dec_Xsu*X_su;
p15 = k_dec_Xaa*X_aa;
p16 = k_dec_Xfa*X_fa;
p17 = k_dec_Xc4*X_c4;
p18 = k_dec_Xpro*X_pro;
p19 = k_dec_Xac*X_ac;
p20 = k_dec_Xh2*X_h2;
p21 = k_dec_Xet*X_et;

% Acid-base transfer rates
p_A_va = k_A_Bva*(S_vaac*(K_a_va + S_H) - K_a_va*S_va);
p_A_bu = k_A_Bbu*(S_buac*(K_a_bu + S_H) - K_a_bu*S_bu);
p_A_pro = k_A_Bpro*(S_proac*(K_a_pro + S_H) - K_a_pro*S_pro);
p_A_ac = k_A_Bac*(S_acac*(K_a_ac + S_H) - K_a_ac*S_ac);
p_A_co2 = k_A_Bco2*(S_ICac*(K_a_co2 + S_H) - K_a_co2*S_IC);
p_A_IN = k_A_BIN*(S_INac*(K_a_IN + S_H) - K_a_IN*S_IN);

% p_A_va = k_A_Bva*(S_vaac*S_H - K_a_va*S_va);
% p_A_bu = k_A_Bbu*(S_buac*S_H - K_a_bu*S_bu);
% p_A_pro = k_A_Bpro*(S_proac*S_H - K_a_pro*S_pro);
% p_A_ac = k_A_Bac*(S_acac*S_H - K_a_ac*S_ac);
% p_A_co2 = k_A_Bco2*(S_ICac*S_H - K_a_co2*S_IC);
% p_A_IN = k_A_BIN*(S_INac*S_H - K_a_IN*S_IN);

% Gas tranfer rates
p_T_h2 = kLa*(S_h2 - 16*K_H_h2*P_gas_h2);
p_T_ch4 = kLa*(S_ch4 - 64*K_H_ch4*P_gas_ch4);
p_T_co2 = kLa*(S_co2 - K_H_co2*P_gas_co2);

% Sum of concentration for inorganic carbon or CO2
s1 = (-1)*C_xc + f_sI_xc*C_sI + f_ch_xc*C_ch + f_pr_xc*C_pr + f_li_xc*C_li
+ f_xI_xc*C_xI;
s2 = (-1)*C_ch + C_su;
s3 = (-1)*C_pr + C_aa;
s4 = (-1)*C_li + (1-f_fa_li)*C_su + f_fa_li*C_fa;
s5 = (-1)*C_su + (1-Y_su)*(f_bu_su*C_bu + f_pro_su*C_pro + f_ac_su*C_ac) +
Y_su*C_bac;
s6 = (-1)*C_aa + (1-Y_aa)*(f_va_aa*C_va + f_bu_aa*C_bu + f_pro_aa*C_pro +
f_ac_aa*C_ac) + Y_aa*C_bac;
s7 = (-1)*C_fa + (1-Y_fa)*0.7*C_ac + Y_fa*C_bac;
s8 = (-1)*C_va + (1-Y_c4)*0.54*C_pro + (1-Y_c4)*0.31*C_ac + Y_c4*C_bac;
s9 = (-1)*C_bu + (1-Y_c4)*0.8*C_ac + Y_c4*C_bac;
s10 = (-1)*C_pro + (1-Y_pro)*0.57*C_ac + Y_pro*C_bac;
s11 = (-1)*C_ac + (1-Y_ac)*C_ch4 + Y_ac*C_bac;
s12 = (1-Y_h2)*C_ch4 + Y_h2*C_bac;
s13 = (-1)*C_bac + C_xc;
s_IC = s1*p1 + s2*p2 + s3*p3 + s4*p4 + s5*p5 + s6*p6 + s7*p7 + s8*p8 +
s9*p9 + s9*p9 + s10*p10 + s11*p11 + s12*p12 +
s13*(p13+p14+p15+p16+p17+p18+p19);

% ====================== Dynamic liquid state variables
==========================
% S - Soluble component
% X - Particulate component
% Stored as array to plot the change in parameters
% All concentrations calculated in kg-COD/m3
% dS = HRT*Ss_in - HRT*S_i + sigma
```

Stellenbosch University https://scholar.sun.ac.za

```
sigma = [0 0 0 0 0 0 0 0 0 0 0 0 0 0 0 0 0 0 0 0 0 0 0 0 0 0 0 0 0 0 0 0 0 0 0 0 
0 0 0 0];

sigma = sigma.';    % Make sigma a column vector

sigma(1) = p2 + (1-f_fa_li)*p4 - p5;  % Monosaccharides
sigma(2) = p3 - p6;   % Amino acids
sigma(3) = f_fa_li*p4 - p7;   % LCFA
sigma(4) = (1-Y_aa)*f_va_aa*p6 - p8;  % Total valerate

sigma(5) = (1-Y_su)*f_bu_su*p5 + (1-Y_aa)*f_bu_aa*p6 - p9;    % Total 
butyrate
sigma(6) = (1-Y_su)*f_pro_su*p5 + (1-Y_aa)*f_pro_aa*p6 + (1-Y_c4)*0.54*p8 - 
p10;  % Total propionate
sigma(7) = (1-Y_su)*f_ac_su*p5 + (1-Y_aa)*f_ac_aa*p6 + (1-Y_fa)*0.7*p7 + 
(1-Y_c4)*0.31*p8 + (1-Y_c4)*0.8*p9 + (1-Y_pro)*0.57*p10 - p11 + 2/3*(1-
Y_et)*p13;    % Total acetate
sigma(8) = (1-Y_su)*f_h2_su*p5 + (1-Y_aa)*f_h2_aa*p6 + (1-Y_fa)*0.3*p7 + 
(1-Y_c4)*0.15*p8 + (1-Y_c4)*0.2*p9 + (1-Y_pro)*0.43*p10 - p12 + 1/3*(1-
Y_et)*p13 - p_T_h2; % Hydrogen gas in liquid

sigma(9) = (1-Y_ac)*p11 + (1-Y_h2)*p12 - p_T_ch4;   % Methane gas in liquid
sigma(10) = (-1)*s_IC - p_T_co2;    % CO2 in liquid
sigma(11) = (-1)*Y_su*N_bac*p5 + (N_aa-Y_aa*N_bac)*p6 - Y_fa*N_bac*p7 - 
Y_c4*N_bac*p8 - Y_c4*N_bac*p9 - Y_pro*N_bac*p10 - Y_ac*N_bac*p11 - 
Y_h2*N_bac*p12 + (N_bac-N_xc)*(p13+p14+p15+p16+p17+p18+p19) + (N_xc - 
f_xI_xc*N_I - f_sI_xc*N_I - f_pr_xc*N_aa)*p1 - Y_et*N_bac;  % Ammonium
sigma(12) = f_sI_xc*p1;   %  Soluble inerts

sigma(13) = -p13; % Ethanol

sigma(14) = (-1)*p1 + (p14+p15+p16+p17+p18+p19+p20);  % Particulate 
composites
sigma(15) = f_ch_xc*p1 - p2;  % Particulate carbohydrates
sigma(16) = f_pr_xc*p1 - p3;  % Particulate proteins
sigma(17) = f_li_xc*p1 - p4;  % Particulate lipids

sigma(18) = Y_su*p5 - p14;    % Particulate sugar degraders
sigma(19) = Y_aa*p6 - p15;    % Particulate amino acid degraders
sigma(20) = Y_fa*p7 - p16;    % Particulate LCFA degraders
sigma(21) = Y_c4*p8 + Y_c4*p9 - p17;  % Particulate valerate and butyrate 
degraders

sigma(22) = Y_pro*p10 - p18;  % Particulate propionate degraders
sigma(23) = Y_ac*p11 - p19;   % Particulate acetate degreders
sigma(24) = Y_h2*p12 - p20;   % Particluate hydrogen degraders
sigma(25) = f_xI_xc*p1;   % Particulate inerts

sigma(26) = Y_et*p13 - p21;   % Particulate ethanol degraders

% Cations and anions
sigma(27) = dS_Cat_add;    % Cations
sigma(28) = dS_An_add;    % Anions

% Ion states
sigma(29) = -p_A_va;    % Valerate anion
sigma(30) = -p_A_bu;    % Butyrate anion
```

Stellenbosch University https://scholar.sun.ac.za

```
sigma(31) = -p_A_pro;    % Propionate anion
sigma(32) = -p_A_ac;     % Acetate anion -
sigma(33) = -p_A_co2;    % Bicarbonate anion - HCO3^-
sigma(34) = -p_A_IN;     % Ammonia anion - NH3

% dS gas sigma
sigma(35) = V_liq/V_gas*p_T_h2;
sigma(36) = V_liq/V_gas*p_T_ch4;
sigma(37) = V_liq/V_gas*p_T_co2;

sigma(38) = 0;

S_liq = s;  % s is a column vector input
S_in = feed;    % feed is a column vector input

% sigma is a column vector
% S_liq is a column vector
% S_in is a column vector

S_liq = s;  % s is a column vector input
S_in = feed;    % feed is a column vector input

% dS for soluble components
for n = 1:13
    dS(n) = q_in*(S_in(n)-S_liq(n))/(V_liq) + sigma(n);
end

% dS for degraders (sludge components include solids retention
alpha = 0.01; % Flow rate ratio 0.1565 // 0.175
beta = 10; % Sludge concentration ratio 10
for n = 14:26
    dS(n) = q_in*(S_in(n)-S_liq(n))/(V_liq) + sigma(n) +
alpha*beta*S_liq(n)*q_out/V_liq - (1+alpha)*S_liq(n)*q_out/V_liq;
end

% dS for ion states
for n = 27:34
    dS(n) = q_in*(S_in(n)-S_liq(n))/(V_liq) + sigma(n);
end

% dS for gas in vapour phase
dS(35) = -S_gas_h2*q_gas/V_gas + p_T_h2*V_liq/V_gas;
dS(36) = -S_gas_ch4*q_gas/V_gas + p_T_ch4*V_liq/V_gas;
dS(37) = -S_gas_co2*q_gas/V_gas + p_T_co2*V_liq/V_gas;

dS(38) = -pH;   % Change in pH for each step

dS = dS.';  % Change to column vector

end
```

Stellenbosch University https://scholar.sun.ac.za

E.3. PLC data analysis

```
function plotPLCdata = plotPLCRecordedDataGasRate(filename)
tic;
% ============ Get test from csv file of the PLC ==============
fid = fopen(filename);  % Open file
headers = fgetl(fid);   % get first line
headers = textscan(headers, '%s', 'delimiter', ';');    % read first line
format = repmat('%s', 1, size(headers{1,1},1));   % Count columns and make
format string
dataRaw = textscan(fid, format, 'delimiter', ';'); % read rest of file
dataRaw = [dataRaw{:}];

[m,n] = size(dataRaw); % Size of data matrix. m = amount of rows, n =
amount of columns
dataProcessed = zeros(m,10);  % Zero matrix for processed data. 1-Time, 2-
Temp, 3-pH, 4-PhaseID, 5-Dosing IO, 6-MixingIO, 7-MixingRate, 8-
Conductivity, 9-ORP, 10-BiogasProduced

strDateTimeStart = strcat(dataRaw(1,2), dataRaw(1,1));
formatIn = 'mm/dd/yyyyHH:MM:SS';
DateTimeStart = datevec(strDateTimeStart, formatIn);
dataProcessed(1,1) = 0;
dataProcessed(1,2) = cellfun(@str2num, dataRaw(1,3))/10;  % Temperature [C]
dataProcessed(1,3) = cellfun(@str2num, dataRaw(1,4))/100;  % pH
dataProcessed(1,4) = cellfun(@str2num, dataRaw(1,5));  % Phase ID
dataProcessed(1,5) = cellfun(@str2num, dataRaw(1,6));  % Dosing IO
dataProcessed(1,6) = cellfun(@str2num, dataRaw(1,7));  % Mixing IO
dataProcessed(1,7) = cellfun(@str2num, dataRaw(1,10));  % ORP [mV]
dataProcessed(1,8) = (cellfun(@str2num, dataRaw(1,11)) +
20000*cellfun(@str2num, dataRaw(1,12)))*0.26;  % Biogas produced [mL]

for k = 2:m
    strDate = dataRaw(k,2);
    strTime = dataRaw(k,1);
    strDateTime1 = strcat(strDate, strTime);
    formatIn = 'mm/dd/yyyyHH:MM:SS';
    DateTime1 = datevec(strDateTime1, formatIn);
    deltaTime = etime(DateTime1, DateTimeStart);
    dataProcessed(k,1) = deltaTime/3600; % Time in seconds from the first
line in the csv file

    dataProcessed(k,2) = cellfun(@str2num, dataRaw(k,3))/10;  % Temperature
[C]
    dataProcessed(k,3) = cellfun(@str2num, dataRaw(k,4))/100;  % pH
    dataProcessed(k,4) = cellfun(@str2num, dataRaw(k,5));  % Phase ID
    dataProcessed(k,5) = cellfun(@str2num, dataRaw(k,6));  % Dosing IO
    dataProcessed(k,6) = cellfun(@str2num, dataRaw(k,7));  % Mixing IO
    dataProcessed(k,7) = cellfun(@str2num, dataRaw(k,10));  % ORP [mV]

end

totalTime = dataProcessed(m,1);

% Find where phase 2 begins
k = 1;
while dataProcessed(k,4) == 1
    dataProcessed(k,8) = 0;
    k = k+1;
```

Stellenbosch University https://scholar.sun.ac.za

```
end

a = k;
phase1 = dataProcessed(k, 1);
removeGasError = cellfun(@str2num, dataRaw(k,11)) + 20000*cellfun(@str2num,
dataRaw(k,12)); % Bubble counter initial value at start of phase 2. Remove
from all values.
for j = k:m
    dataProcessed(j,8) = (cellfun(@str2num, dataRaw(j,11)) +
20000*cellfun(@str2num, dataRaw(j,12)) - removeGasError)*0.26;  % Biogas
produced [mL]
end

% Find where phase 2 ends/phase 3 begin
while dataProcessed(a,4) == 2
    a = a+1;
end
phase2 = dataProcessed(a-1,1);

% Find where phase 3 ends/phase 4 begin
while dataProcessed(a,4) == 3
    a = a+1;
end
phase3 = dataProcessed(a-1,1);
phase4 = dataProcessed(m,1);

feedTimeMin = floor(phase1*60); % Feed time minute
feedTimeSecond = (phase1*60 - feedTimeMin)*60;   % Feed time second

reactTimeHour = floor(phase2 - phase1);
reactTimeMinute = (phase2 - reactTimeHour)*60;

settleTimeMin = floor(phase3*60-phase2*60);
settleTimeSec = (phase3*60 - settleTimeMin)/60;

decantTimeMin = floor(phase4*60-phase3*60);
decantTimeSec = (phase4*60-decantTimeMin)/60;

totalBubbles = dataProcessed(m,8)/0.26;
totalBiogas = dataProcessed(m,8);

fprintf('Feed time:   %4.0f min %4.0f sec \n', feedTimeMin,
feedTimeSecond);
fprintf('React time:  %4.0f hour%4.0f min \n', reactTimeHour,
reactTimeMinute);
fprintf('Settle time: %4.0f min %4.0f sec \n', settleTimeMin,
settleTimeSec);
fprintf('Decant time: %4.0f min %4.0f sec \n', decantTimeMin,
decantTimeSec);
fprintf('Bubbles: %8.0f \nBiogas:\t\t %5.3f mL \n', totalBubbles,
totalBiogas);

ORPdataSmoothed = smooth(dataProcessed(:,7),'rlowess');
pHdataSmoothed = smooth(dataProcessed(:,3),'rlowess');

excelDataPlot =
horzcat(dataProcessed(:,1),dataProcessed(:,2),ORPdataSmoothed,
pHdataSmoothed,dataProcessed(:,8));
```

Stellenbosch University https://scholar.sun.ac.za

```
% To write data to a txt file.
fid = fopen('myFile.txt','wt');
for ii = 1:m
    fprintf(fid,'%d\t',excelDataPlot(ii,:));
    fprintf(fid,'\n');
end
fclose(fid);

time(1) = 0;    %time vector
gasRate(1) = 0;    % Biogas production rate
n = 2;
for i = 31:30:m
    i_old = i-30;

    timeCurrent = dataProcessed(i,1);
    timePrev = dataProcessed(i_old,1);

    gasCurrent = dataProcessed(i,8);
    gasPrev = dataProcessed(i_old,8);

    time(n) = timeCurrent;  % Time in hours of cycle
    gasRate(n) = (gasCurrent-gasPrev)/((timeCurrent-timePrev)*60);  % Gas
Production rate in mL/min

    n=n+1;
end

time = time.';
gasRate = gasRate.';
gasTime = size(time);
gasSmoothed = smooth(gasRate,9);

excelDataPlotGas = horzcat(time,gasSmoothed);

% To write data to a txt file.
fid = fopen('myFileGas.txt','wt');
for ii = 1:gasTime
    fprintf(fid,'%d\t',excelDataPlotGas(ii,:));
    fprintf(fid,'\n');
end
fclose(fid);

if totalTime < 25
    endPlot = 25;
elseif totalTime < 50;
    endPlot = 50;
end

subplot(2,2,1);
[ax, h1, h2] = plotyy(dataProcessed(:,1),
dataProcessed(:,2),dataProcessed(:,1), dataProcessed(:,4));
ylabel(ax(1), 'Temperature [C]','FontSize',14); %14
ylabel(ax(2), 'Phase ID','FontSize',14);%14
xlabel(ax(1), 'Time [h]','FontSize',14);%14
axes(ax(1)); hold on;
set(gca, 'YGrid','on','YMinorGrid','on','FontSize',12); % 12
set(gca, 'GridLineStyle', '-');
```

Stellenbosch University https://scholar.sun.ac.za

```
ylim(ax(2), [0 5]);
xlim(ax(1), [0 endPlot]);
xlim(ax(2), [0 endPlot]);
axes(ax(2)); hold on;
set(gca, 'YTick', [0,1,2,3,4,5],'FontSize',12);%12
set(h1, 'LineWidth', 2);
set(h2, 'LineWidth', 2);

subplot(2,2,2)
[ax, h1, h2] = plotyy(dataProcessed(:,1),
pHdataSmoothed,dataProcessed(:,1), dataProcessed(:,4));
ylabel(ax(1), 'pH','FontSize',14);%14
ylabel(ax(2), 'Phase ID/Dosing','FontSize',14);%14
xlabel(ax(1), 'Time [h]','FontSize',14);%14
set(h1, 'LineWidth', 2);
set(h2, 'LineWidth', 2);
axes(ax(1)); hold on;
%ylim(ax(1), [6 9]);
%set(gca, 'YTick', [6,7,8,9]);
set(gca, 'YGrid','on','YMinorGrid','on','FontSize',12);%12
set(gca, 'GridLineStyle', '-');
axes(ax(2)); hold on;
plot(dataProcessed(:,1), dataProcessed(:,5),'r', 'LineWidth',2);
ylim(ax(2), [0 5]);
xlim(ax(1), [0 endPlot]);
xlim(ax(2), [0 endPlot]);
axes(ax(2)); hold on;
set(gca, 'YTick', [0,1,2,3,4,5],'FontSize',12);%12
hold off

subplot(2,2,3);
plot(dataProcessed(:,1),ORPdataSmoothed);
ylabel('ORP [mV]','FontSize',14,'Color','b');%14
xlabel('Time [h]','FontSize',14);%14
set(gca, 'YGrid','on','YMinorGrid','on','FontSize',12);%12

subplot(2,2,4);
plot(time,gasSmoothed);
ylabel('Biogas production rate [mL/min]','FontSize',14,'Color','b');%14
xlabel('Time [h]','FontSize',14);%14
set(gca, 'YGrid','on','YMinorGrid','on','FontSize',12);%12

suptitle(filename);

toc;
end
```